Università
degli Studi
di Padova

Sede Amministrativa: Università degli Studi di Padova
Dipartimento di Ingegneria Industriale

---

corso di dottorato di ricerca in: ingegneria industriale
curriculum: ingegneria chimica e ambientale
ciclo: XXXII

Design and optimisation of European supply chains for carbon capture, transport, and sequestration

Direttore della Scuola: Ch.mo Prof. Paolo Colombo
Coordinatore d'Indirizzo: Ch.mo Prof. Andrea C. Santomaso
Supervisore : Ch.mo Prof. Fabrizio Bezzo

Dottorando: Federico d'Amore

Foreword

The research project presented in this Thesis has involved the financial and intellectual support of many people, to whom the author is grateful. The research activity reported and discussed in this Thesis has been mainly conducted at the Department of Industrial Engineering of the University of Padova (Italy) under the supervision of Prof. Fabrizio Bezzo. Part of the work has been carried out at the Department of Chemical Engineering of Imperial College London (United Kingdom) under the supervision of Prof. Nilay Shah and partially funded by Fondazione Aldo Gini (Padova, Italy). All the material presented in this Thesis is original, unless explicit references provided by the author. The full list of publications drawn from this research project is reported below.

Peer-reviewed journal articles

d'Amore, F., Bezzo, F., 2019. Optimising the design of supply chains for carbon capture, utilisation and sequestration in Europe: a preliminary study. *Front. Energy Res.*, in preparation.

d'Amore, F., Lovisotto, L., Bezzo, F., 2019. Introducing social acceptance into the design of CCS supply chains: a case study at a European level. *J. Clean. Prod.*, Accepted. `https://doi.org/10.1016/j.jclepro.2019.119337`.

d'Amore, F., Bezzo, F., 2019. Optimal design of European cooperative supply chains for carbon capture, transport and sequestration with costs share policies. *AIChE J.*, Accepted. `https://doi.org/10.1002/AIC.16872`.

d'Amore, F., Sunny, N., Iruretagoyena, D., Bezzo, F., Shah, N., 2019. European supply chains for carbon capture, transport and sequestration, with uncertainties in geological storage capacity: insights from economic optimisation. *Comp. Chem. Eng.*, 129, 106521.

d'Amore, F., Mocellin, P., Vianello, C., Maschio, G., Bezzo, F., 2018. Economic optimisation of European supply chains for CO_2 capture, transport and sequestration, including societal risk analysis and risk mitigation measures. *Appl. Energy* 223, 401-415.

d'Amore, F., Bezzo, F., 2017. Economic optimisation of European supply chains for CO_2 capture, transport and sequestration. *Int. J. Greenh. Gas Control* 65, 99-116.

Peer-reviewed conference proceedings

d'Amore, F., Sunny, N., Iruretagoyena, D., Bezzo, F., Shah, N., 2019. Optimising European supply chains for carbon capture, transport and sequestration, including uncertainty on geological storage availability. *Comput. Aided Chem. Eng.* 46, 199-204.

d'Amore, F., Mocellin, P., Vianello, C., Maschio, G., Bezzo, F., 2018. Towards the economic optimisation of European supply chains for CO_2 capture, transport and sequestration, including societal risk analysis. *Comput. Aided Chem. Eng.* 44, 2305-2310.

Peer-reviewed conference abstracts

d'Amore, F., Bezzo, F., 2019. Optimal design of supply chains for carbon capture, storage, and utilisation. 12th European congress on chemical engineering (ECCE12), Florence, Italy. Selected as keynote talk.

d'Amore, F., Baldo, V., Bezzo, F., 2019. The contribution of CO_2 utilisation to GHG emission reduction: some results based on a European supply chain optimisation. 12th European congress on chemical engineering (ECCE12), Florence, Italy.

Iruretagoyena, D., Hedberg, S., Puhan, D., Zhang, D., Sunny, N., **d'Amore, F.**, Costantini, T., Shaffer, M., Mac Dowell, N., Shah, N., 2019. Novel hierarchical neworks as support for hydrotalcites for pre-combustion CO_2 capture. Fundamentals of Adsorption (FOA) 2019, Cairns, Australia.

Other presentations

d'Amore, F., Sunny, N., Iruretagoyena, D., Shah, N., Bezzo, F., 2019. Ottimizzazione di filiere europee per la cattura, stoccaggio e trasporto della CO_2, con incertezza nelle capacità dei bacini geologici. Congresso GRICU 2019, Palermo, Italy.

d'Amore, F., Lovisotto, L., Bezzo, F., 2019. Can we include acceptance effects in the optimal design of CCS supply chains? A European case study. Gordon Research Conference (GRC) CCUS, Les Diablerets, Switzerland.

Abstract

The global anthropogenic emissions of greenhouse gasses experienced an exponential increase compared to pre-industrial levels and, among these, CO_2 is the most abundant, with an overall emission that rose globally from 2 Gt/year in 1850 to over 35 Gt/year in 2010. Carbon capture and storage has been highlighted among the most promising options to decarbonise the energy sector, especially considering the European context which heavily relies on fossil fuel-fed facilities. When dealing with the strategic design and planning of a European carbon capture and storage infrastructure, the necessity of employing quantitative mathematical tools to treat the combinatorial complexity of such large-scale and multi-echelon networks clearly emerges. In this work, mixed integer linear programming models were utilised for carbon capture and storage supply chain optimisation at European scale.
The modelling framework has been developed according to a mixed integer linear programming model representing Europe in terms of emissions from large-stationary sources (i.e., coal and gas power plants). Regarding the capture facilities, post-combustion, pre-combustion and oxy-fuel combustion have been included as possible options, whereas both pipelines and ships have been described in techno-economic terms as potential transport means. The European geological storage potential has been retrieved from the EU GeoCapacity Project. Uncertainty in geological storage capacities has emerged among the major challenges for fostering an effective implementation of such complex systems. Accordingly, a tailored mathematical technique has been employed to tackle such risks and obtain optimal network configurations in terms of resiliency of the transport infrastructure. Then, a risk assessment has been incorporated within the modelling framework. This evaluation accounted for the societal risk generated by a potential leakage in the transport system (quantified according to the seriousness of the hazard) and was coupled with the choice of installing risk mitigation options (e.g., concrete slabs, deep burying, marker tape, surveillance). The societal response to carbon capture and storage has been further analysed through the concept of social acceptance, described through the amount of risk perceived by a given population inhabiting the region where an infrastructure is planned. The social response has been modelled as proportional to the project size, to the amount of population and to the differential behaviour of the European countries. Besides, a set of constraints has been employed to balance the spread of installation and operation costs among countries, with the aim of enhancing eco-

nomic costs share and cooperation policies between the different players. Finally, a preliminary analysis has been assessed on possible utilisation pathways for carbon conversion and utilisation into products.

The carbon capture and storage models were optimised using the GAMS software through the CPLEX solver. Results from the deterministic framework demonstrated the good European potential for carbon sequestration and gave some indications on the total cost for CO_2 capture, transport and sequestration. Capture costs were found to be the major contribution to total cost, while transport and sequestration costs were never higher than 10% of the investment required to set in motion and operate the whole network. The overall costs for a European carbon capture and storage SC were estimated in the range of 27-38 €/t of CO_2. The risk generated by uncertainty in geological storage capacities was found negligible with respect to the overall cost of the network, but slightly higher investments for transport and sequestration were needed to improve the resiliency of the system. The societal risk-constrained optimisation demonstrated the possibility to design a safe transport infrastructure with minor additional costs. In fact, mitigation actions never represented more than 11% of cost for installing and operating the transport network. However, no feasible solution could be found for a carbon reduction target higher than 50%, because of the unacceptable level of societal risk. When maximising social acceptance from the public (through minimising risk perception), results led to a massive exploitation of offshore sequestration solutions with a (possibly unacceptable) total costs of about 50.88 €/t of sequestered CO_2, i.e. +34% with respect to the economic optimum, due to a more complex network configuration characterised by high transport (+434%) and sequestration (+853%) costs. A multi-objective optimisation analysis, however, allowed identifying a possible intermediate solution between the two conflicting objectives (i.e., economics against acceptance), capable of limiting risk perception without excessively compromising the economic performance of the network. Regarding the model including costs share mechanisms among European countries, results showed that the additional European investment for cooperation (max. +2.6% with respect to a non-cooperative network) might not constitute a barrier towards the installation and operation of such more effective network designs. Finally, a preliminary model investigated the production of chemicals from CO_2 (specifically, polyether carbonate polyols and methanol) as an alternative to geological sequestration. The results showed that CO_2 conversion and utilisation mainly affects the total cost of the supply chain, which could be reduced with respect to a mere carbon capture and storage network. On the other hand, the contribution of CO_2 utilisation over capture in terms of environmental benefits was shown to be almost negligible.

Contents

Foreword 3

Abstract 5

1. Literature review and Thesis objectives 29
1.1 Greenhouse gases and global warming 29
1.2 The role of carbon capture and storage 33
1.3 Carbon capture and storage networks 34
1.3.1 Capture, transport, and sequestration 34
1.3.2 Capture, transport, and utilisation 38
1.4 Modelling carbon capture and storage 39
1.4.1 The need for a system perspective 39
1.4.2 Geographic scales and contexts 41
1.4.3 Effects of uncertainties 44
1.4.4 Safety issues, risk of hazards 46
1.4.5 Public acceptance, risk perception 47
1.4.6 Hedging risk and responsibilities 49
1.4.7 Utilisation pathways 50
1.5 Thesis objectives 52

2. Optimising carbon capture and storage in Europe 57
2.1 Chapter summary 57
2.2 Modelling framework 58
2.2.1 Emission sources 60
2.2.2 Capture options 66
2.2.3 Transport modes 67
2.2.4 Sequestration basins 69
2.3 Mathematical formulation 71
2.3.1 The capture problem model 71
2.3.2 The transport problem model 75
2.3.3 The sequestration problem model 77
2.3.4 Two stage LP-MILP model 78
2.4 Results 79

2.5 Discussion . . . 85
2.6 Chapter conclusions . . . 88

3. Effects of uncertainty in geological storage capacities . . . 91
3.1 Chapter summary . . . 91
3.2 Modelling framework . . . 92
3.2.1 Single stage MILP model . . . 93
3.2.2 Two stage MILP-LP model . . . 96
3.3 Mathematical formulation . . . 97
3.3.1 Single stage MILP model . . . 97
3.3.2 Two stage MILP-LP model . . . 101
3.3.3 Summary . . . 103
3.4 Results and discussion . . . 104
3.4.1 Scenarios . . . 104
3.4.2 Choosing the sample size . . . 104
3.4.3 Forecasting flexibility for resilient networks . . . 107
3.4.4 Resolving uncertainty as second stage decision . . . 109
3.4.5 Measuring the confidence in volume availability . . . 111
3.4.6 Assessing the effects of an extended time horizon . . . 112
3.4.7 Assessing legal restrictions on onshore sequestration . . . 113
3.5 Chapter conclusions . . . 114

4. Societal risk and risk mitigation measures . . . 117
4.1 Chapter summary . . . 117
4.2 Modelling framework . . . 118
4.2.1 Definition of societal risk . . . 120
4.2.2 Definition of risk mitigation measures . . . 123
4.3 Mathematical formulation . . . 123
4.3.1 Risk mitigation problem model . . . 124
4.3.2 Societal risk constraints . . . 128
4.4 Results . . . 128
4.5 Discussion . . . 134
4.6 Chapter conclusions . . . 135

5. Public risk perception and social acceptance . . . 137
5.1 Chapter summary . . . 138
5.2 Modelling social acceptance . . . 138
5.3 Modelling framework . . . 141
5.4 Mathematical formulation . . . 145
5.5 Results . . . 147
5.5.1 Scenarios . . . 147
5.5.2 Minimum cost network . . . 148
5.5.3 Minimum risk network . . . 150

5.5.4 Trade-off network . . . 150
5.5.5 Sensitivity analysis . . . 154
5.6 Discussion and limitations . . . 154
5.7 Chapter conclusions . . . 157

6. Cooperation policies and costs share . . . 159
6.1 Chapter summary . . . 159
6.2 Problem statement . . . 159
6.3 Modelling framework . . . 161
6.4 Mathematical formulation . . . 162
6.5 Results and discussion . . . 167
6.5.1 Scenarios . . . 167
6.5.2 Policies and cooperation levels . . . 167
6.5.3 Network configurations . . . 171
6.5.4 Assessing the European carbon reduction target . . . 174
6.5.5 Assessing legal restrictions on onshore sequestration . . . 175
6.6 Chapter conclusions . . . 176

7. A preliminary study to encompass CO_2 utilisation . . . 179
7.1 Chapter summary . . . 179
7.2 Modelling framework . . . 180
7.3 Mathematical formulation . . . 184
7.4 Results . . . 190
7.5 Discussion and limitations . . . 192
7.6 Chapter conclusions . . . 194

8. Conclusions and future work . . . 197

Bibliography . . . 201

List of Figures

1.1 Annual CO_2 emissions by world regions from 1751 to 2015 (CDIAC, 2017). 31

1.2 Global share of CO_2 emission from fossil fuels combustion in different sectors from 1960 to 2014 (IEA, 2015). 31

1.3 Annual CO_2 emission from solid fuel (e.g., coal), liquid (e.g., oil), gas (e.g., natural gas), cement production, or gas flaring between 1751 to 2013 (CDIAC, 2017). 32

1.4 Bibliometric analysis on scientific contributions for different decarbonisation options (source: Scopus). Sought keywords: 'CCS' or 'carbon capture' and ('storage' or 'sequestration'), 'CCUS' or 'CCU' or ('carbon capture' and 'utilisation'), 'nuclear energy' or 'nuclear power', 'solar energy', 'hydroelectric', 'geothermal', 'wind energy' or 'wind power'. 35

1.5 General scheme of the CCS, CCU, and CCUS echelons and technological options. 36

1.6 Possible carbon conversion and utilisation pathways (adapted from: National Accademy of Sciences, 2019). 39

1.7 Bibliometric analysis on scientific contributions on CCS and CCUS, focusing on keywords and acronyms that are typical of the process systems engineering fields (source: Scopus). Sought keywords: 'CCS' or 'CCUS' and: 'optimisation' or 'mathematical programming', or 'planning', or 'SC' (or 'supply chain'), or 'MILP', or 'MINLP'. 42

1.8 Results from the literature review in terms of: (a) percentage of contributions at different spatial modelling scales (the Unites States are inserted within the category 'continent'), and (b) percentage of contributions on either CCS or CCUS. 42

1.9 Thesis structure. Chapter 2 will propose an optimisation tool for a deterministic CCS SC which will deliver the base case scenario. Starting from this, Chapters 3-5 will investigate CCS technologies in terms of risk in order to provide insights into the design of resilient, safe and socially acceptable SCs. Conversely, Chapter 6 will investigate the policy-framework that may determine the installation of cooperative international CO_2 networks in Europe. Finally, Chapter 7 will preliminary discuss the possibility of conversion and utilisation of the CO_2 for the production of chemicals. 56

2.1 CCS SC echelons, including emission sources, capture option, transport modes and sequestration basins. The objective is the minimisation of the total cost to install and operate the entire European network. 58
2.2 European grid map and cells enumeration. 62
2.3 Spatially-explicit representation of Europe and surrounding regions. Only point sources emitting more than 10^6 t of CO_2/year are considered in this study. 62
2.4 Definition of inter-connection between region g and g' and of intra-connection within cell g, according to the inter-distance between cell g and g' and to the maximum intra-distance within cell g, respectively. 77
2.5 Scenario A-B-C-D, CCS SC final configuration under Scenario A (a), Scenario B (b), Scenario C (c), and Scenario D (d). 81
2.6 Scenario A-B-C-D, European regions g exploited potentials at $t = 20$ for capture and sequestration. 82
2.7 Scenario E, CCS SC final configuration at $t = 5$ (a), $t = 10$ (b), $t = 15$ (c), and $t = 20$ (d). 83
2.8 Scenario A-B-C-D-E, TCC, TTC and TSC contributions to overall TC in Scenario A-B-C-D (a), and their continuous variation in t specifically plotted for Scenario E (b). 85
2.9 Scenario A-B-C-D-E, Capture technologies selection in Scenario A-B-C-D (a), and their continuous variation in t specifically plotted for Scenario E (b). 86
2.10 Scenario A-B-C-D-E, specific costs for capture, transport, and sequestration for Scenario A-B-C-D (a), and their continuous variation in t specifically plotted for Scenario E (b). 86

3.1 Basic operating principle of model 1s 94
3.2 Basic operating principle of model 2s 95
3.3 Example of general planning scheme for sequestration for sample j on basin s in region g at time period t, and consequent values assumed by decision variables $Y_{j,s,g,t}$, $Y^{start}_{j,s,g,t}$, $Y^{keep}_{j,s,g,t}$ and $Y^{end}_{j,s,g,t}$. 101
3.4 Mathematical formulation of: (a) model 1s and (b) 2s. 105

3.5 Scenario A, comparison between models 1s (a) and 2s (b) on the dependency of the estimate of $risk$ [€/t of CO_2] from the sample size N_j, given a carbon reduction target $\alpha = 50\%$. 108
3.6 Scenario A, comparison between models 1s and 2s on the share of TCC, TTC, TSC and $risk$ over TC. 110
3.7 Resulting SC configuration from model 1s (a) and 2s (b): location of sequestration basins, deficits and surpluses of CO_2 and risk. 110
3.8 Dependency on A^{tune} of $risk$ and on ratios of $risk/TSC$ for model 1s and 2s. 112
3.9 SC storage configuration for model 1s for (a) Scenario A and (b) Scenario C. 113
3.10 Scenario D, storage configuration for model 1s (a) and model 2s (b). . 114

4.1 Scheme of the multi-echelon CCS SC framework with quantitative analysis of societal risk and mitigation options. The objective is total cost minimisation subject to the constraint that societal risk is kept below a threshold of acceptability value. Risk mitigation measures can be installed and/or operated on the resulting CO_2 transport infrastructure. 119
4.2 Comparison of SC configurations between Scenario A (a) and Scenario B (b). 131
4.3 Total societal risk SR_g [events] in region g for Scenario A (a), Scenario B (b), Scenario C (c). 132
4.4 Comparison of SC configurations for Scenario A (a) and Scenario A* (b) (the latter includes legal constraints on onshore sequestration). . . 133
4.5 Specific mitigation cost (i.e., total cost TTC^m for installing and operating mitigation options with respect to the overall amount of sequestered CO_2, [€/t of CO_2]) (a), and percentage mitigation cost (i.e., total cost TTC^m for installing and operating mitigation options with respect to total transport cost TTC, [%]) (b). 133

5.1 Basic operating principle of the CCS SC MILP optimisation framework, including social acceptance evaluation through risk perception. 146
5.2 Pareto curve under bi-objective optimisation: the tree Scenarios are indicated. 149
5.3 Scenarios A-B-C: results from the bi-objective optimisation in terms capture TCC [€/t of sequestered CO_2, and %], transport TTC [€/t of sequestered CO_2, and %], and sequestration TSC [€/t of sequestered CO_2, and %] costs contribution to overall investment TC. 151
5.4 Scenarios A, B, and C: resulting SC configurations. Dark dots represent capture and sequestration nodes. 152

5.5 Main contributors to sequestration as results from optimal CCS SC optimisations for Scenarios A, B, and C. dk=Denmark, pl=Poland, ita=Italy, esp=Spain, pt=Portugal, nl=Netherlands, uk=United Kingdom, no=Norway, de=Germany, fr=France, mkd=Macedonia. 153

5.6 CCS SC configuration under Scenario C, for different values of carbon reduction target α. Dark dots represent capture and sequestration nodes. 155

6.1 CCS SC countrywide per capita or per emitted unit cost ($\widehat{TC}_c$ [€/person, or €/t of CO_2 emitted], as resulting from a global optimisation-driven approach reported in Chapter 2. 161

6.2 Representation of the modelling framework aiming at the minimisation of total cost for CCS, such that the imposed costs share level between countries c is accomplished, according to a proportionality between national per capita costs $\widehat{TC}_c^{tot}$ and the chosen policy for cooperation δ_c. 163

6.3 Countrywide variation of total per capita cost $\widehat{TC}_c^{tot}$ [€/person] on cooperation level ε_j at iteration j (shown until the model reaches convergence for $\varepsilon_j = \varepsilon_j^*$), for Scenario A (a), Scenario B (b), and Scenario C (c). Black vertical bars represent the threshold cooperative configurations obtained for ε_j^*. 168

6.4 Total per capita costs (TC_c^{tot} [€/person] for each country c, for Scenario A, Scenario B, and Scenario C. 171

6.5 Contribution each country c in terms of total network cost $\widehat{TC}_c^{network}$, debit ($debit_c$), and credit ($credit_c$), for Scenario (a), Scenario B (b), and Scenario C (c). 172

6.6 Final SC configurations for Scenario A (a), Scenario B (b), and Scenario C (c). Dark dots represent capture and sequestration nodes. . . 173

6.7 Increase in specific total cost TC^{tot} [€/t] when limitations in onshore storage are taken into account (Instance II), with respect to base Scenarios A-B-C. 176

6.8 Countrywide share of sequestered CO_2 for Scenario A-B-C in case of no constraints on storage (a) and for Instance II (b). 177

7.1 Overview of the proposed framework for the CCUS SC optimisation. 183

7.2 Principal flowrates and conversion schemes for producing either (a) PPP (Fernández-Dacosta et al., 2017), or (b) MeOH (Wiesberg et al., 2016). 184

7.3 Final SC configurations for (a) Scenario 0 and (b) Scenario A. 193

7.4 Comparison between Scenario C and Scenario A in terms of: (a) relative variations in total cost (TC) and exploitation of geological sequestration (S); and (b) effective net CO_2 utilisation ($Netutilis.$), with respect to the change in the productions of the chemical being considered (U^{max}). 193

List of Tables

1.1 Literature review on currently published contributions on optimisation tools for CCS/CCUS. 43

1.2 Cited literature on currently published contributions on optimisation and assessment tools for cooperation, collaboration or compensation schemes in multinational energy systems, possibly including CCS or CCUS among the decarbonisation options. 51

2.1 Yearly CO_2 emissions P_g^{max} [t of CO_2/year] in region g, with null values for cells $g = [125 - 134]$ (JRC, 2016). 61

2.2 Terrain factors τ_g, evaluated following the analogy between pipeline transport of CO_2 and electrical transmission: the multiplicative cost factor ranges from a minimum of 1.00 (i.e., grassland) to a maximum of 1.50 (i.e., highly mountainous region), with null values for cells $g = [125 - 134]$ (IEAGHG, 2002). 64

2.3 Coal- and gas-based power generation percentage contributions on total CO_2 emission in 2013 for $\gamma_{k,g}$ [t/t] definition, with null values for cells $g = [125 - 134]$ (Eurostat, 2016). 65

2.4 Plants performances when current CO_2 capture technologies are implemented (IPCC, 2005; Rubin et al., 2015). Both the adjusted values [*] (IPCC, 2005) and the current ones [**] (Rubin et al., 2015) are reported. A \$-€ exchange rate of 1.0487 (2002) and of 1.3791 (2013) was applied. 68

2.5 Transport unitary cost $UTC_{p,l}$ [€/t of CO_2/km] according to the discretisation p of transport capacities Q_p [t of CO_2/year]. The constant value for ship transport ($UTC_{p,ship} = 0.03215$ €/t of CO_2/km) is then lowered according to a kilometric slope ($fship = -0.00001385$ €/t of CO_2/km), the latter representing economies of scale on total transport distance. 70

2.6 Minimum deterministic storage potential $S_{s,g}^{D,min}$ [Mt of CO_2] of basin s in region g, where i= *deep saline aquifers*, ii= *hydrocarbon fields*, iii= *coal fields*. Basins typologies are discussed in Chapter 3. 72

2.7 Maximum deterministic storage potential $S_{s,g}^{D,max}$ [Mt of CO_2] of basin s in region g, where i= *deep saline aquifers*, ii= *hydrocarbon fields*, iii= *coal fields*. Basins typologies are discussed in Chapter 3. 73
2.8 Capture efficiencies (η_k) and unitary capture cost (UCC_k [€/t of CO_2]) for each technology k. Data summarise representative values that were previously reported in Table 2.4. 74
2.9 Scenario A-B-C-D-E, objective (Obj.), carbon reduction target (α) and its variation in time ($\Delta\alpha$), and chosen optimisation technique (Opt. technique). 80
2.10 Scenario A-B-C-D-E, problem size (number of equations and variables) and computational performance (solution time - Sol. time, optimality gap - Opt. gap) of different capture scenarios (depending on α selection) to compare exact (e) and 2-stage ($2s$) solution methods. 84
2.11 Scenario E, sensitivity analysis on unitary capture costs UCC_k [€/t of CO_2]. 88

3.1 Results from model 1s and 2s (Scenario 0-A-B-C-D), according to the European carbon reduction target α [%] and to the sample size N_j: total cost TC [€/t of CO_2] (including $risk$), total capture cost TCC [€/t of CO_2], total transport cost TTC [€/t of CO_2] and $risk$ [€/t of CO_2]. Specific costs [€/t] are expressed in terms of total sequestered amount of CO_2. 106
3.2 Results from model 1s and 2s (Scenario 0-A-B-C-D) in terms of computational performance according to the European carbon reduction target α [%] and to the sample size N_j: number of continuous variables, number of discrete variables and solution time [s]. 107

4.1 Definition of hazardous incidents h, failure frequency [events/km] and percentage probability [events/km] according to the assumed failure distribution [%] and to the chosen methodology (LC50, 60000 ppm, or IDLH). As regards failure frequency, a rare-event probabilistic law is assumed for the calculation of probability. The Poisson's law is used. A 1 year time-framework is here assumed as a reference unit for the calculations. 121
4.2 Population P_g [people] and population density Pd_g [people/km^2] in region g, evaluated by intersecting the information of population data in raster format (CIENSIN, 2015) with the European squared cells g through the QGIS software (QGIS, 2017). 125
4.3 Values of mitigation factor ($MF_{m,l}$ [%]) and unitary cost ($UMC_{m,l}$ [€/km]) of mitigation options m (Knoope et al., 2014) 126
4.4 Scenarios A-A*-B-C, economic results (transport cost - TTC, mitigation cost - TTC^m) and computational information (solution time - Sol. time, optimality gap - Opt. gap). 129

4.5 Scenario A, economic results (transport cost - TTC, mitigation cost - TTC^m) and computational information (solution time - Sol. time, optimality gap - Opt. gap), for different values of α [%]. No feasible solutions were found for $\alpha \geq 50\%$. Specific costs are intended per unit of sequestered CO_2. 131

5.1 Values of $dim_{d,c}$ of Hofstede's cultural dimensions d in country c (Hofstede et al., 2010). 142

5.2 Weights W_d^{risk} and $W_d^{benefit}$ of cultural dimensions d (Karimi and Toikka, 2018). 142

5.3 Parameter for the calculation of risk perception $risk_g$ [(people)$^{-1}\cdot$(t of CO_2)$^{-1}$] in region g within country c (calculated following the methodology proposed by Karimi and Toikka, 2018). Because of lack of data, for some countries approximations are used: for Ukraine (ukr) and Moldavia (mda) the value of Romania (ro) is used; for Bosnia (ba) and Albania (alb) the value of Serbia (srb) is used; for Macedonia (mkd) the value of Greece is used (gr); for Algeria (alg) and Tunisia (tun) the value of Morocco (mo) is used 6.1. 143

5.4 Inner pipeline diameter (i.e., Φ_p [m]) and mass flowrates (i.e., Q_p [Mt of CO_2/year]) employed for the calculation of holdup areas $A_{p,g,g'}$, according to the pipelines capacity discretisation p. The values are taken from Knoope et al. (2013). 148

5.5 Scenarios A-B-C: results from the bi-objective optimisation in terms of total cost TC [B€ or €/t of sequestered CO_2], risk perception RP, optimality gap Opt. gap [%], and solution time Sol. time [s]. 149

6.1 List of countries c. 160

6.2 Differential countrywide weighting factors δ_c^A, δ_c^B and δ_c^C for each country c (Eurostat, 2019a; 2019b). 166

6.3 Scenario 0-A-B-C, main computational data and results: European carbon reduction target α [%], countrywide differential weighting factor δ_c, resulting threshold cooperative convergence rate ε_j^* and corresponding European total cost TC^{tot} [B€ or €/t of sequestered CO_2], maximum optimality gap (Opt. gap [%]) and solution time (Sol. time [s]). 168

6.4 Scenario 0-A-B-C, European carbon reduction target α [%], resulting threshold convergence rate ε_j^*, European total cost TC^{tot} [B€ or €/t of sequestered CO_2], and increase in European total cost ΔTC^{tot} [%] with respect to the α-corresponding economic result in Scenario 0. . . 175

7.1 List of chemicals that can be produced from CO_2 and their effective compliance with the design requirements: (*i*) *minimum production threshold*, (*ii*) *techno-economic data availability*, (*iii*) *environmentally promising* and (*iv*) *economically promising*. Only PPP and MeOH meet all the requirements. 182

7.2 Prices of natural gas (gas p.) and electricity (el. p.), labour cost (lab_c [k€/y]) and corporate tax rate (tax_c, set then identical for each region g within country c) in the analysed countries c (Eurostat, 2017a; 2017b; 2017c). 187

7.3 Cost of raw materials $raw_{\psi,g}$ [€/t] for producing chemical ψ in region g (Eurostat, 2017a; 2017b; 2017c; Baldo, 2018), with null values for cells $g = [125 - 134]$. 188

7.4 Cost of utilities $util_{\psi,g}$ [€/t] for producing chemical ψ in region g (Eurostat, 2017a; 2017b; 2017c; Baldo, 2018), with null values for cells $g = [125 - 134]$. 189

7.5 Arrays of slopes FCI_{ψ}^{slope} [€/t of chemical] and intercepts $FCI_{\psi}^{intercept}$ [€] coefficients for the calculation of the facility capital costs for producing chemical ψ (Aasberg-Petersen et al., 2008). Carbon quantity U_{ψ}^{saved} [t of CO_2/t of chemical ψ] that is saved from the production of a unitary quantity of chemical ψ (von der Assen and Bardow, 2014; Roh et al., 2016), and carbon quantity U_{ψ}^{conv} [t of CO_2/t of chemical ψ] that is converted to produce a unitary quantity of chemical ψ (Langanke et al., 2014; Sakakura and Kohno, 2009; Roh et al., 2016). 190

7.6 Scenarios 0-A-B-C, main assumptions and results. All scenarios aim at reaching a European carbon reduction target $\alpha = 50\%$ of emissions from large stationary sources. Results are summarised in terms of total cost TC total capture cost TCC, total transport cost TTC, total sequestration cost TSC, and $profit$. Intensive values (i.e., [€/t]) are referred to the overall captured quantity of CO_2. Results for Scenario C are those considering the triplication of the European production of chemicals with respect to the base case. 191

List of Symbols

Acronyms

1s	Single stage model
2s	Two stage model
BECCS	Bio-energy carbon capture and storage
CCS	Carbon dioxide capture and storage
CCU	Carbon dioxide capture and utilisation
CCUS	Carbon dioxide capture, utilisation, and storage
COE	Cost of electricity
COP	Conference of the Parties
DMC	Dimethylcarbonate
EOR	Enhanced oil recovery
EC	European Commission
EU	European Union
GHG	Greenhouse gas
IDLH	Immediately dangerous to life or death
IDV	Individualism vs. collectivism
IEA	International Energy Agency
IGCC	Integrated gasification combined cycle
IPCC	Intergovernmental Panel on Climate Change
IVR	Indulgence vs. restraint
JRC	Joint Research Centre
LC50	Lethal concentration 50%
LCA	Life cycle analisis
LP	Linear programing
LTO	Long-term orientation
MAS	Masculinity vs. femininity
MeOH	Methanol
MILP	Mixed integer linear programming
NGCC	Natural gas combined cycle
NIMBY	Not-in-my-back-yard
Opt. gap	Optimality gap
PDI	Power distance index

PPP	Polyether carbonate polyols
SC	Supply chain
Sol. time	Solution time
UAI	Uncertainty avoidance index
ZEP	Zero Emission Platform

Sets

c	Country, $c = [aut, ..., no]$
d	Cultural dimensions, $d = [PDI, ..., IVR]$
g	Region, $g = [1, ..., 134]$
h	Hazard, $h = [i, ii, iii, iv]$
j	Sample or iteration, $j = [1, ..., 400]$
k	Capture option, $k = [post^{comb}_{coal}, ..., pre^{comb}]$
l	Transport mode, $l = [pipeline, ship]$
m	Mitigation option, $m = [none, ..., surveillance]$
p	Transport capacity, $p = [1, ..., 7]$
ψ	Chemical output, $\psi = [PPP, MeOH]$
s	Basin, $s = [saline\ aquifer, ..., coal\ field]$
t	Time period, $t = [1, ..., 20]$

Parameters

A	Area of the hole [m^2]
A^{ψ}	Scalar A for calculation of manufacturing cost of chemical ψ
α	European carbon reduction target [%]
A^{tune}	Tuning parameter of model 2s
$A_{p,g,g'}$	Sectional area of pipeline transporting p from g to g' [m^2]
B^{ψ}	Scalar A for calculation of manufacturing cost of chemical ψ
$b(x)$	Half-width of the pipeline section [m]
$benefit_c$	Benefit parameter in country c
CCR^{seq}	Capital cost rate for injection well [%]
C_d	Release hole of discharge [0.61]
C^{ψ}	Scalar A for calculation of manufacturing cost of chemical ψ
d_g	Average injection well depth in region g [km]
$dim_{d,c}$	Hofstede's cultural dimension d in country c
δ^A_c	Differential weighting factor based on emissions
δ^B_c	Differential weighting factor based on emissions·GDP
δ^C_c	Differential weighting factor based on emissions/GDP
ε_j	Costs convergence rate at iteration j
ε^*_j	Threshold costs convergence rate at iteration j

γ	Viscosity correction factor [1.00]
$\gamma_{g,k}$	Ratio of coal- and gas- fired power plants in region g for capture technology k to be employed
f^{ship}	Cost factor for ship transport [€/t of CO_2/km]
$FCI_{\psi}^{intercept}$	Array of intercept coefficients of the linearized facility capital cost for producing chemical ψ [€]
FCI_{ψ}^{slope}	Array of slope coefficients of the linearized facility capital cost for producing chemical ψ [€/t]
g_c	Gravitational constant [m/s^2]
$lab_{\psi,g}$	Labour cost for producing chemical ψ in region g [€/t]
LD_g	Size of cell g [km]
$LD_{g,g'}$	Matrix of distances between region g and g' [km]
L_h	Liquid release distance of hazard h [km]
μ	Average failure rate [faults/year]
m_1	Cost parameter 1 for injection well [€]
m_2	Cost parameter 2 for injection well [€]
$\dot{m}_{\zeta,\psi}$	Mass flowrate of output ζ for producing chemical ψ [t/year]
$MF_{m,l}$	Mitigation factor of measure m on mode l [%]
N_j	Sample size
η_k	Capture efficiency for technology k [%]
off_g	Additional cost of offshore injection well
OM^{seq}	Maintenance rate for injection well [%]
P^{atm}	Atmospheric pressure [kPa]
Pd_g	Population density in region g [people/km^2]
$\bar{Pd}_g$	Average population density between region g and g' [people/km^2]
$Pf_{h,l}$	Probability of hazard h on mode l [events/km]
P_g	Population in region g [people]
$P_{g'}$	Population in region g' [people]
$\bar{P}_{g,g'}$	Average population between region g and g' [people]
$P_{\zeta,g}$	Unitary price of commidity ζ for producing chemical ψ [€/t]
P_g^{max}	Amount of anthropogenic CO_2 that is generated in region g [t of CO_2]
Q_p	Transported capacity discretisation according to set p [t of CO_2]
ρ_{l,CO_2}	Liquid density of CO_2
$raw_{\psi,g}$	Unitary cost of raw materials for producing chemical ψ in region g [€/t]
ϕ_p	Pipeline inner diameter for transporting flowrate p [m]
$risk_g$	Risk parameter in region g within country c [(people)$^{-1}$·(t of CO_2)$^{-1}$]
$\bar{risk}_{g,g'}$	Average risk parameter between regions g and g' [(people)$^{-1}$·(t of CO_2)$^{-1}$]
$\widehat{R}_{\psi,g}$	Unitary revenue from chemical ψ in region g [€/t]
SR_g^{max}	Maximum societal risk in region g [events]

$S_y(x)$	Lateral dispersion parameter [m]
$S_z(x)$	Vertical dispersion parameter [m]
S^{max}	Maximum capacity of each injection well [t of CO_2]
S_g^D	Deterministic average sequestration potential in region g [t of CO_2]
$S_{s,g}^{D,max}$	Deterministic maximum sequestration potential of basin s in region g [t of CO_2]
$S_{s,g}^{D,min}$	Deterministic minimum sequestration potential of basin s in region g [t of CO_2]
$S_{j,s,g}^{U,min}$	Uncertain minimum upper bound for storage for sample j on basin s in region g [t of CO_2]
τ_g	Terrain factor in region g
tax_g	Taxation in region g
$Total_{g,l,g'}^{Q}$	Total links allowed for transport from g through l to g'
UCC_k	Unitary capture cost for technology k [€/t of CO_2]
U_{ψ}^{conv}	Amount of CO_2 needed to produce a unitary amount of chemical ψ
U_{ψ}^{saved}	Amount of CO_2 saved because of its usage in a conversion process to produce a unitary amount of chemical ψ, instead of utilising a traditional input
$UMC_{m,l}$	Unitary mitigation cost for measure m through mode l [€/km]
$U\bar{T}C$	Unitary intra-connection cost [€/t of CO_2/km]
$UTC_{p,l}$	Unitary transport cost for size p through mode l [€/t of CO_2/km]
$util_{\psi,g}$	Unitary cost of utilities for producing chemical ψ in region g [€/t]
$U_{\psi,g}^{max}$	Productivity upper bound for chemical ψ in region g [t]
U_{ψ}^{ref}	Reference chemical plant capacity [t/year]
$W_d^{benefit}$	Weight of cultural dimension d for benefit calculation
W_d^{risk}	Weight of cultural dimension d for risk calculation

Continuous variables

$\alpha^{stability}$	Stability factor
$c(x, y, z)$	Vapour concentration at ground level [ppm]
$c_c(x)$	Centreline ground-level concentration of CO_2 [ppm]
$CF_{\psi,g}$	Cash flow from sale of chemical ψ in region g [€]
$C_{g,t}^{ratio}$	Carbon captured in region g at time period t with respect to local capture potential [%]
$C_{k,g,t}$	Carbon captured through k in region g at time period t [t of CO_2/year]
$COM_{\psi,g}$	Manufacturing cost for chemical ψ in region g [€]
$credit_{j,c}$	Credit at iteration j in country c [€]
$d_{\psi,g}$	Depreciation of chemical ψ in region g [€]
$debit_{j,c}$	Debit at iteration j in country c [€]

$\delta Q_{j,g,g',t}$	Differential flowrate for sample j from region g to region g' at time period t [t of CO_2/year]
$FCI_{\psi,g}$	Fixed capital investment for producing chemical ψ in region g [€]
$H_{g,g'}$	Pipeline holdup between region g and g' [t of CO_2]
$L_{l,t}$	Total transport distance through l at time period t [km/year]
$\dot{m}_{CO_2}$	Discharged flowrate of CO_2
$N_{g,t}$	Number of injection wells in region g at time period t
$P_{k,g,t}$	Carbon selected for processing through k in region g at time period t [t of CO_2/year]
$profit$	Profit earned from sale of chemicals [€]
P_t	Failure probability based on Poisson distribution of rare events
$Q_{g,l,g',t}$	Carbon flowrate transported from g through l to g' at time period t [t of CO_2/year]
R_i	Richardson dimensionless number
R_t	Reliability based on Poisson distribution of rare events
$R_{\psi,g}$	Revenue from sale of chemical ψ (and by-products) in region g [€]
$risk$	Total risk [€]
$risk_{j,g,t}$	Risk for sample j in region g at time period t [€/year]
$risk^{inter}_{j,g,t}$	Risk due to inter-connection for sample j in region g at time period t [€/year]
$risk^{intra}_{j,g,t}$	Risk due to intra-connection for sample j in region g at time period t [€/year]
RP	Risk perception
RP^{seq}	Risk perception on sequestration stage
RP^{trans}	Risk perception on transport stage
P^{net}_g	Net amount of CO_2 emitted in region g considering its utilisation for chemicals production
$P^{saved}_{\psi,g}$	Amount of CO_2 not emitted because employed for the production of chemical ψ in region g, instead of a traditional input [t]
S^{ratio}_g	Carbon sequestered in region g with respect to local sequestration potential [%]
$S_{g,t}$	Carbon sequestered in region g at time period t [t of CO_2/year]
$S^D_{s,g,t}$	Deterministic sequestered amount on basin s in region g at time period t [t of CO_2/year]
$S^U_{j,s,g,t}$	Uncertain sequestered amount for sample j on basin s in region g at time period t [t of CO_2/year]
$S^{U,max}_{j,s,g}$	Uncertain maximum upper bound for storage for sample j on basin s in region g [t of CO_2]
$S^{U,max}_{j,s,g,t}$	Uncertain maximum upper bound for storage for sample j on basin s in region g at time t [t of CO_2]
$S^I_{s,g,t}$	Yearly storage resulting from stage I on basin s in region g at time period t [t of CO_2/year]

$S^{II}_{j,s,g,t}$	Yearly storage resulting from stage II for sample j on basin s in region g at time t [t of CO_2/year]
$S^{deficit}_{j,s,g,t}$	Deficit of storage for sample j on basin s in region g at time period t [t of CO_2/year]
$S^{surplus}_{j,s,g,t}$	Surplus of storage for sample j on basin s in region g at time period t [t of CO_2/year]
$Sh^{inter}_{h,g,g'}$	Surface affected by hazard h between region g and g' [km^2]
$Sh^{intra}_{h,g}$	Surface affected by hazard h in region g [km^2]
SR_g	Total societal risk in region g [events]
SR^{inter}_g	Societal risk in region g produced by inter-connection systems [events]
$SR^{inter}_{g'}$	Societal risk in region g' produced by inter-connection systems [events]
SR^{intra}_g	Societal risk in region g produced by intra-connection systems [events]
$SR^{inter}_{p,g,l,g'}$	Local societal risk produced by flowrate p transported from g through l to g' [people·events]
$SR^{intra}_{g,l}$	Local societal risk for intra-connection within region g through mode l [people·events]
TC	Total cost [€]
$TC^{network}_{j,c}$	Infrastructural cost at iteration j in country c [€]
$\widehat{TC}^{network}_{max}$	Upper bound for per capita infrastructural cost [€/person]
$\widehat{TC}^{network}_{min}$	Lower bound for per capita infrastructural cost [€/person]
TC^{tot}_j	European total cost at iteration j [€]
$TC^{tot}_{j,c}$	Total cost at iteration j in country c [€]
$\widehat{TC}^{tot}_{j,c}$	Total per capita cost at iteration j in country c [€/person]
$\widehat{TC}^{tot}_{j,max}$	Upper bound for total per capita cost at iteration j [€/person]
$\widehat{TC}^{tot}_{j,min}$	Lower bound for total per capita cost at iteration j [€/person]
TCC	Total capture cost [€]
$TCC_{g,t}$	Total capture cost in region g at time period t [€/year]
TSC	Total sequestration cost [€]
TSC_t	Total sequestration cost at time period t [€/year]
TTC	Total transport cost [€]
TTC^m	Total cost for installing mitigation measures [€]
TTC^m_{inter}	Total cost for mitigation on inter-connection systems [€]
TTC^m_{intra}	Total cost for mitigation on intra-connection systems [€]
TTC_t	Total transport cost at time period t [€/year]
TTC^{size}_t	Scale effect of transport size on total transport cost at time period t [€/year]
TTC^{dist}_t	Scale effect of transport distance on total transport cost at time period t [€/year]

TTC_t^{intra}	Effect of intra-connection cost on total transport cost at time period t [€/year]
U_g	Net amount of CO_2 that is exploited for utilisation in region g [t]
$U_{\psi,g}^{chem}$	Amount of chemical ψ produced in region g [t]

Binary variables

$\delta_{\psi,g}^{chem}$	1 if chemical ψ is produced in region g, 0 otherwise
$\delta_{m,p,g,l,g'}^{inter}$	1 if mitigation m is applied on flowrate p from region g through l to g', 0 otherwise
$\delta_{m,g,l}^{intra}$	1 if mitigation m is applied on intra-connection within region g through l, 0 otherwise
$\lambda_{p,g,l,g'}$	1 if transport of size p is operated from region g through mean l to g', 0 otherwise
$\lambda_{p,g,l,g',t}$	1 if transport of size p is operated from region g through mean l to g' at time period t, 0 otherwise
$Y_{j,s,g,t}$	1 if either injection begins or continues for sample j on basin s in region g at time t, 0 otherwise
$Y_{j,s,g,t}^{end}$	1 if injection has just finished for sample j on basin s in region g at time period t, 0 otherwise
$Y_{j,s,g,t}^{keep}$	1 if is planned to continue the injection for sample j on basin s in region g at time t, 0 otherwise
$Y_{s,g,t}^{keep,I}$	1 if is planned in stage I to continue the injection on basin s in region g at time t, 0 otherwise
$Y_{j,s,g,t}^{start}$	1 if injection begins for sample j on basin s in region g at time period t, 0 otherwise
$Y_{s,g,t}^{start,I}$	1 if in stage I injection begins on basin s in region g at time period t, 0 otherwise

1

Literature review and Thesis objectives

1.1 Greenhouse gases and global warming

The global anthropogenic emissions of greenhouse gasses (GHGs) (mainly constituted of CO_2, CH_4, N_2O and fluorinated gases) have experienced an exponential increase compared to pre-industrial levels. Among all emitted GHGs, CO_2 is the most abundant, and its overall emissions have raised globally from 2 Gt/year in 1850 to over 35 Gt/year in 2010 (IPCC, 2018). It is estimated that a total of 2040 Gt of anthropogenic CO_2 has been emitted so far since 1850, half of which from 1970 to now; the United States, China and Europe are among the largest CO_2 emitters (Figure 1.1). In particular, the increment in GHGs emissions is mainly driven by three causes: population growth, economic growth, and the loss in efficiency for the natural environment to absorb, reflect and emit CO_2 (IPCC, 2018). In fact, it is noted easily that the economic growth of a country is strictly connected to the increase in GHGs emissions, because most countries aim at satisfying the higher energy demand by burning larger quantities of fossil fuels thus, enlarging their carbon footprint (IEA, 2015; BP, 2017). Indeed, nowadays the 80% of the global primary energy demand is met by burning or converting fossil fuels, and in 2013 more than 80% of the total emission of CO_2 derived from the energy-field, accounting for a total of 31 Gt of CO_2 (BP, 2017). Additionally, the trend of CO_2 emissions within the energy sector has not fallen, considering that within a decade (2006-2016) the global emissions from power industry have raised by 1.3%/year (BP, 2017). In general, four activities are mainly responsible for GHGs emissions: power generation,

residential buildings and tertiary, manufacturing industries and constructions and transports (IPCC, 2018). In 2014, considering the overall CO_2 emissions derived from fossil fuels combustion, power and heat generation accounted for the largest share (i.e., 49%), followed by transport (i.e., 20%), manufacturing industry (i.e., 20%), and residential buildings and tertiary (i.e., 8.6%) (Figure 1.2). In addition, focusing on fossil fuels conversion or utilisation, in 2013 solid fuels (e.g., coal) have been responsible for a total of 15 Gt of CO_2, followed by liquid fuels (e.g., oil) with 12 Gt, gaseous fuel (e.g., natural gas) with 6.6 Gt, and 2 Gt of indirect CO_2 emissions from cement industry (Figure 1.3).

The emission in the atmosphere of excessive amounts of anthropogenic GHGs has directly affected the climate. As known, natural GHGs allow the earth to keep acceptable climatic condition for human life by trapping part of the reflected sun radiation coming from the Earth surface (Treut et al., 2007). Indeed, without the blanket-like effect generated by GHGs, the average Earth's surface temperature would be -19°C, against a current value of 14°C (IPCC, 2018). However, due to the anthropogenic GHGs emissions, the atmospheric CO_2 concentration has risen from 280 ppm to 400 ppm since 1860. This has led to an increment of the average surface temperature of about 0.85°C, as measured between 1880 and 2012 (IPCC, 2018). The growing concentration of CO_2 in the atmosphere has also caused a 26% acidification of the oceans (which corresponds to a 0.1 decrease in the pH), a 4% reduction in extension of the Arctic glacier compared to 1979 levels, and a 0.19 m increase in the sea level (IPCC, 2018). If no actions were carried out to prevent and limit CO_2 emissions, the average Earth surface temperature would rise from a minimum of +1.9°C to a maximum of +3.4°C, with respect to pre-industrial levels by 2100 (with a mean increase between +0.1°C and +0.3°C per decade), with drastic consequences on the life of billions of people (IPCC, 2018). The effects of anthropogenic emissions of GHGs on the climate started raising some concern already in 1988, when the Intergovernmental Panel on Climate Change (IPCC) was founded, but it was only in 1997 that 192 countries started moving towards the adoption of a first treat for GHGs emissions reduction through the Kyoto Protocol. Moreover, in 2015 through the Paris Agreement 195 nations agreed on trying to prevent the temperature rise well below +2°C with respect to pre-industrial level. A further effort in trying to limit the rise in average temperature to +1.5°C by 2050 was proposed, too (IPCC, 2018). A 23% reduction of GHG emission has already been achieved in the European Union (EU) compared to 1996 levels, but in order to comply with the Paris Agreement it has been proposed to reduce them by 43% by 2030 with respect to 2005 values. Regarding CO_2 specifically, its concentration in the atmosphere should be limited to less than 450 ppm to stand a good chance of not exceeding the +1.5°C target (IPCC, 2018).

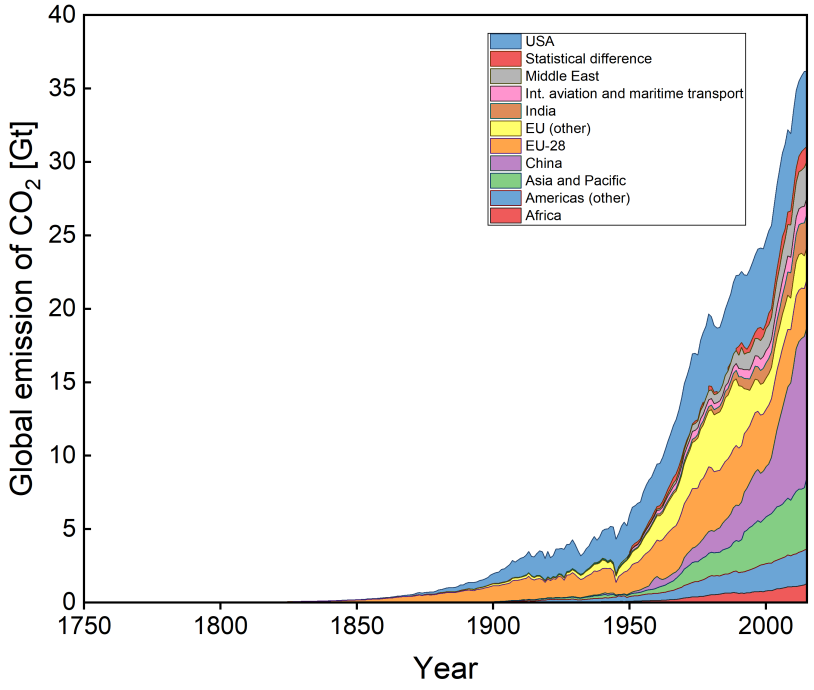

Fig. 1.1: Annual CO_2 emissions by world regions from 1751 to 2015 (CDIAC, 2017).

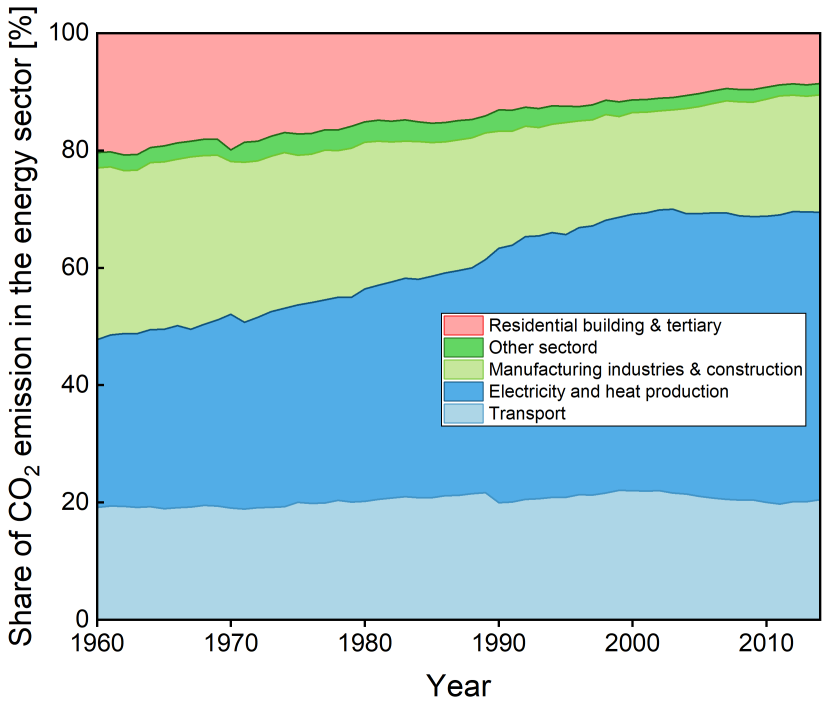

Fig. 1.2: Global share of CO_2 emission from fossil fuels combustion in different sectors from 1960 to 2014 (IEA, 2015).

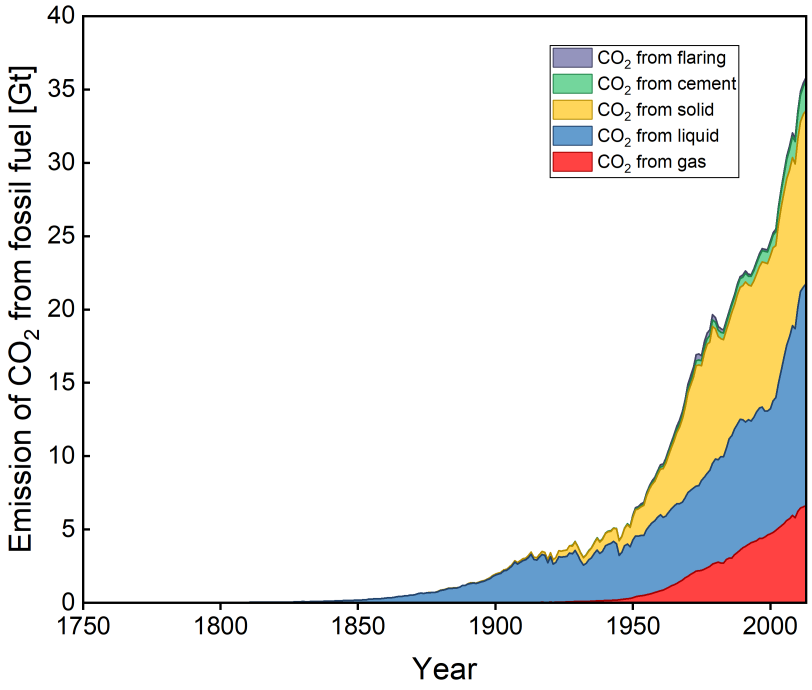

Fig. 1.3: Annual CO_2 emission from solid fuel (e.g., coal), liquid (e.g., oil), gas (e.g., natural gas), cement production, or gas flaring between 1751 to 2013 (CDIAC, 2017).

1.2 The role of carbon capture and storage

The Brundtland Commission of the United Nations on March 20th, 1987 defined 'sustainable development' as that 'development that meets the needs of the present without compromising the ability of future generations to meet their own needs'. From this perspective, carbon capture and storage (CCS) represents an ideal candidate for attaining a sustainable development within that definition, i.e. an economic growth that aims at tackling major environmental issues (global warming), in an era when (unfortunately) power and industry still massively rely on carbon and, more in general, fossil fuels. Along with the progressive implementation of greener alternatives (e.g., through an increasing penetration of renewable energies and low-impact, high-efficiency processes), CCS would allow developed countries to achieve that technological shift that is struggling to occur, without affecting jobs and economic resources allocated in fossil-based businesses (Sustainable Gas Institute, 2016). Moreover, CCS would play a big role in emerging economies as well, such as China and India. In this sense, a bibliometric analysis can easily demonstrate the significant research push that CCS has received during the last decade, since the amount of yearly published contributions (including those entailing carbon capture utilisation and storage, i.e. CCUS) has become significant, and comparable with the number of scientific articles on other decarbonisation approaches (Figure 1.4). These bibliometric results have been confirmed also by Li et al. (2019a). To limit CO_2 concentration to 450 ppm by 2050, CCS must play a significant role in the decarbonisation of carbon intensive sectors. According to WBGU (2011), on a 9 scenarios average, CCS accounts from 7% to 27% contribution in terms of reduction of CO_2 emissions before 2050. In the International Energy Agency (IEA) 450 Scenario (i.e., the scenario aiming at keeping CO_2 concentration in the atmosphere below 450 ppm), a total of 52 Gt of CO_2 between 2015 and 2040 should be captured by CCS technologies from both the industry and the power generation sectors, of which 5.1 Gt in 2040 (IEA, 2015). Furthermore, by comparing the costs of different scenarios designed to limit the temperature increase to +2°C, no-CCS scenarios (i.e., those scenarios in which CCS is not present in the portfolio of technology employed to fight climate change) usually have a higher cost compared to CCS ones. In fact, no-CCS scenarios are expected to entail a +138% additional cost (with values ranging between +29% and +297%) in the period 2015-2100 compared to scenarios utilising CCS (Edenhofer et al., 2014). Higher investments are required by no-CCS scenarios due to the necessity of deploying the available low carbon technologies in all the most crucial areas (e.g., power generation, transport, industries), within a short time framework. For instance, several no-CCS scenarios suggest a fast electrification of the transport sector and a high level of energy efficiency by 2050, which are required to compensate emissions from heavy industry and power generation (WBGU, 2011). Furthermore, only 40% of no-CCS scenarios are able to comply with the +2°C threshold of temperature increase (Global CCS Institute, 2017), be-

cause of the huge challenges imposed by the absence of CCS. Conversely, CCS can be utilised in the short term (i.e., before 2050) to limit the emission of CO_2 from carbon intensive facilities (7%-27% depending on the scenario). Whereas, in the long term (i.e., before 2100), bio-energy powered CCS (BECCS) could be further employed to attain negative emissions of CO_2, which are required to further limit the temperature increase to +1.5°C (Global CCS Institute, 2017; IPCC, 2018).
Particularly considering the European framework, which strongly depends on fossil fuels from other regions and countries, the implementation of CCS would allow other technological alternatives a longer time to enter the market. At the same time, CCS is one of the few technologies completely avoiding the direct emission of CO_2 in the atmosphere. Cuéllar-Franca and Azapagic (2015) extensively reviewed life cycle analysis (LCA) studies on CCS and found that the global warming potential of fossil fuel-based power plants can be decreased by 63-82% by implementing CCS. More recently, Gibon et al. (2017) assessed a consistent set of life cycle inventories for different energy technologies deployed in several regions; it emerged that CCS allows reducing significantly the GHGs emissions of fossil-based technologies, at the cost of increasing other resources use depending on the specific projects. Similarly, Thomas et al. (2017) conducted a LCA, which demonstrated that the implementation of CCS would produce a decrease in the impact of GHGs over human health, against an increase of the ecological impacts, and suggested to address this issue by combining CCS with bioenergy. Farquharson et al. (2017) compared coal- and gas-fed power plants in terms of GHGs mitigation potential through a tailored model: once again the study demonstrated the environmental benefits of including CCS technologies for both types of power plants. The IEA, too, stated that much more attention to CCS (along with other low-carbon alternatives) would be required to meet climate goals (IEA, 2018). Overall, CCS is employed to dispose the CO_2 emitted by the operation of carbon intensive facilities into appropriate geological basins (CCS), in opposition to the possibility of converting it into useful products (CCU), or exploiting a combination of both sequestration and utilisation (CCUS).

1.3 Carbon capture and storage networks

1.3.1 Capture, transport, and sequestration

The idea behind CCS is to avoid the emission into the atmosphere of those CO_2 quantities generated from stationary sources by capturing CO_2 flowrates and sequestering them underground into deep geological formations. Almost 7500 large stationary CO_2 emission sources (i.e., above 10^5 t of CO_2/year) can be identified in the world, mainly in three areas: fuel combustion activities, industrial processes and natural gas processing. Among them, over 2000 coal-fed plants are accounted, followed by 1700 natural gas-fed facilities, 1200 cement industries, and others (IPCC, 2005). Considering the European framework, the great majority of single-point

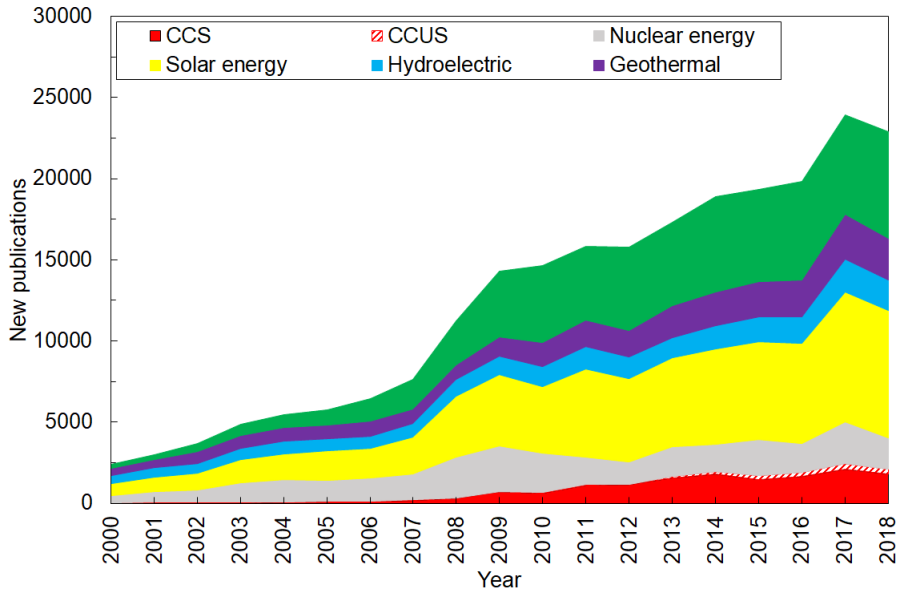

Fig. 1.4: Bibliometric analysis on scientific contributions for different decarbonisation options (source: Scopus). Sought keywords: 'CCS' or 'carbon capture' and ('storage' or 'sequestration'), 'CCUS' or 'CCU' or ('carbon capture' and 'utilisation'), 'nuclear energy' or 'nuclear power', 'solar energy', 'hydroelectric', 'geothermal', 'wind energy' or 'wind power'.

emission sources is constituted by coal- and gas-based power plants. These can be further divided into three categories according to the entity of the emission: large sources (i.e., producing more than 10^5 t of CO_2/year), very large sources (i.e., producing more than 10^6 t of CO_2/year), and extremely large sources (i.e., producing more than 10^7 t of CO_2/year). In particular, large sources currently represent 42% of the European global CO_2 stationary emissions, while very large sources, although accounting for half of the facilities with respect to large sources, still emit 37% of the European global CO_2 from stationary generation. In fact, only a few extremely large sources can be accounted in Europe (JRC, 2016) and as regard refineries, only two highly emitting facilities are both identified just outside European borders, characterised by a carbon footprint of about 10^5 t of CO_2/year and located in Algers (Algeria) and Alexandria (Egypt) (JRC, 2016). On the contrary, considering emission clusters rather than single point-source facilities (which leads to the enumeration of less intensive, but more diffused CO_2 generation points), industry (and particularly, cement industry) plays a role as well in the accounting of overall CO_2 generation in Europe. Nevertheless, as it will be described in Chapter 2, considering the major contribution of power plants in terms of overall CO_2 emissions and the need to reduce the computational burden of a large-scale European optimisation framework, both industry and refineries will be here considered not relevant given their scarse level of pointly emission.

The typical CCS scheme is composed of three echelons: capture, transport and sequestration (IPCC, 2005) (Figure 1.5). The capture echelon consists in separating

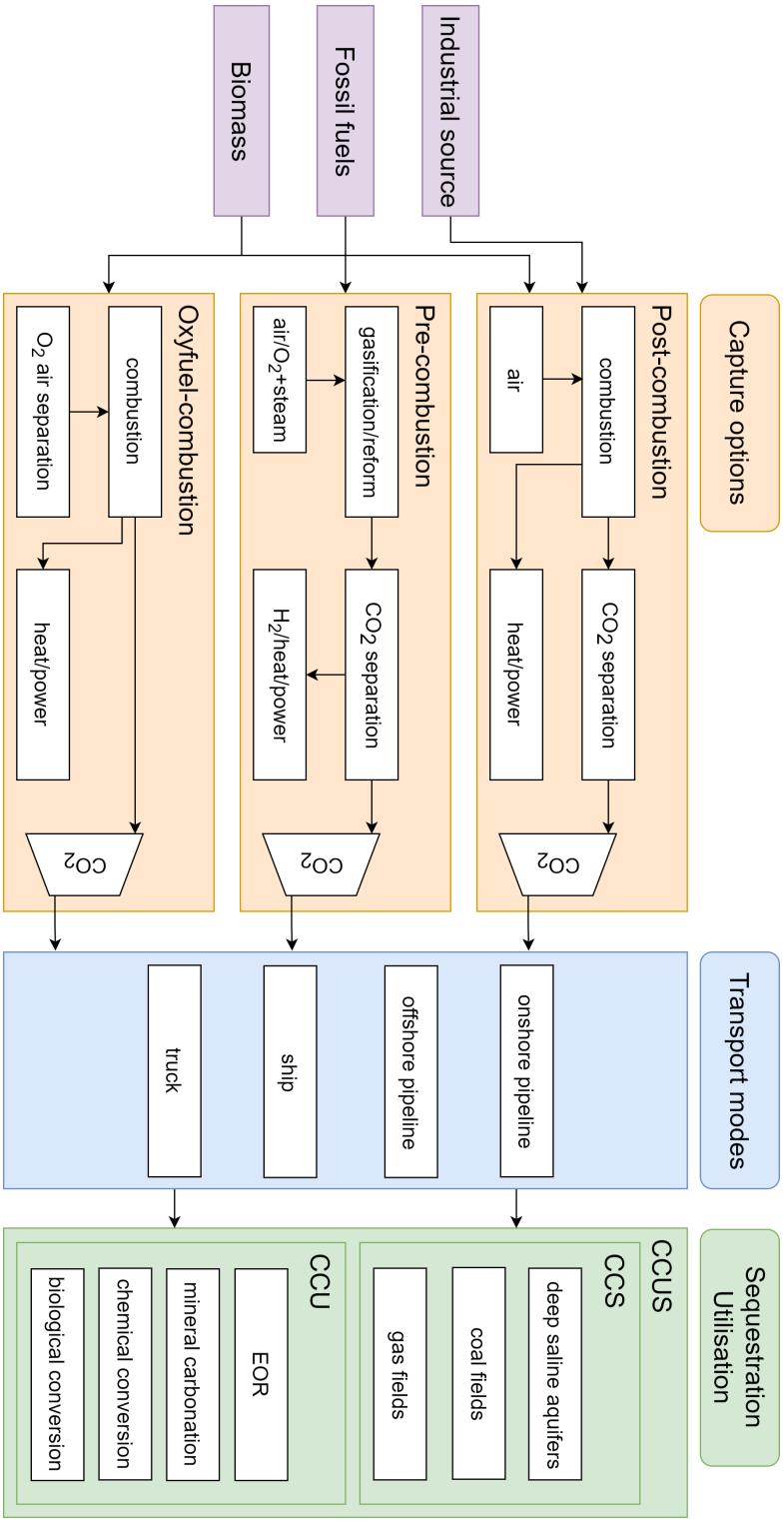

Fig. 1.5: General scheme of the CCS, CCU, and CCUS echelons and technological options.

CO_2 from the other gasses of a process stream: streams with high concentration of CO_2 such as those flowing out of a furnace or turbine in a fossil fuel-fed power plant are preferred because of higher efficiency and lower cost of the capture process (IPCC, 2005). Three main technologies are available for capturing CO_2 from use of fossil fuels: post-combustion capture, oxy-fuel combustion capture, and pre-combustion capture:

- *Post-combustion capture* is based on separating CO_2 from the flue gases produced by the combustion of a fossil fuel or biomass. Further, it can be advantageously retrofitted on already existing plants. By doing so, instead of being released to the athmosphere, the exhaust gas is sent to a separation technology which utilises either absorption systems or membranes. Accordingly, a highly pure CO_2 stream is produced as output (Bui et al., 2018; Mukherjee et al., 2019).

- *Oxy-fuel combustion capture* relies on an air separation process, which is needed to obtain a nearly pure oxygen combustion, to which follows the production of a CO_2-rich flue gas. In this case, oxygen can be traditionally produced through rather efficient but expensive and energy intensive cryogenic air separation units, with the advantage of obtaining a highly pure CO_2 stream as a result of the combustion (Bui et al., 2018).

- *Pre-combustion capture* can be applied to combustion processes involving the utilisation of coal, natural gas, or biomass as input. In particular, this technology relies on the production of an hydrogen rich syngas. Despite the noteworthy investment for the production of syngas, the pros of pre-combustion with respect to post-combustion option is constituted by a higher CO_2 concentration in the output stream, which determines the need for a smaller and cheaper separation stage (Bui et al., 2018).

The concentrated CO_2 flow is then purified and compressed to be cost-effectively transported. The second echelon of the CCS supply chain (SC) is the transportation of CO_2 towards underground stable geological formations. In particular, CO_2 can be transported in three states: compressed gas, liquid, and solid. Although commercial scale transport may include tanks (only suitable for low-scale transport), pipelines (either onshore or offshore), and ships (typically suitable for transporting small quantities of CO_2 for long offshore distances), pipelines constitute the best option when large flowrates need to be transported for long distances in an efficient and cost-effective way (IPCC, 2005). Finally, the third step is the injection of CO_2 below the Earth surface and its consequent sequestration. The most interesting sequestration basins for carbon storage are deep saline aquifers, hydrocarbon fields, and coal fields (Leung et al., 2014), which must then be selected, screened and ranked in terms of storage capabilities. All the aforementioned echelons of the CCS SC (i.e., capture, transport, and sequestration options) will be analised and

discussed in techno-economic terms in Chapter 2, in order to point out the main assumptions and simplifications on which this work relies.

1.3.2 Capture, transport, and utilisation

As an alternative to geological sequestration into appropriate basins, the CO_2 could be diverted into use for other processes (Figure 1.5). Regarding utilisation pathways, different options (Figure 1.6) have been highlighted as promising to attain a reduction of costs of CCS through either CCU or CCUS, and have been gathered into the groups of mineral carbonation, chemical conversion, and biological utilisation:

- *Mineral carbonation* can be employed to produce construction materials, which may represent an appealing option when considering that solid carbonates are already in use in construction material markets, that the chemistry for producing carbonates (based on calcium and magnesium) is well known, and that carbonation is a set of processes that may consume large flowrates of CO_2 by binding it into solid and stable materials (National Accademy of Sciences, 2019).

- *Chemical conversion* routes can be carried out to produce commodity chemicals and fuels (Alper et al., 2017; Bassani et al., 2019), even though some studies questioned the actual effectiveness of this pathway and indicated that only minor environmental benefits could be obtained (Mac Dowell et al., 2017).

- *Biological utilisation* consists in exploiting the natural ability of microorganisms (e.g., microalgae, cyanobacteria) to capture and convert CO_2 through photosynthetic mechanisms, even though major research issues are still open and need to be tackled, such as scalability and costs (National Accademy of Sciences, 2019).

These processes and conversion technologies are generally highly energy intensive and ideally require renewable energy sources to achieve a negative carbon footprint. As a consequence, a comprehensive analysis of the complete value chain is needed in order to provide a sustainable implementation (Jarvis and Samsatli, 2018). Furthermore, despite recognising that carbon utilisation technologies may play an important role in the circular economy of future carbon management, nowadays the commercialisation of routes for CO_2 utilisation are mainly limited to few applications, such as enhanced oil recovery (EOR), where CO_2 is used to increase the efficiency of oil extraction in almost exhausted wells (Mac Dowell et al., 2017). In any case, the aforementioned pathways are currently studied with huge research effort, in order to convert part of the captured CO_2 into valuable products (e.g., construction materials, chemicals, fuels) (National Accademy of Sciences, 2019). These technologies belong to the CCU and CCUS frameworks (Jarvis and Samsatli, 2018). However, in this Thesis CO_2 conversion and utilisation will not be considered as a major and

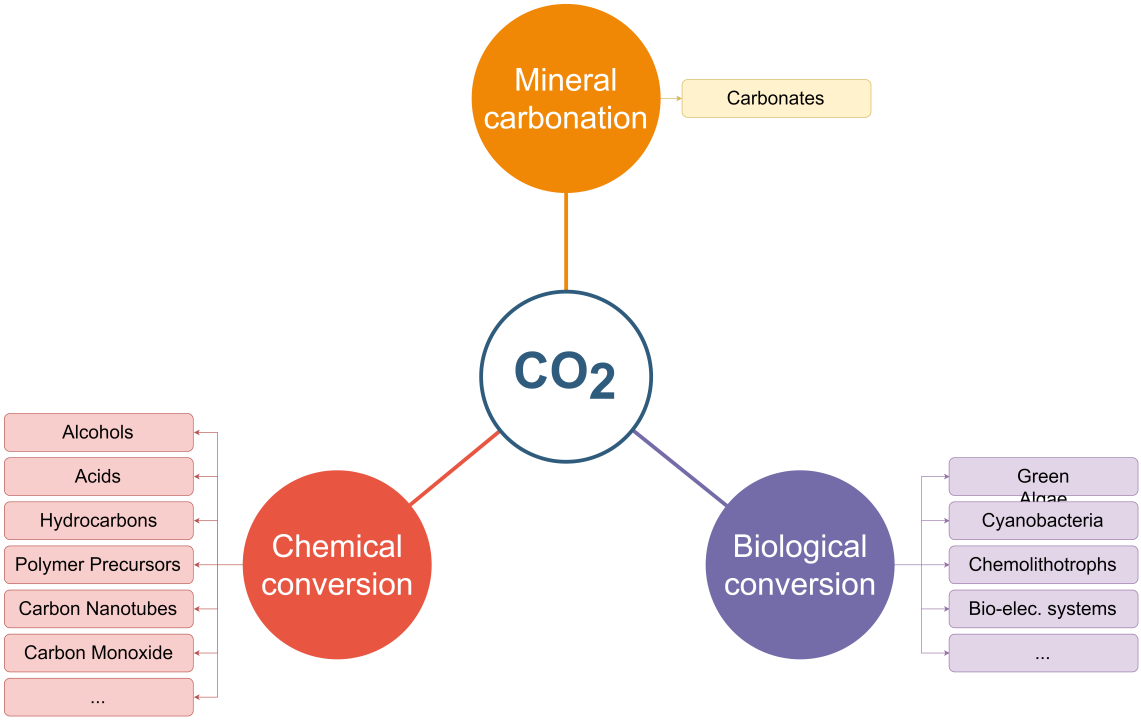

Fig. 1.6: Possible carbon conversion and utilisation pathways (adapted from: National Accademy of Sciences, 2019).

alternative option to geological storage, given its scarce maturity in terms of technologies, applications and high costs. Accordingly, this work will mainly analyse only the mere CCS scheme, i.e. that one contemplating only the possibility of CO_2 storage in geological basins. Utilisation pathways for the optimisation of a comprehensive CCUS framework will be assessed as a preliminary work; the focus will be put on the conversion of CO_2 for the production of high-added value chemicals (see Chapter 7).

1.4 Modelling carbon capture and storage

1.4.1 The need for a system perspective

As stated above, diminishing the anthropogenic generation of GHGs features as one of the key challenges of the twenty-first century and at the same time it is very unlikely that emissions may be reduced without relying on CCS and CCUS, especially when considering a framework in which climate change is addressed by only using known technologies (IPCC, 2018). A few years ago, Pacala and Socolow (2004) proposed the 'wedges model', subsequently revised by Davis et al. (2013), that was based on a business-as-usual starting scenario, and predicted a doubling of CO_2 emissions by 2056 if no action had been taken. Each wedge represented the potential ramping up of a CO_2 abatement technology, possibly resulting in a total worldwide reduction of 175 Gt between 2006 and 2056. A drastic reduction of global

CO_2 emissions should rely on two main pillars: technology advancement in terms of higher conversion efficiencies and/or a further push towards the penetration of renewables (Arnette, 2016), and a significant implementation of CCS (Odenberger et al., 2008; Egmond and Hekkert, 2012). Regarding the latter, energy and industry systems could constitute a fertile ground for the potential abatement forecasted by Pacala and Socolow (2004), considering the possible implementation of CCS or CCUS to reduce those emissions.

Focusing on the European context, the EU has recently financed through the European Commission (EC) several projects (EC, 2019) to assess the techno-economic performance of large-scale systems for CO_2 capture (ZEP, 2011), transport (Morbee et al., 2012), and storage (EU GeoCapacity Project, 2009; Poulsen et al., 2014). Furthermore, the feasibility of implementing a European CCS infrastructure has been investigated through a number of demonstration plants in different countries (CCS Network, 2015; IEA, 2015). Thus, having recognised the importance of CCS for the European framework, the EC has also allocated different research funds (e.g., Horizon 2020, NER 300, LIFE climate action) for the development of techniques allowing a reduction of GHGs and a determination of the techno-economic aspects in the different echelons of the CCS SC (Global CCS Institute, 2017; EC, 2019). This research effort and further academic projects laid the foundations for several studies proposed along the years, which have later provided a deep increase in the techno-economic knowledge of each single stage of the SC. Besides, the necessity of investigating the design, cost and integration of the CCS stages for different geographic contexts and applicative frameworks has emerged, in order to reduce the overall investment, to share local risks and foster the effectiveness of the implementation from a large-scale perspective (Bui et al., 2018). Overall, a huge research effort has been channelled into each single SC stage rather than into the assessment and optimisation of CCS from a systemic standpoint. Obviously, this situation has reflected on the published literature on both CCS and CCUS, since those keywords and acronyms typical of the process systems engineering fields (e.g., mathematical programming, planning, optimisation) are only found in relatively few contributions (Figure 1.7).

In fact, when dealing with the strategic design and planning of a European CCS infrastructure, it clearly emerges the necessity of employing quantitative mathematical tools, such as mathematical programming, to treat the combinatorial complexity of these large-scale and multi-echelon networks, e.g. considering the numerical vastness of locations for the possible capture technologies, the huge amount of feasible transport routes, or the abundancy and spatial distribution of geological sequestration basins. Even though simplified approaches for an early design of the system (e.g., to match the major CO_2 sources with nearby carbon sinks) might represent an economically satisfactory solution, the global result could really turn out far from optimality, especially considering the scale of a continent-wide network. To tackle these issues, mathematical programming models are typically employed in a wide variety of fields

and applications as fundamental tools for the design, planning, and optimisation of large-scale networks. Moreover, the process systems engineering community has extensively employed these methodologies to address different and complex combinatorial optimisation problems (Stephanopoulos and Reklaitis, 2011). Previous studies analysed the problem of designing large-scale infrastructures and networks by determining their optimal size, location and planning through techniques for SC optimisation (Beamon, 1998), in particular via mixed integer linear programming (MILP) approaches (Kallrath, 2000). The latter modelling method represents a well-established technique in many industrial fields and scopes of application, and it is commonly employed to solve large combinatorial optimisation problems without excessively increasing the computational burden (Heuberger et al., 2018). Indeed, to reduce the computational effort and solution complexity, MILP models are the most practical and most commonly adopted option when tackling large-scale instances (Mula et al., 2010). For instance, Calderon and Papageorgiou (2018) recently analysed the key aspects of the strategic planning of a natural gas SC through a MILP mathematical framework. Analogously, Moreno-Benito et al. (2017) proposed an optimal and sustainable hydrogen infrastructure for the United Kingdom through a MILP model. As regards the modelling of CCS and CCUS networks (Table 1.1), the first application of mathematical programming to a proper SC optimisation framework can be retrieved in a study on EOR by Turk et al. (1987). Since then, several contributions have been proposed for the optimisation of either CCS or CCUS systems (Tapia et al., 2018; Li et al., 2019a).
The following subsections will analyse and discuss the scientific literature on CCS and CCUS SCs in terms of: geographic scales and contexts, sources of uncertainty incorporated within the modelling frameworks, safety issues and risk of hazards, public acceptance and risk perception, cooperation policies and hedging strategies, conversion and utilisation pathways.

1.4.2 Geographic scales and contexts

When dealing with the design and optimisation of spatially-explicit (i.e., based on the concepts of scale and geographic location as design variables) CCS SCs, many studies have been focused on regional/national frameworks (Table 1.1) (Figure 1.8), mostly in terms of economic optimisation (e.g., Bakken and von Velken, 2008; Strachan et al., 2011; Middleton et al., 2012a; 2012b; Elahi et al., 2014; Kalyanarengan Ravi et al., 2016), in some cases including CO_2 utilisation for process integration, too (e.g., Turk et al., 1987; Klokk et al., 2010; Han and Lee, 2012; Hasan et al., 2015; Wu et al., 2015; Lee et al., 2019; Leonzio et al., 2019; Kim et al., 2019), or assessing some environmental- or risk-related aspects (e.g., Han and Lee, 2013). For instance, Bakken and Velken (2008) proposed a linear model for Norway aiming at power systems infrastructure economic optimisation including CCS, while transport routing was not specifically considered as part of an optimisation model

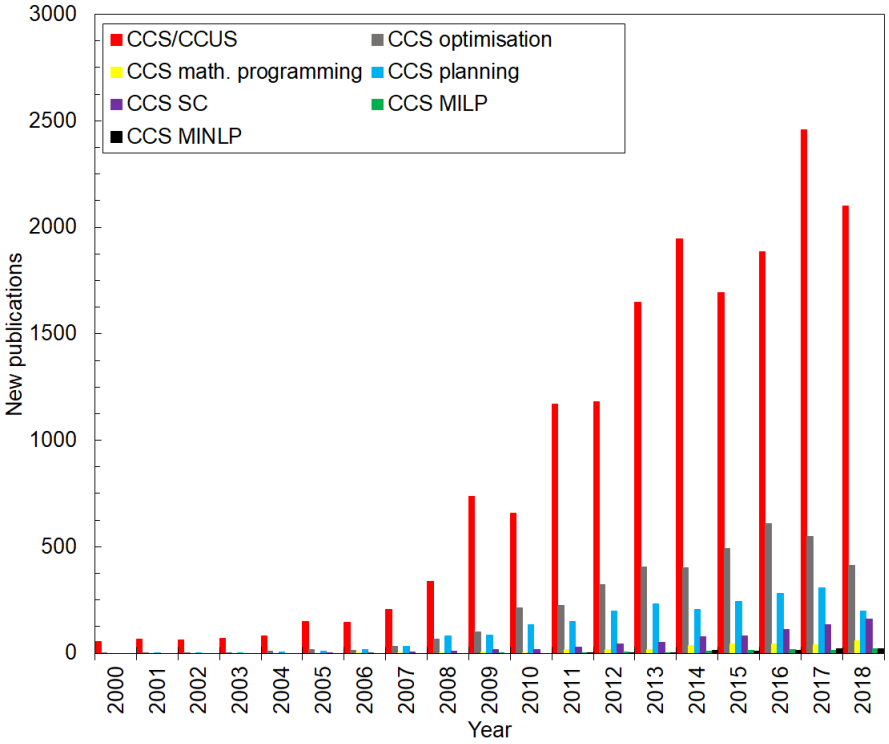

Fig. 1.7: Bibliometric analysis on scientific contributions on CCS and CCUS, focusing on keywords and acronyms that are typical of the process systems engineering fields (source: Scopus). Sought keywords: 'CCS' or 'CCUS' and: 'optimisation' or 'mathematical programming', or 'planning', or 'SC' (or 'supply chain'), or 'MILP', or 'MINLP'.

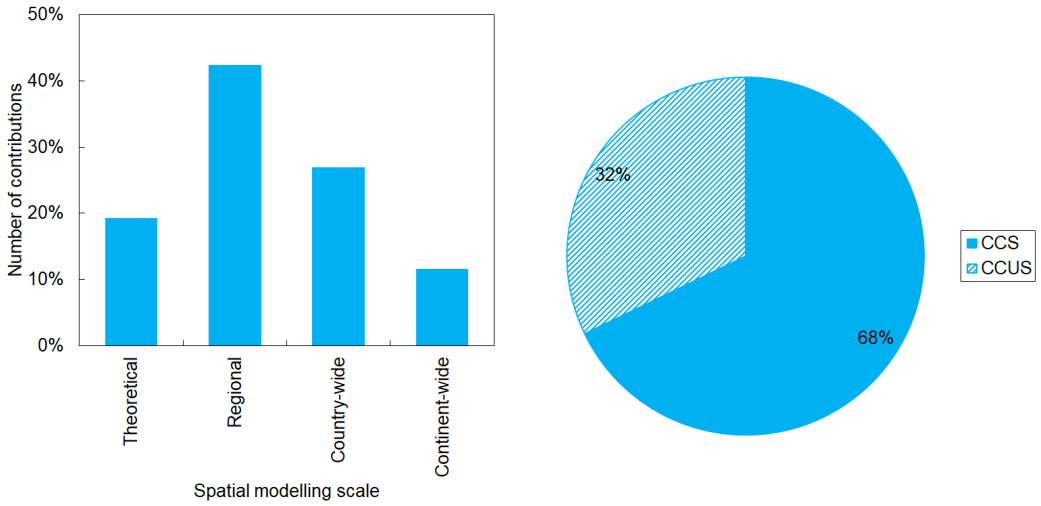

(a) *(b)*

Fig. 1.8: Results from the literature review in terms of: (a) percentage of contributions at different spatial modelling scales (the Unites States are inserted within the category 'continent'), and (b) percentage of contributions on either CCS or CCUS.

Tab. 1.1: Literature review on currently published contributions on optimisation tools for CCS/CCUS.

Authors, year	CC(U)S	MI(N)LP	Utilisation	Scale (Area)	Uncertainty
Turk et al., 1987	CCUS	MILP	EOR	Region (Ohio, United States)	-
Bakken and von Velken, 2008	CCS	LP	-	Region (central Norway)	-
Odenberger and Johnsson, 2010	CCS	-	-	Continent (Europe)	Scenario analysis
Klokk et al., 2010	CCUS	MILP	EOR	Country (Norway)	-
Strachan et al., 2011	CCS	LP	-	Region (North Sea)	-
Han and Lee, 2012	CCS	MILP	-	Region (Pohang, South Korea)	Prices, costs
Middleton et al., 2012a	CCS	MILP	-	Region (Texas, United States)	Storage physics
Middleton et al., 2012b	CCS	MILP	-	Region (Texas, United States)	-
Morbee et al., 2012	CCS	MILP	-	Continent (Europe)	-
Han and Lee, 2013	CCUS	MILP	Biobutanol, polymers	Region (Pohang, South Korea)	Prices, costs
Akgul et al., 2014	BECCS	MINLP	-	Country (United Kingdom)	-
Elahi et al., 2014	CCS	MILP	-	Country (United Kingdom)	-
Petvipusit et al., 2014	CCS	other	-	Region (theoretical)	Storage physics
Hasan et al., 2015	CCUS	MILP	EOR	Country (United States)	-
Wu et al., 2015	CCUS	MILP	EOR	Region (theoretical)	Inexact parameters
Kalyanarengan Ravi et al., 2016	CCS	MILP	-	Country (the Netherlands)	-
Elahi et al., 2017	CCS	MILP	-	Country (United Kingdom)	Carbon prices
Jin et al., 2017	CCS	LP	-	Region (Bazhou, China)	Inexact parameters
Lee et al., 2017	CCS	MILP	-	Region (Pohang, South Korea)	Preference on risk
Nie et al., 2017	CCS	MILP	-	Country (United Kingdom)	Market, subsidies
Noureldin et al., 2017	CCS	other	-	Region (theoretical)	Storage physics
Ağrali et al., 2018	CCUS	MILP	EOR	Country (Turkey)	-
Jeong et al., 2018	CCS	MIP	-	Region (theoretical)	Storage physics
Middleton and Yaw, 2018	CCS	MILP	-	Region (Alberta, Canada)	Storage physics
Zhang et al., 2018a; 2018b	CCS	MILP	-	Region (theoretical)	Storage physics, costs
Lee et al., 2019	CCUS	MILP	Biobutanol, polymers	Region (Pohang, South Korea)	Preference on risk
Leonzio et al., 2019	CCUS	MILP	Methanol	Country (Germany)	-
Kim et al., 2019	CCUS	MILP	Hydrogen	Country (South Korea)	-

in the work by Odenberger and Johnsson (2010) that investigated the quantitative potential of CCS as share of a portfolio for diminishing European CO_2 emissions. Elahi et al. (2014) described a multi-period MILP optimisation aiming at cost minimisation of an integrated CO_2 infrastructure in the United Kingdom. Akgul et al. (2014) optimised a biomass-based SC including CCS (BECCS) again for the United Kingdom, through a spatially-explicit, static, multi-objective, mixed integer nonlinear programming (MINLP) model. Similar CCS economic optimisation approaches have been investigated for different geographic contexts by Klokk et al. (2010) once again for Norway, by Strachan et al. (2011) for the North Sea regions, by Middleton et al. (2012a; 2012b) for Texas, and by Kalyanarengan Ravi et al. (2016) for the Netherlands. Han and Lee (2012) proposed a stochastic multi-period model for CO_2 capture, transport, and utilisation on the eastern coast of Korea that was subsequently updated in Han and Lee (2013) by including techno-economic-, environmental- and risk-related aspects. Wu et al. (2015) provided an optimisation model for CCUS under uncertainty, although the spatial representation was only simplified into four theoretical regions for either CO_2 storage or utilisation. Other studies focussed specifically on the CO_2 logistics, i.e. the transport infrastructure, rather than investigating the whole CCS network either through assessment-based approaches (e.g., Chen et al., 2010; Jensen et al., 2013; Zheng et al., 2010) or through optimisation algorithms, likewise Morbee et al. (2012) optimised a European infrastructure for CO_2 transport by implementing methodological innovations in the solution algorithm in order to reduce the number of nodes and, consequently, the problem size.

All the aforementioned studies provided a deep increase in the knowledge of complex and comprehensive CCS or CCUS systems through tailored modelling, simulation, and optimisation techniques, but their major limitation has been mainly related to the local or at most regional geographic scale investigated (Figure 1.8a). A more thorough SC optimisation (both in terms of spatial resolution and technical detail) was proposed by Hasan et al. (2015) through a multi-echelon model for the entire United States area. The work by Hasan et al. (2015) included the CO_2 utilisation for EOR and the simultaneous selection of materials and capture technologies, but onshore pipelines were considered as the unique possible transport mean. To our knowledge, that proposed by Hasan et al. (2015) is the only comprehensive SC model developed for CCS or CCUS on a geographic vast level. As a consequence, no information can be retrieved in the scientific literature regarding the assessment and optimisation of a CCS SC for the European context which is conversely among the areas in the world where major research effort is put on CCS.

1.4.3 Effects of uncertainties

In the wake of the recent advances in process systems optimisation under uncertainty (Goel and Grossmann, 2004; Grossmann et al., 2016; Yue and You, 2016),

some MILP models have been proposed for serving the same purpose when applied to CCS networks. As a matter of fact, researchers and institutions have analysed the ways of reducing the effects of uncertainties on CCS networks typically through either stochastic/probabilistic (e.g., Han and Lee, 2013; Wu et al., 2015; Jin et al., 2017; Nie et al., 2017; Jeong et al., 2018; Zhang et al., 2018a; 2018b; Lee et al., 2019) or robust (e.g., Petvipusit et al., 2014) techniques; in particular, different methodologies have been proposed, e.g. multiple scenario realisation (Han and Lee, 2012; Nie et al., 2017), or inexact optimisation (Han and Lee, 2013; Wu et al., 2015). Previous research investigated a broad variety of uncertain parameters, typically related to economics (Han and Lee, 2013; Wu et al., 2015; Jin et al., 2017; Noureldin et al., 2017), storage injectivity (Petvipusit et al., 2014; Aminu et al., 2017; Nie et al., 2017; Noureldin et al., 2017; Jeong et al., 2018; Zhang et al., 2018a; 2018b), storage leakage (Aminu et al., 2017; Alcalde et al., 2018; García and Torvanger, 2019) and policy (Jin et al., 2017). In general, these studies addressed the design and optimisation of CCS and CCUS SCs under uncertainties that were commonly related to external factors (e.g., prices, market scenarios) and more rarely addressed the inherent uncertainties within the system (e.g., storage potential) (Table 1.1). Furthermore, comparatively little attention was paid to storage-related uncertainties such as geological capacities, rather than technical aspects such as injectivity or leakage, considering that geological storage capacities are not usually known to a sufficient degree of accuracy before operation (Selosse and Ricci, 2017). For example, geological data on deep saline aquifers, known for having significant storage potential but limited operational experience, would constitute a high-level source of uncertainty for a correct assessment of CCS (Szulczewski et al., 2012). Other basin typologies have been described only vaguely in terms of effective capacity (EU GeoCapacity Project, 2009). In contrast, for geological structures such as hydrocarbon fields, there are abundant sources of information, that were gathered from operational data during periods of hydrocarbon extraction. Therefore, as geological uncertainties may significantly impact overall sequestration costs, a more flexible pipeline network could be necessary rather than that designed using notional values of storage capacities, in order to exploit those basins that are more likely to sustain the captured flowrates (Anderson, 2017; Zhang and Huisingh, 2017; Middleton and Yaw, 2018).

None of the previous studies has focused on the quantification of risk that may emerge as a consequence of uncertainty in the actual geological volume that is available for CO_2 sequestration in the large-scale European context. For instance, Bachu (2003) proposed a set of 15 criteria to assess basins in terms of suitability for storage in the small scale context of Alberta (Canada), but the comprehensive effects on the design of a CCS infrastructure was not addressed. Middleton and Yaw (2018) showed the effects of geologic uncertainty for a single basin (in terms of capacity and injectivity) on the optimal routing of a pipeline network for the case of a shale oil industry, by addressing the physics of bulk permeability, porosity, and thickness

of a reservoir. Jeong et al. (2018) optimised a cost-effective monitoring network under uncertainty concerning brine formation and leakage in storage, but the effect of geological capacity was not considered. Clearly these approaches, despite being appropriate for the correct determination of each single geological carbon sink, would inevitably lead to an intractable optimisation problem when applied to a continent-wide CCS network. In fact, the scientific literature lacks of a general methodology that could permit optimising a noteworthy CCS system under uncertainty in sequestration volumes, rather than investigating each single CO_2 sink from a geological perspective by aim of computationally expensive (even though tailored) mathematical techniques. Accordingly, the necessity of dealing with geological uncertainties in the planning and design of the infrastructure in terms of both capacity and potential leakage must be highlighted as a primary action to improve the economic feasibility and to manage the risk of large-scale CCS infrastructures (Aminu et al., 2017; Noureldin et al., 2017; Alcalde et al., 2018).

1.4.4 Safety issues, risk of hazards

Another key issue that has not been explicitly taken into account when optimising CCS networks is their social sustainability (Karimi and Toikka, 2018) (Table 1.1). Although having been practiced for over 30 years, CCS is nowadays still raising public concern (Perdan et al., 2017), especially when the possibility of leakage is taken into consideration in proximity of densely populated areas (Gough et al., 2014). In fact, even though CO_2 is a non-toxic and non-flammable gas, it has a higher density than air and could locally accumulate up to a dangerous concentration. As a matter of fact, both opinion leaders' (Liang et al., 2011) and public (Chen et al., 2015) perceptions have been highlighted as a key challenge for a wide scale CCS deployment, especially when safety considerations are taken into account. Pipelines corrosion and external sources may affect the transport safety (Barker et al., 2016) and, when transported for long distances through densely populated regions, CO_2 might expose to risk a number of people significantly greater than the number of those exposed to risk from either capture or storage sites (IPCC, 2005; Aminu et al., 2017). In view of the above, the implementation of a CCS network cannot be disjointed from a proper optimisation-driven analysis aiming at risk minimisation, and from the implementation of effective risk mitigation measures at early SC design stage (Onyebuchi et al., 2017). Similarly to what is commonly proposed for gas pipelines (e.g., An and Peng, 2016), some works dealt with risk-constrained CO_2 SC optimisation, but just a few were focused on the hazards related to pipeline transport systems and on the quantification and prevention of their potential loss. Han and Lee (2013) proposed a fuzzy optimisation for the simultaneous techno-economic, environmental and technical risk assessment of a CCS SC in South Korea, in which risk related to transport modes was treated in terms of cost and total technical loss. Khan and Tee (2016) described a general mathematical framework for risk-cost optimisation

of underground pipelines networks, where both pipeline corrosion and other failure modes were taken into account so as to define the life-cycle costs and to propose a maintenance strategy. Knoope et al. (2014) addressed risk for the appropriate design and routing of a CO_2 pipeline, including Geographic Information System (GIS) features and considering different measures of risk mitigation. In particular, as regard risk mitigation options, several contributions were specifically focused either on the optimal positioning of safety valves (e.g., Medina et al., 2012; Rusin and Stolecka, 2015; Witkowski et al., 2015), and on the selection of suitable transportation paths as methods of risk reduction (Vianello et al., 2016). In contrast, other contributions were focused on the risk analysis and assessment of environmental and toxicological impacts related to accidental releases of CO_2 from pipelines. For instance, Koornneef et al. (2008) identified and described the environmental consequences associated with CCS, whereas Hillebrand et al. (2013) proposed a broad toxicological risk assessment on all the main components of CCS-related processes. Furthermore, Lisbona et al. (2014) predicted the dispersion of CO_2 releases from pipelines using a three-dimensional computational fluid dynamic model, while Joshi et al. (2016) also experimentally validated the transient jet release from a pipeline transporting CO_2. On the whole, very little work has been carried out to formally integrate social sustainability within the design and optimisation of plants and infrastructures and with concern to CCS, no study has been presented concerning the design of large-scale SCs and simultaneously including societal risk in the economic optimisation.

1.4.5 Public acceptance, risk perception

Understanding societal risk related to CCS infrastructures is a key driver for fostering their social acceptance. In fact, notwithstanding the undeniable benefits of having CCS in the portfolio of technologies to fight climate change, many criticisms have been raised on their technical viability, efficacy and safety. Apart from concerns on the utilisation and operation of CCS, the problem of social acceptance and public support has been highlighted as of fundamental importance in the process of fostering a large-scale deployment (Ashworth et al., 2015; Global CCS Institute, 2017; Upham et al., 2015). For instance, people might be concerned about the safety issues in terms of risk of hazards deriving from CCS operation thus, the possibility of CO_2 leakage endangering both communities, commodities, and environment in the vicinity of an infrastructure (Yang et al., 2016). In particular, risk perception is intended as a measure of how much worry or concern is perceived by the public as a consequence of the construction and operation of a CCS infrastructure. As a matter of fact, Schumann (2017) assessed the public perception of CO_2 pipelines construction by the general public in Germany, based also on risk perception. This contribution highlighted that citizens' perception is of fundamental importance in the planning of such infrastructures. Similarly, Ashworth et al. (2019) analysed the

results of a survey to determine the different perception of CCS across Australia and China, demonstrating how strongly the level of knowledge affects the public support towards these technologies. Moreover, being CCS an 'end-of-the-pipe' solution, the public might see it as a 'last resource', to which the utilisation of other low carbon technologies should be preferred (e.g., solar, wind, geothermal) (L'Orange Seigo et al., 2014). Besides, the employment of CCS by fossil fuel industries could be interpreted as a way of prolonging their own existence rather than enabling a genuine energy transition. In view of this, different strategies for a stronger engagement of the public living close to a CCS infrastructure have been recently proposed. For example, by providing information on the environmental benefits of CCS, it is possible to stimulate its social acceptance and potentially avoid protests and opposition (Oltra et al., 2012; Ashworth et al., 2012). However, it would be helpful for investors and policy makers to be able to assess a priori the different levels of opposition of different communities and possibly to design a cost-effective CCS supply chain (SC) maximising social acceptance. Due to a social acceptance lack, different injection projects have undergone strong protests and hostility by the communities settled in their vicinity: a case in point was the commercial project promoted by Shell in Barendrecht (The Netherland) which was cancelled due to the firm public opposition. Similarly, the planning by Vattenfall Group of a storage site in Beeskow (Germany) was cancelled too (Oltra et al., 2012).

Some previous contributions aimed at investigating and tackling through tailored strategies the problem of social acceptance for different energy-related fields. Ervural et al. (2018) developed a multi-objective model for renewable energy planning, including a fuzzy social acceptance factor based on experts' opinion. Accordingly, the acceptance of general public was not explicitly taken into account. Li et al. (2019b) proposed a model for promoting low emission vehicles in China, also including aspects of market acceptance, but again based on data retrieved from a limited sample of experts' opinions. Acar et al. (2019) proposed a comprehensive study for investigating energy storage systems considering economic, environmental, social and technical aspects through a fuzzy-based methodology. However, their methodology did not provide any indications in terms of optimal design and planning from a systems perspective. Regarding the CCS framework, Small et al. (2019) modelled a Bayesian framework for establishing which technological and socioeconomic factors could more likely affect the implementation of CCS. Their methodology, again based on experts' judgement, was only aimed at determining the key drivers for acceptance, but did not provide any indications on how to implement such aspects within a comprehensive framework, e.g. SC optimisation. Arning et al. (2019) compared CCS and CCU in terms of public perception and acceptance for the case of Germany. From this study, it emerged that CO_2 disposal and utilisation may help decreasing the risk perception of transport and storage infrastructures. Nevertheless, their study was based on a survey that did not take into account individual sociocultural factors and public attitudes. Summing up, despite the existence in

the literature of quantitative methodologies for the determination of social acceptance related to the installation and deployment of energy systems (less frequently, focussing on CCS or CCU), the possibility to employ the attitude of generic public explicitly as a decision variable for the optimal design of a large-scale infrastructure, was never taken into account.

1.4.6 Hedging risk and responsibilities

Along with concerns related to societal risk and social acceptance, a viable commercialisation of either CCS or CCUS is still far from becoming a reality. Considering the wide-scale of CCS and CCUS systems, some contributions highlighted how cooperation-related aspects (e.g., international collaboration between academics and industry, knowledge transfer, communication, and costs share mechanisms) might represent key issues to be addressed in order to foster a both timely and effective implementation (Table 1.2).
On the one hand, several studies have shown the necessity of enhancing socio-communicative cooperation between researchers on CCS and CCUS systems. Karimi and Khalilpour (2015) proposed a bibliometric analysis based on historical publication trends to assess the level of international collaboration on CCS among researchers from different countries. Gastine et al. (2017) described a methodology for knowledge share in site operation in the context of an integrated, multi-stakeholder platform for a variety of onshore CCS pilot projects. Czernichowski-Lauriol et al. (2018) stressed the need for intensifying the level of scientific advice and technological communication between CCS players through information activities within the framework of the CO_2GeoNet European project.
On the other hand, the necessity of retrieving alternative financial mechanisms based on economic cooperation for relieving single operators (whether these are companies or governments) from too high risks and responsibilities has emerged as a key requirement for balancing the spread of costs that would characterise a European CCS infrastructure (Bui et al., 2018). This problem has been addressed in the past to comprehend the effects of cooperation among players of large-scale infrastructures, especially in the context of environmental modelling and economic optimisation of multinational energy systems. Bahn et al. (1998) proposed a LP optimisation tool solved through decomposition techniques which described a multinational European energy system including cooperation schemes among countries (Belgium, Switzerland, Germany, and the Netherlands were included in the study). In that case, the objective was that of achieving both equity in the differential shares of emissions and economic efficiency in terms of emissions abatement costs; in particular, this model entailed the optimisation of uniform taxes or emission permits among countries, as it resulted from the compensation of individual marginal abatement costs and demonstrated that the cooperative approach (i.e., when a multinational group is committed to achieve a certain emissions reduction target) is more efficient than

the case in which each country reaches autonomously its emission reduction target. Subsequently, Unger and Ekvall (2003) demonstrated the benefits derived from increased cross-border cooperation in the case of a European energy system with a larger number of players and a higher degree of accuracy in the definition of the set of technologies with respect to Bahn et al. (1998). Similarly, Petrosjan and Zaccour (2003) optimised a cooperative game for pollution reduction by considering the different possible coalitions among theoretical participants; their model included costs share mechanisms for achieving an optimal and 'desirable' allocation of total costs for reducing emissions. Recently, Galán-Martín et al. (2018) proposed a MILP framework for the optimal decarbonisation of the United States energy mix, by applying cooperation mechanisms and fair compensation schemes among nations. Among the mentioned above works only that one proposed by Galán-Martín et al. (2018) included CCS within the set of technologies considered, although this study was more focused on the description of the overall energy system rather than specifically on CCS. Conversely, a more CCS-targeted work was published by Wang et al. (2018), who analysed the optimal CCS investment timing by aim of either a 'single-mode' and a 'cooperative-mode' decision-making strategy through real options theory and game theory. However, the SC only included two different players (i.e., power producer and CCS operator), so the problem of cooperation among different entities at international scale was left out. Summarising, very few contributions have explicitly addressed the problem of reducing costs by optimising structure, scale, location and technological choices of large-scale, integrated, multi-stakeholder, and cooperative CCS or CCUS networks (Bui et al., 2018). In fact, despite some research has provided information on the planning, installation and operation of either local or international CCS and CCUS SCs (Table 1.1), there is still no contribution having directly addressed the problem of those huge differences such as of costs spread that a multiplicity of regions and stakeholders should tackle when dealing with such multinational networks.

1.4.7 Utilisation pathways

Carbon conversion and utilisation pathways have also been indicated as potential options to reduce those costs that derive from the installation and operation of a more general CCS and utilisation (CCUS) infrastructure. Several studies have considered the technological feasibility of different routes. For instance, Alper and Orhan (2017) recently reviewed the possible chemical conversion options for CO_2 and from their analysis a broad variety of families of both pathways and products attractive for CCUS emerged (e.g., C1-chemicals, catalytic processes, polymers, inorganics, fine chemicals). Sternberg et al. (2017) analysed the CO_2-based production of some C1-chemicals by assessing the potential benefits in terms of lowering global warming and fossil depletion. On the other hand, other studies questioned the actual effectiveness of the chemical conversion of CO_2 and indicated that only minor en-

Tab. 1.2: Cited literature on currently published contributions on optimisation and assessment tools for cooperation, collaboration or compensation schemes in multinational energy systems, possibly including CCS or CCUS among the decarbonisation options.

Authors, year	Topic	CCS	Main subject	Method
Bahn et al,. 1998	Energy systems optimisation	X	Multinational energy system with cooperation for emissions reduction	LP optimisation with decomposition techniques
Petrosjan and Zaccour, 2003	Energy systems optimisation	X	Cooperative game for pollution reduction with possible coalitions	Game theory optimisation
Unger and Ekvall, 2003	Energy systems optimisation	X	Increased cross-border cooperation for large-scale energy system	LP optimisation with scenarios
Karimi and Khalilpour, 2015	Bibliometric analysis	V	Social international collaboration on CCS between researchers	Historical publication trends
Gastine et al., 2017	Site operation	V	Integrated, multi-stakeholder platform for onshore CCS pilot projects	Knowledge share in site operation
Czernichowski-Lauriol et al., 2018	Knowledge transfer and communication	V	Information on communication activities for CO_2GeoNet Europe	Scientific advice
Galán-Martín et al., 2018	Energy systems optimisation	V	Cooperation and compensation for decarbonising the United States energy mix	MILP optimisation
Wang et al., 2018	Investment timing	V	Investment decision-making for single- and cooperation-mode	Real options theory and game theory

vironmental benefits could be obtained (Mac Dowell et al., 2017). Furthermore, considering the framework of modelling, simulation, and optimisation of CO_2 SCs, very few contributions optimised comprehensive CCUS superstructures and, in particular, most of these considered only EOR as unique utilisation pathway (Figure 1.8b).

As summarised in Table 1.1, the first model on CCUS SC optimisation was proposed by Turk et al. (1987) and included the possibility of employing CO_2 for EOR in Ohio (United States). Klokk et al. (2010) adopted the same approach for an infrastructure located in Norway. Hasan et al. (2015) in their US-wise optimisation framework took again into account EOR as the only possible utilisation option. Ağrali et al. (2018) proposed an optimisation model for CCUS located in Turkey where again only EOR was adopted as carbon utilisation sink. An even more limited number of scientific contributions optimised CCUS systems by considering the conversion and utilisation of CO_2 to generate valuable products. For instance, Han and Lee (2013) and Lee et al. (2019) considered the conversion of CO_2 into either biobutanol or green polymers as an alternative to geological storage within a comprehensive CCUS modelling framework. Leonzio et al. (2019) optimised a CCUS SC through a MILP modelling tool that included the possibility to produce methanol as an alternative to geological storage. Finally, Kim et al. (2019) proposed a MILP formulation for the integration of an hydrogen/CCUS SC in the context of South Korea. As a result, the possibility to implement and optimise multiple CO_2 conversion and utilisation options in the design of large-scale CCUS SCs has only marginally been examined in published literature.

1.5 Thesis objectives

The previous Sections have shown the gap in knowledge that characterises the published literature related to the modelling, design and optimisation of CCS or CCUS technologies, particularly in terms of:

- addressing the problem of design and optimisation of a CCS/CCUS SC in the wide context of Europe;
- considering uncertainty and consequent risk in the geological storage capacities, in view of the need of a large-scale implementation;
- including aspects of societal risk and social acceptance from the public, since almost no contributions have tackled yet these issues, not even at local scale;
- assessing financial schemes for cooperation and costs share between the different countries, considering the international and intrinsically heterogeneous nature of the European framework;
- considering different possible utilisation pathways for the design of a more general CCUS scheme.

The aforementioned aspects are major challenges that this Thesis aims at tackling (Figure 1.9). The main objective of this Thesis is to provide a multi-scale CCS SC economic optimisation in the large geographic context of Europe. In fact, to our knowledge a comprehensive CO_2 SC design has never been optimised within the European context, also taking into account several technological options for each design stage (Leung et al., 2014). Differently from Hasan et al. (2015), neither EOR nor other forms of CO_2 utilisation will be considered at the first implementation stage, since EOR does not represent a viable solution for the European context (Geske et al., 2015) and the direct CO_2 exploitation (e.g., through conversion into chemicals) does not represent a large-scale mature technology yet (Smit et al., 2014).

Chapter 2 will propose a spatially-explicit, multi-echelon and time-dependent MILP model aiming at the total cost minimisation of a European CCS SC. All the SC stages will be here included within the economic optimisation of a European CCS system. The significant computational burden will be tackled through a hierarchical strategy specifically designed for a fast solution. Results will demonstrate the good quantitative potential of the European area at capturing large flowrates of CO_2 from stationary emissions (up to 70% of the considered CO_2 sample), while simultaneously minimising the total costs of the entire SC over a 20 years' time horizon.

The second objective will be to propose a novel adaptive methodology for the computation of risk based on uncertainties in local storage capacities and to develop insights into network design for risk mitigation at European scale. Differently from other contributions on CCS optimisation under uncertainty and in order to keep the problem computationally tractable, neither a stochastic nor a robust approach will be chosen here. Instead, a methodology optimising the SC in terms of resiliency on risk will be developed. Along with a single stage MILP model that aims simultaneously at total cost and risk minimisation, a two stage MILP-LP solution method will be presented. The latter will comprise a deterministic MILP sub-model followed by a LP sub-model in order to reduce computational efforts.

Chapter 3 will describe two models which will be capable of defining economically optimal European SCs whilst simultaneously minimising the economic risk generated by uncertainties in local sequestration availability to ensure a robust design. Risk will be innovatively quantified in terms of additional infrastructure costs that may emerge from the rerouting of CO_2 flowrates upon realisation of geological uncertainty. Therefore, monetary consequences will be interpreted as additional investment costs that may need to be incurred to improve the flexibility of a European CCS infrastructure. The objective will be to assess the design of a European CCS infrastructure in terms of optimal selection, planning and positioning of capture, transport and sequestration nodes, so that the overall system may be intrinsically resilient to uncertainty in the availability of geological volumes.

The third objective will be to develop a MILP model for the economic optimisation of a European SC for CCS in which risk analysis is for the first time incorporated within the modelling framework. Given the high-scale of the investigated problem, societal risk will be utilised to estimate the measure of incident size, since it represents the risk related to a group of people (i.e., a population) located in the effect region of one or more incidents. Societal risk assessment and risk mitigation measures will be included in the design of the transport network and evaluated specifically for pipeline transport. The risk of leakage (and its societal consequences on local population) will be described as a constraint to transport design.

The aim of Chapter 4 will be to design the optimal European SC configuration that minimises the overall cost to install and operate the CCS system such that the transport infrastructure is routed and installed in a way that prevents people from risk of hazards. The overall CCS SC will be economically optimised so to guarantee that the local level of societal risk is lower than a pre-set threshold and to provide stake-holders a valuable tool for assessing social sustainability.

The forth objective will be to propose a decision tool where both economic factors and social acceptance are taken into account as design variables to optimise the installation and deployment of a European CCS infrastructure and to provide indications on the design and cost of those networks that are more likely to be accepted or rejected by local communities. The social acceptance model will be employed to determine which communities are more likely to oppose to CCS within the framework of a comprehensive MILP multi-objective optimisation, i.e. aiming at the simultaneous minimisation of costs for installing and operating the network and at the maximisation of its social acceptance.

The model described in Chapter 5 will be capable of quantifying the additional cost (with respect to an acceptance risk-neutral network) that would be needed to design a CCS SC in the context of Europe while minimising the risk of rejection from local communities. Assessment of costs and of risk of protests and opposition could provide a critical insight into a European large-scale deployment of CCS thus, fostering its implementation more firmly and effectively.

The fifth objective will be to propose a MILP model for the economic optimisation (in terms costs minimisation) of a European CCS SC, including a set of constraints employed to balance the spread of installation and operation costs between countries, with the aim of fostering economic costs share and cooperation policies among the different players and attaining a more timely and effective implementation of the infrastructure at continental scale.

In Chapter 6, the objective function will aim at the minimisation of the European total costs for CCS but the possibility of balancing countrywide contributions through economic share mechanisms will be introduced within the optimisation framework as an original aspect. Overall, this model will provide the best economically optimal SC configurations subjected to the accomplishment of the chosen level of cooperation which will be set through countrywide parameters taking into account the local environmental and/or economic peculiarities, e.g. in terms of national population, CO_2 emissions and gross domestic product (GDP).

Finally, the sixth objective will be to propose a preliminary study to evaluate the effects of CCUS from an economic and environmental perspective and to assess what contribution may derive from CO_2 utilisation for conversion, in particular into valuable chemical products.

In Chapter 7, the goal will be that to incorporate and assess chemical conversion of CO_2 in the strategic design of CCUS SCs. As in previous models, several technological options will be considered for CO_2 capture from European large stationary sources, whereas transport means will include both pipelines (onshore and offshore) and ships. As regards carbon utilisation, some high added value chemicals will be considered as possible outputs in alternative to geological sequestration.

Overall, the goal of this Thesis will be the development of a time-dependent, multi-echelon, spatially-explicit, large-scale, European digital optimisation tool, aiming at the strategic high-level definition of a CCS SC infrastructure. An array of models will provide valuable insights into the optimal economic deployment of CCS technologies at a noteworthy scale that has been never investigated before and it will be able to steer relevant research and policy into addressing correctly the problem of global warming through CCS (and CCUS) and thus, through the direct reduction of GHGs emissions.

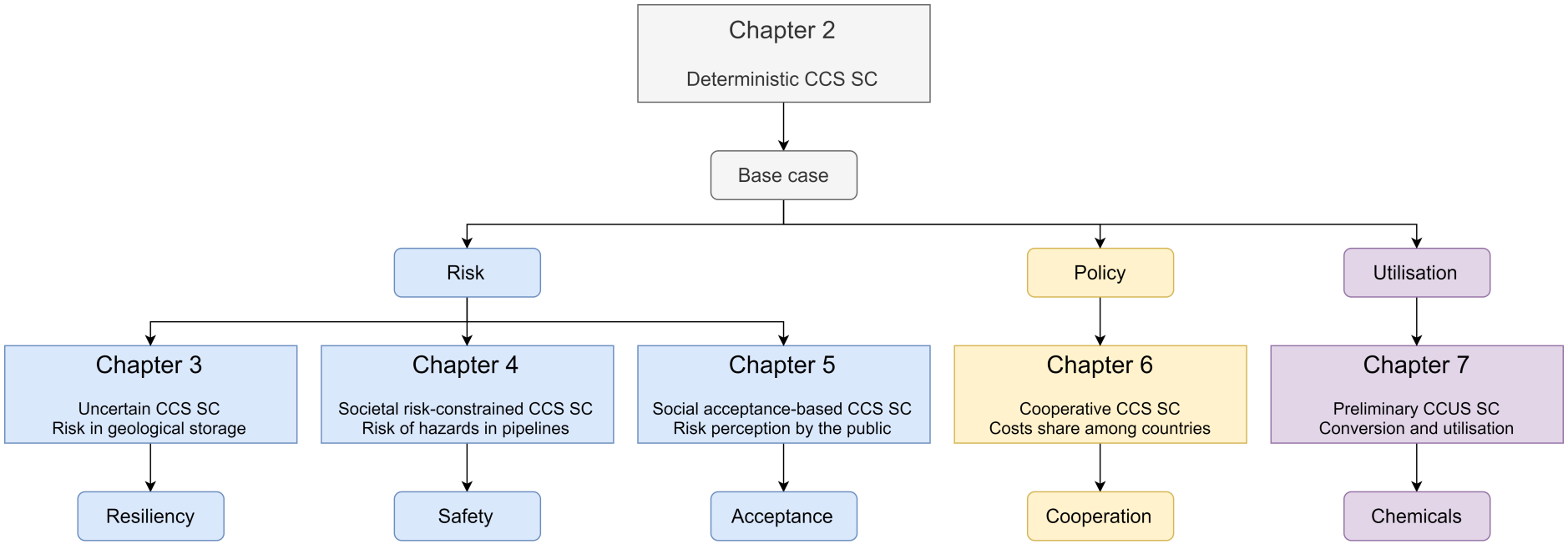

Fig. 1.9: Thesis structure. Chapter 2 will propose an optimisation tool for a deterministic CCS SC which will deliver the base case scenario. Starting from this, Chapters 3-5 will investigate CCS technologies in terms of risk in order to provide insights into the design of resilient, safe and socially acceptable SCs. Conversely, Chapter 6 will investigate the policy-framework that may determine the installation of cooperative international CO_2 networks in Europe. Finally, Chapter 7 will preliminary discuss the possibility of conversion and utilisation of the CO_2 for the production of chemicals.

2

Optimising carbon capture and storage in Europe

2.1 Chapter summary

Diminishing the anthropogenic generation of GHGs is one of the key challenges of the twenty-first century. Considering the current state of affairs, it is nearly impossible to reduce emissions without relying on CCS technologies (to be coupled with other low carbon options, as shown in Chapter 1). In a situation where a large-scale infrastructure is yet to be developed, mathematical programming techniques can provide valuable tools to decision makers for optimising their choices. This Chapter presents a MILP framework for the strategic design and planning of a large European SC for CCS[1]. The European territory is discretised so as to allow for a spatially-explicit definition of large emission clusters. As regards CO_2 capture, post-combustion, oxy-fuel combustion and pre-combustion are considered as possible technological options, whereas both pipelines (onshore and offshore) and ships are taken into account as possible transport means. The overall network is economically optimised over a 20 years' time horizon to provide the geographic location and scale of capture and sequestration sites as well as the most convenient transport means and routes. Different scenarios (capturing up to 70% of European CO_2 emissions from large stationary sources) are analysed and commented on. Results demonstrate the good European potential for carbon sequestration and give some indications on the total cost for CCS. Capture costs are found to be the major contribution to total cost, while transport and sequestration costs are never higher than 10% of the

[1] The content of this Chapter was published in: d'Amore and Bezzo, 2017.

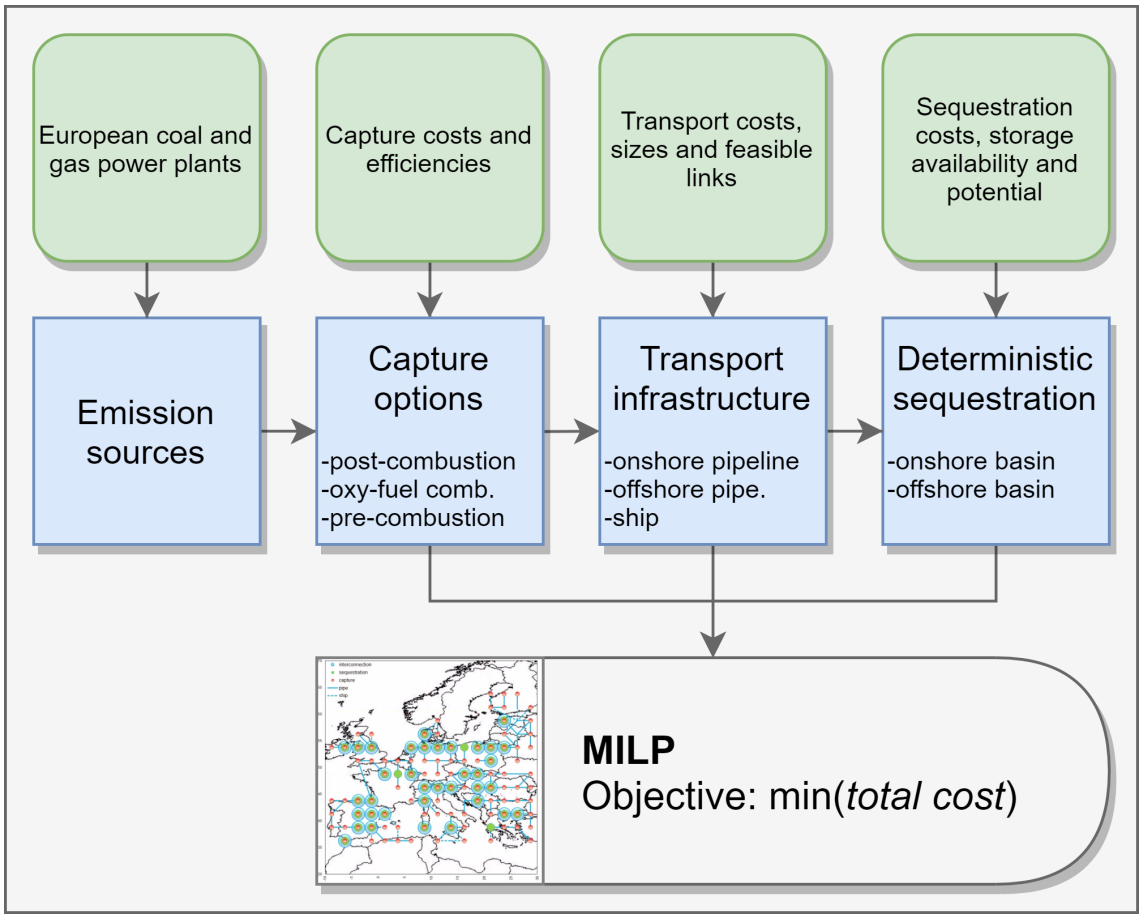

Fig. 2.1: CCS SC echelons, including emission sources, capture option, transport modes and sequestration basins. The objective is the minimisation of the total cost to install and operate the entire European network.

investment required to set in motion and operate the whole network. The overall costs for a European CCS SC were estimated in the range of 27-38 €/t of sequestered CO_2.

2.2 Modelling framework

An optimisation framework is proposed for the design of a CCS SC network within the European context over a 20 years' time horizon. The model is conceived as a single-objective problem to provide the best network in terms of economic performance (i.e., costs minimisation) and is formulated on a grid-based spatially-explicit MILP architecture. The SC evolution in time is described following a multiperiod approach, according to which the time horizon is discretised into 20 yearly time intervals. The optimisation network is geographically described by the set of regions g where the emission sources can be located.
Three sequential echelons are taken into account (Figure 2.1):

- the capture problem, described through the set of capture technologies k, com-

prising post-combustion, oxy-fuel combustion, and pre-combustion options;

- the transport problem, characterized by the set of transport modes l, including onshore pipeline, offshore pipeline, and ship as possible transport means;
- the sequestration problem, described in terms of spatial distribution of onshore and offshore geological basins.

The design problem is formulated as follows. Given the following inputs:

- geographical distribution of CO_2 emission clusters from large stationary sources;
- geographical distribution of CO_2 sequestration areas;
- spatially-explicit features of European territories;
- minimum CO_2 quantity to be captured in Europe across the time horizon;
- CO_2 capture technologies efficiencies;
- CO_2 capture costs as a function of the chosen capture technology;
- transport logistics;
- transport costs as a function of transport mode, quantity and distance;
- CO_2 sequestration costs as a function of selected region;

the objective is to optimise the economic performance (in terms of total cost minimisation) of the system, and therefore to provide:

- geographic location and scale of CO_2 capture sites and technology selection;
- geographic location and scale of CO_2 sequestration sites;
- definition and scale of transport infrastructure;
- exploitation of the European potential for CCS;
- cost performance of the CCS SC over the time horizon.

The computational complexity of large European CCS scenarios has been solved by using a two stage LP-MILP hierarchical strategy aiming at a fast solution of the combinatorial optimisation. The differences between the exact and the heuristic solution methods will be detailed in the mathematical formulation. The following Subsections will provide information on emission sources, and the capture, transport and sequestration stages.

2.2.1 Emission sources

One of the most complete database for emission sources was provided by IEA (2002), including source location, annual CO_2 emission and CO_2 concentrations. Another relevant database was proposed by the EC Science Hub, through the Joint Research Centre (JRC, 2016): this is the Emissions Database for Global Atmospheric Research (EDGAR), which provides a worldwide spatial allocation of GHGs and air pollutants emissions time series and grid-maps from the seventies to 2008, divided into source categories and countries, but without exploring conversion processes specifically (e.g., no information is provided by the EDGAR database in terms of fuel usage for power generation). In this work it was decided to refer to the EDGAR database since it is more updated and was specifically created for the European context. From EDGAR, it can be obtained that in 2008 very large stationary sources (i.e., more than 10^6 t of CO_2/year) emitted 37% of the European global CO_2 and accounted for 336 plants, all of which producing electricity. Considering the noteworthy contribution of such power plants in terms of CO_2 emissions and to reduce the computational burden (this latter aspect will be addressed in the results section), in this Thesis it was chosen to exclude any emissions from other industrial sectors from the possible sources of carbon to be captured. Anyway, this simplification will be further discussed in the conclusive Chapter 8, to set the basis for future work. Furthermore, in order to retain an acceptable computation complexity, a grid consisting of 134 cells (excluding some marginal low/zero-emission areas) was created (Figure 2.2). Emission sources (i.e., coal and gas power plants) within each cells were clustered and assumed to be located at the centre of the cell itself (Figure 2.3).

Each cluster of the grid g represents the overall emission of its area and comprises at least 1 active large emission source (i.e., producing more than 10^6 t of CO_2/year) (Table 2.1). On the whole, assuming the European CO_2 emissions constant since 2008, the grid produces $1.375 \cdot 10^9$ t of CO_2/year, with an average specific emission of $3.722 \cdot 10^6$ t of CO_2/year/facility. According to the grid discretisation and the emission clusters positioning, a spatially-explicit representation of Europe can be provided through a matrix of distances $LD_{g,g'}$ [km] between all potential origins g and destinations g' (where g' is different from g itself). The cell size ranges from 123 km to 224 km according to its position. A methodology for distance calculation for latitude (lat)/longitude ($long$) points is here presented on the basis of a spherical earth (ignoring the ellipsoidal effects). The spherical law of cosines is reported in the following and gives errors typically up to 0.3% (i.e., a maximum error of 3 km over 1000 km of lenght, which can be considered reliable since the spatial resolution of the proposed methodology is in the order of 100 km), thus it seems accurate enough for our purposes:

$$LD_{g,g'} = cos^{-1} \cdot [sin(lat_g) \cdot sin(lat_{g'}) + cos(lat_g) \cdot cos(lat_{g'}) \cdot cos(long_g - long_{g'})] \cdot R \tag{2.1}$$

Tab. 2.1: Yearly CO_2 emissions P_g^{max} [t of CO_2/year] in region g, with null values for cells $g = [125 - 134]$ (JRC, 2016).

g	P_g^{max}	g	P_g^{max}	g	P_g^{max}	g	P_g^{max}
1	1290000	32	9348070	63	13192150	94	3046710
2	1080000	33	14906880	64	1960840	95	41507370
3	1144680	34	11737470	65	3682310	96	10841040
4	7865230	35	10607560	66	1773290	97	10345080
5	2494260	36	46180780	67	4172690	98	8156170
6	0	37	139450560	68	2586690	99	13708240
7	1702930	38	45659040	69	3540190	100	1740120
8	1229100	39	25887690	70	10382000	101	3003740
9	1866730	40	95395370	71	28512840	102	9681650
10	0	41	11459350	72	4066880	103	1819290
11	11301630	42	84301600	73	1173490	104	2414730
12	17466470	43	35533760	74	4260670	105	3843380
13	6008420	44	0	75	8954890	106	1960470
14	10501570	45	2486120	76	13562920	107	8295350
15	6600080	46	0	77	0	108	0
16	1583520	47	8718020	78	0	109	4483710
17	0	48	0	79	10356080	110	3024090
18	2056020	49	18738070	80	26587700	111	17201320
19	8033710	50	32921390	81	19327840	112	3431280
20	6513080	51	5030140	82	5996980	113	3090270
21	17353300	52	1677340	83	6554860	114	1052820
22	96493970	53	8040670	84	2068180	115	4715290
23	3037810	54	11645960	85	0	116	5575650
24	17990540	55	7597960	86	8370360	117	0
25	2762050	56	2485580	87	7808270	118	5440290
26	21133830	57	0	88	4178420	119	0
27	0	58	12857000	89	0	120	5629680
28	2812060	59	14223910	90	4232220	121	4815420
29	2662760	60	0	91	12489060	122	0
30	2356030	61	18959480	92	9993730	123	0
31	10183900	62	14016630	93	8161360	124	12616470

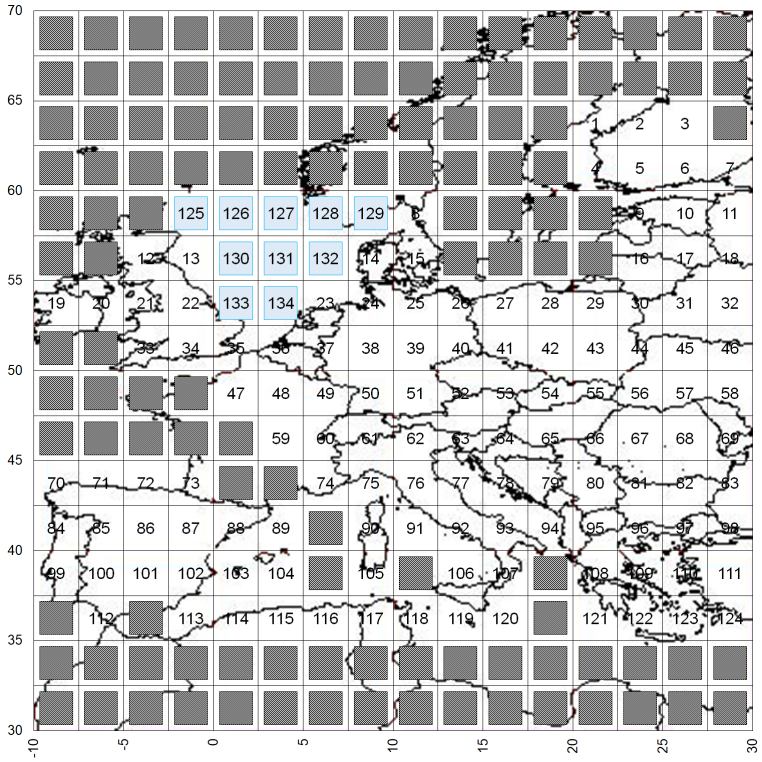

Fig. 2.2: European grid map and cells enumeration.

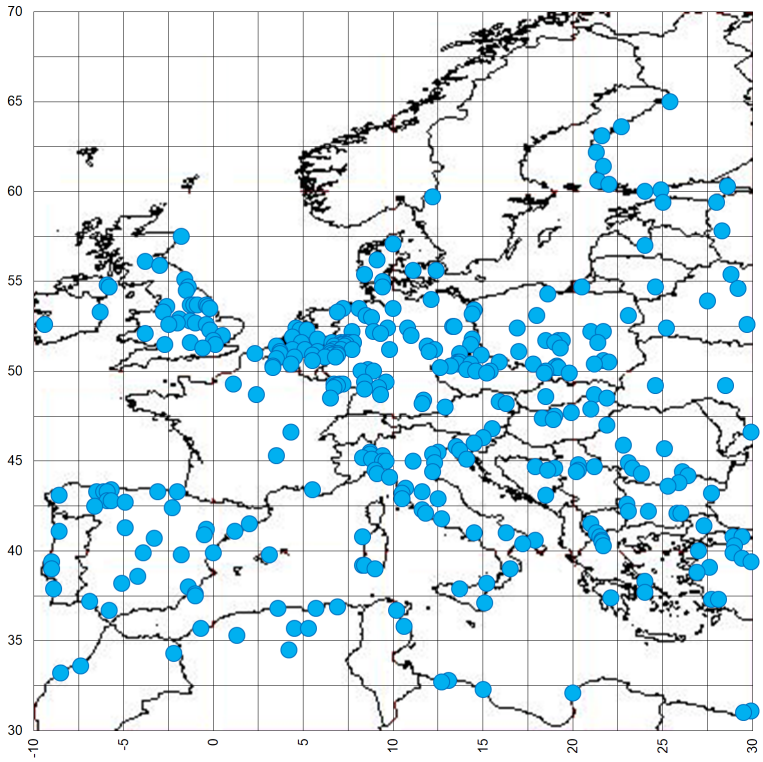

Fig. 2.3: Spatially-explicit representation of Europe and surrounding regions. Only point sources emitting more than 10^6 t of CO_2/year are considered in this study.

where R is equal to 6372.795 km and represents the mean earth's radius. This spherical model gives well-conditioned results down to distances as small as a few metres on earth's surface but, since it gives the shortest 'as-the-crow-flies' distance between g and g', it does not take into account the local geodetic morphology. For this reason, a corrective parameter τ_g was implemented in region g (details in the matematical formulation), to take into account the presence of mountains (Table 2.2).

Since the fuel (gas or coal) used by power stations determines the typology of capture technologies k as well as the input parameters for a capture infrastructure assessment (in terms of capture costs and efficiencies), it is necessary to know in advance which fossil fuel is exploited for electricity generation. The strategy that has been adopted in this work is to refer to the country's specific quotas. As a result, the fuel mix in each grid cell is that of the country the cell belongs to. As a matter of example, Germany is a highly carbon intensive country, in which electricity generated from fossil fuels combustion is mainly produced through coal (almost 81%) and gas (19%) (Eurostat, 2016). Average emissions are 1.04 kg of CO_2 per kWh in the case of a coal-fuelled power station, and 0.383 kg of CO_2 per kWh in the case of gas. Therefore, our assumption is that CO_2 emission within a grid cell in the German territory will be distributed based on the average emissions per technology and the quotas of electricity production per technology; the result is that 92% emissions are related to coal and 8% emissions are related to gas. This is estimated for all cells by introducing a parameter $\gamma_{k,g}$ [%] (Table 2.3), representing the quota of emissions within cell g for which technology k could be employed. Parameter $\gamma_{k,g}$ was calculated according to the 2013 percentages of coal and gas combustion for electricity production for each European country and was then linked with each capture technology k through its possible implementation in region g. The assumption above represents a simplification of the state of things since it is assumed that national quotas of fuel usage are the same throughout the territory of a country. In general, that is not true and some distortions may come up in terms of location of capture technologies and of layout of the CO_2 transportation system. However, it is also important to point out that this is not a shortcoming of the methodology, but a consequence of a lack of available data that hindered a more detailed mapping of emission sources. In particular, the parameter $\gamma_{k,g}$ was calculated by matching the 2013 rates of coal- and gas-based electricity production (in terms of kWh^{coal} and kWh^{gas} compared to kWh^{tot}) for each European country (Eurostat, 2016), and the specific CO_2 production rates (m^{CO_2} [kg of CO_2/kWh]) for both coal- and gas-fed power plants, which were calculated through:

$$m^{CO_2} = c \cdot \frac{13200}{\eta_{el} \cdot K_i} \tag{2.2}$$

where c represents the carbon mass fraction within the fuel (set equal to either 0.95 or 0.75 respectively for coal or gas), η_{el} is the net plant efficiency (set equal to either 0.39 or 0.55 respectively for coal- or gas-based power plants), while K_i is the lower

Tab. 2.2: Terrain factors τ_g, evaluated following the analogy between pipeline transport of CO_2 and electrical transmission: the multiplicative cost factor ranges from a minimum of 1.00 (i.e., grassland) to a maximum of 1.50 (i.e., highly mountainous region), with null values for cells $g = [125 - 134]$ (IEAGHG, 2002).

g	τ_g	g	τ_g	g	τ_g	g	τ_g
1	1	32	1	63	1.3	94	1
2	1	33	1	64	1	95	1
3	1	34	1	65	1	96	1
4	1	35	1	66	1	97	1
5	1	36	1.5	67	1	98	1
6	1	37	1	68	1.3	99	1
7	1	38	1	69	1	100	1
8	1	39	1	70	1	101	1
9	1	40	1.5	71	1.5	102	1.3
10	1	41	1.5	72	1.5	103	1
11	1	42	1	73	1.5	104	1
12	1.5	43	1	74	1.5	105	1.3
13	1	44	1	75	1.5	106	1
14	1	45	1	76	1.5	107	1.3
15	1	46	1	77	1	108	1
16	1	47	1	78	1	109	1
17	1	48	1	79	1	110	1
18	1	49	1	80	1	111	1
19	1	50	1.3	81	1	112	1.3
20	1.5	51	1	82	1	113	1
21	1	52	1	83	1	114	1
22	1	53	1	84	1	115	1
23	1	54	1.3	85	1	116	1
24	1	55	1.5	86	1	117	1
25	1	56	1.3	87	1.3	118	1
26	1	57	1	88	1.5	119	1
27	1	58	1	89	1	120	1
28	1	59	1	90	1.3	121	1
29	1	60	1.5	91	1.3	122	1
30	1	61	1.5	92	1.5	123	1
31	1	62	1.5	93	1.5	124	1

Tab. 2.3: Coal- and gas-based power generation percentage contributions on total CO_2 emission in 2013 for $\gamma_{k,g}$ [t/t] definition, with null values for cells $g = [125-134]$ (Eurostat, 2016).

	$\gamma_{k,g}$			$\gamma_{k,g}$			$\gamma_{k,g}$			$\gamma_{k,g}$	
g	coal	gas	g	coal	gas	g	coal	gas	g	coal	gas
1	0.71	0.29	32	0.95	0.05	63	0.32	0.68	94	0.00	1.00
2	0.71	0.29	33	0.63	0.37	64	0.51	0.49	95	0.93	0.07
3	0.71	0.29	34	0.63	0.37	65	0.55	0.45	96	0.77	0.23
4	0.71	0.29	35	0.63	0.37	66	0.69	0.31	97	0.77	0.23
5	0.71	0.29	36	0.14	0.86	67	0.69	0.31	98	0.47	0.53
6	0.71	0.29	37	0.81	0.19	68	0.69	0.31	99	0.61	0.49
7	0.71	0.29	38	0.81	0.19	69	0.00	1.00	100	0.51	0.39
8	0.79	0.21	39	0.81	0.19	70	0.61	0.39	101	0.51	0.39
9	0.71	0.29	40	0.81	0.19	71	0.51	0.49	102	0.51	0.39
10	0.71	0.29	41	0.95	0.05	72	0.51	0.49	103	0.51	0.39
11	0.71	0.29	42	0.95	0.05	73	0.51	0.49	104	0.51	0.39
12	0.63	0.37	43	0.95	0.05	74	0.54	0.46	105	0.32	0.68
13	0.63	0.37	44	0.95	0.05	75	0.32	0.68	106	0.32	0.68
14	0.79	0.21	45	0.77	0.23	76	0.32	0.68	107	0.32	0.68
15	0.79	0.21	46	0.77	0.23	77	0.32	0.68	108	0.77	0.23
16	0.00	1.00	47	0.54	0.46	78	0.99	0.01	109	0.77	0.23
17	0.00	1.00	48	0.54	0.46	79	0.99	0.01	110	0.47	0.53
18	0.00	1.00	49	0.54	0.46	80	0.97	0.03	111	0.47	0.53
19	0.41	0.59	50	0.81	0.19	81	0.69	0.31	112	0.51	0.49
20	0.41	0.59	51	0.81	0.19	82	0.69	0.31	113	0.51	0.49
21	0.63	0.37	52	0.91	0.09	83	0.69	0.31	114	0.51	0.49
22	0.63	0.37	53	0.91	0.09	84	0.61	0.39	115	0.51	0.49
23	0.34	0.66	54	0.62	0.38	85	0.51	0.49	116	0.51	0.49
24	0.81	0.19	55	0.62	0.38	86	0.51	0.49	117	0.51	0.49
25	0.81	0.19	56	0.77	0.23	87	0.51	0.49	118	0.32	0.68
26	0.81	0.19	57	0.77	0.23	88	0.51	0.49	119	0.32	0.68
27	0.95	0.05	58	0.77	0.23	89	0.51	0.49	120	0.32	0.68
28	0.95	0.05	59	0.54	0.46	90	0.32	0.68	121	0.77	0.23
29	0.95	0.05	60	0.54	0.46	91	0.32	0.68	122	0.77	0.23
30	0.95	0.05	61	0.32	0.68	92	0.32	0.68	123	0.77	0.23
31	0.95	0.05	62	0.32	0.68	93	0.32	0.68	124	0.47	0.53

heating value of coal (31 MJ/kg) or gas (47 MJ/kg). As a result, m^{CO_2} is resulted equal to either 1.040 or 0.383 kg of CO_2/kWh to account the specific carbon emission related respectively to coal or gas-based electricity generation.

2.2.2 Capture options

There are four main technologies for capturing CO_2 from use of fossil fuels: capture from industrial process streams; post-combustion capture; oxy-fuel combustion capture; and pre-combustion capture. Since for each production system different technological configurations are economically feasible under specific conditions (IPCC, 2005), a key aspect of this work entails the definition of the capture technology set. As regards CO_2 capture from industrial processes streams, as stated before, this technological possibility will not be taken into account here. This simplificative choice will be discussed in the conclusions.
When combustion of fossil fuels takes place, post-combustion CO_2 capture can be applied to the flue gasses. The reference systems where it is sensible to apply this technology comprise pulverised coal power plants and natural gas combined cycles, i.e. the best technologies in terms of conversion efficiency. Different process technologies are available for CO_2 separation from post-combustion gases, but currently the preferred options are absorption processes and membranes. Absorption processes offer high capture efficiency and selectivity and the best net energy balance with respect to other postcombustion options, with a typical CO_2 recovery between 80% and 95% (IPCC, 2005). Membrane processes are commercially available for CO_2 removal, but they denote higher energy requirements and lower removal potential than absorption-based systems (Herzog et al., 1991; Feron, 1994), and will not be considered here. An alternative to post-combustion capture is oxy-fuel combustion, in which a pre-combustion air separation process is carried out, in order to obtain a nearly pure oxygen combustion. The flue gas, which contains high concentrations (80–98%) of CO_2 is then compressed, dried and purified for transport and storage. Oxy-fuel technology will be considered as a potential alternative for coal-based plants only since its application to gas systems is still at the design stage (IPCC, 2005). Finally, the pre-combustion technique will be taken into account: starting from syngas, it determines the production of a hydrogen-rich syngas, which can fuel many applications, such as boilers, furnaces, gas turbines, internal combustion engines or fuel cells (IPCC, 2005). Since carbon-based fossil fuels can be processed into syngas, in principle, the pre-combustion option could be applied to different power plant typologies. However, the possibility to convert traditional steam cycles into gasification and pre-combustion based-ones, entails major alteration of both plant design and costs that are difficult to estimate. Thus, only natural gas combined cycles (NGCCs) should be considered. In fact, because of the design similarities, NGCCs could be converted into coal-based integrated gasification combined cycles (IGCCs). Although this represents an interesting perspective, the NGCC repowering

into IGCC option with pre-combustion systems will not be considered in this study, since we are not aware of any industrial NGCC plant being converted, and since there is still little information available in terms of the costs required to implement the transformation. For the above reasons, here it is assumed that pre-combustion CO_2 capture can be applied to general natural gas fired facilities, only. Moreover, it should be pointed out that such facilities are still lacking of industrial applications thus, are still characterised by an uncertain technological development (in terms of both costs, efficiencies, and retrofittability). For this reason, the values reported in this work for the techno-economic description of pre-combustion should be intended as a preliminary attempt, to which further research should follow in the future. Anyway, considering the significant cost uncertainty for this technology, a sensitivity analysis on the capture cost will be provided subsequently.
Summarising, for coal-fed plants, post-combustion and oxy-fuel combustion capture technologies are considered, whereas pre- and post-combustion capture technologies are considered for gas cycles. Overall, capture technologies will be described according to set $k = [post^{comb}_{coal}, post^{comb}_{gas}, oxy^{fuel}_{coal}, pre^{comb}]$. As regards costs for capture, it is here proposed an economical assessment of capture technologies for coal- and gas-fired power plants in terms of capture potential, capital cost, levelised cost of electricity (COE), and cost of CO_2 avoided/captured for both postcombustion, oxy-fuel combustion and pre-combustion systems (Table 2.4). All costs are for capture and compression only, and they do not include the costs for transport and storage. Data were retrieved from IPCC (2005) and updated by taking into account escalation factors and inflation (Rubin et al., 2015; Leung et al., 2014).

2.2.3 Transport modes

Carbon dioxide can be transported in three states: compressed gas, liquid and solid. Commercial scale transport includes tanks (low-scale), pipelines (either onshore or offshore) and ships (long offshore distances). Both solid CO_2 and tanks transportation mode were assumed irrelevant for the wide scale of the CCS problem here investigated.
The IPCC already provided in 2005 the information on total unitary transport cost (UTC [€/t of CO_2/km) for both onshore and offshore pipelines as a function of diameter, length, quantity of CO_2, capital charge and load factor, as well as for ship transport, which becomes cost-competitive with pipelines over large distances. Subsequently, both ZEP (2011) and USDOE (2014) presented their results on CO_2 pipeline transport costs as a combination of length and capacity. Recently, Rubin et al. (2015) reviewed and updated these cost functions for CO_2 transport via pipeline. The economy of scale has a very relevant impact, since unitary costs rapidly decrease when considering large CO_2 flows. Conversely, the effect of transport distance on unitary cost is less significant (Rubin et al., 2015). Following the same methodology, ship transport costs were investigated as a function of traveling distance and

Tab. 2.4: Plants performances when current CO_2 capture technologies are implemented (IPCC, 2005; Rubin et al., 2015). Both the adjusted values [*] (IPCC, 2005) and the current ones [**] (Rubin et al., 2015) are reported. A $-€ exchange rate of 1.0487 (2002) and of 1.3791 (2013) was applied.

	Post-combustion						Oxy-fuel comb.			Pre-combustion		
	Coal-fired			Gas-fired			Coal-fired			Gas-fired		
	Range		Rep.	Range		Rep.	Range		Rep.	Range		Rep.
Cost measure	low	high	value	low	high	value	low	high	value	low	high	value
CO_2 reduction per kWh (%)*	81	88	85	83	88	86	74	100	89	81	91	86
CO_2 reduction per kWh (%)**	86	88	87	88	89	88	90	98	92	82	88	86
Increase in parasitic energy (% input MWh^{-1})*	24	40	31	11	22	16	15	43	25	14	25	19
Increase in parasitic energy (% input MWh^{-1})**	21	44	32	13	18	16	24	29	25	20	35	28
Increase in capital cost (%)*	44	74	63	64	100	76	28	90	62	19	66	37
Increase in capital cost (%)**	58	91	75	76	121	96	67	106	91	30	47	38
Increase in COE (%)*	42	66	57	37	69	46	29	119	65	20	55	33
Increase in COE (%)**	46	69	62	27	61	45	60	84	72	26	41	34
Cost of CO_2 captured ($€^{2002}$/t of CO_2)*	22	33	28	31	54	42	29	29	29	10	31	19
Cost of CO_2 captured ($€^{2013}$/t of CO_2)*	24	42	35	38	63	49	-	-	-	15	37	23
Cost of CO_2 captured ($€^{2013}$/t of CO_2)**	26	38	33	35	80	54	25	41	36	20	30	25
Cost of CO_2 avoided ($€^{2002}$/t of CO_2)*	28	49	39	35	71	51	14	72	40	12	35	22
Cost of CO_2 avoided ($€^{2013}$/t of CO_2)*	32	62	49	46	82	60	-	-	-	17	45	28
Cost of CO_2 avoided ($€^{2013}$/t of CO_2)**	33	51	46	42	88	63	33	53	45	27	42	33

transported capacity.
Oppositely to pipeline transport, ship transport mostly depends on overall transport distance (ZEP, 2011), while transport capacity only slightly affects the unitary shipping cost, especially when large distances are considered. In view of the above, the onshore and offshore pipeline unitary transport costs will be related to the total transported flowrate (and not to the total covered distance), which is here discretised into values Q_p [t of CO_2/year] of capacity $p = [1, 2, ..., 6, 7]$ (Table 2.5). Conversely, the ship unitary transport cost $UTC_{p,ship}$ is set independent of capacity and linearly correlated to distance through regression slope coefficient ($fship = -0.00001385$ €/t of CO_2/km) so as to take into account the scale effect of transport distance on sea shipping. The slope coefficient was estimated from the cost curves proposed by IPCC (2005).
Note that several political and social factors may affect the final configuration of a CO_2 transportation systems, particularly when different national interests and policies need considering simultaneously. The analysis of these factors (and their consequences with respect to the design problem being investigated here) is well beyond the scope of this work. However, we would like to point out that, on the one hand, CO_2 transportation, by either ships or pipelines, has been practised for over 30 years and is governed by various international conventions, national codes and standards, particularly when considering the planning of networks between countries. The Basel Convention (come into force in 1992) did not directly impose any kind of constraint and/or restriction on the CO_2 transportation, despite this has to comply with a multitude of national and international standards, agreement and regulations (IPCC, 2005). On the other hand, despite being classified as a non-flammable and non-toxic gas (or refrigerated liquid), CO_2 is still rising public concern, especially as regards the possibility of a leakage. Accordingly, it should be remembered that the actual design of a CCS infrastructure cannot be finalised without a proper risk assessment and the implementation of effective risk mitigation measures (which will be performed in Chapter 4, which deals with the quantification of societal risk, and implementation of possible risk mitigation measures on the onshore pipeline system).

2.2.4 Sequestration basins

Spatially-explicit data for CO_2 sequestration must be provided in order to optimise the design network for a CO_2 capture and storage infrastructure. Here data on carbon geological sequestration are critically analysed within the European framework. A GIS analysis of European geological formations that can trap the CO_2 efficiently was provided by the EU GeoCapacity Project (2009), which was a research project aiming at the assessment of the storage capacity of deep saline aquifers, hydrocarbon fields and coal fields, i.e. the most interesting sequestration areas (Leung et al., 2014), over a total of 25 countries. Such results are based on a number of criteria for selecting, screening and ranking potential storage sites:

Tab. 2.5: Transport unitary cost $UTC_{p,l}$ [€/t of CO_2/km] according to the discretisation p of transport capacities Q_p [t of CO_2/year]. The constant value for ship transport ($UTC_{p,ship} = 0.03215$ €/t of CO_2/km) is then lowered according to a kilometric slope ($fship = -0.00001385$ €/t of CO_2/km), the latter representing economies of scale on total transport distance.

		$UTC_{p,l}$		
p	Q_p [Mt/year]	onshore [€/t/km]	offshore [€/t/km]	ship [€/t/km]
1	1	0.04009	0.07137	0.03215
2	5	0.01476	0.02215	0.03215
3	10	0.00959	0.01338	0.03215
4	15	0.00746	0.00997	0.03215
5	20	0.00624	0.00808	0.03215
6	25	0.00543	0.00687	0.03215
7	30	0.00485	0.00602	0.03215

- reservoir depth must ensure that the CO_2 is in supercritical phase (under 800 m), but it is advised against drilling deeper than 2 km because of the decrease of the permeability and porosity;
- integrity of the seal must avoid CO_2 leakage;
- storage capacity has to be enough large to be compared with plants emissions;
- petrophysic characteristics must ensure economic feasibility and leakage prevention (Anthonsen et al., 2009).

The study pointed out the remarkable potential of geological storage, stressing the fact that this sequestration option can really constitute, in the majority of the countries analysed, a fertile land for fossil fuel-based electricity generation acceptance. According to these results, a total of over 117 Gt of CO_2 can be captured within European geological formations, equal to 83 times the current yearly carbon generation from those large stationary sources that we included in our model. Excluding Norway (whose capacity is mainly offshore), the sequestration potential lowers to 91 Gt of CO_2, that means the onshore capacity for storing the yearly emissions of the large stationary sources over the next 63 years. The spatially-explicit representation of Europe in terms of CO_2 storage capacity is retrieved from the EU GeoCapacity Project (2009) and reported in Table 2.6 (i.e., $S_{s,g}^{D,min}$ [t of CO_2], which is the minimum deterministic storage potential of basin s in region g), and Table 2.7 (i.e., $S_{s,g}^{D,max}$ [t of CO_2], which is the maximum deterministic storage potential of basin s in region g). In particular, the deterministic model developed in this Chapter 2 will employ data of storage potential which is an average value S_g^D [t of CO_2] between the minimum (Table 2.6) and maximum (Table 2.7) ones. Furthermore, this modelling framework will not distinguish between the different typologies of basins s

(whereas, this aspect will be investigated in Chapter 3, where basins typologies will be discussed as well). Accordingly, major onshore storage potential can be found in Spain (14 Gt of CO_2), Germany (17 Gt of CO_2) and United Kingdom (14 Gt of CO_2). The cost for CO_2 sequestration will be described subsequently, according to the methodology proposed by Ogden (2003, 2004) for injection wells installation, operation and maintenance. Note that onshore CO_2 sequestration is currently not allowed in several countries (e.g., the Netherlands, Germany, Austria). The effect of this legislation constraint will be discussed subsequently.

2.3 Mathematical formulation

According to the qualitative results already reviewed and presented for a European CCS assessment, the aim of this Section is to develop a multi-echelon, multi-period and spatially-explicit MILP model for an economic optimisation of a CO_2 SC in terms of global cost minimisation. The objective is to minimise the total cost (TC [€]) that occurs to set in motion the SC, including total capture costs (TCC [€]), total transportation costs (TTC [€]) and total sequestration costs (TSC [€]), such that all constraints are satisfied:

$$\begin{cases} objective = min(TC) \\ TC = TCC + TTC + TSC \\ s.t. \\ capture\ problem\ model \\ transport\ problem\ model \\ sequestration\ problem\ model \end{cases} \tag{2.3}$$

As will be detailed, the model mathematical architecture is based on three pillars, each generating several constraints to the main problem: the capture problem, the transport problem and, finally, the sequestration problem.

2.3.1 The capture problem model

The spatially-explicit representation of Europe is described through the set g accounting for all the regions constituting the discretisation grid. It is here assumed a time horizon of 20 years t, in which for each region g a possible capture technology k can be selected and installed. For each region g and each time period t, we can define the parameter $P_{g,t}^{max}$ [t of CO_2/year] representing the global yearly CO_2 production and accounting for all the European emitting sources. In general, the CO_2 that is selected for processing ($P_{k,g,t}$ [t of CO_2/year]) through technology k in region g at time period t must be lower than the maximum CO_2 flowrate $P_{g,t}^{max}$ available for capture in a region g at time period t:

$$\sum_k P_{k,g,t} \leq P_{g,t}^{max} \qquad \forall g, t \tag{2.4}$$

Tab. 2.6: Minimum deterministic storage potential $S_{s,g}^{D,min}$ [Mt of CO_2] of basin s in region g, where i= *deep saline aquifers*, ii= *hydrocarbon fields*, iii= *coal fields*. Basins typologies are discussed in Chapter 3.

	s				s				s				s		
g	i	ii	iii	g	i	ii	iii	g	i	ii	iii	g	i	ii	iii
1	0	0	0	35	0	0	0	69	2100	3	17	103	0	0	0
2	0	0	0	36	100	0	0	70	0	0	0	104	0	0	0
3	0	0	0	37	0	0	1090	71	2333	0	0	105	0	0	71
4	0	0	0	38	1714	0	1090	72	2333	0	73	106	0	0	0
5	0	0	0	39	1714	0	0	73	0	0	0	107	934	0	0
6	0	0	0	40	1714	0	0	74	1584	0	0	108	0	0	0
7	0	0	0	41	0	191	0	75	0	0	0	109	0	0	0
8	0	0	0	42	587	0	208	76	0	0	0	110	0	0	0
9	0	0	0	43	0	191	0	77	934	0	0	111	0	0	0
10	0	0	0	44	0	0	0	78	0	0	0	112	2333	0	0
11	0	0	0	45	0	0	0	79	197	0	0	113	0	0	0
12	0	0	0	46	0	0	0	80	0	0	0	114	0	0	0
13	0	0	0	47	1584	0	0	81	0	0	0	115	0	0	0
14	2553	203	0	48	1584	770	0	82	0	0	0	116	0	0	0
15	340	1700	300	49	1584	0	0	83	0	0	0	117	0	0	0
16	8	4	0	50	0	0	0	84	0	0	0	118	0	0	0
17	8	0	0	51	1714	0	0	85	0	0	0	119	0	0	0
18	0	0	0	52	766	0	0	86	2333	0	0	120	0	0	0
19	0	0	0	53	0	17	27	87	0	0	0	121	0	0	0
20	0	0	0	54	1716	0	0	88	2333	0	73	122	0	0	0
21	3550	7300	0	55	0	0	0	89	0	0	0	123	0	0	0
22	0	0	0	56	0	0	0	90	0	0	0	124	0	0	0
23	0	0	0	57	0	0	0	91	0	0	0	125	0	0	0
24	1714	1450	0	58	0	0	0	92	934	0	0	126	4895	0	0
25	1714	1450	0	59	1584	0	0	93	934	0	0	127	4895	0	0
26	1714	0	0	60	0	0	0	94	0	0	0	128	4895	0	0
27	587	0	0	61	0	905	0	95	390	0	0	129	0	0	0
28	587	0	0	62	934	905	0	96	0	0	0	130	0	0	0
29	0	0	0	63	92	2	0	97	0	0	0	131	0	0	0
30	0	0	0	64	2710	95	0	98	0	0	0	132	0	0	0
31	0	0	0	65	0	195	0	99	92	35	0	133	3550	0	0
32	0	0	0	66	3890	750	44	100	0	0	0	134	0	0	0
33	0	0	0	67	3750	750	0	101	0	0	0				
34	0	0	0	68	0	0	0	102	2333	0	0				

Tab. 2.7: Maximum deterministic storage potential $S_{s,g}^{D,max}$ [Mt of CO_2] of basin s in region g, where i= *deep saline aquifers*, ii= *hydrocarbon fields*, iii= *coal fields*. Basins typologies are discussed in Chapter 3.

	s				s				s				s		
g	i	ii	iii	g	i	ii	iii	g	i	ii	iii	g	i	ii	iii
1	0	0	0	35	0	0	0	69	2658	7	27	103	0	0	0
2	0	0	0	36	199	0	0	70	0	0	0	104	0	0	0
3	0	0	0	37	0	0	1400	71	3907	0	0	105	0	0	265
4	0	0	0	38	4000	0	1400	72	3907	34	97	106	0	0	0
5	0	0	0	39	4000	0	0	73	0	0	0	107	1868	0	0
6	0	0	0	40	4000	0	0	74	5427	0	0	108	0	0	0
7	0	0	0	41	0	382	0	75	0	0	0	109	0	0	0
8	0	0	0	42	1174	0	415	76	0	0	0	110	0	0	0
9	0	0	0	43	0	382	0	77	1868	0	0	111	0	0	0
10	0	0	0	44	0	0	0	78	0	0	0	112	3907	0	0
11	0	0	0	45	0	0	0	79	296	0	0	113	0	0	0
12	0	0	0	46	0	0	0	80	0	0	0	114	0	0	0
13	0	0	0	47	5427	0	0	81	0	0	0	115	0	0	0
14	16672	810	0	48	5427	1008	0	82	0	0	0	116	0	0	0
15	430	2700	500	49	5427	0	0	83	0	0	0	117	0	0	0
16	15	7	0	50	0	0	0	84	0	0	0	118	0	0	0
17	15	0	0	51	4000	0	0	85	0	0	0	119	0	0	0
18	0	0	0	52	2863	0	0	86	3907	0	0	120	0	0	0
19	0	0	0	53	0	33	54	87	0	0	0	121	0	0	0
20	0	0	0	54	13708	134	0	88	3907	0	97	122	0	0	0
21	7468	9887	0	55	0	0	0	89	0	0	0	123	0	0	0
22	0	0	0	56	0	0	0	90	0	0	0	124	0	0	0
23	0	0	0	57	0	0	0	91	0	0	0	125	0	0	0
24	4000	3165	0	58	0	0	0	92	1868	0	0	126	9790	0	0
25	4000	3165	0	59	5427	0	0	93	1868	0	0	127	9790	0	0
26	4000	0	0	60	0	0	0	94	20	111	0	128	9790	0	0
27	1174	0	0	61	0	1714	0	95	1050	0	0	129	0	0	0
28	1174	0	0	62	1868	1714	0	96	0	0	0	130	0	0	0
29	0	0	0	63	153	6	0	97	0	0	0	131	0	0	0
30	0	0	0	64	4067	189	0	98	0	0	0	132	0	0	0
31	0	0	0	65	0	389	0	99	184	70	0	133	7468	0	0
32	0	0	0	66	9861	2000	87	100	0	0	0	134	0	0	0
33	0	0	0	67	9300	2000	0	101	0	0	0				
34	0	0	0	68	0	0	0	102	3907	0	0				

Tab. 2.8: Capture efficiencies (η_k) and unitary capture cost (UCC_k [€/t of CO_2]) for each technology k. Data summarise representative values that were previously reported in Table 2.4.

	k			
	$post^{comb}_{coal}$	$post^{comb}_{gas}$	oxy^{fuel}_{coal}	pre^{comb}
η_k	0.87	0.88	0.92	0.86
UCC_k	33	54	36	25

Therefore, $P^{max}_{g,t}$ represents the upper bound for the $P_{k,g,t}$ calculation. The flowrate of CO_2 captured by each technology k in region g at time period t is also constrained through the parameter $\gamma_{k,g}$ [%], representing the feasibility ratios when installing a technology k for capture in region g, according to the spatially-explicit characteristics of the European countries in terms of local coal- and gas-based power generation:

$$P_{k,g,t} \leq P^{max}_{g,t} \cdot \gamma_{k,g} \qquad \forall k, g, t \tag{2.5}$$

Once a technology k is selected for capture region g at time period t, a global lower bound for $P_{k,g,t}$ is set:

$$\sum_{k,g,t} P_{k,g,t} \geq \alpha \cdot \sum_{g,t} P^{max}_{g,t} \tag{2.6}$$

where α represents an a priori-fixed lower bound for minimum European CCS. Thus, a global minimum quantity to be captured (and sequestered) is defined over the time horizon, thus leaving the solver to choose when to install the capture facilities: α sets a global minimum carbon reduction target in Europe in 20 years of simulation, given the total CO_2 emissions from large stationary sources considered in this work. Then, the CO_2 flowrate $C_{k,g,t}$ [t of CO_2/year] that is captured through technology k in region g at time period t is calculated as follows:

$$C_{k,g,t} = \eta_k \cdot P_{k,g,t} \qquad \forall k, g, t \tag{2.7}$$

where η_k is the average capture efficiency of each installed technology k (Table 2.8). The total cost for capture ($TCC_{g,t}$ [€/year]) in region g at time period t is given by expression:

$$TCC_{g,t} = \sum_{k} (UCC_k \cdot C_{k,g,t}) \qquad \forall g, t \tag{2.8}$$

where UCC_k [€/t of CO_2]) is the unitary capture cost through technology k (Table 2.8). Finally, the global European capture cost over the 20-years' time horizon (TCC [€]) is given by the sum for all regions g and time periods t of $TCC_{g,t}$:

$$TCC = \sum_{g,t} TCC_{g,t} \tag{2.9}$$

2.3.2 The transport problem model

Costs for installing and operating the transport infrastructure can be described through unitary transport costs. The linearisation through set p of quantities Q_p [t of CO_2/year] was then implemented to keep the formulation linear as regards shipment size. The CO_2 mass balance in region g at time period t is calculated by imposing that the ingoing flows, given by the captured CO_2 (i.e., $C_{k,g,t}$) and the flowrates from region g' through l to region g at time period t (i.e., $Q_{g',l,g,t}$ [t of CO_2/year]), must be equal to the outgoing flows, given by the sequestered flowrate (i.e., $S_{g,t}$ [t of CO_2/year]) and the quantity shipped from region g through l to region g' at time period t (i.e., $Q_{g,l,g',t}$ [t of CO_2/year]):

$$\sum_{k} C_{k,g,t} + \sum_{l,g'} Q_{g',l,g,t} = \sum_{l,g'} Q_{g,l,g',t} + S_{g,t} \qquad \forall g,t \tag{2.10}$$

where $S_{g,t}$ is the sequestered CO_2 flowrate in region g at time period t (it will be further detailed in the next sections), while g' represents the subset of g of possible origins or destinations that are different from g itself. Then, each transported flowrate $Q_{g,l,g',t}$ is discretised according to Q_p to retain the linear formulation:

$$Q_{g,l,g',t} = \sum_{p} (\lambda_{p,g,l,g',t} \cdot Q_p) \qquad \forall g,l,g',t \tag{2.11}$$

The transport mode sizing, definition and selection is operated through the binary decision variable $\lambda_{p,g,l,g',t}$ representing the possible shipment of a quantity p from g via transport mode l to g' at time t. Then, it is imposed that only feasible combinations between g and g' for each transport mode l may be chosen, according to the transport feasibility set $Total^{Q}_{g,l,g'}$ (e.g., ships must not be in use within the mainland), and that internal transport loops must be avoided (e.g., a flowrate from region g to g itself must not occur):

$$\begin{cases} Q_{g,l,g',t} = 0 & \forall g,l,g' \notin Total^{Q}_{g,l,g'} \\ Q_{g,l,g,t} = 0 \end{cases} \tag{2.12}$$

According to decision variables $\lambda_{p,g,l,g',t}$, it is also possible to evaluate the overall transport distance $L_{l,t}$ [km] covered through a mean l at time period t, and impose an upper bound for the construction speed of pipelines in years t, which is here set equal to 5000 km/year, as retrieved for gas pipeline construction in the US (EIA, 2007):

$$L_{l,t} = \sum_{p,g,g'} (\lambda_{p,g,l,g',t} \cdot LD_{g,g'}) \qquad \forall l,t \tag{2.13}$$

$$L_{l,t} - L_{l,t-1} \leq 5000 \qquad \forall l \neq ship \tag{2.14}$$

where $LD_{g,g'}$ represents the distance between grid points g and g'. This formulation also limits the fluctuations on the pipeline infrastructure installation. Transport costs can be evaluated from the actually transported flowrates, that are described through the decision variable $\lambda_{p,g,l,g',t}$ of and according to the scale factors-based

procedure. Indeed, the total transport cost at time period t (i.e., TTC_t [€/year]) is given by the contribution of scale factors on total transportation size (purposely designed for pipeline transport) at time period t (i.e., TTC_t^{size} [€/year]), of scale factors on total transportation length (purposely designed for ship transport) at time period t (i.e., TTC_t^{dist} [€/year]), and intra-grid connection-related costs (i.e., TTC_t^{intra} [€/year]):

$$TTC_t = TTC_t^{size} + TTC_t^{dist} + TTC_t^{intra} \qquad \forall t \tag{2.15}$$

In the expression above, TTC_t^{size} represents the transport length and shipment size contribution to total transport cost at time period t, by taking particularly into account the scale effects of total transport flowrate as regards pipelines:

$$TTC_t^{size} = \sum_{p.l} UTC_{p,l} \cdot \sum_{g,g'} (\lambda_{p,g,l,g',t} \cdot Q_p \cdot LD_{g,g'} \cdot \tau_g) \qquad \forall t \tag{2.16}$$

Thus, TTC_t^{size} depends on the flowrate size and on the linear distance $LD_{g,g'}$ between regions g and g', which is corrected through a tourtuosity factor τ_g, which represents a corrective parameter of terrain in region g that accounts for specific geographical features (e.g., the presence of mountains) and that may determine the need for a different, typically more tortuous, pipeline path (Table 2.2). In particular, τ_g is calculated following the analogy proposed by IEAGHG (2002) between pipeline transport of CO_2 and electrical transmission. A multiplicative cost factor is therefore introduced, that ranges from a minimum of 1.00 (i.e., grassland) to a maximum of 1.50 (i.e., highly mountainous region).
On the other hand, TTC_t^{dist} includes the contribution of scale effects of total transport distance when considering ships as a transport option from region g to g' at time period t:

$$TTC_t^{dist} = \sum_{l} f^{ship} \cdot \sum_{g,g'} (Q_{g,l,g',t} \cdot LD_{g,g'}) \qquad \forall l = ship, \forall t \tag{2.17}$$

Finally, intra-connection costs TTC_t^{intra} accounts for all the short-distance transport costs within each capture region g:

$$TTC_t^{intra} = U\bar{T}C \cdot \sum_{k,g} (C_{k,g,t} \cdot LD_g \cdot \frac{\sqrt{2}}{2}) \qquad \forall t \tag{2.18}$$

where $U\bar{T}C$ is equal to 0.0126 €/t of CO_2/km and represents the average cost for transporting CO_2 through onshore pipelines, while LD_g [km] represents the size of each single cell g. Since emission sources are clustered in the middle of the cell g, it is assumed that the intra-connection length is equal to $\sqrt{2}/2$ times the cell size LD_g so that (conservatively) pipelines can reach all the cell marginal areas for in loco storage (Figure 2.4).
Finally, TTC_t is summed up in t for the overall transportation cost TTC calculation:

$$TTC = \sum_{t} TTC_t \tag{2.19}$$

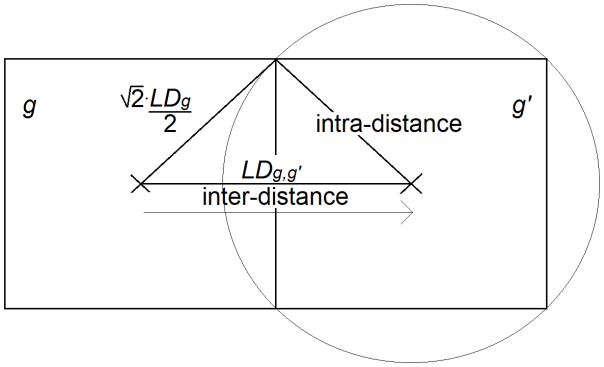

Fig. 2.4: Definition of inter-connection between region g and g' and of intra-connection within cell g, according to the inter-distance between cell g and g' and to the maximum intra-distance within cell g, respectively.

2.3.3 The sequestration problem model

Once CO_2 gets transported, it can be sequestered deep into geological formations according to the sequestration flowrates $S_{g,t}$. An upper bound is imposed for the total amount that can be stored in each region g over the time horizon:

$$\sum_t S_{g,t} \leq S_g^D \qquad \forall g \tag{2.20}$$

where S_g^D [t of CO_2] represents the deterministic average upper bound for storage in region g as retrieved from the spatially-explicit representation of geological formations in Europe, and is equal to average values of storage potential between the minimum (Table 2.6) and maximum (Table 2.7) ones. The sequestration ratio S_g^{ratio} [%] can be then defined for each region g by comparing the actually sequestered CO_2 (i.e., $S_{g,t}$) with the maximum storage potential S_g^D in the same g:

$$S_g^{ratio} = \frac{S_{g,t}}{S_g^D} \qquad \forall g \tag{2.21}$$

As regards the yearly total sequestration cost TSC_t [€/year], according to the indications by Kwak and Kim (2017) and to the formulation proposed by Hasan et al. (2015), the cost for injecting CO_2 can be calculated following Ogden (2003, 2004) by summing up for each region g the yearly investment for wells installation, operation and maintenance:

$$TSC_t = \sum_g [(CCR^{seq} \cdot OM^{seq}) \cdot off_g \cdot (m_1 \cdot d_g + m_2) \cdot N_{g,t}] \qquad \forall t \tag{2.22}$$

where CCR^{seq} [%] represents the yearly capital charge rate of ownership of cost, OM^{seq} [%] is the yearly operation and maintenance cost rate, m_1 [set equal to 1.6 M€/km] and m_2 [set equal to 1.3 M€] are cost parameters for well construction and subsequent CO_2 injection, while d_g [km] is the spatially-explicit injection depth in region g, ranging from a minimum value of 0.8 km to a maximum of 2 km.

Furthermore, off_g represents the additional cost to install and operate offshore wells instead of onshore ones, and was set equal to 5 according to the literature (van den Broek et al., 2010). Finally, $N_{g,t}$ determines the number of injection wells in region g at time period t and is calculated by dividing the actual sequestered flowrate $S_{g,t}$ for the maximum injection capacity of a well S^{max} [t of CO_2/year]:

$$N_{g,t} = \frac{S_{g,t}}{S^{max}} \qquad \forall g, t \tag{2.23}$$

The results of the EU GeoCapacity Project (2009), although qualitatively describing the minimum geomorphological properties that characterise suitable formations, do not always provide spatially-explicit information on specific geological parameters (e.g., permeability). Accordingly, here we assumed an average injectivity of 1.56 Mt of CO_2/year per injection well (Ogden, 2003, 2004), which is comparable with the minimum injectivity to ensure remunerative investments (0.1 Mt of CO_2/year, EU GeoCapacity Project (2009)) and capable of dealing with the range of transported CO_2 flowrates in the model (1–30 Mt of CO_2/year).
Finally, the overall sequestration cost TSC [€] is defined as follows:

$$TSC = \sum_t TSC_t \tag{2.24}$$

2.3.4 Two stage LP-MILP model

According to exact mathematical formulation previously described, $\lambda_{p,g,l,g',t}$ is a binary variable needed to decide whether a transport option l of size p is selected to move CO_2 from region g to region g'. For large values of carbon reduction target α, the solution of the optimisation problem requires a very high computational time, since decision variables grow exponentially with the amount of CO_2 to be captured. To tackle this issue, here we consider a two stage LP-MILP heuristic formulation based on a hierarchical strategy aiming at a fast solution of highly complex CCS SCs, i.e. whenever the problem size becomes too large for an exact solution method implementation. This formulation, built-up on Moreno-Benito et al. (2017), allows for the optimisation to be performed within the range of CO_2 capture limits considered in this work (Table 2.9). The solution procedure is based on two sequential optimisation steps:

- at first a continuous relaxation of binary variables (i.e., continuous $\lambda^{i}_{p,g,l,g',t}$) is performed; the results that are obtained for CO_2 capture (i.e., $C^{i}_{k,g,t}$) through technology k in region g at time period t are stored for the second stage (ii);

- in second optimisation stage (ii), a reduced version of the exact optimisation (now with with discrete $\lambda^{ii}_{p,g,l,g',t}$) is performed and, by imposing $C^{i}_{k,g,t} = C^{ii}_{k,g,t}$, it is possible to reduce the computational effort, while guaranteeing the goodness of the results as proven by Agnolucci et al. (2013) and Sabio et al. (2010), and as will be confirmed by our results, too.

For instance, when it is chosen $\alpha = 0.25$, the exact model and the heuristic one show a difference in TC final result of less than 2%, which is assumed to be perfectly acceptable. Table 2.10 summarises the results for different values of α.
Considering the available computational power, $\alpha = 0.25$ represented the upper value for a rigorous solution to be obtained before the problem becomes computationally intractable. The following equations summarise the previously described two stage procedure:

$$\begin{cases} objective = min(TC^{i}) \\ s.t. \\ 0 \leq \lambda^{i}_{p,g,l,g',t} \leq 1 \\ \lambda^{i}_{p,g,l,g',t} \in R \\ C^{i}_{k,g,t} \end{cases} \tag{2.25}$$

$$\begin{cases} objective = min(TC^{ii}) \\ s.t. \\ 0 \leq \lambda^{ii}_{p,g,l,g',t} \leq 1 \\ \lambda^{ii}_{p,g,l,g',t} \in Z \\ C^{i}_{k,g,t} = C^{ii}_{k,g,t} \end{cases} \tag{2.26}$$

As a result, for small values of $\alpha = [0.05, 0.25]$ the exact method will be applied, while the two stage optimisation will be introduced for large values of $\alpha = [0.50, 0.70]$. Note that a limitation is imposed on the maximum value of α. In fact, by performing a simulation to evaluate the maximum achievable level of CO_2 capture in Europe over the 20 years' time horizon according to the following formulation:

$$objective = max(\sum_{g,t} S_{g,t}) \tag{2.27}$$

It results that about 23 Gt of CO_2 can be captured and sequestered (at a cost of over 2300 B€). This corresponds to $\alpha = 0.81$. As a consequence, $\alpha = 0.70$ was set as the maximum feasible value for the simulated case studies.

2.4 Results

Results from both the exact and the two stage formulation will be here presented. In particular (Table 2.9, Table 2.10), the exact method will be applied up to a carbon reduction target $\alpha = 25\%$ (i.e., Scenario A-B for $\alpha = [0.05, 0.25]$), while the hierarchical methodology will be introduced for higher values of sequestered CO_2 (i.e., Scenario C-D for $\alpha = [0.50, 0.70]$). In these scenarios, α sets the overall CO_2 that is captured in Europe over 20 years of simulation, on the basis of the total emission that is produced over the time horizon, thus leaving the solver the possibility to choose the optimal CCS deployment according to the time-dependent features of the model. A fifth Scenario E will be presented as well, in which the hierarchical methodology is applied to optimise the CCS infrastructure according to a linearly

Tab. 2.9: Scenario A-B-C-D-E, objective (Obj.), carbon reduction target (α) and its variation in time ($\Delta\alpha$), and chosen optimisation technique (Opt. technique).

Scenario	Obj.	α	$\Delta\alpha$	Opt. technique
A	min(TC)	0.05	Constant	Exact-e
B	min(TC)	0.25	Constant	Exact-e
C	min(TC)	0.50	Constant	Exact-e
D	min(TC)	0.70	Constant	Exact-e
E	min(TC)	0.00-0.70	Linear	Hierarchical-2s

increasing quantity of CO_2 in years t (from $\alpha = 0.00$ at $t = 1$, to $\alpha = 0.70$ at $t = 20$): within Scenario E, the increasing value of α sets the yearly quantity to be captured according to the emission of that specific year t, thus determining a continuous development of the CCS system over the time horizon, and probably representing a more realistic design option with respect to previous scenarios A-B-C-D.
Figure 2.5 shows the final SC configurations at $t = 20$ for scenarios A-B-C-D. It can be observed that there is an increasing complexity in the resulting infrastructure as long as α increases and larger flowrates of CO_2 are moved across Europe (the totally sequestered amount varies from a minimum of 1.2 Gt of CO_2 in Scenario A, to a maximum of 16.9 Gt of CO_2 in Scenario D). Capture is at first operated (Scenario A-B) within regions in which suitable geological formations are available (e.g., Northern Germany, central United Kingdom, Poland), but when larger quantities are imposed (Scenario C-D), transportation via shipping is needed to balance the increasing CO_2 capture for storage (Figure 2.6). In general, in most regions g, much larger quantities can be sequestered rather than captured, thus demonstrating the good quantitative potential of European onshore territories for CCS applications. As a matter of facts, offshore potential is never exploited, considering the higher cost of this option. The same situation can be observed in Scenario E, where the linearly increasing value of α reflects on the continuous development of the SC over the years (Figure 2.7). In Scenario C-D-E, it is also possible to observe the shutdown of some sequestration sites, which reached their maximum capacity limit within the time horizon considered in this study. In general, the economic results are mainly determined by the capture stage costs, representing up to the 94.3% (in Scenario A) of the overall investment, while costs for transport and sequestration are consistently lower in all scenarios (the maximum value is obtained in scenario C where they reach 8.6% of the overall costs as illustrated in Figure 2.8). It can also be observed that, since stable yearly carbon emission are assumed, the amount of CO_2 that is sequestered every year in Scenarios A-B-C-D is almost constant and variations occur either because the sequestration amount is limited by the rate at which the transport infrastructure is being established or because some sequestration regions get saturated.
As regards capture technologies selection (Figure 2.9a), the oxy-fuel combustion op-

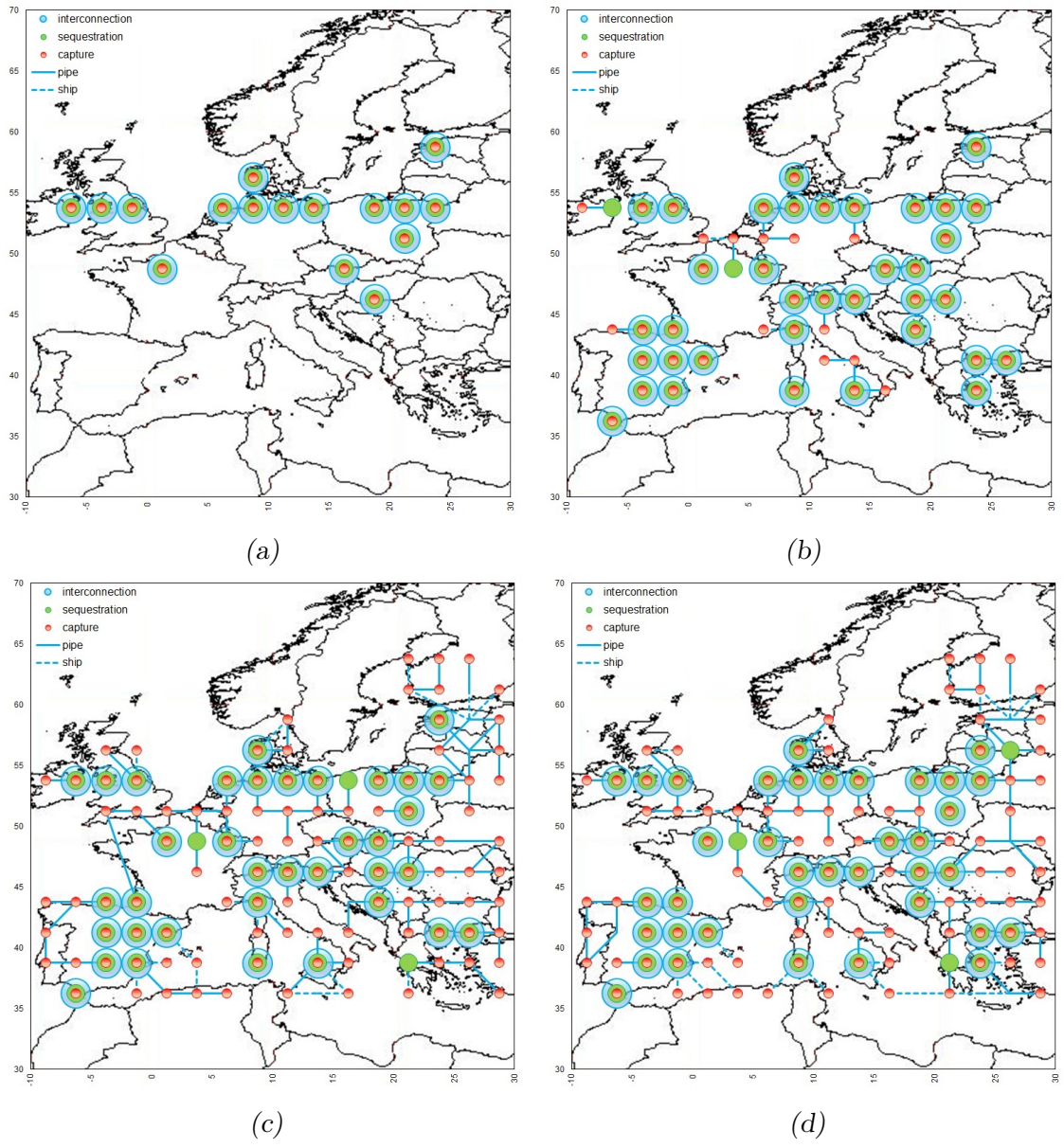

Fig. 2.5: Scenario A-B-C-D, CCS SC final configuration under Scenario A (a), Scenario B (b), Scenario C (c), and Scenario D (d).

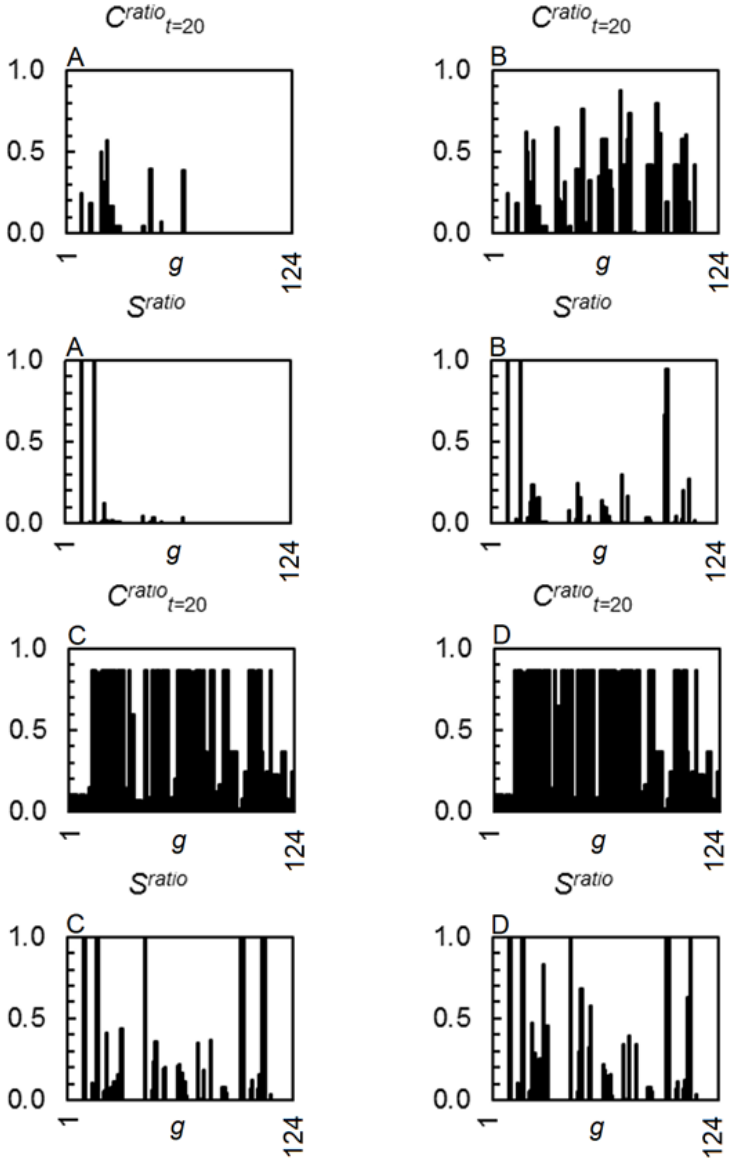

Fig. 2.6: Scenario A-B-C-D, European regions g exploited potentials at $t = 20$ for capture and sequestration.

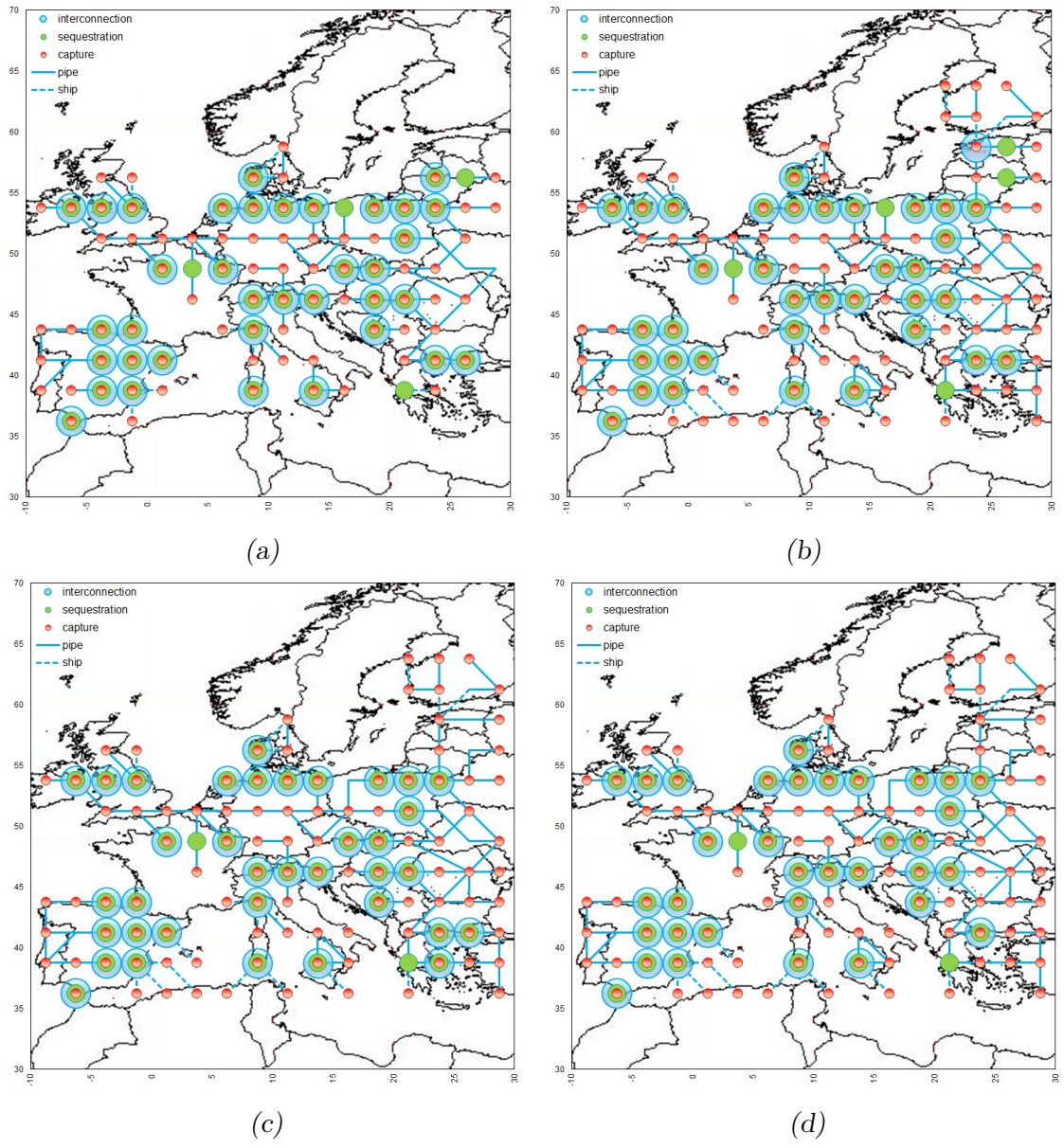

Fig. 2.7: Scenario E, CCS SC final configuration at $t = 5$ (a), $t = 10$ (b), $t = 15$ (c), and $t = 20$ (d).

Tab. 2.10: Scenario A-B-C-D-E, problem size (number of equations and variables) and computational performance (solution time - Sol. time, optimality gap - Opt. gap) of different capture scenarios (depending on α selection) to compare exact (e) and 2-stage ($2s$) solution methods.

α	Sol.	Scen.	Equations	Variables	Sol. time [s]	Opt. gap[%]
0.05	e	A	8337435	13876309	143	0.0
0.05	$2s$	-	14783078	13866433	167+402	0.0+1.7
0.25	e	B	8337435	13876309	132	2.8
0.25	$2s$	-	14782958	13866433	130+12300	0.0+4.1
0.50	e	-	8337435	13876309	≥40000	-
0.50	$2s$	C	14783078	13866433	166+30594	0.0+3.3
0.70	e	-	8337555	13876309	≥40000	-
0.70	$2s$	D	14783078	13866433	164+22471	0.0+2.3
0.00-0.70	$2s$	E	14783078	13866433	67+21817	0.0+3.8

tion is never chosen by the solver, whereas post-combustion and pre-combustion are massively installed in all scenarios. In particular, as far as we move from Scenario A to Scenario D (i.e., α from 0.05 to 0.70), the captured CO_2 quota through coal-based post-combustion increases against the initially preferred pre-combustion technology, which was installed for low values of α because of its better economic performance, although it can be applied to natural gas-based power plants only. The same situation can be observed for Scenario E (Figure 2.9b), in which the continuous variation of α in time produces a progressively increasing quota of post-combustion technologies against pre-combustion ones, since in this simulation the pre-combustion option reaches its maximum CO_2 exploitation limit at $t = 6$. In fact, as long as it is possible to exploit CO_2 from gas-powered plants, specific capture costs (i.e., with respect to the yearly sequestered tons of CO_2) are lower and constant (25.0 €/t of CO_2), whereas they progressively increase up to 31.1 €/t of CO_2 after the sixth year of simulation, in which coal-based power plants are considered, too by the solver for post-combustion techniques installation (Figure 2.9b).

According to the mathematical formulation of transports, sea shipping is an alternative and, in some cases, cheaper option with respect to offshore pipelines, especially for small quantities Q_p. As a result, at the end of the simulation a combination of offshore pipelines and ships are in use in the Mediterranean area and in the Baltic Sea (Scenario C-D-E), whereas onshore pipelines are massively installed within the European mainland. At the end of the time horizon, the grown infrastructure can move CO_2 flowrates for more than 24000 km every year (Scenario C-D-E), covered either through pipelines or ships. As regards the financial optimisation result, in particular referring to Scenario E, it is possible to observe that once the inter-grid transport infrastructure is massively set in motion (at $t = 6$), scale effects benefit the specific cost for transport (i.e., with respect to the yearly sequestered t of CO_2), which varies from a maximum of 5.0 €/t of CO_2 (at $t = 6$) to a minimum of

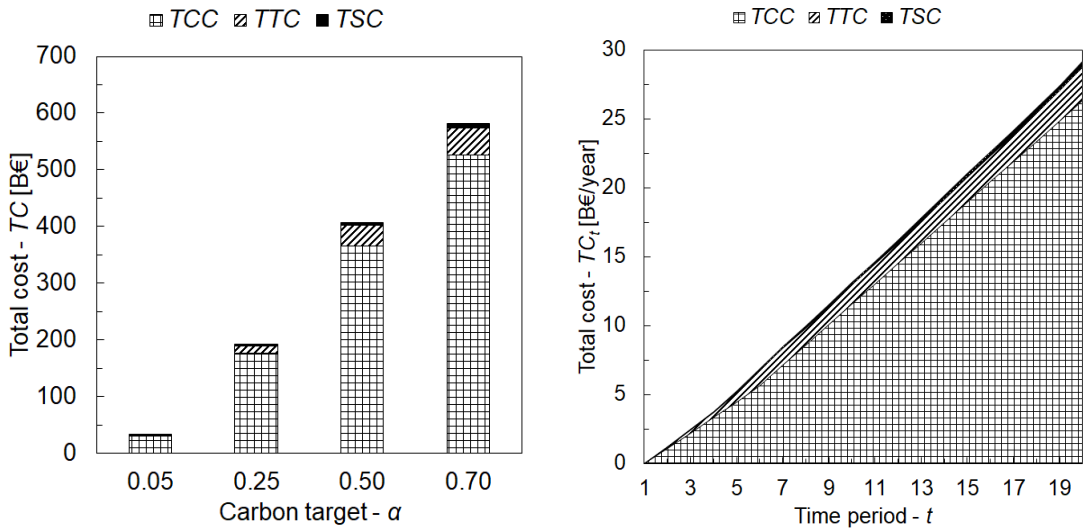

(a) *(b)*

Fig. 2.8: Scenario A-B-C-D-E, TCC, TTC and TSC contributions to overall TC in Scenario A-B-C-D (a), and their continuous variation in t specifically plotted for Scenario E (b).

2.7 €/t of CO_2 (at $t = 20$) (Figure 2.10). In fact, according to our mathematical formulation, shipping costs were calculated on the bases of the set p for quantities discretisation, and lower specific costs were assumed for large-scale CO_2 carriage, which is the actually observed situation in the last years of simulation (i.e., when a noteworthy capture infrastructure is set).
CO_2 sequestration costs were previously shown to be much lower than those for transport and, above all, those for capture. Furthermore, costs for injecting CO_2 underground are not affected by scale effects but are just linearly correlated with the overall captured quota α. For example, Scenario E exhibits an average of 0.469 €/t of CO_2 for geologically confining CO_2.

2.5 Discussion

Results demonstrate the good quantitative potential of European territories for carbon sequestration, considering that only few storage sites are saturated within the 20 years' time horizon, even when the highest reduction targets (e.g., Scenario D) are chosen for a massive infrastructure installation. In fact, all Scenarios denote that the sequestration ratio S_g^{ratio}, representing the local geological exploitation for CO_2 storage, is generally lower than 1 in most of the European regions g. Conversely, a widespread introduction of capture technologies on power plants is highlighted, since most of the regions appear to be heavily equipped for CO_2 capture, as shown by the often nearly unitary local capture potential C_g^{ratio}. Only post-combustion (for coal-based power plants) and pre-combustion (for gas-fed cycles) is selected by the

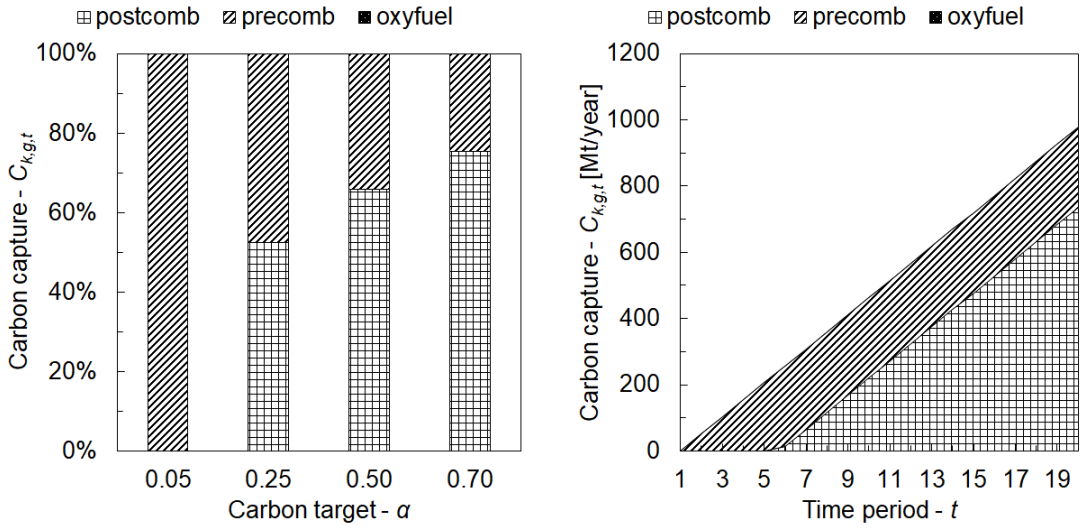

(a) *(b)*

Fig. 2.9: Scenario A-B-C-D-E, Capture technologies selection in Scenario A-B-C-D (a), and their continuous variation in t specifically plotted for Scenario E (b).

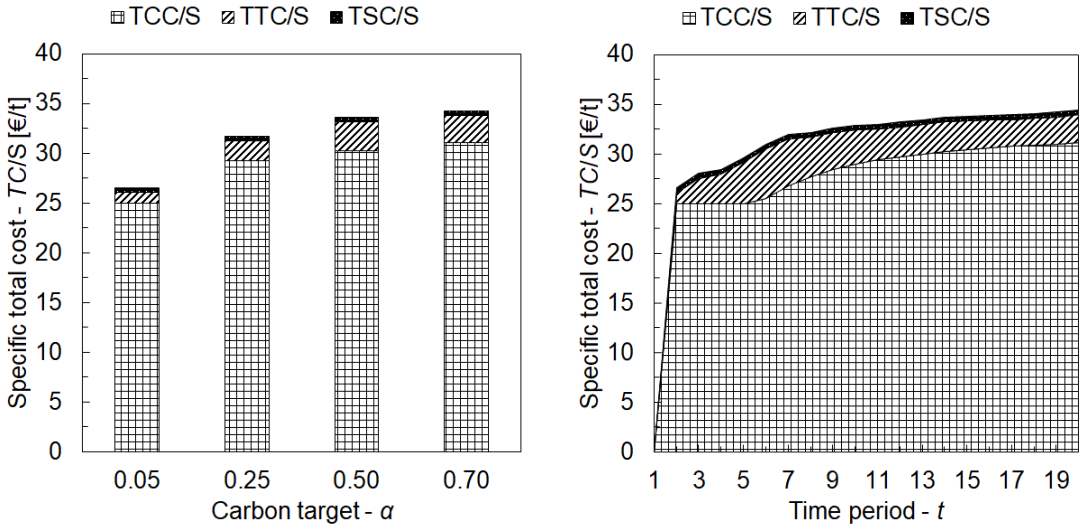

(a) *(b)*

Fig. 2.10: Scenario A-B-C-D-E, specific costs for capture, transport, and sequestration for Scenario A-B-C-D (a), and their continuous variation in t specifically plotted for Scenario E (b).

solver in all scenarios, being the oxy-fuel technology non-competitive at this stage of technological development with respect to other capture options. As regards the CCS SC optimisation design, in the case of a carbon sequestration target lower than 25%, the installation of the pre-combustion option is always preferred due to its better economic performance with respect to the post-combustion. On the other hand, when aiming at reduction targets larger than 25% of CO_2, being the coal-related emission preponderant on the gas-based one in most of the European regions, post-combustion emerges as the most sensible design alternative. For instance, nearly 80% of power plants is equipped with the post-combustion option when capturing 70% of European emission.

As regards the SC economics, being capture the key contributor to total cost in all scenarios, the cost for transport and sequestration is never higher than 10% of the investment necessary to set in motion and operate the European CCS network. As a matter of fact, the yearly specific cost for capture (i.e., the yearly cost for capturing CO_2 with respect to the yearly European sequestered flowrate of CO_2) becomes even larger when post-combustion CO_2 flowrates must be captured from coal-powered facilities, since the maximum contribution of gas fed plants gets totally exploited. For example, Scenario E exhibit a specific European capture cost that increases from 25 €/t of CO_2 to about 31 €/t of CO_2, since capture technologies must be applied to coal plants according to α growth.

Since capture costs TCC were found to be the major contributor to total SC costs TC, it was decided to carry out a sensitivity analysis on unitary costs for capture UCC_k through technology k on the basis of the range proposed by Rubin et al., 2015 (Table 2.11). Results of new Scenario E*-E** will be here discussed with respect to the reference base case of Scenario E, in which the representative values were selected for capture costs calculation. The economic optimisation results of Scenario E*-E** show, as expected, a respectively decreased and increased value of TCC, while TTC and TSC are not affected by the UCC_k selection. Scenario E* and E** entail a TC respectively equal to 229 B€ (i.e., -18.5% with respect to Scenario E) and to 323 B€ (i.e., +15.1% with respect to Scenario E). On the other hand, the selection of capture technologies k at time period t is the same in all scenarios, since it is assumed that the costs for all technologies increase or decrease simultaneously. Results of Scenario E were assessed considering possible variations of pre-combustion costs, too. It was verified that this technological option is not competitive with respect to post-combustion systems when its capture cost becomes greater than 36 €/t of CO_2, i.e. 44% higher than the reference value used in this study.

Legislation constraints (e.g. barriers on onshore storage in some EU countries) were not explicitly considered in the main analysis, since they may change in time and reduce the generality of the presented methodology and results. However, the consequences of the latest country-specific legislations will be presented here. Indeed, the EC (2017) updated the list of European members that are not allowing or limiting

Tab. 2.11: Scenario E, sensitivity analysis on unitary capture costs UCC_k [€/t of CO_2].

		UCC_k			
Range	Scenario	$post^{comb}_{coal}$	$post^{comb}_{gas}$	oxy^{fuel}_{coal}	pre^{comb}
low	E*	26	35	25	20
rep. value	E	33	54	36	25
high	E**	38	80	41	30

onshore CO_2 storage option (Austria, Croatia, Estonia, Ireland, Latvia, Slovenia, the Netherlands, UK, Sweden, Czech Republic, Germany and Poland). In view of the above, it is here proposed the Scenario E^{reg}, in which it is assumed that geological sequestration is completely forbidden in the above-listed countries. As a consequence, the overall European storage capacity is diminished by 37%. As expected, the limitations on the sequestration potential directly affect transport costs, whose increase (+28.3%) determines higher CCS costs (more than 34 €/t of CO_2, against 33 €/t of CO_2 in Scenario E). On the other hand, capture and sequestration costs do not change significantly, and the same capture technologies are selected. The final SC configuration of Scenario E^{reg} at $t = 20$ reveals a different and (in some areas) more complex transport infrastructure with respect to Scenario E.
To summarise, the overall costs for CCS are estimated in the range 27-38 €/t of CO_2, which may also represent an estimate for a possible carbon tax to compensate for the investment and operation costs for capturing, transporting and sequestering CO_2.
In term of the computational effort, the definition of the optimal SC, particularly when a large CO_2 reduction target is required, imposes the solution of a complex mathematical programming method. However, the hierarchical strategy for fast solution of complex SCs appears to perform well, still guaranteeing reliable results when compared to the exact solution method. The heuristic method allows for optimising a multi-choices logistic network in less than 10 h on a 2.80 GHz (32 GB RAM) laptop.

2.6 Chapter conclusions

This Chapter presented a MILP model for the strategic design and optimisation of a spatially-explicit, multiechelon and time-dependent European SC for CCS at European scale. The investigated scenarios, capturing up to the 70% of 20 years' CO_2 production through either pre- or post-combustion technologies, demonstrated the good European potential for sequestration and, simultaneously, the good computational performance of the solution approach.
Costs for capture emerged as the key economic challenge of the system, being the transport- and, even more, the sequestration-related costs a negligible part of the

overall investment, necessary to install and operate the whole CO_2 network. In particular, the yearly cost for capture became even larger when post-combustion CO_2 flowrates had to be captured from coal-powered facilities, since the maximum contribution of gas-fed plants was proven to be easily exploitable and post-combustion for coal plants is a more expensive option than the pre-combustion one.
Starting from these results, Chapters 3-5 will investigate CCS technologies in terms of risk, in order to provide insights into the design of resilient, safe and socially acceptable SCs. In particular, the ensuing Chapter 3 will consider uncertainty effects in geological storage potentials.

3

Effects of uncertainty in geological storage capacities

3.1 Chapter summary

CCS is widely recognised as a promising technology for decarbonising the energy and industrial sectors. An integrated assessment of technological options is required for effective deployment of large-scale infrastructures between the nodes of production and sequestration of CO_2. Additionally, design challenges due to uncertainties in the effective storage availability of sequestration basins must be tackled for the optimal planning of long-lived infrastructure. The objective of this Chapter is to quantify the financial risks arising from geological uncertainties in European SC networks, whilst also providing a tool for minimising storage risk exposure[1]. For this purpose, a methodological approach utilising MILP optimisation is developed and subsequent analysis demonstrates that risks arising from geological volumes are negligible compared to the overall network costs (always $\leq$ 1% of total cost) although they may be significant locally. The model shows that a slight increase in transport (+11%) and sequestration (+5%) costs is required to obtain a resilient SC, but the overall investment is substantially unchanged (max. +0.2%) with respect to a risk-neutral network. It is shown that risks in storage capacities can be minimised via careful design of the network, through distributing the investment for storage across Europe, and incorporating operational flexibility.

[1] The content of this Chapter was published in: d'Amore et al., 2019a; 2019b.

3.2 Modelling framework

Chapter 3 proposes a MILP optimisation under uncertainty based on the deterministic CCS SC model described in Chapter 2. The objective is to minimise the total costs required to install and operate, along a 10 year time horizon $t = [1, 2, ..., 9, 10]$, the overall network for CCS, considering the financial risks that are generated by uncertainties in both onshore and offshore European sequestration basins.
European large stationary CO_2 sources are included in the model instance according to data retrieved from JRC (JRC, 2016). The capture stage and associated constraints are described following the methodology proposed in Chapter 2, i.e. through a set of technological options k. The transport set includes different options $l = [onshore\ pipeline, offshore\ pipeline, ship]$, each discretised through a set of possible flowrate capacities p that ranges from a minimum of 1 Mt of CO_2/year to a maximum of 30 Mt of CO_2/year. The entire European area is discretised into a grid of regions g, analogous to that described in Chapter 2 (Figure 2.2). The sequestration basins are distinguished into different categories according to a set $s = [deep\ saline\ aquifers, hydrocarbon\ fields, coal\ fields]$ (EU GeoCapacity Project, 2009). In particular, as reported in Chapter 2, basins s will be described on the basis of their minimum deterministic storage potential (Table 2.6) and maximum deterministic storage potential (Table 2.7).
Focusing on the sequestration stage, along with the optimisation of the deterministic sequestration model, this study quantitatively evaluates (and minimises) risk that may be generated due to uncertainty on the effective volumetric capacity of geological basins. As will be detailed subsequently within this Chapter 3, local storage availability is forecasted according to two contributions: (i) a precautionary base storage potential preventively defined at the beginning of the storage operations on the basis of randomly generated minimum upper bounds of available volume (every sample j entails a different random combination of minimum upper bounds for storage capacity); and (ii) the possibility of a yearly rate of increase in the confidence on the actual availability of storage as far as the injection is performed. Accordingly, the local storage availability is forced to increase from the randomly generated worst case towards the best deterministic upper bound if it is considered to exploit a certain basin s in region g for several years t, with the drawback of generating risk for more consecutive years.
Overall, the main inputs to this CCS SC optimisation under uncertainty are:

- the spatial distribution of European upstream sources of CO_2;
- the techno-economic parameters of capture options k;
- the European carbon reduction target α to be pursued along the time horizon t;
- the techno-economic parameters of transport means l;

- the spatial distribution of deterministic minimum and maximum upper bounds of local geological potential of sequestration basins s (Tables 2.6,2.7);
- the random matrix of uncertain minimum upper bounds of local geological potential of sequestration basins.

Therefore, the key variables to be optimised are:

- the planning (i.e., investment date), location, scale and cost of the capture system;
- the planning, location, scale and cost of the transport infrastructure;
- the planning, location, scale and cost of the deterministic-driven sequestration system;
- the total cost to install and operate the capture, transport, sequestration infrastructure;
- the adaptive, uncertainty-dependent upper bound of local geological potential for storage;
- the planning, location, scale and consequent risk of the uncertainty-driven sequestration system;
- the differential flowrates that may be generated (i.e., surplus and deficit) between the deterministic and the uncertainty-driven sequestration stage;
- the total risk generated by uncertainty according to the planning features and the location of the sequestration infrastructure.

In particular, this study addresses the problem of storage uncertainty by aim of two different formulations: a single stage MILP model (1s) (Figure 3.1) and a two stage MILP-LP model (2s) (Figure 3.2), both evaluating risk in geological storage capacity. The following Sections will describe the modelling framework and, specifically, the key aspects related to the formulations of model 1s and 2s.

3.2.1 Single stage MILP model

Model 1s addresses uncertainty through a unique objective function that aims to minimise over samples j the total cost for capture, transport and sequestration, including total financial risk generated by the sequestration stage. For this purpose, an innovative adaptive (i.e., both decision-dependent and time-dependent) methodology is implemented for the calculation of risk. In fact, risk is dependent on: (i) the strategic planning of storage sites; (ii) the deterministic minimum and maximum upper bounds for local storage availability; and (iii) a multi-sampling procedure for

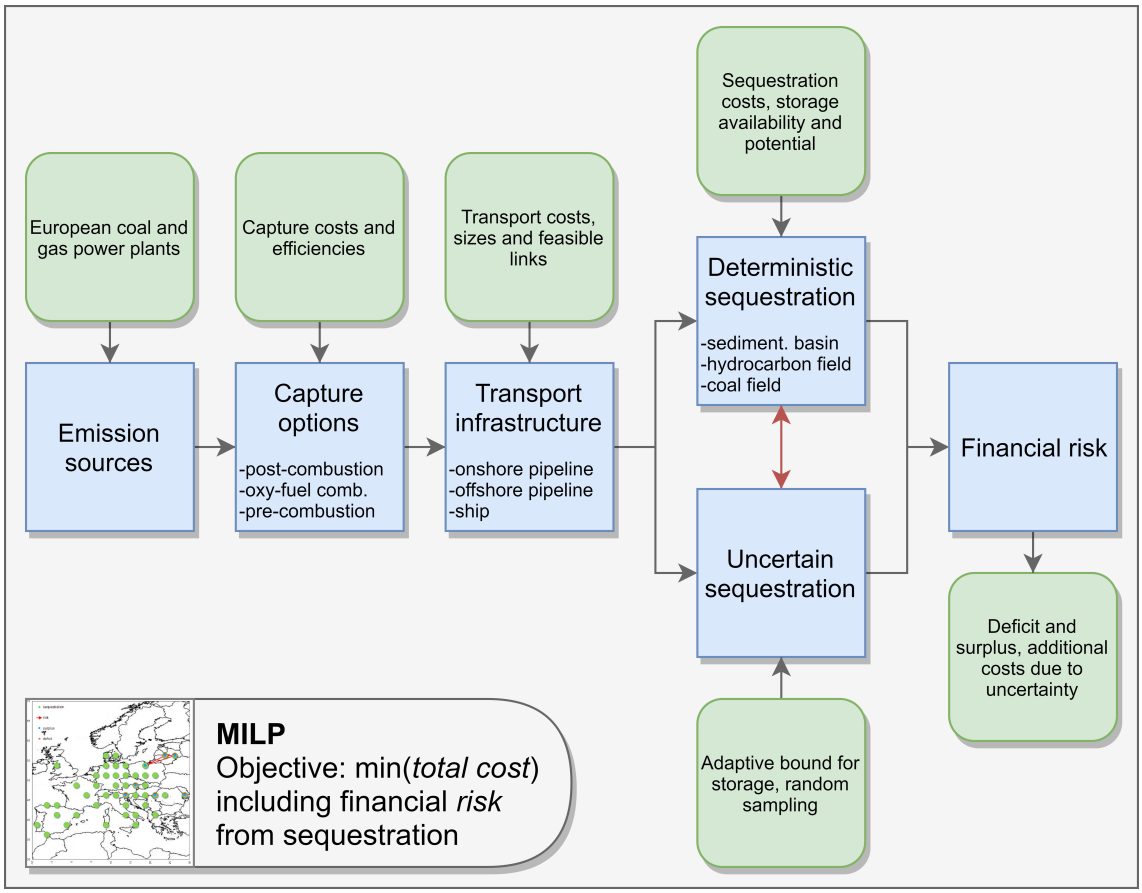

Fig. 3.1: Basic operating principle of model 1s

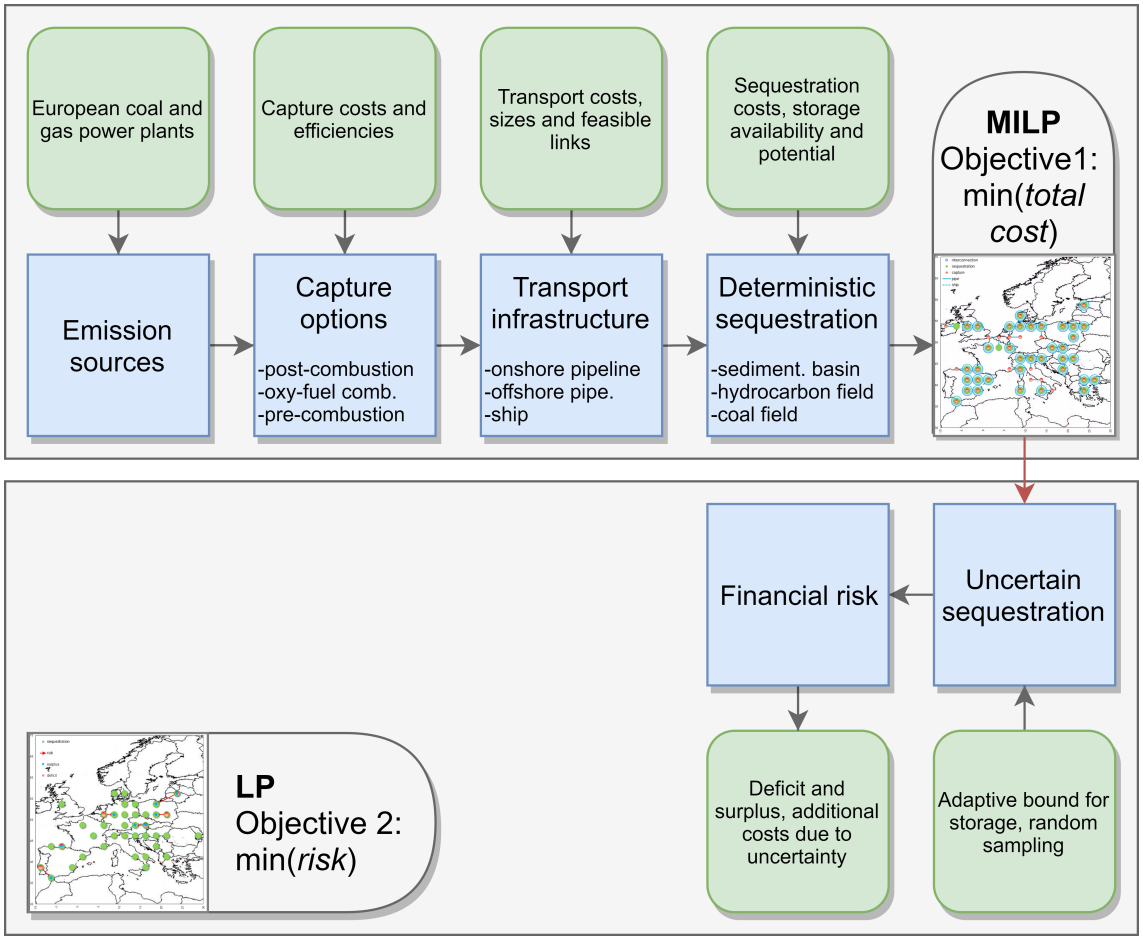

Fig. 3.2: Basic operating principle of model 2s

the random generation of minimum upper bounds within the likely range of local geological potential. It is likely that the geological volume availability of a basin varies substantially as a result of the incorporation of uncertainties. Thus, the model is capable of quantifying, for a given sample size N_j, quantitative differences between the volumes stored in the deterministic sequestration stage and those stored in the uncertain sequestration stage. Such discrepancies in stored quantities (described in terms of deficits and/or surpluses of CO_2) must therefore, be balanced among the regions and transported between basins s and/or between regions g, and its corresponding costs must be evaluated accordingly. Thus, financial risk is calculated in terms of potential additional transport costs that may emerge as a consequence of uncertainty on geological storage capacities. The basic operating principle of this MILP optimisation under uncertainty is the following: the CCS network (i.e., entailing the deterministic stages of capture, transport and sequestration) is optimised (in terms of total costs that occur to install and operate the overall network) considering the discrepancies between the deterministic- and the uncertainty-resulting stored volumes, which may determine the existence of either a sequestration deficit or surplus in basin s within region g. Accordingly, the model minimises both the additional inter-regional and intra-regional transport of CO_2 flowrates generated as a consequence of storage deficits. Financial risk is minimised together with other costs, and is defined here as the total costs that are required to nullify a potential release of CO_2 due to a lack of storage volume availability in a particular basin. A comprehensive description of the mathematical formulation is given subsequently.

3.2.2 Two stage MILP-LP model

Model 2s addresses uncertainty in the storage availability of basin s in European region g according to a sequential optimisation procedure. Stage I entails a MILP mathematical framework for the economic optimisation of a European CCS SC. It is optimised according to deterministic data on storage volumes as shown in Chapter 2. The quantitative results in terms of spatially-explicit geological sequestration are the CO_2 sequestered amount and the planning features of the site (i.e., the year in which injection starts and continues being performed). These variables are all stored for stage II, which evaluates risk by comparing the deterministic storage features with those resulting from the uncertain sequestration model. In fact, stage II optimises a multi-sampling LP model that aims at minimising the financial risk generated by potential deficit (i.e., loss) or surplus (i.e., gains). Overall, this model evaluates the financial risk related to the uncertainty on storage volumes for the optimal economic CCS SC configuration that was determined deterministically in the absence of uncertainty. In particular, stage I constitutes the upper bound for the local theoretical storage capacity of stage II in which, conversely, the actual geological potential is in general unknown, and is therefore randomly chosen (for each basin s in region g) within the range given by literature (Tables 2.6,2.7). The

mathematical procedure is reported subsequently.

3.3 Mathematical formulation

3.3.1 Single stage MILP model

The objective of the single stage MILP model is the total cost minimisation (TC [€]) of the entire CCS SC network, where the risk generated by uncertainty is included to produce an overall objective function which is minimised:

$$\begin{cases} objective = min(TC) \\ TC = TCC + TTC + TSC + risk_j \qquad \forall j, loop \\ s.t. \\ capture\ problem\ model \\ transport\ problem\ model \\ deterministic\ sequestration\ problem\ model \\ + \\ uncertain\ sequestration\ problem\ model \\ logical\ constraints \end{cases} \tag{3.1}$$

In particular, the capture problem model defines the quantity $C_{k,g,t}$ [t of CO_2/year] of CO_2 that is captured through technology k in region g at time period t and, consequently, evaluates the total capture cost TCC [€] of Eq.(3.1). Similarly, the transport problem model determines the total transport cost TTC [€] of Eq.(3.1) by evaluating the total flowrate $Q_{g,l,g',t}$ [t of CO_2/year] that is transported through mean l at time period t according to the mass balance between region g and region g'. Both the capture problem model and the transport problem model are unchanged with respect to Chapter 2. Conversely, the sequestration stage and in particular the quantification of its related uncertainty are the key features of the modelling formulation proposed in this Chapter 3. Accordingly, both the deterministic sequestration model (determining total sequestration cost TSC [€] of Eq.(3.1)) and the uncertain sequestration model (quantifying $risk$ [€] of Eq.(3.1)), as well as the description of risk-related logical constraints (describing the planning and operation of injection sites through binary decision variables) will be discussed in the following.
According to the results from mass balances that are defined in Chapter 2 for the inter-connection transport between regions g and g', deterministic quantities $S^D_{s,g,t}$ [t of CO_2/year] of CO_2 are set to be stored in chosen basin s in region g at time period t. These quantities are constrained to be lower than the deterministic upper bound for geological sequestration $S^{D,max}_{s,g}$ [t of CO_2] (Table 2.7) on basin s in region g:

$$\sum_t S^D_{s,g,t} \leq S^{D,max}_{s,g} \qquad \forall s, g \tag{3.2}$$

Then, the number of injection wells $N_{s,g,t}$ that is needed on basin s in region g at time period t to sequester the quantity $S^D_{s,g,t}$ can be evaluated according to the

maximum capacity S^{max} [t of CO_2] of each single well described in Chapter 2:

$$N_{s,g,t} = \frac{S^D_{s,g,t}}{S^{max}} \qquad \forall s, g, t \tag{3.3}$$

Given $N_{s,g,t}$ by Eq.(3.3), the total sequestration costs (TSC) required to install and operate the injection wells are determined as follows:

$$TSC = \sum_{s,g,t} (N_{s,g,t} \cdot USC_g) \tag{3.4}$$

where the unitary sequestration cost USC_g [€/well] for each region g depends on capital charge, operation and maintenance cost rates, and on the local injection depth of the basin, as detailed in Chapter 2.
Uncertainty is then introduced through a purposely designed methodology that aims at evaluating regional sequestration potential (and minimising its associated risk) on the basis of a multi-sampling strategy. The random sampling is obtained through the Mersenne Twister algorithm (Rubinstein and Kroese, 2017), which generates random values with uniform probability distribution between the deterministic minimum and upper bounds for local storage potential. Analogously to Eq.(3.2), that determined the deterministic regional upper bound for storage, the uncertainty-dependent decision variable for sequestration $S^U_{j,s,g,t}$ [t of CO_2/year] for sample j on basin s in region g at time period t is constrained to be lower than the maximum local storage availability $S^{U,max}_{j,s,g}$ [t of CO_2] for sample j on basin s in region g:

$$\sum_t S^U_{j,s,g,t} \leq S^{U,max}_{j,s,g} \qquad \forall j, s, g \tag{3.5}$$

Nevertheless, differently from the deterministic approach, the upper bound $S^{U,max}_{j,s,g}$ of Eq.(3.5) is not a fixed parameter, but is calculated by summing the yearly adaptive storage potentials $S^{U,max}_{j,s,g,t}$ [t of CO_2/year] for sample j on basin s in region g at time period t:

$$S^{U,max}_{j,s,g} = \sum_t S^{U,max}_{j,s,g,t} \qquad \forall j, s, g \tag{3.6}$$

Indeed, $S^{U,max}_{j,s,g,t}$ of Eq.(3.6) is evaluated according to the actual timing of the injection, i.e. given the chosen year t in which the sequestration starts on basin s in region g and the number of years in which the site is active:

$$S^{U,max}_{j,s,g,t} = S^{U,min}_{j,s,g} \cdot Y^{start}_{j,s,g,t} + 0.1 \cdot (S^{D,max}_{s,g} - S^{U,min}_{j,s,g}) \cdot Y^{keep}_{j,s,g,t} \qquad \forall j, s, g, t \tag{3.7}$$

where $S^{U,min}_{j,s,g}$ [t of CO_2] of Eq.(3.7) is the matrix of uncertain minimum values of upper bound of local sequestration potential, and is constituted (for every j, each basin s and each region g) by random values comprised within the deterministic range $[S^{D,min}_{s,g}, S^{D,max}_{s,g}]$. Furthermore, $Y^{start}_{j,s,g,t}$ and $Y^{keep}_{j,s,g,t}$ of Eq.(3.7) are binary decision variables that define, respectively, when the injection starts and/or continues being performed for sample j on basin s in region g at time period t. Overall, Eq.(3.7) defines the uncertainty in sequestration potential through $S^{U,max}_{j,s,g,t}$, thus according to

two contributions: (i) a precautionary base storage potential preventively defined at the beginning of the storage operations according to $Y^{start}_{j,s,g,t}$; and (ii) the possibility of a yearly rate of increase in the confidence on the actual availability of storage as far as the injection is performed according to $Y^{keep}_{j,s,g,t}$. As a result, the local storage availability is forced to increase from the randomly generated worst case $S^{U,min}_{j,s,g}$ toward the best deterministic upper bound $S^{D,max}_{s,g}$ if it is considered to exploit a certain basin s in region g for several years t. The rate of increase is fixed equal to 0.1 [year^{-1}] so as to allow, by exploiting the overall 10 years' time horizon, the theoretical possibility of reaching the best deterministic upper bound $S^{D,max}_{s,g}$ (but clearly at the cost of generating risk for more years).
Having defined $S^{U}_{j,s,g,t}$ according to the adaptive upper bound $S^{U,max}_{j,s,g,t}$, it is possible to compare the uncertain sequestration model with the deterministic storage capacity $S^{D}_{s,g,t}$ that was previously calculated through Eq.(3.2):

$$S^{U}_{j,s,g,t} = S^{D}_{s,g,t} - S^{deficit}_{j,s,g,t} + S^{surplus}_{j,s,g,t} \qquad \forall j,s,g,t \tag{3.8}$$

where $S^{deficit}_{j,s,g,t}$ [t of CO_2/year] and $S^{surplus}_{j,s,g,t}$ [t of CO_2/year] are variables that define, for every j, the differences between the uncertain and the deterministic amounts of CO_2 that are stored on basin s in region g at time period t. If for sample j, a basin s in region g presents at time period t a value of $S^{U}_{j,s,g,t} \geq S^{D}_{s,g,t}$, this implies that $S^{surplus}_{j,s,g,t} \geq 0$ is generated in region g (and in this case g is potentially capable of receiving a deficit from g'). Conversely, when $S^{U}_{j,s,g,t} \leq S^{D}_{s,g,t}$, then $S^{deficit}_{j,s,g,t} \geq 0$, implying that a deficit occurs in region g (and must be transported to g' in which a surplus will be generated). Accordingly, these quantities must be transported from region g to g' according to a differential mass balance:

$$\sum_{s} S^{deficit}_{j,s,g,t} + \sum_{g'} \Delta Q_{j,g',g,t} = \sum_{g'} \Delta Q_{j,g,g',t} + \sum_{s} S^{surplus}_{j,s,g,t} \qquad \forall j,g,t \tag{3.9}$$

The variable $\Delta Q_{j,g,g',t}$ [t of CO_2/year] represents the flowrates of CO_2 that must be transported for sample j between region g and g' at time period t according to sequestration discrepancies between the deterministic and the uncertain models. Note that the flowrates $\Delta Q_{j,g,g',t}$ of previous equation are merely generated by uncertainty in storage capacities and, therefore, they are evaluated differently from those of the deterministic transport infrastructure (reported in the transport problem model in Chapter 2). Indeed, the associated $risk^{inter}_{j,g,t}$ [€/year] can be defined, for every j in region g at time period t, as the additional cost (i.e., with respect to that for transport of the deterministic SC model) to install and operate further inter-connection transport links between region g and g' according to the additional flowrates $\Delta Q_{j,g,g',t}$:

$$risk^{inter}_{j,g,t} = \sum_{g'} \left(\Delta Q_{j,g,g',t} \cdot LD_{g,g'} \cdot \tau_g \cdot \bar{UTC}\right) \qquad \forall j,g,t \tag{3.10}$$

In particular, $\bar{UTC}$ [€/t of CO_2/km] represents the average unitary cost for transport (Chapter 2), $LD_{g,g'}$ [km] is the linear distance between region g and g' and

τ_g is a tortuousity factor for region g (Table 2.2). Thus, $risk^{inter}_{j,g,t}$ describes the economic penalties of transporting CO_2 flowrates between region g and region g', independently from the specific basins s that are chosen in origin or destination. On the other hand, risk related to the intra-connection transport within region g of a $S^{deficit}_{j,s,g,t} > 0$ is taken into account through the variable $risk^{intra}_{j,g,t}$ [€/year]:

$$risk^{intra}_{j,g,t} = \sum_{s} (S^{deficit}_{j,s,g,t} \cdot LD_g \cdot \tau_g \cdot U\bar{T}C) \qquad \forall j, g, t \tag{3.11}$$

As expected, $risk^{intra}_{j,g,t}$ describes the economic expenditure as a result of transporting CO_2 between different basins s within the same region g. Finally, total $risk$ [€] is given by its average value over the chosen sample size N_j, and takes into account both the contribution of risk related to the inter-connection system between region g and g' and of that related to the intra-connection within cell g:

$$risk = \sum_{j,g,t} \frac{risk^{inter}_{j,g,t} + risk^{intra}_{j,g,t}}{N_j} \tag{3.12}$$

Regarding the logical constraints reported in Eq.(3.1), they define the relations between the binary decision variables $Y^{start}_{j,s,g,t}$ and $Y^{keep}_{j,s,g,t}$ that were employed in Eq.(3.7) for the calculation of the adaptive $S^{U,max}_{j,s,g,t}$. $Y^{start}_{j,s,g,t}$ defines whether the injection of CO_2 begins for sample j on basin s in region g at time period t, or not. Therefore, it must be imposed that, for every j on basin s in region g, at most 1 starting point can be planned along the time horizon t:

$$\sum_{t} Y^{start}_{j,s,g,t} \leq 1 \qquad \forall j, s, g \tag{3.13}$$

$Y^{keep}_{j,s,g,t}$ indicates whether it is planned to keep (i.e., to continue) the injection for sample j on basin s in region g at time period t, or not. Accordingly, the overall planning of the sequestration site is given by $Y_{j,s,g,t}$, which describes if injection takes place for sample j on basin s in region g at time period t:

$$Y_{j,s,g,t} = Y^{start}_{j,s,g,t} + Y^{keep}_{j,s,g,t} \qquad \forall j, s, g, t \tag{3.14}$$

In particular, the previous equation defines, at time period t, whether it is planned that the injection starts (i.e., $Y_{j,s,g,t} = Y^{start}_{j,s,g,t}$), or that the injection is continuing (i.e., $Y_{j,s,g,t} = Y^{keep}_{j,s,g,t}$), or that no injection is planned at all (i.e., $Y_{j,s,g,t} = 0$). Then, the binary decision variable $Y_{j,s,g,t}$ is linked with the actual presence of a sequestration structure for sample j on basin s in region g at time period t, according to the maximum deterministic amount $S^{D,max}_{s,g}$ of storage availability (that constitutes the big-M constraint for decisional planning):

$$S^{U,max}_{j,s,g,t} \leq Y_{j,s,g,t} \cdot S^{D,max}_{s,g} \qquad \forall j, s, g, t \tag{3.15}$$

Furthermore, it is also necessary to introduce a binary variable $Y^{end}_{j,s,g,t}$, that defines whether injection has just finished for sample j on basin s in region g at time period

t	1	2	3	4	5	6	7	8	9	10
Y	0	0	1	1	1	1	1	0	0	0
Y^{start}	0	0	1	0	0	0	0	0	0	0
Y^{keep}	0	0	0	1	1	1	1	0	0	0
Y^{end}	0	0	0	0	0	0	0	1	0	0

Fig. 3.3: Example of general planning scheme for sequestration for sample j on basin s in region g at time period t, and consequent values assumed by decision variables $Y_{j,s,g,t}$, $Y^{start}_{j,s,g,t}$, $Y^{keep}_{j,s,g,t}$ and $Y^{end}_{j,s,g,t}$.

t (i.e., sequestration has been actively performed until the previous year $t-1$), or not. Analogously to the starting point, also the planning of $Y^{end}_{j,s,g,t}$ must be at most equal to a value of 1 over the time horizon for every j on basin s in region g:

$$\sum_{t} Y^{end}_{j,s,g,t} \leq 1 \qquad \forall j,s,g \tag{3.16}$$

The need for the implementation of the decision variable $Y^{end}_{j,s,g,t}$ is justified by the necessity of imposing that even the most general planning scheme (Figure 3.3) can be contemplated as a solution of the optimisation, i.e. that $Y^{start}_{j,s,g,t}$ assumes unitary value only at the effective beginning of the sequestration and that $Y^{keep}_{j,s,g,t}$ can become null even when it is eventually chosen to plan the end of sequestration before the end of the time horizon:

$$Y^{keep}_{j,s,g,t} - Y^{keep}_{j,s,g,t-1} = Y^{start}_{j,s,g,t-1} - Y^{end}_{j,s,g,t} \qquad \forall j,s,g,t \tag{3.17}$$

3.3.2 Two stage MILP-LP model

In the two stage model, the objective of the MILP model (stage I) is the total cost minimisation (TC [€]) of the entire deterministic CCS SC network in the absence of uncertainty (i.e., the deterministic model described in Chapter 2). However, the subsequent LP model (stage II) focuses on the quantification of uncertainty related to the sequestration stage:

$$\begin{cases} objective^{I} = min(TC) \\ TC = TCC + TTC + TSC \\ s.t. \\ capture\ problem\ model \\ transport\ problem\ model \\ deterministic\ sequestration\ model \end{cases} \tag{3.18}$$

$$\begin{cases} objective^{II} = min(risk_j) \quad \forall j, loop \\ s.t. \\ uncertain\ sequestration\ model \end{cases} \tag{3.19}$$

The objective of stage II is the total risk minimisation ($risk$), which is calculated analogously to the single stage model through Eq.(3.12), therefore according to the contribution of both inter-connection between regions g and g' (through $risk^{inter}_{j,g,t}$) and intra-connection within basins in cell g (through $risk^{intra}_{j,g,t}$). Again identically to the previously described single stage model, the transported flowrates $\Delta Q_{j,g,g',t}$ and the storage surplus ($S^{surplus}_{j,s,g,t}$) or deficit ($S^{deficit}_{j,s,g,t}$) for sample j on basin s in region g at time period t are determined through the same mass balance as reported in Eq.(3.9). In contrast, the peculiar feature of the two stage formulation is that both deficit and surplus are evaluated by comparing the deterministic amounts of CO_2 ($S^{I}_{s,g,t}$ [t of CO_2/year]) that are sequestered on basin s in region g at time period t in stage I, with those quantities $S^{II}_{j,s,g,t}$ [t of CO_2/year] that are actually stored in stage II:

$$S^{II}_{j,s,g,t} = S^{I}_{s,g,t} - S^{deficit}_{j,s,g,t} + S^{surplus}_{j,s,g,t} \qquad \forall j, s, g, t \tag{3.20}$$

According to the previous equation, if the quantity $S^{I}_{s,g,t}$ that was sequestered in stage I exceeds the local maximum storage availability for that specific j, a positive amount $S^{deficit}_{j,s,g,t}$ is then generated and must therefore, be transported to another region $g' \neq g$ as defined through Eq.(3.9). Alternatively, a region g can receive an amount $S^{surplus}_{j,s,g,t}$ and, overall, financial risk is therefore generated. Given a certain sample j, $S^{II}_{j,s,g,t}$ is to be intended as a net sequestration potential that comes from the consequences of both deficit and surplus of CO_2 from stage I. Furthermore, Eq.(3.20) allows for the possibility to move CO_2 flowrates between basins s that are located within the same region g.

The upper bound for the actually sequestered amount $S^{II}_{j,s,g,t}$ for sample j on basin s in region g is given by:

$$\sum_t S^{II}_{j,s,g,t} \leq \sum_t [S^{U,min}_{j,s,g} \cdot Y^{start,I}_{s,g,t} + A^{tune} \cdot (S^{D,max}_{s,g} - S^{U,min}_{j,s,g}) \cdot Y^{keep,I}_{s,g,t}] \qquad \forall s, g, t \tag{3.21}$$

where $S^{U,min}_{j,s,g}$ of Eq.(3.21) is defined analogously to the single stage problem as the matrix of uncertain minimum values of upper bound of local sequestration potential, and is constituted (for every j, each basin s and each region g) by random volumes comprised within the deterministic range $[S^{D,min}_{s,g}, S^{D,max}_{s,g}]$ (Tables 2.6,2.7). On the other hand, Eq.(3.21) represents the adaptive behaviour of the uncertain upper bound for local storage through the planning binaries $Y^{start,I}_{s,g,t}$ and $Y^{keep,I}_{s,g,t}$, as they result from stage I for each basin s in region g that is employed at time period t for storage of CO_2. Furthermore, a tuning parameter $0 \leq A^{tune} \leq 0.1$ is implemented in this stage, in order to consider the possibility to exclude (or restrict) the adaptive component in the calculation of the uncertain upper bounds for storage. The reason for accounting for this possibility in the evaluation of $S^{II}_{j,s,g,t}$ is given by the intrinsic architecture of the two stage formulation: differently from the single

stage model (which implies a simultaneous foresight planning of both deterministic aspects and risk), the two stage model minimises risk with the benefit of hindsight, i.e. on the basis of the best economic SC obtained in the absence of uncertainty. Accordingly, A^{tune} is here introduced in order to take into account every possible financial scenario that may emerge as a consequence of the risk generated by an already set SC configuration. Results reported in subsequently have been firstly calculated by setting as a reference case $A^{tune} = 0$ (i.e., worst case scenario of risk evaluation) in order to be both conservative and precautionary in the evaluation of financial risk.
Then, the overall European stored amount of CO_2 in stage II is constrained to be yearly identical to the total sequestered amount in stage I for every j:

$$\sum_{s,g} S^{II}_{j,s,g,t} = \sum_{s,g} S^{I}_{s,g,t} \qquad \forall j,t \tag{3.22}$$

The previous equation imposes that the European sequestered CO_2 must be identical between stages I and II, in order to meet the carbon reduction target α (i.e., the ratio between the total amount of sequestered CO_2 and the overall European emissions from large stationary sources).

3.3.3 Summary

Figure 3.4a illustrates the mathematical formulation of the single stage MILP model. The deterministic uncertainty model deals with the definition of the captured ($C_{k,g,t}$), transported ($Q_{g,l,g',t}$) and sequestered ($S^{D}_{s,g,t}$) quantities of CO_2, the latter calculated according to deterministic input data in terms of local sequestration potential ($S^{D,max}_{s,g}$). As a result, TCC, TTC and TSC are evaluated and optimised within the objective function that aims at TC minimisation. Concurrently, the deterministic sequestered amount ($S^{D}_{s,g,t}$) is compared with that deriving from the uncertain sequestration problem ($S^{U}_{j,s,g,t}$). The uncertain geological volume is determined according to an adaptive upper bound for local sequestration potential ($S^{U,max}_{j,s,g,t}$), which depends on the planning features of the site itself ($Y_{j,s,g,t}$, defined by $Y^{start}_{j,s,g,t}$, $Y^{keep}_{j,s,g,t}$, and $Y^{end}_{j,s,g,t}$), and is also derived according to both deterministic ($S^{D,min}_{s,g}$) and randomly generated ($S^{U,min}_{j,s,g,t}$) data on local storage potential. The eventual presence of a surplus ($S^{surplus}_{j,s,g,t}$) and/or of a deficit ($S^{deficit}_{j,s,g,t}$) generates either new CO_2 flowrates ($\Delta Q_{j,g,g',t}$) between regions g and g' or intra-cell additional transport nodes between basins, that can be quantified in economic terms to provide financial $risk_{j,g,t}$. Then, the total $risk$ generated by uncertainty in storage capacity is optimised within the objective function in order to minimise TC (both deterministic and uncertain components) of the CCS SC.
Similarly, the mathematical formulation of the two stage MILP-LP model is summarised in Figure 3.4b. Here, the deterministic model is purposely optimised in a specific stage I that aims at total cost TC minimisation excluding any uncertainties. Accordingly, the sequestered amount $S^{I}_{s,g,t}$ and the planning binaries $Y^{start,I}_{s,g,t}$ and

$Y^{keep,I}_{s,g,t}$ are determined and given as an input for the calculation of the uncertain stored volume $S^{II}_{j,s,g,t}$ in stage II (Figure 3.4b reports the case in which $A^{tune} = 0$). The presence of either a surplus ($S^{surplus}_{j,s,g,t}$) or a deficit ($S^{deficit}_{j,s,g,t}$) must be balanced and transported according to a positive $\Delta Q_{j,g,g',t}$ and $risk$ is therefore, generated and minimised for every j.

3.4 Results and discussion

3.4.1 Scenarios

The CCS SC optimisation under uncertainty minimises cost and risk given the spatial distribution of CO_2 sources and the techno-economic parameters related to capture options, transport modes and sequestration basins. Results will be presented and analysed using three different scenarios. Scenario 0 optimises the SC network in the absence of uncertainty, using nominal storage capacities for all basins. Accordingly, in Scenario 0 risk is not included within the objective function, which coincides with the risk neutral optimisation of stage I from model 2s. Scenario A optimises the CCS SC under uncertainty in storage capacity with the aim to achieve (constantly throughout a 10 years' time framework) a European carbon reduction target $\alpha = 50\%$ of CO_2 emissions from large stationary sources (EC, 2018). Uncertainty is approximated by $10 \leq N_j \leq 400$ random samples in order to test the efficacy of the proposed mathematical formulation. Results from Scenario A are compared with those from Scenario 0, with the aim of quantifying the effects of uncertainty in storage capacity on the optimal planning and operation of a CCS SC. Then, Scenario B investigates how the choice in the minimum carbon reduction target $10\% \leq \alpha \leq 70\%$ affects the uncertainty-driven network in terms of both costs and risk. The main optimisation outputs are reported in Table 3.1. Regarding model 2s, Scenarios A-B are optimised setting $A^{tune} = 0$, a parameter that describes the increase of confidence in the storage capacity as a consequence of the planning features of the injection site itself. Then, the response of model 2s on the variation of A^{tune} between 0 and 0.1 is investigated. Furthermore, models have been verified by aim of two additional scenarios, dealing with a test on the extension of the time horizon to 20 years (i.e., Scenario C), and a test on legal restrictions on CO_2 onshore sequestration (i.e., Scenario D). Both models were implemented in the GAMS software and optimised using the CPLEX solver on a 24-Core cluster machine with 96 GB RAM, by imposing a maximum optimality gap of 2% for each sample/stage.

3.4.2 Choosing the sample size

From Scenario A it emerges that the two models have slightly different responses to the chosen sample size N_j, but in general they both achieve accurate results in

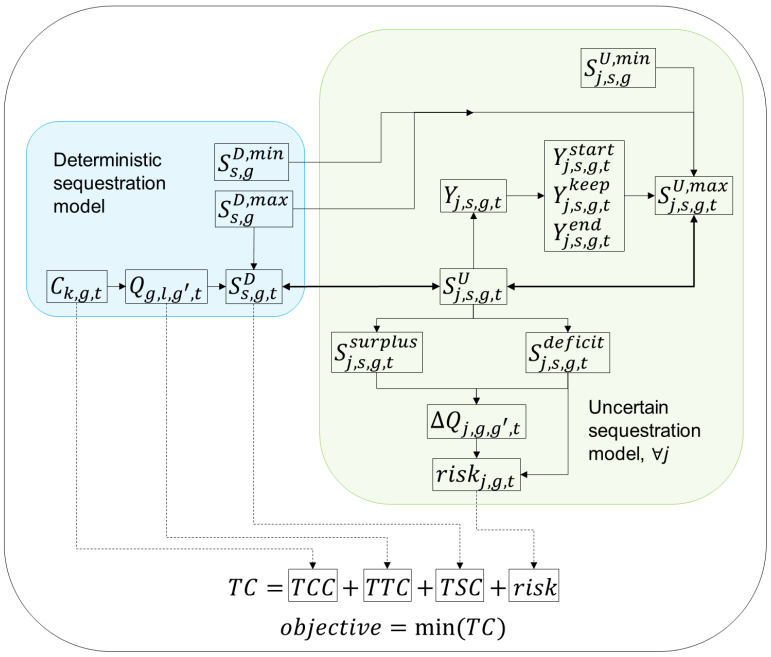

(a)

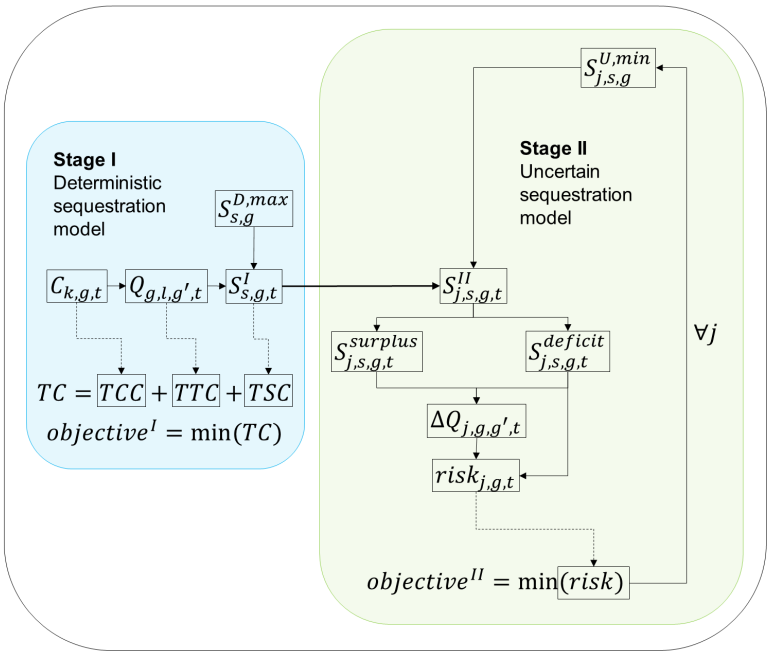

(b)

Fig. 3.4: Mathematical formulation of: (a) model 1s and (b) 2s.

Tab. 3.1: Results from model 1s and 2s (Scenario 0-A-B-C-D), according to the European carbon reduction target α [%] and to the sample size N_j: total cost TC [€/t of CO_2] (including $risk$), total capture cost TCC [€/t of CO_2], total transport cost TTC [€/t of CO_2] and $risk$ [€/t of CO_2]. Specific costs [€/t] are expressed in terms of total sequestered amount of CO_2.

Scenario	α [%]	N_j	TC [€/t]	TCC [€/t]	TTC [€/t]	TSC [€/t]	$risk$ [€/t]
2s-0	0.50	-	38.250	35.867	2.112	0.271	-
1s-A	0.50	10	38.299	35.716	2.287	0.295	0.000
1s-A	0.50	50	38.272	35.664	2.323	0.285	0.000
1s-A	0.50	100	38.302	35.637	2.377	0.287	0.000
1s-A	0.50	200	38.324	35.622	2.413	0.288	0.000
2s-A	0.50	50	38.373	35.867	2.112	0.271	0.123
2s-A	0.50	100	38.384	35.867	2.112	0.271	0.134
2s-A	0.50	200	38.376	35.867	2.112	0.271	0.126
2s-A	0.50	400	38.377	35.867	2.112	0.271	0.127
1s-B	0.10	100	32.319	29.568	2.470	0.282	0.000
1s-B	0.30	100	36.736	34.314	2.152	0.271	0.000
1s-B	0.50	100	38.302	35.637	2.377	0.287	0.000
1s-B	0.70	100	39.207	36.131	2.764	0.310	0.002
2s-B	0.10	100	32.826	30.189	2.204	0.425	0.008
2s-B	0.30	100	36.901	34.423	2.203	0.260	0.014
2s-B	0.50	100	38.384	35.867	2.112	0.271	0.134
2s-B	0.70	100	39.273	36.156	2.658	0.323	0.136
1s-C	0.50	100	38.773	35.679	2.814	0.281	0.000
1s-D	0.50	94	40.199	35.617	4.153	0.429	0.000
2s-D	0.50	100	40.936	35.530	4.990	0.416	0.038

Tab. 3.2: Results from model 1s and 2s (Scenario 0-A-B-C-D) in terms of computational performance according to the European carbon reduction target α [%] and to the sample size N_j: number of continuous variables, number of discrete variables and solution time [s].

Scenario	α [%]	N_j	Cont. var.	Disc. var.	Sol. time [s]
2s-0	0.50	-	8128879	82220	78
1s-A	0.50	10	83278800	822200	13187
1s-A	0.50	50	416394000	4111000	117202
1s-A	0.50	100	832788000	8222000	154497
1s-A	0.50	200	1665576000	16444000	301785
2s-A	0.50	50	18078929	82220	253
2s-A	0.50	100	28028979	82220	414
2s-A	0.50	200	47128879	82220	862
2s-A	0.50	400	87729279	82220	1624
1s-B	0.10	100	832788000	8222000	35581
1s-B	0.30	100	832788000	8222000	175320
1s-B	0.50	100	832788000	8222000	154497
1s-B	0.70	100	832788000	8222000	261500
2s-B	0.10	100	28028979	82220	464
2s-B	0.30	100	28028979	82220	420
2s-B	0.50	100	28028979	82220	414
2s-B	0.70	100	28028979	82220	687
1s-C	0.50	100	832788000	8222000	508777
1s-D	0.50	94	832788000	8222000	191432
2s-D	0.50	100	28028979	82220	632

as few as $N_j = 100$ (Figure 3.5). Therefore, from here onwards, $N_j = 100$ will be set as the reference sample size and the results will be presented and discussed accordingly. The present tuning allows reaching optimality within reasonable time limits (less than 2 days). As expected and independently from scenarios (Table 3.2), the computational effort required to solve model 1s is significantly larger than the case 2s. This can be explained by the fact that the simplified 2s formulation entails a much smaller amount of discrete variables than the optimisation of model 1s.

3.4.3 Forecasting flexibility for resilient networks

Model 1s aims at defining, over a 10 year time horizon, the optimal SC in terms of both cost and risk, and therefore provides those CCS configurations that are the most robust given the uncertainties in regional storage capacities. Appropriate sequestration basins are chosen not only as a consequence of the minimisation of transport and injection costs, but also given the eventual necessity of balancing the

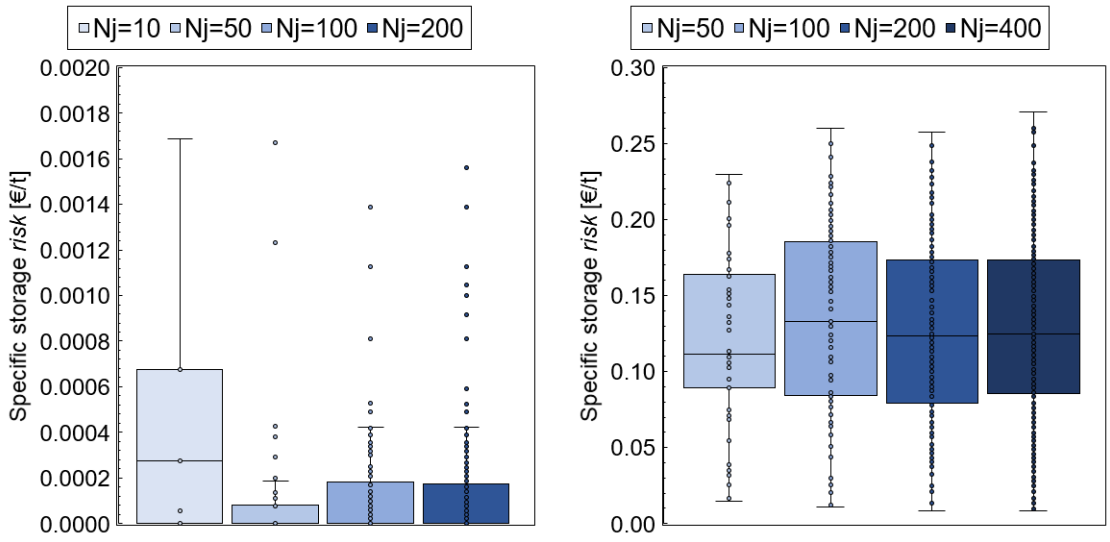

Fig. 3.5: Scenario A, comparison between models 1s (a) and 2s (b) on the dependency of the estimate of *risk* [€/t of CO_2] from the sample size N_j, given a carbon reduction target $\alpha = 50\%$.

future variations/re-routing induced by uncertainty in storage itself. It should be noted that this formulation assumes that a decision-maker has perfect information with respect to geological volumes upon the realisation of uncertainty in each distinct sample. Furthermore, the constraints for the calculation of the adaptive storage capacity additionally improve the implicit flexibility of the sequestration network, since the algorithm chooses those basins that are more likely to exhibit a good trade-off between 'being exploited for' and 'generating risk for' more consecutive years. Considering Scenario A (i.e., $\alpha = 50\%$), model 1s entails (Figure 3.6) a total cost TC for installing and operating the CCS system (including the contribution of financial risk) of 232.1 B€ (i.e., 38.302 €/t of sequestered CO_2), of which the major contribution is represented by the capture stage with a total cost TCC of 216.0 B€ (i.e., 35.637 €/t of sequestered CO_2). Interestingly, the transport cost TTC (with 14.4 B€, i.e. 2.377 €/t of sequestered CO_2) and the sequestration cost TSC (with 1.8 B€, i.e. 0.287 €/t of sequestered CO_2) constitute altogether only the 7.0% of TC. With respect to *risk*, its final value is negligible, thus from the optimisation of model 1s (in which risk is minimised along with the other costs) the best SC configuration emerges in terms of robustness to storage uncertainty. However, comparing the results with those from Scenario 0 (i.e., an equivalent risk-neutral network), despite having an almost identical total cost (+0.1% with respect to TC of Scenario 0), the cost of mitigating and ensuring low values of risk is reflected in slightly higher transport (+11.2% with respect to TTC of Scenario 0) and sequestration (+5.5% with respect to TSC of Scenario 0) costs. These additional infrastructural costs are the direct consequence of the choice of improving flexibility to minimise the contribution of risk to overall costs. Furthermore, results from Scenario B show

that model 1s provides optimal SC configurations with (almost) null values of risk for a wide range of carbon reduction targets ($\alpha \leq 70\%$).
Regarding the SC configuration resulting from model 1s under Scenario A (Figure 3.7a), the number of basins in which a deficit of storage may occur is minimised and in general it is strategically chosen to exploit the sequestration potential of a larger number of regions (and basins) compared to a deterministic SC (with the drawback of increasing transport costs). Accordingly, distributing the investment for storage across different European regions, and particularly exploiting those with abundancy of basins, is an effective hedging strategy when risk on storage volume availability is taken into account. On the other hand, when some risk is unavoidable, slightly risky basins are only chosen for storage in areas in which nearby regions are likely and able to receive a surplus of CO_2, in order to minimise additional transport costs. In fact, the regions near the Baltics and Northern Poland are the only areas in which storage risk necessitates the balancing of carbon deficits and surpluses, but the resulting potential flowrates are in the range of $33 \leq \Delta Q_{g,g',t} \leq 720$ kt of CO_2/year, therefore minimal with respect to the expected rates of CO_2 shipped yearly between regions (these comprised between 1 Mt of CO_2/year and 30 Mt of CO_2/year). Other deficits are scattered in Slovenia and near the Black Sea, but the CO_2 is diverted towards different basins within the same region and constitutes only a minor contribution to total economic risk, overall still negligible with respect to the total cost to install and operate the CCS network. Model 1s proves that it is possible to design an optimal CCS SC, which mitigates risk on storage capacity with just minor hedging design modifications in the sequestration network configuration and with a slight increase in infrastructure costs with respect to a deterministic equivalent risk-neutral network.

3.4.4 Resolving uncertainty as second stage decision

Model 2s is constituted by two sequential stages, reflecting two separated but consecutive levels of decision making. The first MILP optimises the CCS network as an initial planning by risk-neutral stakeholders in the absence of uncertainty, and therefore provides the best deterministic SC (that of Scenario 0). In this stage, risk is not included within the objective function, as if the stakeholders were not aware of any uncertainty on storage capacity. The resulting SC configuration (i.e., the overall capture, transport and sequestration network) is then given as an input to the second LP stage, in which risk is minimised by a subsequent revision of the sequestration operational decisions based on a sudden awareness of geological uncertainties. On the one hand, one aim of model 2s is to decrease the computational burden by treating uncertainty through a LP formulation. On the other hand, model 2s is capable of answering the following question: what is the amount of risk generated by the realisation of uncertainty on an already fixed European CCS SC? Results showed that under Scenario A (i.e., $\alpha = 50\%$), model 2s entails (Figure 3.6) a total cost TC

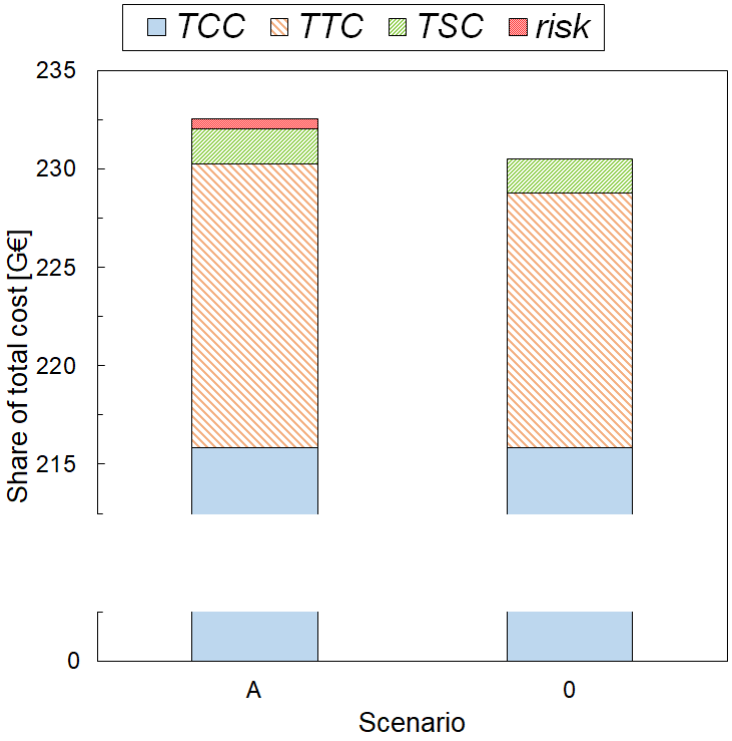

Fig. 3.6: Scenario A, comparison between models 1s and 2s on the share of TCC, TTC, TSC and $risk$ over TC.

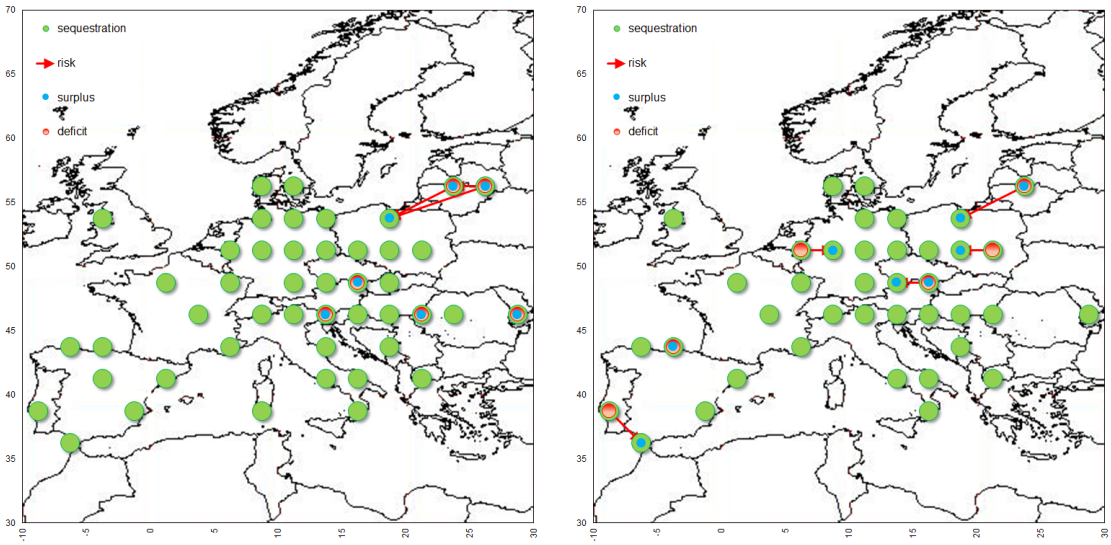

(a) *(b)*

Fig. 3.7: Resulting SC configuration from model 1s (a) and 2s (b): location of sequestration basins, deficits and surpluses of CO_2 and risk.

of 232.7 B€ (i.e., 38.384 €/t of sequestered CO_2), of which for capture (TCC) 217.4 B€ (i.e., 35.867 €/t of sequestered CO_2). The minor contribution of the transport and sequestration stages is noted, with TTC equal to 12.8 B€ (i.e., 2.112 €/t of sequestered CO_2) and a final TSC of 1.6 B€ (i.e., 0.271 €/t of sequestered CO_2). Conversely, from the optimisation of the second LP stage emerges a non-negligible value of $risk$ (809 M€, i.e. 0.134 €/t of sequestered CO_2), which proportionally increases up to 1.2 B€ (i.e., 0.136 €/t of sequestered CO_2) for $\alpha = 70\%$ in Scenario B. Nevertheless, considering the combined contributions of both costs and risk, the SC resulting from model 2s entails an almost identical total cost TC (+0.2% with respect to model 1s, extensively equal to 538 M€). Differently from model 1s, in model 2s the selection of the sequestration basins and regions is determined as a strategic choice from the first deterministic stage (Figure 3.7b). Accordingly, storage locations are chosen with the aim of minimising the deterministic costs of the CCS system, whereas risk is deliberately minimised through the subsequent second stage. As a result, risk is generated from the necessity of balancing deficits and surpluses of CO_2 between the Baltic States and Poland, within Poland, within Germany, between Czech Republic and Austria and between Portugal and Spain, with potential additional flowrates up to 2 Mt of CO_2/year each.

3.4.5 Measuring the confidence in volume availability

The results from model 2s are reliable even when it is chosen to change the value of the tuning parameter A^{tune}, defining whether to (also partially) omit the adaptive component in the calculation of the regional uncertain minimum upper bounds for sequestration. The reason for accounting for this possibility in the evaluation of stored volumes is given by the intrinsic architecture of the two stage formulation: in comparison to the single stage model (which implies a simultaneous foresight planning of both deterministic aspects and risk), the two stage model minimises risk with the benefit of hindsight, i.e. on the basis of the best economic SC obtained in the absence of uncertainty. Accordingly, A^{tune} is introduced here in order to take into account every possible financial scenario that may emerge as a consequence of the risk generated by a fixed SC configuration. Model 2s exhibits a $risk$ (Figure 3.8) that decreases from 809 M€ for $A^{tune} = 0$ ($risk$ is 49.2% of TSC) to a minimum of 63 M€ for $A^{tune} = 0.1$ ($risk$ is 3.8% of TSC), i.e. the latter is still higher than the negligible value that was found with model 1s. Independently from the selection of the tuning parameter A^{tune}, results from model 1s in terms of risk are consistently better than those from model 2s, even though the presence of uncertainty in storage capacity still represents at most a marginal contributor when comparing its effects with the overall costs of the CCS SC. This is a positive outcome, since the additional flexibility to deal with storage risk is never particularly expensive. Furthermore, it was verified that if it was chosen to implement A^{tune} in model 1s, results would entail a maximum value of risk (Scenario A, $A^{tune} = 0$) of 3 M€ (i.e., 0.001 €/t of

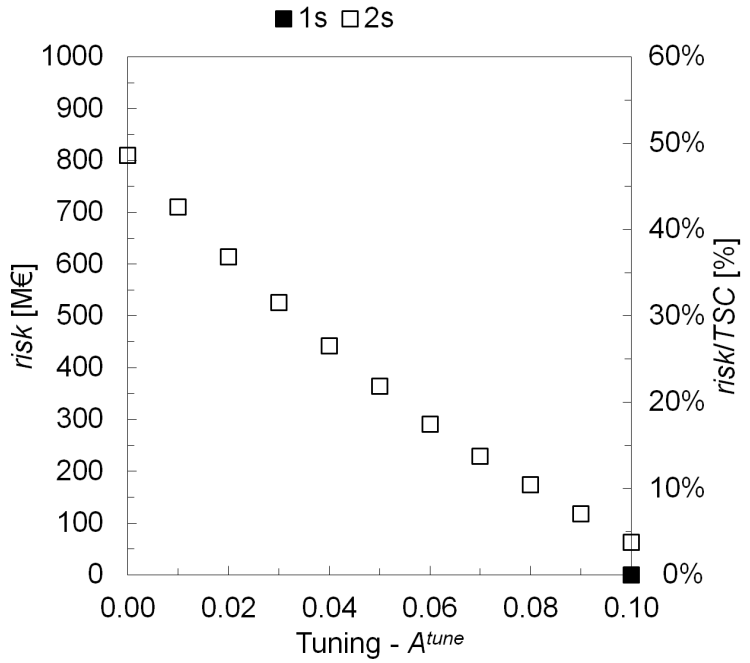

Fig. 3.8: Dependency on A^{tune} of $risk$ and on ratios of $risk/TSC$ for model 1s and 2s.

sequestered CO_2) with only minor modifications to the SC configuration, therefore still consistently lower than the minimum value of risk found for model 2s in the less precautionary configuration. In summary, even if a methodology that incorporates risk within the first planning decision is not considered initially, a two-level formulation might constitute a satisfactory solution, even though the consequences of rerouting pipelines and repositioning sequestration basins might lead to issues and difficulties that have not been investigated here (e.g., additional costs for authorisations and bureaucracy, insufficient time for the building of new transport links).

3.4.6 Assessing the effects of an extended time horizon

In order to test the efficacy of the proposed methodology, model 1s was tested on Scenario C, which entails the extension of the time horizon to 20 years (instead of 10 years in Scenario A). Results are reported in Table 3.1 and do not denote any particular quantitative difference in terms of risk with respect to the 10 years' Scenario A. Furthermore, the SC configurations reported in Figure 3.9a (Scenario A) and Figure 3.9b (Scenario C) confirm that it is possible to design optimally resilient European CCS networks even when an extended time horizon is considered in the study. The drawback of Scenario C is mainly computational, since the solution time, as reported in Table 3.2, is more than doubled with respect to the base-case Scenario A.

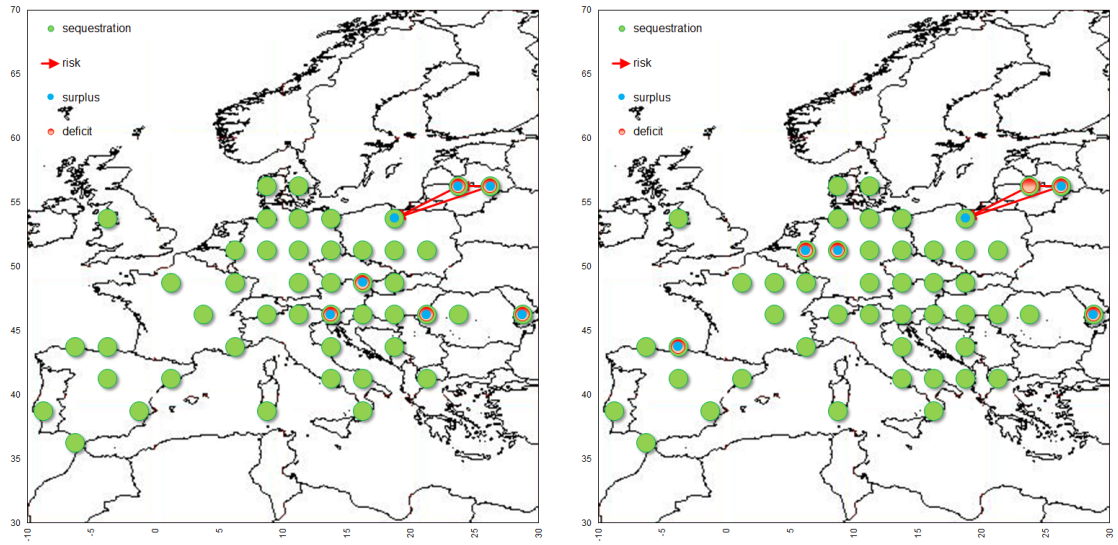

(a) (b)

Fig. 3.9: SC storage configuration for model 1s for (a) Scenario A and (b) Scenario C.

3.4.7 Assessing legal restrictions on onshore sequestration

Here we consider the fact that some countries either restrict (Czech Republic, Germany, Poland, Sweden, the Netherlands, and United Kingdom) or forbid (Austria, Croatia, Estonia, Ireland, Latvia, Finland and Belgium) onshore sequestration (EC, 2017). Even though United Kingdom, Poland and the Netherlands might be in the process of authorising it (EC, 2017), Scenario D prudently optimises the CCS SC while excluding all the aforementioned states from those in which onshore storage is allowed.

Results from model 1s under Scenario D (Table 3.1) show that regulations have negative effects on both transport TTC (i.e., +74.7%) and sequestration TSC (i.e., +49.5%) costs, despite the model is still capable of providing economically optimal SCs with negligible values of *risk*. Overall, the results from this test entail a total cost TC of 40.199 €/t of sequestered CO_2 (i.e., +5.0%). The reason for this additional infrastructure expenditures has to be found in the greater complexity of the resulting SC, which is a consequence of the necessity of transporting the CO_2 for longer distances since available basins are not homogeneously distributed across Europe (Figure 3.10a). Furthermore, the computational effort to solve Scenario D was larger than that of the base case Scenario A, with a solution time of more than 859 ks by employing the same cluster machine, and with 6% of sampling cases that did not provide any feasible solution within this time limit (these are excluded from the results reported in Table 3.1).

Regarding model 2s, Scenario D (Table 3.1) denotes an increase of total cost TC (+7.0% with respect to Scenario A), of transport costs TTC (+136.3% with respect to Scenario A), and of sequestration costs TSC (+53.3% with respect to Scenario A). Interestingly, risk is not particularly affected by the introduction of regulations

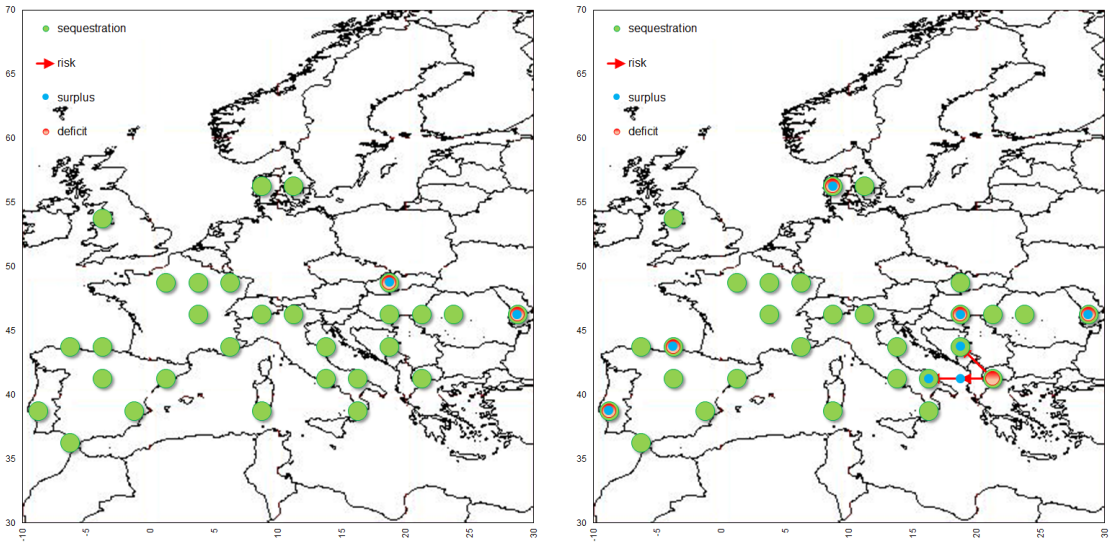

(a) (b)

Fig. 3.10: Scenario D, storage configuration for model 1s (a) and model 2s (b).

according to Scenario D, and its final value is even lower (and still negligible with respect to other costs) than that found for Scenario A. Similarly to model 1s, also model 2s entails a less homogenous exploitation of sequestration basins across Europe as a result of the legal restrictions on onshore storage (Figure 3.10b).
Overall, Scenario D proves that regulations and limitations on onshore CO_2 sequestration might have much larger effects on transport and sequestration costs than on risk, and therefore regional legal frameworks are more likely to affect the initial planning of a European CCS system rather than its deployment because of uncertainty in geological capacity.

3.5 Chapter conclusions

This Chapter explored the risks related to uncertainty in geological storage in the planning and operation of a European CCS SC. It was demonstrated the possibility to design optimal European CCS networks, while keeping the overall risk on storage to low values. In particular, financial risks due to geological uncertainties were found to be comparatively small because of the combination of: (i) abundancy and homogeneous distribution of basins across Europe, (ii) relative position of large emission clusters (more attractive for capture and transport than isolated point sources) with respect to basins. Accordingly, it was shown that only minor modifications should be taken into account with respect to the European deterministic CO_2 network as depicted in Chapter 2, in order to increase the level of flexibility of the transport infrastructure long enough to guarantee that uncertainty in storage capacity does not affect the final deployment of the overall system. The effects of uncertainty were quantified in terms of risk related to the necessity of installing further transport links

with respect to the risk-neutral solution of the model, with the aim of improving the intrinsic flexibility of European CO_2 infrastructure in relation to geological uncertainties. The proposed tool provides economically optimal network configurations resilient to risk and allows a decision-maker to understand the financial penalties associated with designing infrastructures in the absence of uncertainty, by quantifying the monetary consequences of dealing with uncertainty either in the initial planning of the system or as a second step reactive choice. The basins emerging here as more suitable (i.e., less risky) for storage would then require deeper analyses to assess their geo-physical characteristics.

From the results discussed within Chapter 3, it emerged the good resiliency of the European area on uncertainty in geological storage. However, apart from the strategic planning of an effective SC design, concerns from the public may constitute a main driver for the implementation of such networks. Chapter 4 will explore this issue, by proposing a societal risk-constrained European CCS SC optimisation, i.e. including the risk of a potential release of CO_2 from the pipeline system.

4

Societal risk and risk mitigation measures

4.1 Chapter summary

Although being practiced for over 30 years, CO_2 transportation is intrinsically characterised by the risk of leakage. Chapter 4 aims at assessing and tackling this issue within the CCS design problem, by proposing a spatially-explicit MILP approach for the economic optimisation of a European SC for CCS, where societal risk assessment is formally incorporated within the modelling framework[1]. Post-combustion, oxy-fuel combustion and pre-combustion are considered as technological options for CO_2 capture, whereas both pipelines (onshore and offshore) and ships are taken into account as transport means. Both inland-onshore and offshore injection options are available for carbon geological sequestration. Risk mitigation measures are considered in the design of the transport network. The overall SC is economically optimised for different minimum carbon reduction scenarios. Results demonstrate that accounting for societal risk may impact the overall carbon sequestration capacity, and that the proposed approach may represent a valuable tool to support policy makers in their strategic decisions.

[1] The content of this Chapter was published in: d'Amore et al., 2018a; 2018b.

4.2 Modelling framework

This work proposes a single objective, multi-echelon, time-static, spatially-explicit MILP model for the strategic design of a risk-constrained CCS SC within the European geographical context. The objective is the total cost minimisation, while simultaneously including societal risk analysis on CO_2 transport modes and implementing the possibility of installing specific risk mitigation measures on the resulting logistic network, according to the locally accepted level of societal risk. Furthermore, it is here introduced a probabilistic approach for considering different hazardous scenarios according to the type of failure of the pipeline. All the SC stages (i.e., capture, transport and sequestration) are simultaneously optimised within the mathematical framework. In order to decrease the computational burden, the time-period evolution of the SC is not considered, and only the final configuration is optimised. The spatial resolution is achieved by aim of a grid $g = [1, 2, 3, ..., 133, 134]$ discretising Europe mainland and offshore storage in the North Sea region (Fig. 2.2). The offshore and onshore storage potential are those reported in Tables 2.6,2.7. Capture technologies are introduced through a set of options k that includes post-combustion absorption from the flue gasses of coal-fired power plants, post-combustion absorption from the flue gasses of gas-fired power plants, oxy-fuel technology applied to coal-fired power plants, in which air separation is obtained for a nearly pure oxygen combustion, and pre-combustion, which entails the production of a hydrogen-rich syngas to fuel gas-fired facilities. Transport is described through a set of modes $l = [onshore\,pipeline, offshore\,pipeline, ship]$; flowrates are discretised according to a capacity set $p = [1, 2, ..., 6, 7]$ to speed up computing. The risk analysis is characterised by the implementation of different classes of scenarios $h = [i, ii, iii, iv]$ according to the magnitude of the hazard, whereas risk mitigation measures, whose selection may affect both societal risk and total cost of specific transportation paths, are included within a set of possible options $m = [none, marker\,tape, concrete\,slabs, deep\,burying, surveillance\,interval]$. All the input parameters for the CCS SC optimisation are retrieved from the scientific literature, except those related to the implementation of risk (which are calculated as detailed subsequently).
Overall, the strategic optimisation problem is formulated giving the following inputs (Figure 4.1):

- spatially-explicit features of European territories in terms of CO_2 emission sources;
- spatially-explicit features of European territories in terms of CO_2 onshore/offshore storage potential;
- minimum European CO_2 reduction target;
- technical and economic parameters of capture technologies k;

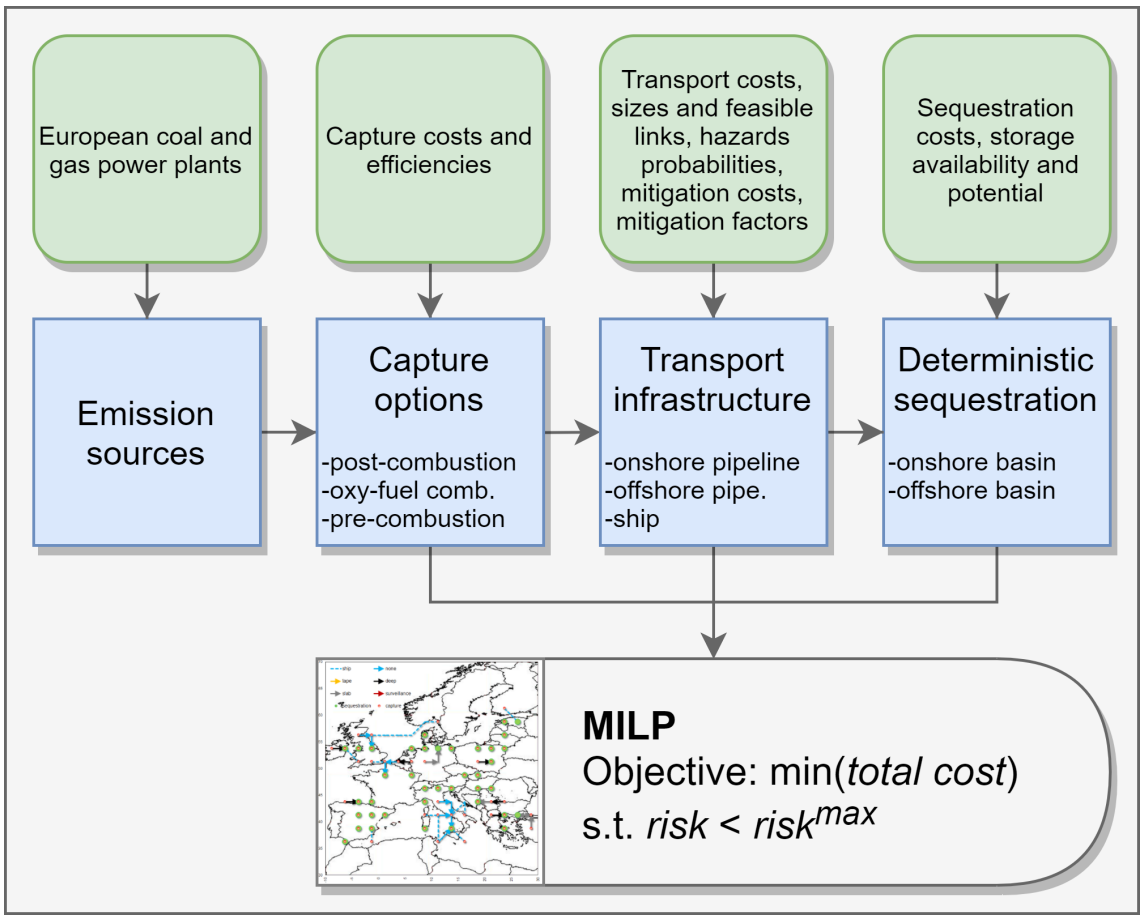

Fig. 4.1: Scheme of the multi-echelon CCS SC framework with quantitative analysis of societal risk and mitigation options. The objective is total cost minimisation subject to the constraint that societal risk is kept below a threshold of acceptability value. Risk mitigation measures can be installed and/or operated on the resulting CO_2 transport infrastructure.

- technical and economic parameters of transport options l;
- probabilistic classes of incident according to scenario h;
- technical and design parameters for societal risk calculation;
- spatially-explicit implementation of maximum societal risk acceptability;
- technical and economic parameters of risk mitigation options m.

The objective is to minimise the total cost for setting into motion and operating the European CCS network, while keeping societal risk below regional levels of acceptability. Therefore, the model output includes:

- location, scale and cost of capture sites, capture technologies selection;
- location, scale and cost of both onshore and offshore sequestration sites;
- design and cost of transport infrastructure, transport modes selection;
- total societal risk produced when operating the European CCS network;
- selection and cost of suitable risk mitigation measures;
- cost performance of the CCS SC according to locally accepted levels of societal risk;
- validation of the CCS model on different European CO_2 reduction targets.

4.2.1 Definition of societal risk

Societal risk, which was formally introduced in the nuclear industry for the reactor safety-related investigations (Rasmussen, 1975), is defined as the risk of health consequences related to the number of people (i.e., population) that may be affected by hazardous incidents h in a certain region g. This work discretises hazardous cases into different potential types h, according to the seriousness of the situation (Table 4.1). Given the previously discussed definition of societal risk, onshore pipelines only are considered for risk analysis, being the offshore and the ship options away from densely populated areas. Risk related to docking operations is not considered either, since the aggregated societal risk is negligible with respect to the one derived from the presence of the CO_2 pipeline: docking operations are not considered dangerous because of the non-flammable nature of the CO_2 and of the desultoriness of such operations (DNV, 2011). CO_2 can generate adverse effects on health depending on both its concentration and the duration of the exposure (Vianello et al., 2016). Following the most appropriate exposure examples resulting from Ridgway (2007) and from Hedlund (2012), three scenarios are here chosen to describe the damage surface:

Tab. 4.1: Definition of hazardous incidents h, failure frequency [events/km] and percentage probability [events/km] according to the assumed failure distribution [%] and to the chosen methodology (LC50, 60000 ppm, or IDLH). As regards failure frequency, a rare-event probabilistic law is assumed for the calculation of probability. The Poisson's law is used. A 1 year time-framework is here assumed as a reference unit for the calculations.

h	Definition	Method	Frequency [events/km]	Distr. [%]	Probability [events/km]	Distance [km]
i	Rupture	LC50	$2.6 \cdot 10^{-4}$	10	0.002600	1.800
ii	Large puncture	LC50	$2.6 \cdot 10^{-4}$	10	0.002600	0.450
iii	Med. puncture	LC50	$2.6 \cdot 10^{-4}$	30	0.007800	0.108
iv	Small puncture	LC50	$2.6 \cdot 10^{-4}$	50	0.013000	0.027
i	Rupture	60000 ppm	$2.6 \cdot 10^{-4}$	10	0.000780	2.300
ii	Large puncture	60000 ppm	$2.6 \cdot 10^{-4}$	10	0.000780	0.587
iii	Med. puncture	60000 ppm	$2.6 \cdot 10^{-4}$	30	0.002340	0.139
iv	Small puncture	60000 ppm	$2.6 \cdot 10^{-4}$	50	0.003900	0.035
i	Rupture	IDLH	$2.6 \cdot 10^{-4}$	10	0.000026	2.700
ii	Large puncture	IDLH	$2.6 \cdot 10^{-4}$	10	0.000026	0.725
iii	Med. puncture	IDLH	$2.6 \cdot 10^{-4}$	30	0.000078	0.171
iv	Small puncture	IDLH	$2.6 \cdot 10^{-4}$	50	0.000130	0.044

- a strong impact generated by a lethal concentration of 50% (LC50), defined as the concentration for which unconsciousness leads to death of 50% of the affected population (Vianello et al., 2016), resulting in a toxic dose of 10000 ppm for 15 min;
- an intermediate situation with 60000 ppm for 10 min;
- an area of irreversible damage resulting in immediate danger to life or death (IDLH), defined as the maximum concentration to which a healthy person can be exposed for 30 min, without resulting in irreversible effects (Vianello et al., 2016), generated by a dose of 40000 ppm for 30 min.

The definition of risk is based on the quantification of both the accident scenario probability and its magnitude, namely the effect of the CO_2 release on the exposed target. The probabilistic assessment assumes that a failure, on average, occurs after a certain period of time t. The average failure rate, μ [faults/year], is based on expert judgement, heuristic or historical records of pipelines accidents and is used to estimate the probability that a component will not fail during the time interval $[0, t]$:

$$R_t = e^{-\mu t} \qquad \forall t \tag{4.1}$$

R_t is called reliability and the mathematical formulation is based on the Poisson distribution of rare events (Roffel and Rijnsdorp, 1982). The complement of the

reliability is called the failure probability P_t that is thus given by:

$$P_t = 1 - R_t = 1 - e^{-\mu t} \qquad \forall t \tag{4.2}$$

Historical failure frequencies of Table 4.1 are used to assess the failure probability of a specific failure scenario. A specific failure distribution discerns among scenarios characterised by different degree of severity (rupture, large puncture, medium puncture, small puncture). Dedicated release and dispersion models are then employed to estimate the effect, or impact, of the failure scenario. The released quantity of liquid CO_2 (i.e., $\dot{m}_{CO_2}$) as a result of the failure, is estimated following the indications provided by Lees (2004) therefore, according to its physical properties, the pipeline operative conditions, and the size of the release hole:

$$\dot{m}_{CO_2} = C_d \cdot \gamma \cdot \rho_{l,CO_2} \cdot A \cdot \sqrt{\frac{2g_c \cdot (P - P^{atm})}{\rho_{l,CO_2}}} \tag{4.3}$$

where C_d is the release hole coefficient of discharge assumed to be equal to 0.61, γ is the viscosity correction factor that is function of Reynolds number at the discharge location and conservatively assumed to be 1.0, ρ_{l,CO_2} is the CO_2 liquid density at the pipeline operative conditions, A is the hole area associated to the release hole size, g_c [m^2/s] is the gravitational constant, P [kPa] is the operative pressure and P^{atm} [kPa] is the atmospheric pressure. Indeed, the released vapour CO_2 flowrate $\dot{m}_{CO_2}$ resulting from induced phase change mechanisms is the input to the dense gas dispersion model that allows for the estimation of the CO_2 concentration at a certain location (Lees, 2004). The CO_2 concentration at ground-level $c(x, y, z)$ is assessed with the dense gas dispersion model DEGADIS (Havens and Spicer, 1985) that accounts for the plume gravity spreading and stratification phenomena. The following equation applies:

$$c(x,y,z) = \begin{cases} c_c(x) \cdot e^{-[(|y|-b(x))/S_y]^2} - (z/S_z)^{1+n} & |y| > b(x) \\ c_c(x) \cdot e^{-(z/S_z)^{1+n}} & |y| \leq b(x) \end{cases} \tag{4.4}$$

In the previous equation, c_c [ppm] is the centreline ground-level concentration of CO_2, $S_y(x)$ [m] is the lateral dispersion parameter, $S_z(x)$ [m] is the vertical dispersion parameter, $b(x)$ [m] stands for the half-width of the core section, whereas n is the constant in the power-law wind profile (Lees, 2004). Dispersion parameters are quantified in terms of balance between the downwind gradient in concentration and either the vertical or the lateral turbulent diffusion and a stability factor $\alpha^{stability}$ based on a corrected Richardson dimensionless number R_i:

$$\alpha^{stability}(R_i) = 0.88 + 0.099 \cdot R_i^{1.04} + 1.4 \cdot 10^{-25} \cdot R_i^{5.7} \tag{4.5}$$

The stability factor is used to correct the vertical dispersion induced by stratification phenomena. Dispersion effects are quantified in terms of CO_2 concentration threshold values according to different methodologies (Table 4.1), and an equal impact distance on both pipeline sides is considered. Dispersion parameters are based

on European average weather conditions and a Pasquill-Gifford stability class D is employed (neutral conditions). Resulting damage distances are expressed in terms of isopleths, namely impact distances characterised by a CO_2 concentration at least equal to that pertaining to the adopted methodology (Table 4.1). Finally, with a Probit function (Molag and Raben, 2006), the link between the exposure to the CO_2 and the effect on the human target is integrated in the modelling procedure. Resulting mapped, individual risk contours are then matched with the local population density to determine the societal risk as will be described subsequently.

4.2.2 Definition of risk mitigation measures

Within the framework of pipeline transport systems, a risk mitigation measure can be defined as either a physical or a planning safety option that, if implemented, leads to: (i) a decrease in the failure frequency or in the quantity of CO_2 released, i.e. a beneficial influence on societal risk, but (ii) also an increase in the costs of the transport system, i.e. a disadvantageous effect on economics. Following the indications by Knoope et al. (2014), the following risk mitigation measures were included in this study within the set of options m:

- the installation of marker tape above the pipeline;
- the installation of protective concrete slabs that may prevent an excavator driver from punching a hole in the pipeline;
- the deep burying of pipelines (at 2.0 m) that may reduce the possibility to hit the pipeline;
- the establishment of a weekly surveillance interval to detect illicit excavations and therefore prevent damages.

In addition, the 'none' mitigation option, too, was included within set m in order to keep the mathematical formulation linear when considering the 'no-action' choice. On the other hand, other mitigation options that are related to the specific flowrate characteristics (e.g., the optimisation of block valves distance, or the choice of the design factor for calculating walls thickness), were not considered in this study, given the size of the problem and the large spatial resolution that is here considered. The mathematical implementation of risk mitigation measures will be discussed subsequently, as regards both societal risk reduction and costs increase.

4.3 Mathematical formulation

The objective is the economic optimisation of a European CCS SC in terms of total cost (TC [€]) minimisation, in such a way as to guarantee that the local level of risk is lower than a pre-set threshold. TC is given by the contributions of the cost for

capture (TCC [€]), the cost for transport (TTC [€]), and the cost for sequestration (TSC [€]):

$$\begin{cases} objective = min(TC) \\ TC = TCC + TTC + TSC \\ s.t. \\ capture\ problem\ model \\ transport\ problem\ model \\ sequestration\ problem\ model \\ + \\ risk\ mitigation\ problem\ model \\ societal\ risk\ constraints \end{cases} \tag{4.6}$$

On the one hand, the capture problem model, the transport problem model and the sequestration problem model were previously described in Chapter 2. On the other hand, the risk mitigation problem model and the societal risk constraints are the innovative core of this study, and permit the calculation of societal risk and the selection of suitable mitigation options, respectively.

4.3.1 Risk mitigation problem model

Mitigation options m can mitigate regional societal risk, so that the probability of consequences on population may be significantly reduced without considering other safety measures (AIChE, 2000), like for instance the optimisation of the distance between block valves (Medina et al., 2012), the selection of a preservative design factor (Knoope et al., 2014), or a changing in the path toward uninhabited regions (Vianello et al., 2016). Mitigation options can be applied on both inter-connection modes among region g and g' through either onshore pipeline, offshore pipeline or ship, and on intra-connection within cell g through onshore pipeline. It is assumed that intra-connection, being originated from the necessity of linking capture facilities with local storage capacities, is operated neither through offshore pipelines, nor through ships.

On the one hand, as regards inter-connection between region g and g', it is possible to evaluate the local societal risk $SR^{inter}_{p,g,l,g'}$ [people·events] according to the effects of the mitigation measure m that may be adopted between transport nodes and according to the spatially-explicit features of each specific region g and g':

$$SR^{inter}_{p,g,l,g'} = \sum_{m} (\delta^{inter}_{m,p,g,l,g'} \cdot MF_{m,l}) \cdot \sum_{h} (\bar{Pd}_{g,g'} \cdot Sh^{inter}_{h,g,g'} \cdot Pf_{h,l} \cdot LDg, g') \qquad \forall p, g, l, g' \tag{4.7}$$

where $\bar{Pd}_{g,g'}$ [people/km^2] (Table 4.2) represents the average value of population density between region g and g', while $Sh^{inter}_{h,g,g'}$ [km^2] is the surface affected by hazardous case h between region g and g'. Each incident typology h is then weighted according to the probability $Pf_{h,l}$ [events/km] (Table 4.1) that incident h through mode l generates an event. Then, $LD_{g,g'}$ evaluates the distance between region g and

Tab. 4.2: Population P_g [people] and population density Pd_g [people/km^2] in region g, evaluated by intersecting the information of population data in raster format (CIENSIN, 2015) with the European squared cells g through the QGIS software (QGIS, 2017).

g	P_g [people]	Pd_g [people/km^2]	g	P_g [people]	Pd_g [people/km^2]	g	P_g [people]	Pd_g [people/km^2]	g	P_g [people]	Pd_g [people/km^2]
1	623338	41.21493562	35	17425077	575.2763982	69	7149345	193.3739765	103	2528046	53.76084907
2	1444089	95.48276403	36	26442966	872.9955247	70	2615241	64.82235419	104	926370	19.69997292
3	1138663	75.28808165	37	29740921	981.8751396	71	2314727	57.37370034	105	1187523	25.253593
4	1968386	110.0493875	38	22497971	742.754349	72	5967721	147.9181935	106	6006687	127.7368344
5	5344278	298.7902376	39	17420852	575.1369129	73	9723700	241.0153119	107	4151164	88.27770588
6	4142946	231.6256414	40	18038080	595.5142518	74	11996446	297.3484553	108	3680987	78.27902915
7	1225066	68.49152704	41	17327507	572.0551948	75	7854909	194.6947502	109	5657679	120.3149099
8	5554491	266.97638	42	22487959	742.42381	76	11991306	297.2210533	110	7563776	160.8495336
9	7322399	351.9508048	43	23022237	760.0626144	77	4360803	108.0885152	111	13279758	282.4043018
10	4406072	211.7776683	44	24126788	796.5285721	78	1845221	45.73634675	112	5020666	64.93114437
11	1990982	95.6964674	45	46977319	1550.922436	79	12728932	315.5041308	113	1793237	35.6624784
12	6873434	288.0243766	46	33351472	1101.074887	80	32031815	793.9527016	114	0	0
13	3619151	151.6569026	47	20622020	613.5700139	81	42373045	1050.274346	115	0	0
14	5373260	225.1610857	48	9114312	271.1794742	82	12593705	312.1523432	116	0	0
15	9818152	411.4198389	49	12076934	359.3268052	83	3373639	83.62029433	117	0	0
16	6251886	261.9790294	50	20502070	610.0011238	84	8411228	192.4682341	118	429112	8.533839883
17	27114025	1136.186097	51	14078576	418.8819559	85	4110680	94.06180887	119	3066682	60.98774483
18	6060678	253.9666494	52	9169064	272.8085186	86	8623897	197.3345897	120	1760777	35.01693961
19	3739335	138.3368607	53	13164287	391.6789799	87	5861966	134.1352588	121	579655	11.52771994
20	4563479	168.8261037	54	29700915	883.6957209	88	11273828	257.9711032	122	4646671	92.40931576
21	15766328	583.2759889	55	27000884	803.3612988	89	6879932	157.4286611	123	2491814	49.55522496
22	23407982	865.9793104	56	11513991	342.5774787	90	1145620	26.21441938	124	4760194	94.66697135
23	6650423	246.0326876	57	11980548	356.4590182	91	4954248	113.3645841	125	0	0
24	13801479	510.5863148	58	15537520	462.2901327	92	21584173	493.8955003	126	0	0
25	10960259	405.4752575	59	9455965	255.762948	93	7104495	162.5671789	127	0	0
26	9867184	365.0369005	60	12926570	349.6351405	94	8554502	195.7466726	128	0	0
27	5687484	210.4087175	61	42298841	1144.090135	95	21993064	503.2518664	129	0	0
28	10066478	372.4097906	62	19151247	517.9988918	96	17924647	410.1571322	130	0	0
29	12724572	470.7460936	63	7475558	202.197317	97	7783208	178.0976927	131	0	0
30	19531358	722.5634372	64	8101485	219.1272585	98	17652641	403.9330096	132	0	0
31	35166724	1300.994481	65	19896347	538.1521996	99	5872477	124.8827552	133	0	0
32	21682044	802.1281591	66	24303916	657.3671968	100	7884497	167.6699131	134	0	0
33	8257058	272.6008376	67	9508152	257.174491	101	12191710	259.2661214			
34	25029302	826.3244234	68	10898807	294.7886343	102	8250115	175.445062			

Tab. 4.3: Values of mitigation factor ($MF_{m,l}$ [%]) and unitary cost ($UMC_{m,l}$ [€/km]) of mitigation options m (Knoope et al., 2014)

	m				
	none	marker tape	concrete slabs	deep burying	surveillance
$MF_{m,l}$	100.0	59.9	20.0	29.0	70.0
$UMC_{m,l}$	0	220	110000	51500	1337

g' (i.e., the transportation length). Binary variable $\delta^{inter}_{m,p,g,l,g'}$ is a decision variable representing whether a mitigation option m is taken into account on a specific inter-connection path, and is then coupled with mitigation factors $MF_{m,l}$ [%] (Table 4.3) to consider the possible selection of suitable measures for risk mitigation. Note that a null mitigation option $m = [none]$ is included, too, in the formulation in order to take into account the possibility of not installing any of these options. As reported in Table 4.3, in the absence of mitigation measures ($m = [none]$) we have a unitary value of $MF_{none,l}$ (therefore, this option does not reduce societal risk), and a null installation cost, since no additional costs occur with respect to the original pipeline. Thus, Eq.(4.7) defines the local societal risk in region g not only as a consequence of population presence, transport mode l selection and incident typology h definition, but also by considering the possible implementation of a mitigation option m on each chosen transportation path. For each hazardous incident h between region g and g', $Sh^{inter}_{h,g,g'}$ is calculated according to the liquid release distance from the pipeline L_h [km] (Table 4.1) and the overall distance $LD_{g,g'}$ between region g and g':

$$Sh^{inter}_{h,g,g'} = 2 \cdot L_h \cdot LD_{g,g'} \qquad \forall h, g, g' \tag{4.8}$$

On the other hand, as regards intra-connection within cell g, regional societal risk $SR^{intra}_{g,l}$ [people·events] can be estimated, analogously to $SR^{inter}_{p,g,l,g'}$, according to the possible implementation of mitigation measures (i.e., through a binary variable $\delta^{intra}_{m,g,l}$, representing whether a mitigation option m is implemented in region g on intraconnection mode l) and on the basis of the potential impact surface ($Sh^{intra}_{h,g}$ [km^2]) that may be affected by hazardous incident h in region g:

$$SR^{intra}_{g,l} = \sum_m (\delta^{intra}_{m,g,l} \cdot MF_{m,l}) \cdot \sum_h (Pd_g \cdot Sh^{intra}_{h,g} \cdot Pf_{h,l} \cdot LDg \cdot \frac{\sqrt{2}}{2}) \qquad \forall g, l \tag{4.9}$$

where Pd_g [people/km^2] (Table 4.2) is the population density in region g. Here we consider a maximum intra-connection length that is equal to $\sqrt{2}/2$ times the cell size LD_g (Figure 2.4). For each hazardous case h on intra-connection within region g, $Sh^{intra}_{h,g}$ is calculated according to the liquid release distance from the pipeline L_h [km] (Table 4.1) and the size LD_g of each cell g:

$$Sh^{intra}_{h,g} = 2 \cdot L_h \cdot LD_g \cdot \frac{\sqrt{2}}{2} \qquad \forall h, g \tag{4.10}$$

Binary decision variable $\delta^{inter}_{m,p,g,l,g'}$ inter in Eq.(4.7) describes whether a mitigation strategy m is chosen for flowrate p from region g through transport mode l to region g'. $\delta^{inter}_{m,p,g,l,g'}$ is linked with the actually established transport system (described in Chapter 2) through the following equation:

$$\sum_{m} \delta^{inter}_{m,p,g,l,g'} = \lambda_{p,g,l,g'} \qquad \forall p, g, l, g' \tag{4.11}$$

According to the previous equation, if there is no flowrate p transport from region g through l to g' (i.e., $\lambda_{p,g,l,g'} = 0$), no mitigation measures are therefore chosen and installed (i.e., $\delta^{inter}_{m,p,g,l,g'} = 0$). Conversely, if any flowrate p transport is carried out from region g through l to g' (i.e., $\lambda_{p,g,l,g'} = 1$), then one mitigation measure may be taken into account (i.e., $\delta^{inter}_{m,p,g,l,g'} \geq 0$). Note that just one mitigation m at a time can be applied on each specific transportation path from region g to g'. Moreover, the definition of mitigation factors $MF_{m,l}$, as retrieved from Knoope et al. (2014), does not permit the quantification of the residual value of societal risk that is generated from the combination of different options m. Nevertheless, according to the definition of $\lambda_{p,g,l,g'}$, no limitations are introduced on the size and number of transport links that can be effectively installed and operated between regions g and g'. For instance, CO_2 can be transported in parallel through onshore pipelines of different sizes p, to whom different measures m can be respectively operated. Therefore, the possibility of installing different mitigation measures between the same geographic nodes is indirectly implemented (although we recognise that this may lead to an overestimation of actual transport costs).
The decision of installing a mitigation option m on the intra-connection system within cell g is defined through the binary variable $\delta^{intra}_{m,g,l}$ of Eq.(4.9), which is then linked with the actual presence of a capture infrastructure in region g through the binary variable Y_g, which assumes a unitary value when a capture system is installed and operated in region g:

$$\sum_{m} \delta^{intra}_{m,g,l} = Y_g \qquad \forall g \tag{4.12}$$

According to the decision variables $\delta^{inter}_{m,p,g,l,g'}$ of Eq.(4.7) and $\delta^{intra}_{m,g,l}$ of Eq.(4.9), a mitigation measure m can be specifically applied to each installed transport system. As a result, the total cost TTC described in Chapter 2 (transport problem model) for transporting flowrates $Q_{p,g,l,g'}$ [t of CO_2] of size p from region g through l to g', that in general is given by the contributions of transport size (TTC^{size}), distance (TTC^{dist}) and intra-connection within each cell (TTC^{intra}) is increased by TTC_m. Cost TTC_m for installing and operating risk mitigation measures is given by the contribution of both inter-connection and intra-connection transport:

$$TTC^m = TTC^m_{inter} + TTC^m_{intra} \tag{4.13}$$

Cost TTC^m_{inter} [€] for the risk mitigation on inter-connection transport between region g and g' is calculated according to the unitary mitigation cost $UMC_{m,l}$ [€/km]

(Table 4.3) of chosen measure m on specific mode l and on the basis of the distance $LD_{g,g'}$ between region g and g':

$$TTC^{m}_{inter} = \sum_{m,p,g,l,g'} (\delta^{inter}_{m,p,g,l,g'} \cdot UMC_{m,l} \cdot LD_{g,g'}) \tag{4.14}$$

Cost TTC^{m}_{intra} [€] for the risk mitigation on intra-connection transport within region g is calculated according to the unitary mitigation cost $UMC_{m,l}$ [€/km] (Table 4.3) of chosen measure m on specific mode l and on the basis of the size LD_g of cell g:

$$TTC^{m}_{intra} = \sum_{m,g,l} (\delta^{intra}_{m,g,l} \cdot UMC_{m,l} \cdot LD_g \cdot \frac{\sqrt{2}}{2}) \tag{4.15}$$

4.3.2 Societal risk constraints

As regards inter-connection between region g and g', the regional societal risk SR^{inter}_{g} [events] in origin region g is given by the sum of local societal risk $SR^{inter}_{p,g,l,g'}$ of Eq.(4.7) produced by each flowrate p that is transported from region g through transport mean l to region g' (oppositely, $SR^{inter}_{g'}$ [events] refers to destination region g'):

$$SR^{inter}_{g} = \sum_{p,l,g'} \frac{SR^{inter}_{p,g,l,g'}}{P_g} \qquad \forall g \tag{4.16}$$

$$SR^{inter}_{g'} = \sum_{p,l,g} \frac{SR^{inter}_{p,g,l,g'}}{P_{g'}} \qquad \forall g' \tag{4.17}$$

where P_g [people] and $P_{g'}$ [people] are the populations in region g and g', respectively (Table 4.2). Conversely, as regards intra-connection within cell g, the regional societal risk SR^{intra}_{g} [events] in region g is given by the contribution of local societal risk $SR^{intra}_{g,l}$ of Eq.(4.9) in region g through intra-connection mode $l = [onshore\ pipeline]$, which is then weighted for the population P_g inhabiting region g:

$$SR^{intra}_{g} = \sum_{l} \frac{SR^{intra}_{g,l}}{P_g} \qquad \forall g \tag{4.18}$$

Finally, the total regional societal risk SR_g [events], which is given by the contribution of SR^{inter}_{g}, $SR^{inter}_{g'}$ and SR^{intra}_{g}, is here constrained to be lower than the maximum regional societal risk SR^{max}_{g} [events] that is imposed by national standards (AIChE, 2000):

$$SR_g = SR^{inter}_{g} + SR^{inter}_{g'} + SR^{intra}_{g} \qquad \forall g \tag{4.19}$$

$$SR_g \leq SR^{max}_{g} \qquad \forall g \tag{4.20}$$

4.4 Results

The spatially-explicit, multi-echelon MILP mathematical framework (comprising 61 million variables, of which 25 million are discrete ones) was optimised in less than

Tab. 4.4: Scenarios A-A*-B-C, economic results (transport cost - TTC, mitigation cost - TTC^m) and computational information (solution time - Sol. time, optimality gap - Opt. gap).

Scenario	SR_g^{max}	α	TTC		TTC^m		Sol. time	Opt. gap
	[events]		[M€]	[€/t]	[M€]	[€/t]	[s]	[%]
A	0.01	0.50	1982.3	3.34	243.8	0.41	950	2.8
A*	0.01	0.50	3039.1	5.12	322.8	0.54	632	2.7
B	0.01	0.50	1473.6	2.48	99.1	0.17	682	1.6
C	0.01	0.50	1441.7	2.43	0.0	0.00	634	0.8

20 min by aim of the GAMS modelling tool using the CPLEX solver on a 2.80 GHz laptop (32 GB RAM). The regional upper bound SR_g^{max} for societal risk calculation of Eq.(4.20) was set equal to 0.01 events (following the indications provided by the United Kingdom regulations; AIChE, 2000), whereas the lower bound α for minimum European carbon reduction target was imposed equal to 50%, in order to compare the results with those from Chapter 2 and Chapter 3. Three scenarios are investigated according to the employed methodology for damage evaluation: Scenario A with LC50, Scenario B with 60000 ppm and Scenario C with IDLH criteria. The main hypotheses behind the three scenarios, as well as the economic results in terms of transport costs, along with the computational information of each simulation, are reported in Table 4.4. Scenario A, where the SC is sequestering more than 600 Mt of CO_2, exhibits a total cost TC of 20.60 B€ (corresponding to a specific cost for installing and operating the entire network of 34.74 €/t of CO_2), of which TTC is 1.98 B€, i.e. 3.34 €/t of CO_2 (9.6% of TC). The solution entails the installation of strong mitigation measures (deep burying and concrete slabs) on the onshore pipeline system (Figure 4.2a), in order to keep the local societal risk SR_g always lower than SR_g^{max} (Figure 4.3a). This produces a total cost for mitigation TTC^m of 243.8 B€, i.e. 0.41 €/t of CO_2 (12.3% of TTC). Furthermore, a noteworthy part of the transport infrastructure is developed within offshore areas, in order to exploit the beneficial effect of low population density on societal risk. As regards Scenario B (Figure 4.2b), the implementation of the 60000 ppm methodology generates a lower mitigation cost (TTC^m is 99.1 B€, i.e. 0.17 €/t of CO_2) since mostly marker tape is now installed as mitigation option, which consequently produces a lower value of TTC (1.47 B€, i.e. 2.48 €/t of CO_2) and also a small decrease in TC (20.56 B€, i.e. 34.67 €/t of CO_2), despite an identical amount of sequestered CO_2 with respect to Scenario A. Within Scenario B, the majority of the transport infrastructure is developed within the mainland, with some deep burying operated in densely populated areas. In general, Scenario B entails lower values of societal risk than Scenario A (Figure 4.3b). The IDLH approach (Scenario C) is less cautionary then the other scenarios and as a consequence it exhibits the best results in terms of societal risk

(Figure 4.3c), since it suggests the installation of no mitigation measures, thus producing the best economic performance (TC is 20.37 B€, i.e. 34.35 €/t of CO_2), and the lowest cost for transport (TTC is 1.44 B€, i.e. 2.43 €/t of CO_2). Therefore, according to the IDLH methodology for safety distance calculation, it is possible to design an economically optimal European transport network, which already satisfies the regional risk constraints without implementing any mitigation measure on the onshore system.

The North Sea potential for offshore sequestration of CO_2 is not exploited by the solver in any scenario as it represents a more expensive option with respect to onshore geological storage. However, we need to consider that currently several European countries do not allow or severely limit the practice of onshore storage for CO_2. To assess the effect of these regulations, a new instance was analysed (Scenario A*) by forbidding onshore sequestration in countries where it is currently limited or prohibited (i.e., in Austria, Croatia, Estonia, Ireland, Latvia, Slovenia, Netherlands, UK, Sweden, Czech Republic, Germany and Poland). The SC was optimised considering the most conservative LC50 methodology. Results are summarised in Table 3. Scenario A*, as expected, exhibits a higher cost for transporting CO_2 (TTC is 3.04 B€, i.e. 5.12 €/t of CO_2, i.e.+53.3%) and the introduction of even larger mitigation actions on pipeline systems (TTC^m is 322.8 B€, i.e. 0.54 €/t of CO_2, i.e. +32.4%) with respect to Scenario A. This result reflects the necessity of transporting the CO_2 far from the emission sources, given the legal constraints for certain areas in sequestering within the mainland. As a consequence, it can be seen (Figure 4.4b) that Scenario A* entails a more complex SC network with respect to Scenario A (Figure 4.4a). Furthermore, Scenario A* exploits the offshore storage potential of the North Sea region, since the sequestration of 29 Mt of CO_2 is operated in $g = [126]$. This choice also generates higher costs for sequestering CO_2 (329.7 B€, i.e. 0.56 €/t of CO_2, i.e. +18.7%) leading to a total cost TC of 22.5 B€, i.e. 37.94 €/t of CO_2, therefore 8.7% higher than that of Scenario A. As regards mitigation measures, both deep burying and concrete slabs are implemented in Scenario A* on the onshore pipeline system.

Finally, the effect of the minimum European carbon reduction target α was evaluated. Table 4.5 summarises the results of a sensitivity analysis where Scenario A (i.e., criterion LC50) was optimised for different values of reduction α from a minimum of 10%. The specific mitigation cost (i.e., the total cost TTC^m for installing and operating mitigation options with respect to the overall amount S of sequestered CO_2) increases from a zero value to a maximum of 0.41 €/t of CO_2, the latter corresponding to a carbon reduction target $\alpha = 50\%$ (Figure 4.5a). Consequently, also the share of TTC^m over total transport cost TTC reaches its maximum value (12.3%) for $\alpha = 50\%$ (Figure 4.5b). The value $\alpha = 50\%$ represents the maximum carbon reduction target, after which no feasible (i.e., with acceptable values of regional societal risk) SC configurations can be found. When $\alpha > 50\%$, local societal risk exceeds the imposed threshold of 0.01 events.

Tab. 4.5: Scenario A, economic results (transport cost - TTC, mitigation cost - TTC^m) and computational information (solution time - Sol. time, optimality gap - Opt. gap), for different values of α [%]. No feasible solutions were found for $\alpha \geq 50\%$. Specific costs are intended per unit of sequestered CO_2.

Scenario	SR_g^{max}	α	TTC		TTC^m		Sol. time	Opt. gap
	[events]		[M€]	[€/t]	[M€]	[€/t]	[s]	[%]
A	0.01	0.10	235.9	1.96	0.0	0.0	667	1.9
A	0.01	0.20	445.3	1.84	7.1	0.03	606	1.0
A	0.01	0.30	697.4	1.93	22.0	0.06	600	0.8
A	0.01	0.40	1109.1	2.23	53.7	0.11	604	1.3
A	0.01	0.50	1982.3	3.34	243.8	0.41	950	2.8
A	0.01	≥ 0.50	-	-	-	-	-	-

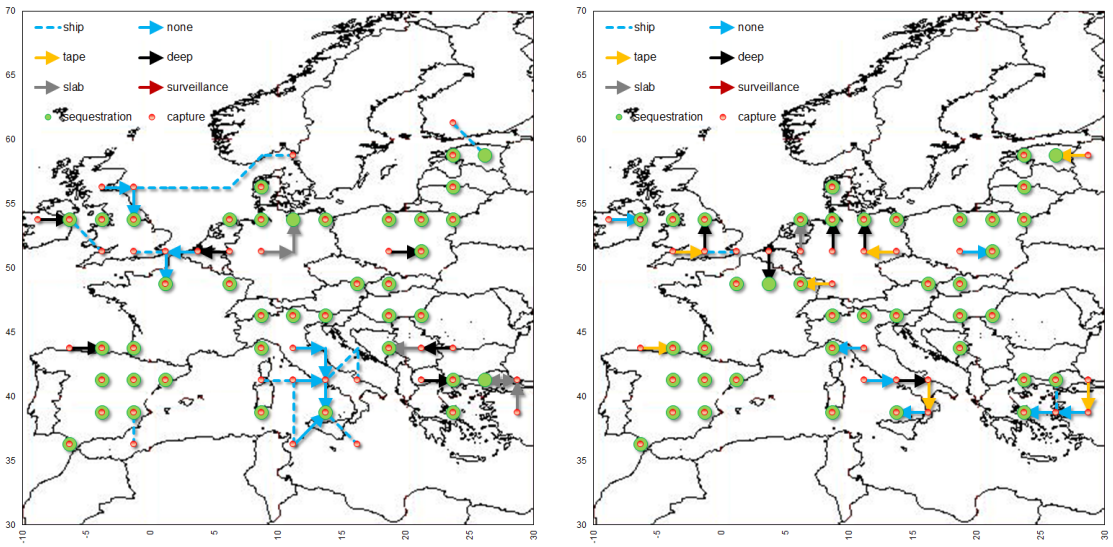

(a) *(b)*

Fig. 4.2: Comparison of SC configurations between Scenario A (a) and Scenario B (b).

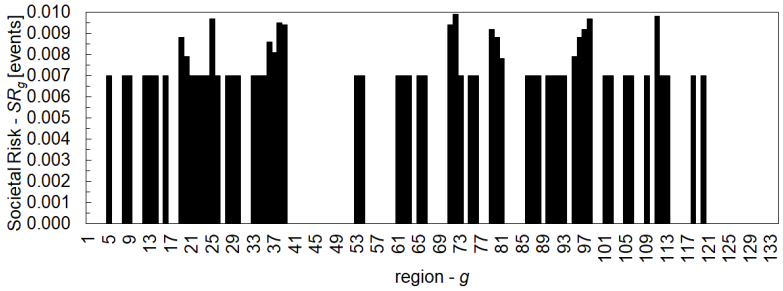

(a)

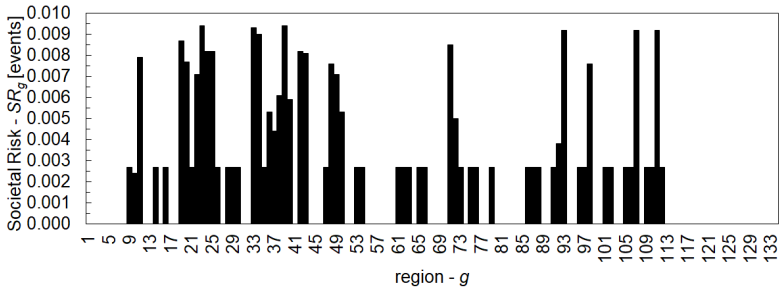

(b)

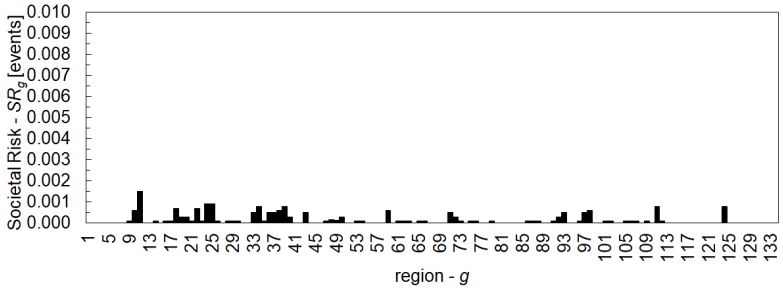

(c)

Fig. 4.3: Total societal risk SR_g [events] in region g for Scenario A (a), Scenario B (b), Scenario C (c).

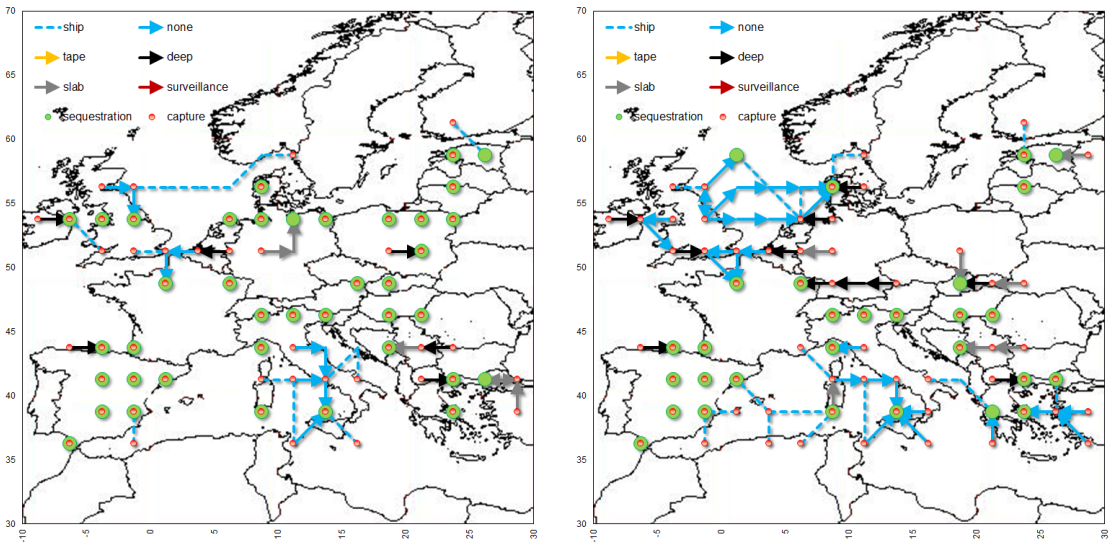

(a) (b)

Fig. 4.4: Comparison of SC configurations for Scenario A (a) and Scenario A* (b) (the latter includes legal constraints on onshore sequestration).

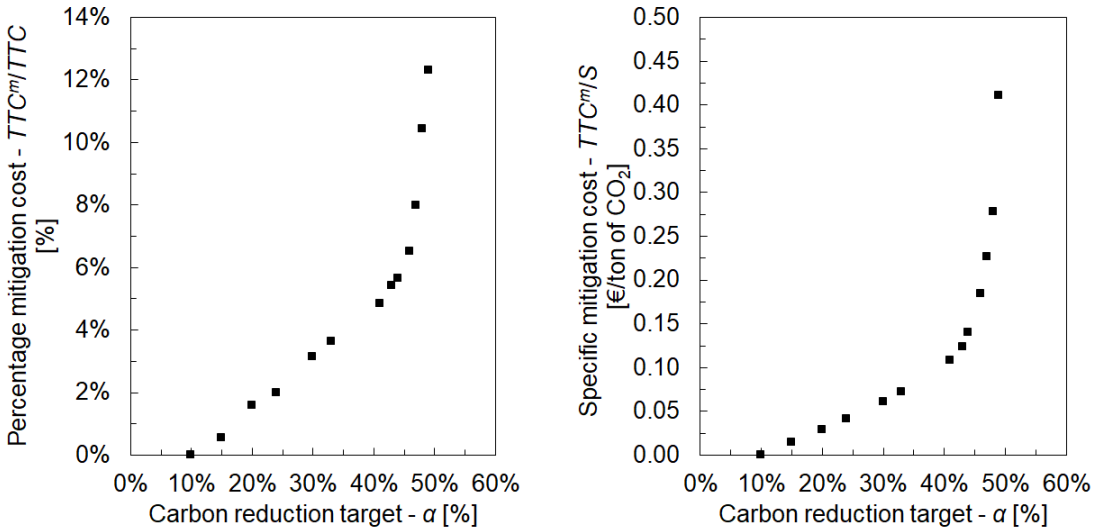

(a) (b)

Fig. 4.5: Specific mitigation cost (i.e., total cost TTC^m for installing and operating mitigation options with respect to the overall amount of sequestered CO_2, [€/t of CO_2]) (a), and percentage mitigation cost (i.e., total cost TTC^m for installing and operating mitigation options with respect to total transport cost TTC, [%]) (b).

4.5 Discussion

Three methodologies have been tested for societal risk quantification: LC50, 60000 ppm and IDLH. When choosing the LC50 method for release distance calculation, Scenario A demonstrates that the transport of CO_2 is almost completely avoided in regions that are typically characterised by high values of population density (e.g. Germany). Conversely, the sequestration potential of the Mediterranean area is rather exploited, being the offshore/ship transports considered safer (in terms of societal risk) with respect to the onshore option. On the other hand, when evaluating societal risk through the 60000 ppm methodology, Scenario B shows that the optimal SC configuration suggests the installation of mostly onshore transport networks, being this in general a cheaper option with respect to the offshore ones, despite the necessity of installing even strong and expensive mitigation measures between the nodes characterised by high population density (Northern Germany and United Kingdom). The IDLH approach emerges as even less cautionary from the results of Scenario C. According to this scenario, it appears that mitigation options are not necessary to obtain acceptable levels of risk. In general, the specific cost TTC^m/S for keeping societal risk below acceptable levels is never higher than 0.41 €/t of CO_2 and constitutes the 11% of overall transport costs; therefore the implementation of mitigation measures on a European CCS SC should not be considered an economic obstacle when modelling a safe transport infrastructure. The situation is slightly different when testing the model on the application of current national regulations on onshore storage, since from Scenario A* it emerges the necessity of carrying out large CO_2 flowrates from Germany, where the high population density obliges to install expensive mitigation options between the transport nodes. In fact, Scenario A* exhibits larger costs for mitigation (+32%) and overall larger costs for transport (+53%) with respect to Scenario A (i.e., the case in which onshore storage is allowed in every European country). Thus, the debate on Germany's "no" to onshore storage (Vögele et al., 2018), although being clearly beyond the scope of this work, appears at least quantified in terms of monetary consequences from the results of this model.

Finally, it was observed (through a sensitivity analysis on the selection of the minimum European carbon reduction target α) that if $\alpha \geq 50\%$ is chosen, local societal risk exceeds the imposed threshold of 0.01 events. As a matter of facts, this upper bound can be compared with (and confirms) the overall target that the EC has suggested for capture (i.e., 43% of total CO_2 emitted by sectors that are interested by the Emissions Trading System) (EC, 2018).

In general, it was demonstrated that the proposed methodology is capable of providing a preliminary tool for a European CCS assessment, aiming at a strategic and overviewing analysis of potential CO_2 transport pathways that minimise both the overall costs of the SC and the risk of failure hazards on the population. The resulting optimal CO_2 networks demonstrated the applicability of European directives in

terms of both carbon abatement and local safety, having shown that the societal risk generated by pipeline transport can be kept within acceptable levels, also through the installation of suitable mitigation options, up to carbon reduction targets of 50% of overall emissions.
Furthermore, although remarking the necessity of coupling CCS with other strategies for reduction of carbon emissions (e.g., improvements in processes efficiencies or large deployment of renewable energies), this work has pointed out the concrete possibility of direct action on the already installed fossil-based European energy system. The flexibility and generality of the modelling approach has been demonstrated through the optimisation of several scenarios, being the proposed mathematical framework applicable in other contexts or easily adaptable to account for policy changes or country-based choices. Having stated this, it should also be remarked that the proposed approach delivers a general tool for a high-level strategic analysis and optimisation of a large-scale CCS infrastructure. As a consequence details concerning, for instance, the exact pipeline route or the risk analysis of a potential leakage in a specific context (and related safety measures) cannot be included in the optimisation framework. These further studies would represent an essential second-level analysis, which nonetheless makes sense only when the big picture is obtained, i.e. when decision makers and stakeholders approximatively know the actual CCS potential, the cost for taxpayers, the effects of implementing risk-mitigation measures, the most convenient transport routes and storage locations, the consequences of some country policies (e.g. the decision of refusing CO_2 storage), and so on. The proposed methodology provides a quantitative tool to answer the latter questions.

4.6 Chapter conclusions

A wide-scale European risk-constrained economic optimisation was presented in Chapter 4, in which the minimisation of the total cost for capturing, transporting and sequestering CO_2 from large stationary sources was coupled with a societal risk assessment. In the most conservative scenario, mitigation actions represented 10% of total cost for installing and operating the transport network. For the two additional scenarios being considered, mitigation costs never represented more than 11% of transport costs (less than 1.5% of the overall costs for deploying the CCS infrastructure). The offshore sequestration potential was only exploited when limitations on onshore storage were taken into account according to country legislations. No feasible solution could be found for a carbon reduction target higher than 50%, because of the unacceptable level of societal risk.
The design of a safe transport infrastructure is vital for an effective deployment of the CCS network, and also to attain a favourable reception from the public. In view of this, Chapter 5 will propose an innovative methodology for quantifying social acceptance related to a CCS SC. In particular, risk perception by inhabitants will be employed as proxy for the calculation of social acceptance.

5

Public risk perception and social acceptance

"Once an inventor has discovered a use for a new technology, the next step is to persuade society to adopt it. Merely having a bigger, faster, more powerful device for doing something is no guarantee of ready acceptance. Innumerable such technologies were either not adopted at all or adopted only after prolonged resistance. Notorious examples include the U.S. Congress's rejection of funds to develop a supersonic transport in 1971, the world's continued rejection of an efficiently designed typewriter keyboard, and Britain's long reluctance to adopt electric lighting. What is it that promotes an invention's acceptance by a society? Let's begin by comparing the acceptability of different inventions within the same society. It turns out that at least four factors influence acceptance. The first and most obvious factor is relative economic advantage compared with existing technology [...]. A second consideration is social value and prestige, which can override economic benefit (or lack thereof). Still another factor is compatibility with vested interests [...]. The remaining consideration affecting acceptance of new technologies is the ease with which their advantages can be observed."

- Jared Diamond, *Guns, Germs and Steel: the Fates of Human Societies*

5.1 Chapter summary

The installation of infrastructures for CCS to tackle the problem of CO_2 emissions from European power plants and carbon intensive industries, is of strategic importance to reach future GHGs reduction targets. However, the public reaction to the deployment of these technologies is still uncertain, and opposition may result in either cancellations or delays. Chapter 5 provides quantitative insights into how social acceptance affects the design of a European CO_2 infrastructure[1]. A multi-objective MILP model is developed to optimise the design the entire SC, by simultaneously addressing the minimisation of the costs to install and operate the infrastructure and the maximisation of its community acceptance. The goal is to provide optimal network designs in terms of costs, whilst considering the social behaviour of inhabitants towards the installation and operation of either CO_2 pipelines or injection wells. Results demonstrate how the methodology may be exploited to assess the response of local communities and identify design strategies aiming at a trade-off between economic objectives and social acceptance. Although the maximisation of social acceptance leads to a +34% increase in costs with respect to the economic optimum, it is shown that an intermediate solution between the two objectives (i.e., economics against acceptance) entails a just slight increase of +8% with respect to the cost of the best economic configuration.

5.2 Modelling social acceptance

Considering the wide range of industrial sectors and applications covered (e.g., energy systems, civil engineering, infrastructures), social acceptance-related studies have so far become of key importance for governments, industries and academics (Upham et al., 2015). Concepts like public opinion, perceptions, acceptance, attitude, behaviour, values and practise cannot be overlooked anymore, and social acceptance has come to be noticed as one of many aspects that may lead to the successful implementation of new developments or policies, especially in the energy field.

The energy sector is commonly considered as one of the key fields of research on social acceptance (Wolsink, 2018), and might constitute a fertile land for retrieving quantitative methodologies that may be applied to CCS modelling. For instance, Van der Horst and Toke (van der Horst and Toke, 2010) proposed a study on acceptance of wind farms in the United Kingdom. Their model was based on a list of either approved or rejected wind farms between 1991 and 2006, and on a dataset concerning socio-economical information (e.g., education, health, demography, employment) obtained from inhabitants of rural areas. Similarly, Roddis et al. (2018) proposed a study on social acceptance focused on both wind and solar farms in

[1] The content of this Chapter was published in: d'Amore et al., 2019c.

the United Kingdom, by aim of a dataset of either approved or rejected facilities between 1990 and 2017, together with the description of both attitudinal and social arguments. This class of methods, however, requires both a dataset of quantitative parameters based on material or attitudinal/social arguments, and a list of previous accepted or rejected infrastructure applications, which in the case of CCS is practically unavailable, considering the early stage of implementation of this technology (Reiner, 2015; 2016; Global CCS Institute, 2017).

Regarding studies specifically focussed on public perception of CCS, during the last decade researchers tried to understand the correlations between aspects such as acceptance, knowledge of the technology, trust in institutions, attitude, fairness, perceived cost, perceived benefit, and perceived risk (Götz et al., 2016; Karimi and Toikka, 2018). Oltra et al. (2012) and Ashworth et al. (2012) compared several case studies of CCS projects, indicating a series of factors that may influence public reaction towards CCS and its acceptance. However, none of these factors has been quantified in strict mathematical terms. Additionally, given the scarcity of active industrial applications of CCS, surveys and interviews cannot be always employed as sources of information on public perception, being often the respondents too few and endangered by a lack of impartiality (L'Orange Seigo et al., 2014). Other studies aimed at measuring the general public reactions in localities in the near vicinity of a proposed energy facility and, in some cases, a CCS system. Huijts et al. (2007) discussed the results from a survey on acceptance of CCS nearby a potential storage site. Groothuis et al. (2008) assessed the compensation level required to attain the acceptance of windmills in North Carolina. Subsequently, monetary compensation was indicated also as a potential help to foster also CCS implementation (ter Mors et al., 2012). These aspects were additionally revised and expanded by Terwel and ter Mors (2015) for the context of the Netherlands. Terwel et al. (2009) applied a methodology for evaluating perceived benefit, risk, and trust, in the context of CCS. Dütschke (2011) analysed the main drivers for local public acceptance for two case studies located in Germany. The public response in the vicinity of a planned sequestration basin was investigated by Oltra et al. (2012) for different case studies. Then, the consequences of informing public opinions about CCS were investigated by ter Mors et al. (2013). From this contribution, it emerged that information-choice questionnaires delivered higher-quality opinions than focus groups. Overall, from these studies, it emerged a general support for CCS but an opposition to local projects, which is addressed in the literature as the "not-in-my-back-yard" (NIMBY) effect (Braun, 2017). Nonetheless, this class of studies alone cannot be used to set up a quantitative methodology supporting CCS SC optimisation.

On the other hand, models based on the concepts of risk and benefit perception can be considered of significant importance for the optimisation problem addressed by this contribution. Pietzner et al. (2011) uncovered how different countries have a different public perception of CCS technologies. Wallquist et al. (2012) employed risk and benefit perception as proxies for evaluating the acceptance of the CCS echelons.

Following these studies, Karimi et al. (2016) developed a methodology showing how cross-cultural characteristics of countries play a role in risk and benefit perception of a technology, concluding that some nations are more likely to accept a new technology compared to others. This study was subsequently updated by Karimi and Toikka (2018), which proposed a model for investigating the socio-cultural orientation/attitudes of countries and their influences in the reaction (and acceptance) of people towards CCS technologies, to understand if a countrywide cultural behaviour determines how people perceive CCS. The model was built by taking into account:

- A survey conducted by the EU commission on the knowledge of CCS technology in 12 European countries, specifically countries where CCS projects were already started or planned (Eurobarometer, 2011). This study entails a total of 13901 respondents (with a minimum countrywide sample of 1000 respondents) and has been conducted in Bulgaria, Czech Republic, Finland, France, Germany, Greece, Italy, Netherlands, Poland, Romania, Spain and United Kingdom.

- A study by Hofstede et al. (2010), which aimed at characterising the socio-attitudinal characteristic (or cultural dimensions) of each country by aim of different factors. These quantities describe the general attitude of a citizen of a country in relative terms with respect to others and each dimension indicates how people living in that country tend to behave or approach certain issues. In particular, six main dimensions emerged as highly influential from that study: power distance index (PDI), individualism vs. collectivism (IDV), masculinity vs. femininity (MAS), uncertainty avoidance index (UAI), long-term orientation (LTO) and indulgence vs. restraint (IVR) (Hofstede et al., 2010).

In their work, Karimi and Toikka (2018) analysed the results from the Eurobarometer survey (Eurobarometer, 2011) and extended them to further countries according to the methodology proposed by Hofstede et al. (2010) (and other articles on social acceptance), by describing the public perception towards CCS through risk perception (i.e., $risk_g$) and benefit perception (i.e., $benefit_g$) parameters in region g belonging to country c (6.1):

$$risk_g = \sum_d (W_d^{risk} \cdot dim_{d,g}) \qquad \forall g \tag{5.1}$$

$$benefit_g = \sum_d (W_d^{benefit} \cdot dim_{d,g}) \qquad \forall g \tag{5.2}$$

where $dim_{d,g}$ represents the countrywide values of Hofstede's cultural dimensions (Hofstede et al., 2010) $d = [PDI, UAI, LTO, IDV, MAS, IVR]$ and assumes the same value in every region g belonging to the same country c (Table 5.1), while the parameters W_d^{risk} and $W_d^{benefit}$ (Table 5.2) are the weights (Karimi and Toikka, 2018) of cultural dimension d for the calculation of either $risk_g$ or $benefit_g$. Thanks

to its quantitative approach, the method proposed by Karimi and Toikka (2018) can be incorporated within a CCS SC optimisation framework, with the aim of designing optimal large-scale networks in terms of both minimum costs and maximum acceptance from inhabitants. The idea was implemented in this work, under the following assumptions:

- It is here chosen to exclude benefits from the formulation of social acceptance, since these are related to a rather generic perception of the large-scale mitigation effect of CCS on climate change and cannot be related to specific facilities, as required in a design problem. Conversely, the size of the planned/installed infrastructure and the number of inhabitants clearly affect social acceptance in terms of risk perception, since larger projects combined with high population densities are likely to generate stronger response by the public and a higher opposition may be expected (Braun, 2017; Roddis et al., 2018).

- It is here chosen to exclude the capture stage from those infrastructures generating acceptance-related issues. In fact, the addition of a capture system to an already existing fossil fuel-based facility does not directly concern the public living in the vicinity of the plant. Moreover, capture is assumed to concern less the society than the CCS infrastructure. Therefore it is here assumed that the capture stage does not generate any acceptance-related issues. On the other hand, pipelines and sequestration basins may generate a strong social response as the infrastructure may be placed in areas in close contact with the public.

Accordingly, this model will only take into account the risk perception parameter as proxy for the quantification of social acceptance, as results from Eq.(5.1) (Table 5.3).

5.3 Modelling framework

The model will provide a MILP strategic optimisation of a European CCS infrastructure (in terms of selection, positioning, and operation of capture and sequestration nodes, and transport routes), whilst considering the maximisation of social acceptance from the public inhabiting nearby the infrastructure (Figure 5.1). The spatial framework is geographically described through a grid of 134 squared cells g as described in Chapter 2, whose size ranges from 123 km to 224 km. This discretisation includes the European continent, few regions of North Africa and some offshore regions in the North Sea, where offshore sequestration basins are located and may be exploited (along with onshore storage options). Data and location of emission sources of CO_2 are obtained from the Emission Database for Global Atmospheric Research (EDGAR) published by Joint Research Centre (JRC, 2016). In particular, only large stationary emission sources (i.e., emitting more than 10^6 t of CO_2/year, corresponding to 37% of overall European CO_2 emissions) are considered, according

Tab. 5.1: Values of $dim_{d,c}$ of Hofstede's cultural dimensions d in country c (Hofstede et al., 2010).

	d					
c	PDI	UAI	LTO	IDV	MAS	IVR
Belgium	67	93	82	75	53	57
Croatia	73	80	58	33	40	33
Czech Republic	57	74	70	58	57	29
Denmark	18	23	35	74	16	70
Finland	33	59	38	63	26	57
France	68	86	63	71	43	48
Germany	35	65	83	67	66	40
Greece	60	112	45	35	57	50
Hungary	46	82	58	80	88	31
Ireland	28	35	24	70	68	65
Italy	50	75	61	76	70	30
Lithuania	42	65	82	60	19	16
Morocco	70	68	14	46	53	25
Netherlands	38	53	67	80	14	68
Norway	31	50	35	69	8	55
Poland	68	93	38	60	64	29
Portugal	63	104	28	27	31	33
Romania	90	90	52	30	42	20
Serbia	86	92	52	25	43	28
Slovakia	104	51	77	52	110	28
Spain	57	86	48	51	42	44
Turkey	66	85	46	37	45	49
United Kingdom	35	35	51	89	66	69

Tab. 5.2: Weights W_d^{risk} and $W_d^{benefit}$ of cultural dimensions d (Karimi and Toikka, 2018).

d	W_d^{risk}	$W_d^{benefit}$
PDI	-0.2	1.6
UAI	0.9	-1.7
LTO	0.7	-1.3
IDV	-0.1	-0.9
MAS	0.2	0.6
IVR	0.4	-0.8

Tab. 5.3: Parameter for the calculation of risk perception $risk_g$ [(people)$^{-1}$·(t of CO_2)$^{-1}$] in region g within country c (calculated following the methodology proposed by Karimi and Toikka, 2018). Because of lack of data, for some countries approximations are used: for Ukraine (ukr) and Moldavia (mda) the value of Romania (ro) is used; for Bosnia (ba) and Albania (alb) the value of Serbia (srb) is used; for Macedonia (mkd) the value of Greece is used (gr); for Algeria (alg) and Tunisia (tun) the value of Morocco (mo) is used 6.1.

g	c	$risk_g$	g	c	$risk_g$	g	c	$risk_g$	g	c	$risk_g$
1	fin	94.8	35	uk	92.1	69	mda	112.8	103	esp	120.5
2	fin	94.8	36	be	153.6	70	pt	117.3	104	esp	120.5
3	fin	94.8	37	de	132.1	71	esp	120.5	105	ita	118.6
4	fin	94.8	38	de	132.1	72	esp	120.5	106	ita	118.6
5	fin	94.8	39	de	132.1	73	esp	120.5	107	ita	118.6
6	fin	94.8	40	de	132.1	74	fr	128.6	108	gr	148.2
7	fin	94.8	41	pl	115.1	75	ita	118.6	109	gr	148.2
8	dk	65.4	42	pl	115.1	76	ita	118.6	110	tur	120.4
9	fin	94.8	43	pl	115.1	77	ita	118.6	111	tur	120.4
10	fin	94.8	44	pl	115.1	78	ba	119.3	112	esp	120.5
11	fin	94.8	45	ukr	112.8	79	ba	119.3	113	alg	73.0
12	uk	92.1	46	ukr	112.8	80	srb	119.3	114	alg	73.0
13	uk	92.1	47	fr	128.6	81	ro	112.8	115	alg	73.0
14	dk	65.4	48	fr	128.6	82	ro	112.8	116	alg	73.0
15	dk	65.4	49	fr	128.6	83	ro	112.8	117	tun	73.0
16	ltu	111.7	50	de	132.1	84	pt	117.3	118	tun	73.0
17	ltu	111.7	51	de	132.1	85	esp	120.5	119	ita	118.6
18	ltu	111.7	52	cz	121.4	86	esp	120.5	120	ita	118.6
19	irl	75.3	53	cz	121.4	87	esp	120.5	121	gr	148.2
20	irl	75.3	54	svk	107.0	88	esp	120.5	122	gr	148.2
21	uk	92.1	55	svk	107.0	89	esp	120.5	123	gr	148.2
22	uk	92.1	56	ukr	112.8	90	ita	118.6	124	tur	120.4
23	nl	109.0	57	ukr	112.8	91	ita	118.6	125	uk	92.1
24	de	132.1	58	ukr	112.8	92	ita	118.6	126	uk	92.1
25	de	132.1	59	fr	128.6	93	ita	118.6	127	no	80.0
26	de	132.1	60	fr	128.6	94	alb	119.3	128	no	80.0
27	pl	132.1	61	ita	118.6	95	mkd	148.2	129	no	80.0
28	pl	115.1	62	ita	118.6	96	gr	148.2	130	uk	92.1
29	pl	115.1	63	ita	118.6	97	gr	148.2	131	no	80.0
30	pl	115.1	64	hrv	127.2	98	tur	120.4	132	dk	94.8
31	pl	115.1	65	hun	127.2	99	pt	117.3	133	uk	92.1
32	pl	115.1	66	ro	112.8	100	esp	120.5	134	nl	109.0
33	uk	92.1	67	ro	112.8	101	esp	120.5			
34	uk	92.1	68	ro	112.8	102	esp	120.5			

to the indications provided by Chapter 2. These emissions can be captured according to a set of technologies k thus, including post-combustion from either coal or gas power plants, oxy-fuel combustion applied to coal plants, and pre-combustion capture applied to gas plants (described in Chapter 2). CO_2 flowrates can be transported from region g to region g' by mean of either onshore or offshore pipelines l, towards sequestration in geological basins. Note that the model developed within this Chapter 5 will not take into account the potential use of ships for transporting the CO_2 to reduce the computational burden. This seems a reasonable simplification, considering that ships were almost never employed from the results of previous Chapters. Data on the location, capacity and characterisation of the most promising formations for CO_2 storage (i.e., deep saline aquifers, hydrocarbon and coal fields) is obtained from the EU GeoCapacity Project (2009).
The design and operation of the resulting CCS infrastructure will generate a public response which is proportional to the risk perception, and will depend on the project size, on the population inhabiting the region, and on the differential behaviour of countries. Depending on the choice of optimising either costs, or risk perception, or a combination of both, the MILP model will minimise the corresponding objective function, and thus determine the optimal CCS SC configuration that allows reaching the chosen target. When pursuing an economic objective, the resulting network will be arranged in such a way as to minimise the costs to install and operate the various CCS stages (i.e., capture, transport, and geological sequestration). When aiming at optimising the social acceptance, the SC will be planned and operated in those regions that allow keeping risk perception on transport and sequestration at minimum levels. Otherwise, trade-off configurations will be obtained for combinations of the two conflicting objectives (i.e., economics against acceptance). Overall, the model is designed as follows. Given the following inputs:

- geographical distribution of CO_2 emission clusters from large stationary sources;
- geographical distribution of CO_2 sequestration basins;
- spatial features of European territories;
- minimum CO_2 quantity to be captured in Europe;
- techno-economic parameters describing CO_2 capture options;
- techno-economic parameters describing possible transport logistics;
- techno-economic parameters describing CO_2 storage sites and injection wells;
- spatial quantification of inhabitants in the model regions;
- differential behaviour of countries in terms of risk perception.

The objective is to optimise the economic (i.e., costs minimisation) and the community acceptance (i.e., risk minimisation) performances of the resulting CCS network. Accordingly, the model will provide as an output:

- geographic location, scale, and selection of CO_2 capture sites;
- geographic location, scale, and selection of CO_2 sequestration basins;
- definition and scale of transport infrastructure;
- exploitation of the European potential for CCS;
- economic performance of the CCS SC;
- risk perception performance of the transport network;
- risk perception performance of the injection system;
- social performance of the CCS SC in terms of risk perception.

5.4 Mathematical formulation

A European CCS SC is represented through a multi-echelon, time-static, spatially-explicit, multi-objective, MILP model, aiming at the simultaneous minimisation of total costs (TC [€]) and risk perception (RP):

$$\begin{cases} objective = min(TC, RP) \\ s.t. \\ capture\ problem\ model \\ transport\ problem\ model \\ sequestration\ problem\ model \\ + \\ social\ acceptance\ problem\ model \end{cases} \tag{5.3}$$

The modelling framework includes the capture, transport, sequestration, and social acceptance problems. In particular, the value of TC of Eq.(5.3) is given by the sum of the overall installation and operation costs deriving from the capture (i.e., TCC [€]), transport (i.e., TTC [€]), and sequestration (i.e., TSC [€]) stages, while RP of Eq.(5.3) is obtained according to the contributions of both transport (RP^{trans}) and sequestration (RP^{seq}) infrastructures in terms of risk perception:

$$TC = TCC + TTC + TSC \tag{5.4}$$

$$RP = RP^{trans} + RP^{seq} \tag{5.5}$$

Details on TCC, TTC, and TSC of Eq.(5.4) can be found in Chapter 2, whereas the quantification of RP^{trans} and RP^{seq} of Eq.(5.5) is detailed through the social

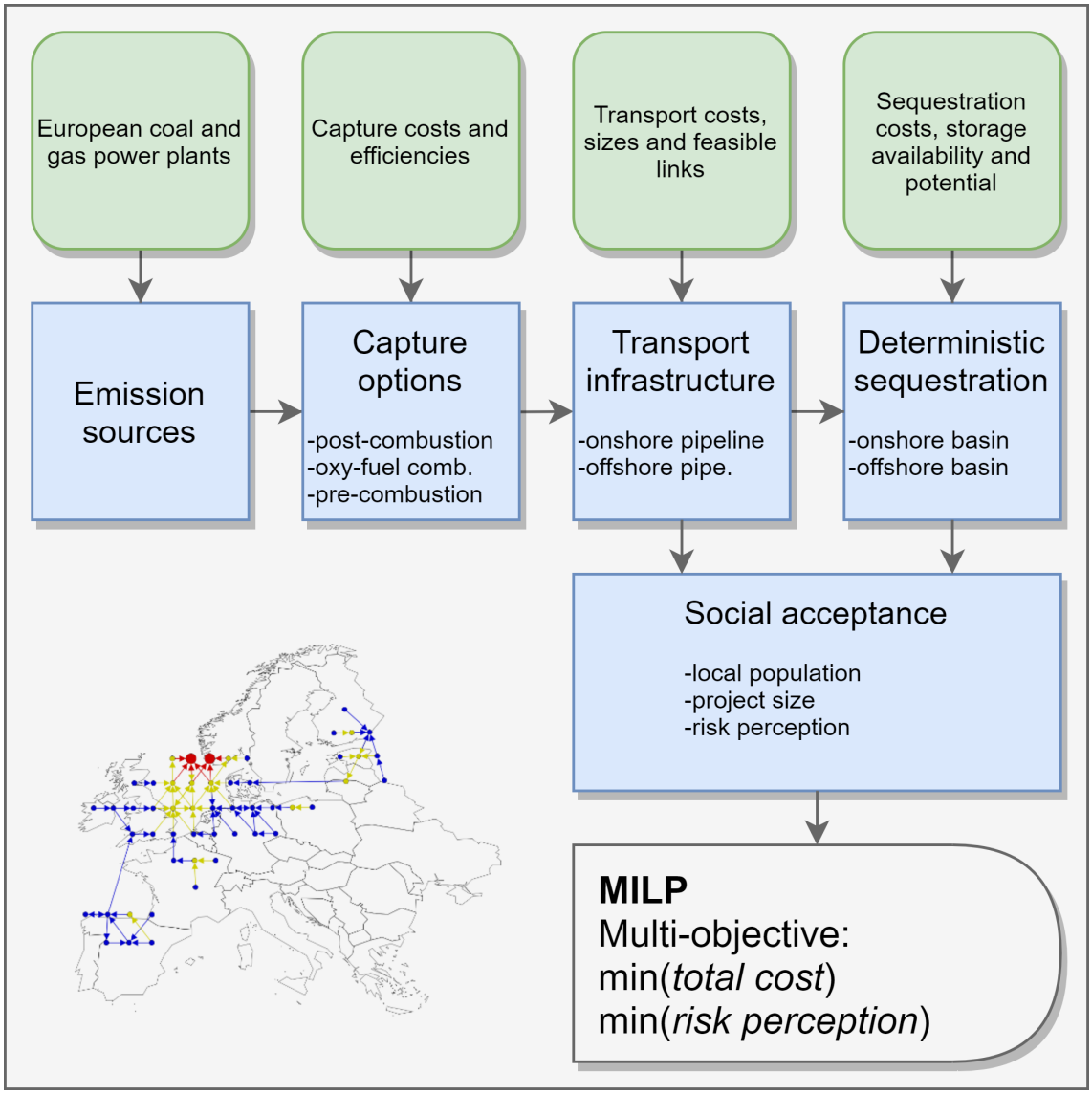

Fig. 5.1: Basic operating principle of the CCS SC MILP optimisation framework, including social acceptance evaluation through risk perception.

acceptance problem. Overall, as it will be detailed in the following, RP is calculated on the basis of the size of the CCS project, of the population inhabiting the region, and of the differential behaviour of countries in terms of risk perception. Indeed, RP^{trans} of Eq.(5.5) is calculated considering the massive CO_2 holdup in the pipelines $H_{g,g'}$ [t of CO_2] as variable accounting for the project size, the average population $\bar{P}_{g,g'}$ inhabiting between regions g and g' (Table 4.2), and the average parameter $\bar{risk}_{g,g'}$ [(people)$^{-1}$·(t of CO_2)$^{-1}$] for risk perception calculation of regions g and g' (Table 5.3):

$$RP^{trans} = \sum_{g,g'} (H_{g,g'} \cdot \bar{P}_{g,g'} \cdot \bar{risk}_{g,g'}) \tag{5.6}$$

In particular, $H_{g,g'}$ depends on the inner characteristics of the pipeline:

$$H_{g,g'} = \sum_{p,l} (\lambda_{p,g,l,g'} \cdot A_{p,g,g'} \cdot LD_{g,g'} \cdot \rho^{CO_2}) \qquad \forall g, g' \tag{5.7}$$

where $\lambda_{p,g,l,g'}$ is a binary variable representing whether a pipeline l of size p is installed between regions g and g', $A_{p,g,g'}$ [m^2] is calculated from the average values of inner diameters reported in Table (5.4) and represents the summation of pipelines sectional areas for transport capacities p between regions g and g', $LD_{g,g'}$ [m] is the length of the pipeline installed between regions g and g', while ρ^{CO_2} [0.85 t/m^3] is the average value of density of the CO_2 as taken from IPCC (2005), considering an average pressure of 15 MPa and temperature of 30°C. Furthermore, regarding risk perception on intra-connection systems within regions g, this formulation assumes that their contribution is indirectly accounted within that generated by the sequestration basins installed in region g. Indeed, if a sequestration basin is installed in region g therefore, at least one intra-connection mode is installed within the same region and its social acceptance is already quantified through the risk perception of the sequestration stage.

On the other hand, the risk perception RP^{seq} of Eq.(5.5) generated by the installation and operation of injection facilities is calculated according to the population P_g [people] inhabiting region g (Table 4.2), to the size of the sequestration S_g in region g, and to the parameter $risk_g$ for risk perception calculation in region g (Table 5.3):

$$RP^{seq} = \sum_{g} (S_g \cdot P_g \cdot risk_g) \tag{5.8}$$

5.5 Results

5.5.1 Scenarios

The model was implemented in the GAMS software and optimised through CPLEX solver on a quad core 2.3 GHz computer (32 GB RAM). The multi-objective optimisation was performed by aim of the ε-constrain method (Laumanns et al., 2006),

Tab. 5.4: Inner pipeline diameter (i.e., Φ_p [m]) and mass flowrates (i.e., Q_p [Mt of CO_2/year]) employed for the calculation of holdup areas $A_{p,g,g'}$, according to the pipelines capacity discretisation p. The values are taken from Knoope et al. (2013).

	p						
	1	2	3	4	5	6	7
Q_p	1	5	10	15	20	25	30
Φ_p	0.20	0.40	0.50	0.59	0.66	0.72	0.79

which allows to optimise a bi-objective problem under a Pareto-based criterium, i.e. a situation in which an improvement in the solution of one first objective equals necessarily to worsening the solution of the secondary objective. Following the indications provided by the EC (2018), and to compare the results with those from previous Chapters, the minimum European carbon reduction target α was set equal to 50% of European emissions (i.e., the model aims at capturing and permanently sequestering 50% of the total European emissions from large stationary sources). The response of the model to different values of carbon reduction target will be tested as well. Results clearly show the conflict between costs and risk perception (Figure 5.2), as those SC configurations positively affecting economics (i.e., lower total cost TC) exhibit a poor performance in terms of social acceptance (i.e., higher risk perception RP). Three case studies will be here investigated according to the multi-objective solution of the optimisation:

- Scenario A (Figure 5.2, point A), entailing the economic optimisation of the CCS SC in terms of TC minimisation;
- Scenario B (Figure 5.2, point B), entailing the social acceptance optimisation of the CCS SC in terms of RP minimisation;
- Scenario C (Figure 5.2, point C), entailing an intermediate situation between the two conflicting objectives, corresponding to a trade-off network that manages to keep RP low without penalising excessively the CCS SC in terms of TC.

5.5.2 Minimum cost network

The European CCS system resulting under Scenario A entails (Table 5.5) a total cost TC to install and operate the network of 462.4 B€ (i.e., 38.18 €/t of sequestered CO_2), of which TCC for capture is 432.3 B€ (i.e., 35.69 €/t of sequestered CO_2), TTC for transport is 26.4 B€ (i.e., 2.18 €/t of sequestered CO_2), and TSC for sequestration is 0.3 B€(i.e., 0.28 €/t of sequestered CO_2) (Figure 5.3). Furthermore,

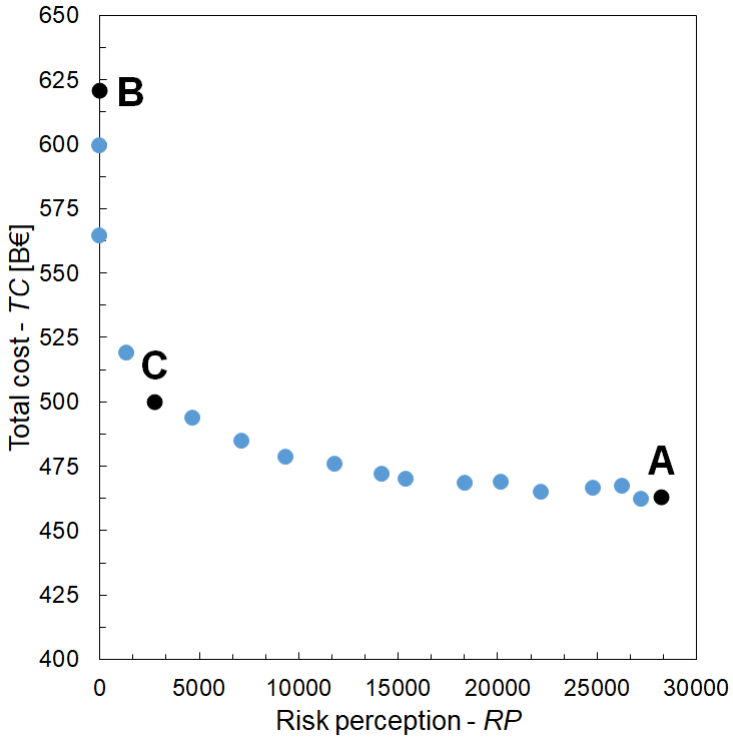

Fig. 5.2: Pareto curve under bi-objective optimisation: the tree Scenarios are indicated.

Tab. 5.5: Scenarios A-B-C: results from the bi-objective optimisation in terms of total cost TC [B€ or €/t of sequestered CO_2], risk perception RP, optimality gap Opt. gap [%], and solution time Sol. time [s].

Scenario	α	TC		RP	Opt. Gap	Sol. Time
		[B€]	[€/t]		[%]	[s]
A	0.50	462.4	38.15	27204.1	1.6	<60
B	0.50	620.7	50.88	6.3	6.6	4969
C	0.50	499.8	41.25	2752.2	5.2	14579

the optimal solution of the best economic SC entails the overall risk perception RP is equal to 27204, and constituted by a negligible transport risk perception RP^{trans} of about 1, opposed to a very large sequestration risk perception RP^{seq} of 27203. The resulting SC configuration (Figure 5.4) is mainly developed within the mainland to minimise both transport and sequestration costs by avoiding offshore logistics and injection points, which generates noticeable values of risk perception as an obvious shortcoming. Moreover, risk perception generated by sequestration is much larger than that generated by the transport infrastructure. This difference can be explained considering the fact that the quantity of CO_2 that may be planned to be stored in geological basins can be up to the order of magnitude of 10^9 t of CO_2, whereas pipelines are designed to transport a maximum flowrate of 30 Mt of CO_2 on a yearly basis. Therefore, considering a CCS project in a region g with a certain population, RP^{trans} and RP^{seq} are calculated on the basis of pipelines holdups and stored quantities, and as a consequence RP^{trans} is likely to be quantitatively smaller than RP^{seq}.

5.5.3 Minimum risk network

The situation is completely different under Scenario B in terms of both economic result, community acceptance, and SC configuration. In fact, Scenario B exhibits (Table 5.5) a total cost TC of 620.7 B€ (i.e., 50.88 €/t of sequestered CO_2), i.e. +34% with respect to that of Scenario A. In particular, Scenario B entails a remarkable increase in transport TTC (equal to 140.9 B€, or 11.55 €/t of sequestered CO_2, i.e. +434%) and sequestration TSC (equal to 25.9 B€, or 2.13 €/t of sequestered CO_2, i.e. +853%) costs with respect to the best economic configuration obtained from Scenario A (Figure 5.3). These additional expenditures are needed to keep the levels of risk perception to minimum levels and to obtain the best network in terms of social acceptance: RP^{trans} is almost null and RP^{seq} is reduced to zero. The increase in TTC and TSC costs with respect to Scenario A is explained considering the SC network generated from Scenario B (Figure 5.4b): offshore sequestration in the North Sea is preferred to the (cheaper) onshore option (Figure 5.5). Regarding the positioning of capture facilities, CO_2 is captured in regions that are as close as possible to offshore basins to minimise the length of the pipelines and, accordingly, RP^{trans} as well.

5.5.4 Trade-off network

As expected, Scenario C depicts an intermediate situation between the two extreme SC configurations represented by the solutions of Scenario A and Scenario B. In fact, Scenario C exhibits (Table 5.5) a total cost TC of 499.8 B€ (i.e., 41.25 €/t of sequestered CO_2, +8% and –189% with respect to Scenario A and Scenario B, respectively), constituted by a capture cost TCC of 432.9 B€ (i.e., 35.72 €/t of sequestered CO_2), a transport cost TTC of 59.6 B€ (i.e., 4.91 €/t of sequestered

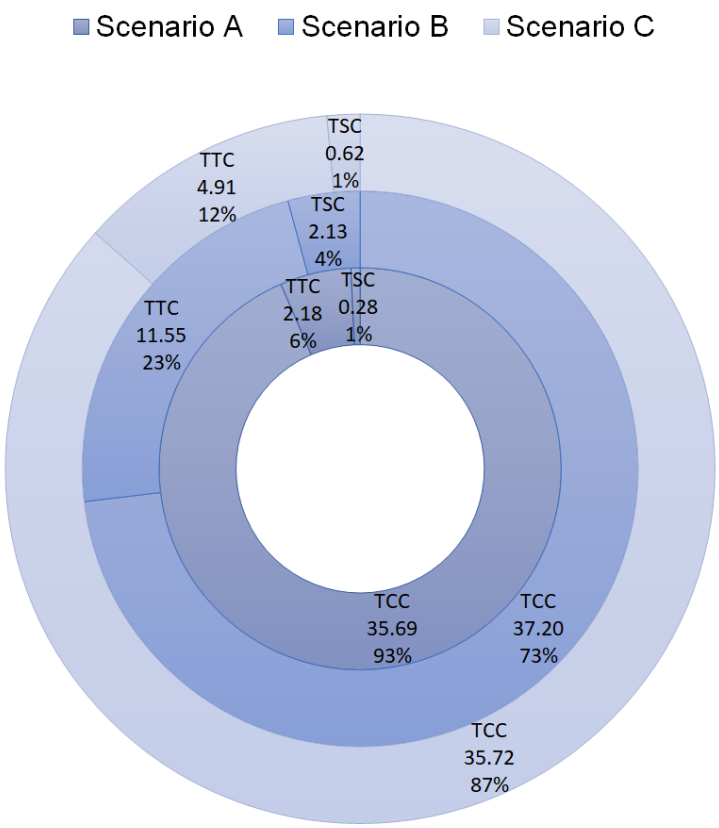

Fig. 5.3: Scenarios A-B-C: results from the bi-objective optimisation in terms capture TCC [€/t of sequestered CO_2, and %], transport TTC [€/t of sequestered CO_2, and %], and sequestration TSC [€/t of sequestered CO_2, and %] costs contribution to overall investment TC.

CO_2), and a sequestration cost TSC of 7.5 B€ (i.e., 0.62 €/t of sequestered CO_2) (Figure 5.3). The slight increase in TC with respect to Scenario A is needed to obtain an acceptable infrastructure in terms of risk perception RP, the latter equal to 2752 and significantly reduced (-899%) with respect to the optimal economic SC obtained for Scenario A. Unlike Scenario B (Figure 5.4b), in Scenario C (Figure 5.4c) offshore sequestration is only performed on basins nearby the United Kingdom (i.e., fairly close to the mainland), to limit the additional costs deriving from further transportation towards the North Sea. Concerning onshore sequestration, the most exploited basins for CO_2 storage are located nearby the Netherlands, Denmark, Spain, Italy, and Portugal (Figure 5.5). Just minor quantities are stored in locations within countries with high carbon intensity and high risk perception (e.g., Germany, Poland), at the cost of allowing some decrease in public acceptance with respect to Scenario B, while keeping infrastructural costs not too high with respect to Scenario A.

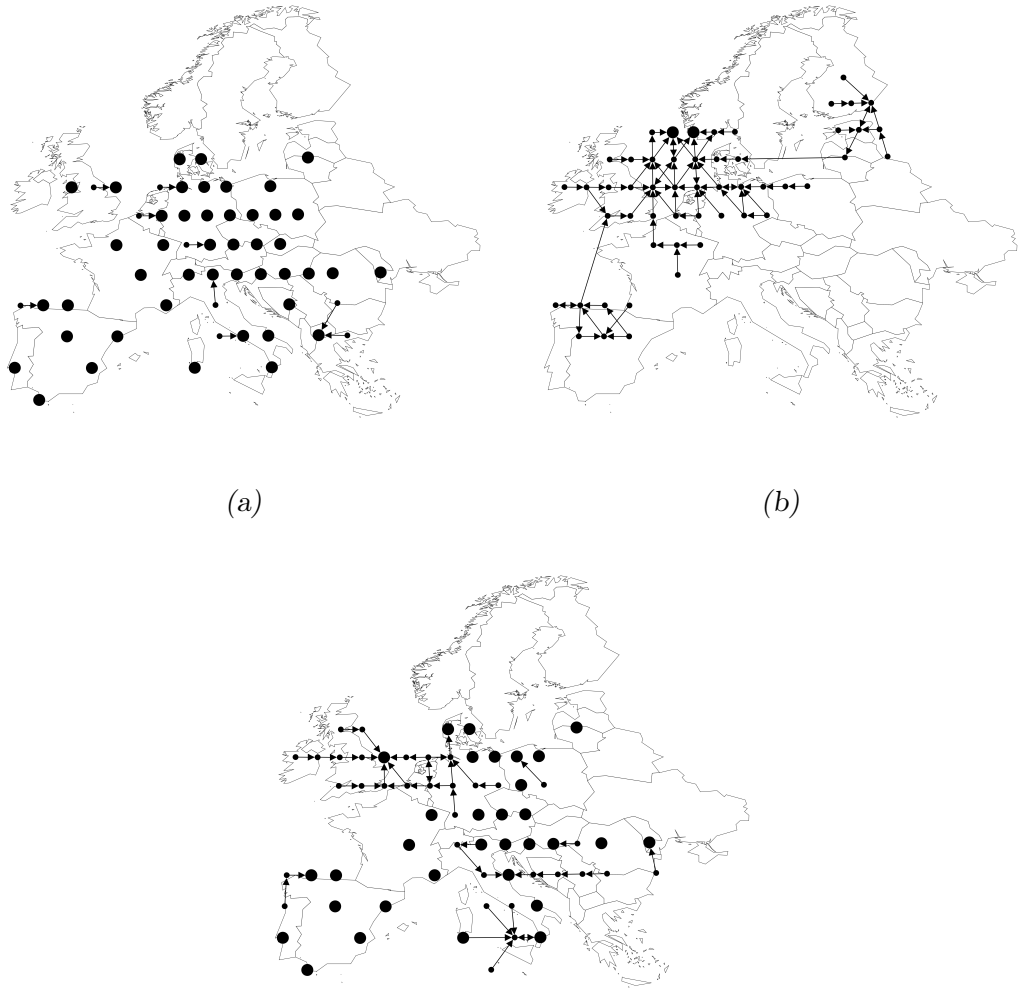

(a) *(b)*

(c)

Fig. 5.4: Scenarios A, B, and C: resulting SC configurations. Dark dots represent capture and sequestration nodes.

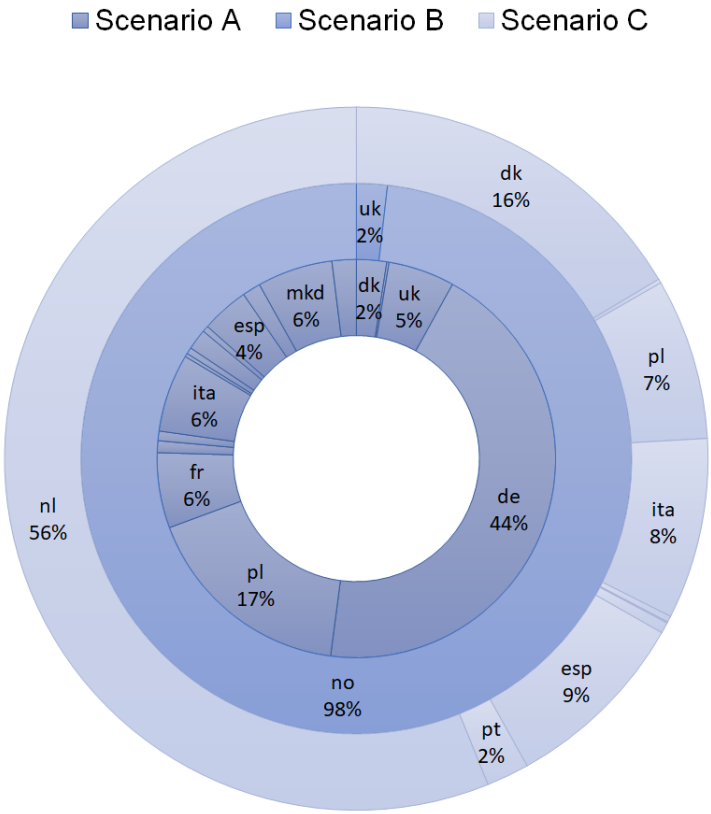

Fig. 5.5: Main contributors to sequestration as results from optimal CCS SC optimisations for Scenarios A, B, and C. dk=Denmark, pl=Poland, ita=Italy, esp=Spain, pt=Portugal, nl=Netherlands, uk=United Kingdom, no=Norway, de=Germany, fr=France, mkd=Macedonia.

5.5.5 Sensitivity analysis

This Section analyses the response of model to the variations of the European carbon reduction target α under Scenario C (i.e., the trade-off scenario between economic and social acceptance optimisations), from a minimum value of 20% to a maximum of 50%. Results in terms of SC configuration clearly show the evolution of the system when the lower bound for overall CO_2 capture is increased (Figure 5.6). Offshore geological potential is the main storage option chosen to be exploited for low carbon reduction targets (in order to keep the level of risk perception as low as possible, without compromising too much the economic performance of the system) but, as long as α increases, more and more CO_2 gets sequestered onshore, at the cost of generating some risk in terms of acceptance, while keeping infrastructural costs not too high. Overall, changing the European carbon reduction target confirms the results in terms of optimal configuration obtained for $\alpha = 50\%$ and described within the main text.

5.6 Discussion and limitations

Different SC configurations emerged from the multi-objective optimisation of the system, depending on the choice of minimising either costs (Scenario A) or public risk perception (Scenario B), or a combination of both (Scenario C). The economic optimisation (Scenario A) confirms the results from previous Chapters in terms of both SC configuration and range of costs, and suggests sequestering the CO_2 in the same region where it is captured, in order to minimise the transport costs (Figure 5.5). The resulting SC is constituted by an infrastructure, which is rather uniformly spread across Europe. The best configuration in terms of public acceptance (Scenario B) suggests sequestering all the CO_2 in the North Sea (Figure 5.5) to exploit basins that are located in regions with no population (thus, generating very low risk perception). Nevertheless, the resulting network is too complex and expensive, and unlikely to be practically implemented. Conversely, the intermediate solution (Scenario C) represents a trade-off between economics and public acceptance, and could be employed to characterise the additional costs (+8% with respect to an acceptance risk-neutral network) deriving from the design of a European CCS SC that takes into account, along with the economic decision variables, the attitude and criticism of people towards these technologies (Figure 5.5).
The mathematical formulation of this study is based on two main pillars: a deterministic economic optimisation of a European network for CCS (as described in Chapter 2), and a quantitative technique for measuring public acceptance through risk perception at countrywide level (Karimi and Toikka, 2018). We recognise that there are a number of assumptions and simplifications, which are discussed in the following:

- the installation of transport/sequestration infrastructure in a country will

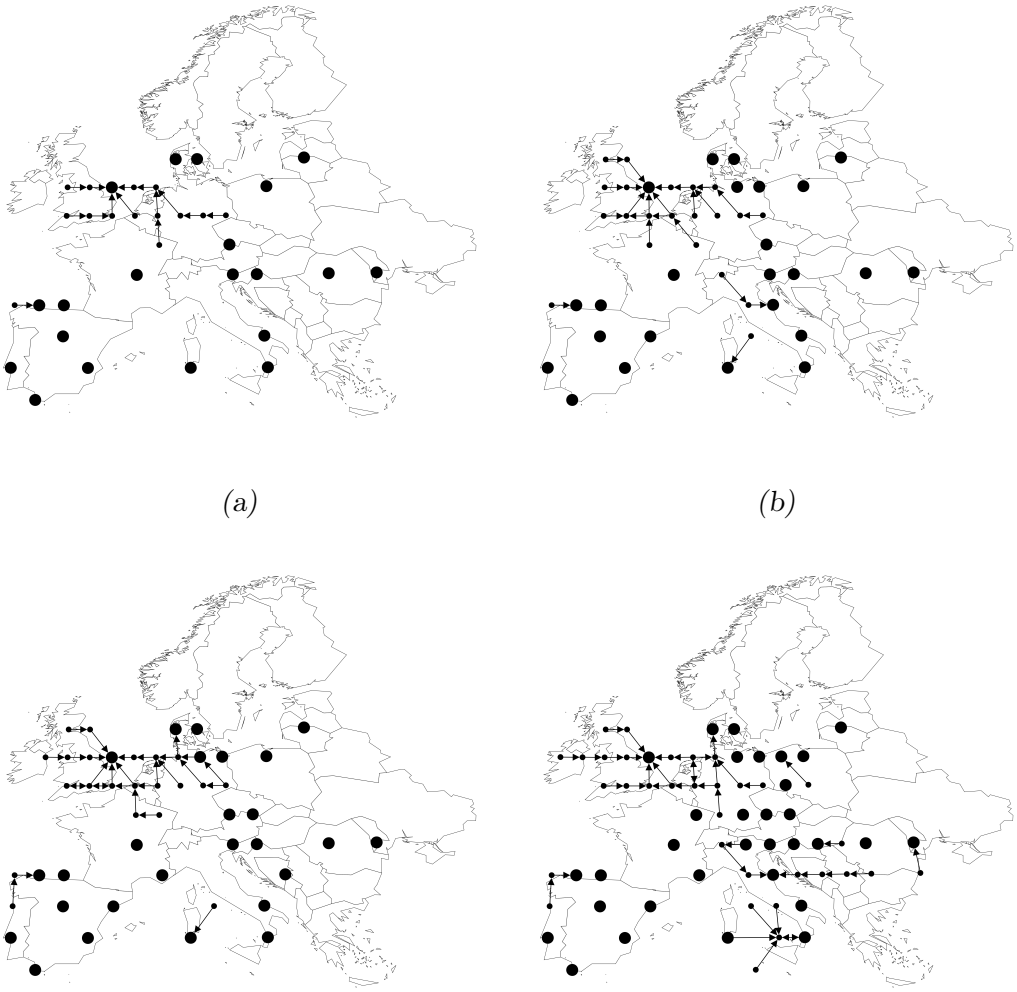

(a) *(b)*

(c) *(d)*

Fig. 5.6: CCS SC configuration under Scenario C, for different values of carbon reduction target α. Dark dots represent capture and sequestration nodes.

likely create a debate, which may modify the perception on CCS and affect how future enlargements or installation may be perceived; in our model we assume that the entire European CCS SC is simultaneously built, thus neglecting possible positive or negative feedback effects on perception depending on the evolution in time of the CCS infrastructure;

- it is assumed that risk is proportional to the size of the transportation pipeline and/or sequestration basin; although this seems a sensible approach, there is no information available assessing whether risk perception indeed increases linearly with size or an alternative correlation would be more realistic;

- it is well known that political propaganda, mass media, information campaigns may change people perception even in a relatively short-term; this introduces a level of uncertainty, whose effects can be neither quantified, nor forecasted, and therefore they are not taken into account in the proposed framework;

- also in view of the above, survey data should be periodically updated; we have referred to the most recent data available at a European level (Eurobarometer, 2011), but the situation is continuously changing and evolving;

- as shown in previous Chapters, coal- and gas-fired power plants are considered as the only sources of CO_2, neglecting the contribution of industrial facilities to overall emissions. Although this is a simplification, it is nonetheless a fact that these power plants are the only points of very high emission of CO_2 and they generate about 37% of the overall yearly stationary CO_2 emissions in Europe (IPCC, 2018);

- the potential of combined carbon utilisation and sequestration (CCUS) is not taken into account; although its impact in terms GHGs emissions is still debated (Mac Dowell et al., 2017; Alper and Orhan, 2017), a recent study (Arning et al., 2019) suggests that carbon utilisation has a more favourable response in terms of public acceptance; it may therefore be used synergistically to maximise acceptance.

Notwithstanding such limitations, this model represents a significant step forward to assess the design of CCS infrastructures. For the first time, a model of public perception was incorporated within an optimisation framework to provide a quantitative tool to assess how social acceptance may affect the effective planning and deployment of a CCS infrastructure, and the costs incurred to address and minimise that risk. Furthermore, a positive feedback comes from the fact that in several cases, higher specific risk perception values are assigned to those countries where legislation was enforced to limit or even ban CO_2 storage on their territory (e.g., Germany, Poland); accordingly, results (Scenario C) show some correspondence between those countries where CCS deployment is avoided to reduce risk perception, and those in which CO_2 storage is indeed forbidden by actual regulations (EC, 2017). Although

this cannot be deemed as a proper validation (additional political and social factors can contribute to this result), it nonetheless demonstrates that there is a good agreement between the model predictions and the actual national response to such issues.

5.7 Chapter conclusions

This Chapter 5 proposed a MILP model for the design and optimisation of a European CCS SC, including a quantitative assessment of countrywide community acceptance through measures of risk perception. The objective was to minimise the installation and operation costs of a continent-scale network, while simultaneously minimising the additional costs deriving from the necessity of avoiding the possibility of local protests and opposition against the implementation of the transport and sequestration infrastructural nodes.
Results showed that the maximisation of social acceptance through the minimisation of risk perception (regardless of considerations on economic aspects) leads to offshore sequestration solutions with a (possibly unacceptable) total costs of about 621 B€ (equal to 50.88 €/t of sequestered, i.e. +34% with respect to the economic optimum), due to a more complex network configuration characterised by high transport (+434%) and sequestration (+853%) costs. A multi-objective optimisation analysis, however, allowed identifying a possible intermediate solution between the two conflicting objectives (i.e., economics against acceptance), capable of limiting risk perception, without excessively compromising the economic performance of the network. This configuration still entailed a massive deployment of offshore sequestration to minimise overall risk perception, but also several onshore basins were exploited in regions within Denmark, Spain, Italy and Portugal. Overall, the specific total cost of the SC increased to 41.25 €/t of sequestered CO_2 (+8% with respect to the best economic configuration), thus demonstrating that this configuration could represent a reasonable trade-off between the economic and community acceptance objectives. The methodology presented in this Chapter may provide investors and policy makers with a quantitative tool to assess the possible response of local communities to the deployment of such technologies. The combination of this analysis with more inclusive strategies for a stronger engagement of local communities might constitute a key tool to foster an effective implementation of CCS technologies. Cooperation policies for costs share should be taken into account too, in order to relieve single countries from too high investment risk. The next Chapter will deal with this issue by introducing costs share policies among European nations.

6

Cooperation policies and costs share

6.1 Chapter summary

Considering a large-scale CCS infrastructure at European level, economic cooperation has been highlighted as a key requirement to relieve single countries from too high risk and commitment. This Chapter 6 proposes an economic optimisation for cooperative SCs for CCS, by adopting policies that balance the spread of costs among countries, according to local features in terms of population, CO_2 emissions and macroeconomic outcome[1]. Results show that the additional European investment for cooperation (max. +2.6% with respect to a non-cooperative network) should not constitute a barrier towards the installation and operation of such more effective network designs.

6.2 Problem statement

A common assumption in the establishment of a CCS infrastructure is that each player (i.e., each country) should pay the costs for what of the network is actually installed within its borders. Therefore, it is clear that the adoption of this globally optimal solution entails the drawback of polarising countrywide per capita and per emitted unit infrastructural costs ($\widehat{TC}_c$ [€/person or €/t of CO_2 emitted] in country c (Figure 6.1) (the list of countries is reported in Table 6.1). For instance,

[1] The content of this Chapter was published in: d'Amore and Bezzo, 2019d.

Tab. 6.1: List of countries c.

c	Country	c	Country
alb	Albania	ita	Italy
aut	Austria	ltu	Lithuania
ba	Bulgaria	lv	Latvia
be	Belgium	mda	Moldova
ch	Switzerland	mdk	Macedonia
cz	Czech Republic	nl	Netherlands
de	Germany	no	Norway
dk	Denmark	pl	Poland
dz	Algeria and Tunisia	pt	Portugal
esp	Spain	ro	Romania
est	Estonia	se	Sweden
fin	Finland	si	Slovenia
fr	France	srb	Serbia
gr	Greece	svk	Slovakia
hrv	Croatia	tur	Turkey
hun	Hungary	uk	United Kingdom
irl	Ireland	ukr	Ukraine

Chapter 2 described a modelling framework for the optimisation of a European CCS SC with a carbon reduction target of 50% of overall emissions from large stationary source over a 20 years' time span. The resulting globally optimal European SC entailed a countrywide cost ranging from zero to over 2000 €/person (corresponding to an average cost of 673.6 € per European inhabitant). This could locally constitute a non-satisfactory investment solution, e.g. for those medium-large emitting countries paying high per capita infrastructural costs (i.e., €/person) compared to those per emission unit (i.e., €/t of CO_2). On the contrary, CO_2 emitters located in marginal areas might not be considered as part of the CCS network from the results of an approach aiming at global optimality, since they would not pay high enough per capita infrastructural costs (considering their contribution to overall emission) given their decentralised position. Balancing the spread of costs for CCS across European countries might be an effective strategy for a more timely and fair implementation of such a large-scale and complex network. This can be achieved by pushing towards the adoption of policies for financial cooperation, meaning that every country c should play a role in the investment for CCS, also independently of the presence of an operative infrastructure on their territory. Therefore, more cooperative system configurations might constitute a better (i.e., more likely to be implementable) solution with respect to that resulting from a global optimum-driven approach. The proposed modelling approach will be discussed in the following.

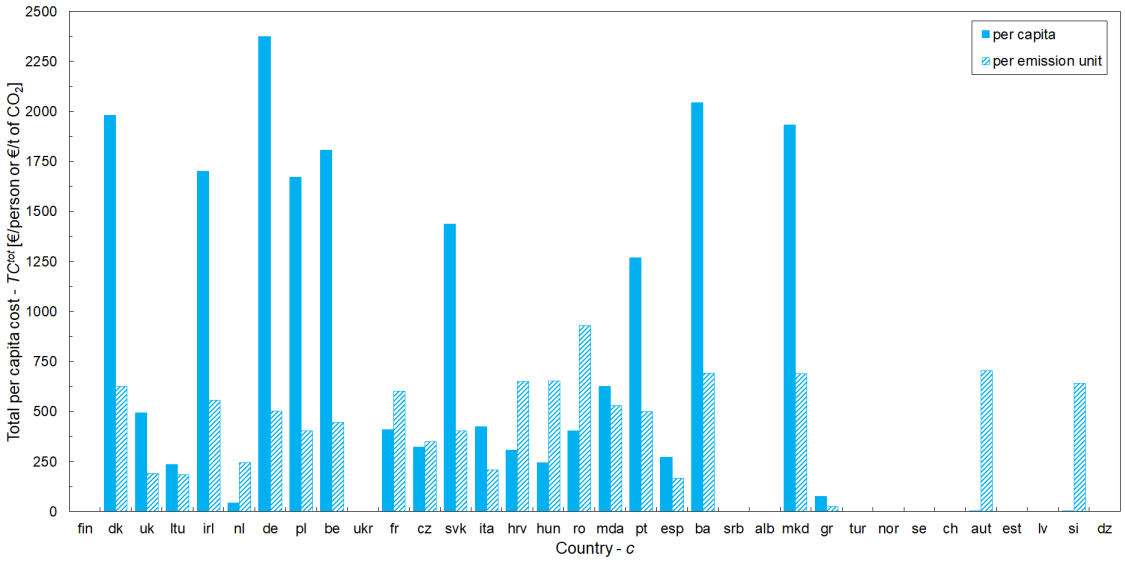

Fig. 6.1: CCS SC countrywide per capita or per emitted unit cost ($\widehat{TC}_c$ [€/person, or €/t of CO_2 emitted], as resulting from a global optimisation-driven approach reported in Chapter 2.

6.3 Modelling framework

A multi-echelon, spatially-explicit, time-static, MILP model for the economic optimisation of a European CCS SC is presented, with the aim of providing a financial tool that evaluates the additional cost required to attain balancing strategies among countries and thus, to foster implementation through costs share and cooperation (Figure 6.2). In particular, the model builds up from a previous deterministic mathematical framework (as described in Chapter 2), by discussing further such a large-scale European CCS network, in which notably most of the infrastructure resulting from a global optimisation-driven approach needs to be built heterogeneously among different countries and across many borders, with no clear consensus on either individual financial responsibilities, or communal investment duties. However, differently from previous contributions, this model does not aim at providing insights into the optimal deployment and evolution of the CCS SC along a certain time horizon, but rather investigates how the choice in cooperation mechanisms would affect the final optimal configuration of the European system, independently from any time-dependent considerations. This is done to reduce the much higher computational burden that would be required by a time-dependent model, also considering that the final CCS SC configuration does not differ in the two cases significantly (d'Amore and Bezzo, 2017). On the one hand, along with the implementation of spatial-geographic features at European scale by aim of grid g of squared regions, this contribution focuses as well on the nationwide-scale commitment for installing and operating the optimal CO_2 network through the set of countries $c = [fin, dk, uk, ..., lv, si, dz]$. On the other hand, considering the size and resolution of the investigated network, in

which cells g are broader than 150 km, Cyprus, Luxemburg and Malta have not been here considered as part of the optimisation. The spatial description of large stationary point sources is retrieved from the EDGAR database (JRC, 2016) and only constituted by coal and gas power plants emitting more than 10^6 t of CO_2/year (i.e., corresponding to the 37% of European overall CO_2 emissions from large stationary sources), following the indications provided by Chapter 2. On the one hand, the techno-economic characterisation of capture options k (i.e., unitary capture costs, capture efficiencies, matching with CO_2 sources) is retrieved from data provided by IPCC (2005), subsequently updated by Rubin et al. (2015). On the other hand, the techno-economic description of the transport infrastructure (i.e., unitary transport costs, scale factors on distance and scale, feasible connection arcs) is taken from Chapter 2 according to possible transport modes l that can be installed and operated for either intra-connection within cell g, or inter-connection between region g and g'. Finally, the geolocation and volumetric description of European sequestration basins s are retrieved from the EU GeoCapacity Project (JRC, 2016). Injection wells are economically described according to the unitary installation and operation costs as proposed in Chapter 2.
In order to foster a timely development of the network, each country should play a role to achieve an effective financing strategy at both local and global scale, also independently from the installation of the CCS network on their territory. However, large stationary point sources are not homogeneously distributed across Europe (JRC, 2016); thus, a methodology that does not penalise members with an already accomplished policy for low carbon intensity is here taken into account. Furthermore, from a macroscopic point of view in terms of living standards, European countries are not only characterised by highly differentiated population densities (Eurostat, 2019a), but also by relatively large macroeconomic differences (Eurostat, 2019b). These phenomena are included within the MILP model to achieve a satisfactory balance between an ideally equalitarian costs share system (i.e., maximum sub-optimality), and a fairer network that locally considers both capture and economic necessities.

6.4 Mathematical formulation

The objective function is the minimisation, for every iteration j, of the total European cost TC_j^{tot} [€] that is required to install and operate the CCS network:

$$\begin{cases} objective = min(TC_j^{tot}) \\ TC_j^{tot} = \sum_c TC_{j,c}^{tot} \qquad \forall j \end{cases} \tag{6.1}$$

In particular, at iteration j every country c entails a total cost $TC_{j,c}^{tot}$ [€], which is given by the combined contribution of infrastructural cost $TC_{j,c}^{network}$ [€] and an either positive (i.e., $debit_{j,c}$ [€]) or negative (i.e., $credit_{j,c}$ [€]) additional differential

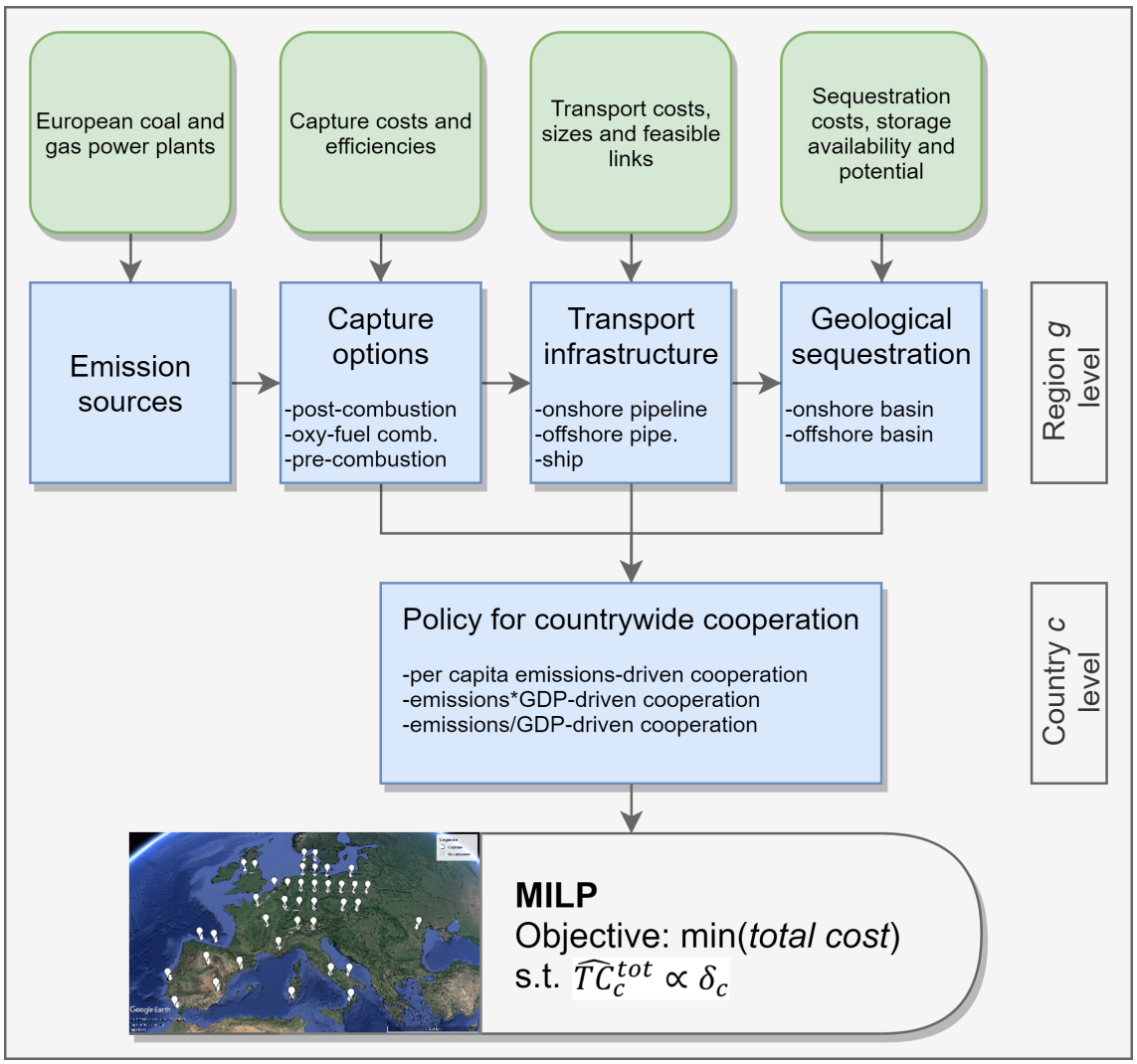

Fig. 6.2: Representation of the modelling framework aiming at the minimisation of total cost for CCS, such that the imposed costs share level between countries c is accomplished, according to a proportionality between national per capita costs $\widehat{TC}_c^{tot}$ and the chosen policy for cooperation δ_c.

investment that might be required to balance the spread of costs for CCS across Europe:

$$TC_{j,c}^{tot} = TC_{j,c}^{network} + debit_{j,c} - credit_{j,c} \qquad \forall j, c \tag{6.2}$$

Eq.(6.2) defines a funding mechanism, through which every country c can either actively contribute to the infrastructural costs to install and operate the SC stages (i.e., $TC_{j,c}^{network} > 0$), or passively compensate through a debit (i.e., $debit_{j,c} > 0$) those countries c' that are investing more than a certain threshold (and will conversely receive $credit_{j,c'} > 0$). The debit/credit system is introduced to prevent non-sensible configurations in the optimised solution. For instance, the scope is to avoid that a highly emitting country located in a marginal area is forced to invest in a CCS infrastructure in its territory that would lead to an excessive distortion of the optimal CCS configuration and accordingly too high an increase in the overall investment. Thus, the debit/credit system allows to compensate with money the additional investment of other countries. On the other hand, $TC_{j,c}^{network}$ of Eq.(6.2) is calculated by summing up the cost contributions of the capture ($TCC_{j,c}$ [€]), transport ($TTC_{j,c}$ [€]) and sequestration ($TSC_{j,c}$ [€]) stages:

$$TC_{j,c}^{network} = TCC_{j,c} + TTC_{j,c} + TSC_{j,c} \qquad \forall j, c \tag{6.3}$$

In particular, $TCC_{j,c}$ of Eq.(6.3) is evaluated according to the optimal selection, location and scale of capture options k, which might be installed at iteration j in regions g of country c, and depends on the captured quantity $C_{j,g,k}$ [t of CO_2] in regions g within country c through technology k, and on the unitary cost UCC_k [€/t of CO_2] for installing and operating capture option k (described in Chapter 2):

$$TCC_{j,c} = \sum_{k,g \in c} (C_{j,g,k} \cdot UCC_k) \qquad \forall j, c \tag{6.4}$$

Regarding $TTC_{j,c}$ of Eq.(6.3), it is determined through mass balances and logical constraints reported in Chapter 2 as result from the optimal routing, selection and scale at iteration j of transport modes l between region g and g' located across country c. $TTC_{j,c}$ is given by the combined contributions of countrywide-scale effects on transport size ($TCC_{j,c}^{size}$) [€], of scale effects on transport distance ($TCC_{j,c}^{dist}$) [€] and of a corrective cost component ($TCC_{j,c}^{intra}$) [€] that accounts the intra-connection systems within each cell:

$$TTC_{j,c} = TCC_{j,c}^{size} + TCC_{j,c}^{dist} + TCC_{j,c}^{intra} \qquad \forall j, c \tag{6.5}$$

Finally, $TSC_{j,c}$ of Eq.(6.3) is calculated at iteration j according the optimal choice in the number and size of injection wells $N_{j,g}$ that are positioned in regions g of country c:

$$TSC_{j,c} = \sum_{g \in c} (N_{j,g} \cdot USC_g) \qquad \forall j, c \tag{6.6}$$

where USC_g [€/well] is the unitary sequestration cost for installing and operating one injection well in region g described in Chapter 2.

Regarding $debit_{j,c}$ and $credit_{j,c}$ of Eq.(6.2), this model assumes that Europe is an economically 'adiabatic' system, i.e. no outsource subsidies or external debits are allowed. Therefore, the financial debit generated in a given country must be necessarily balanced by an identical amount of credit (or by the sum of many credits) somewhere else at every iteration j. Thus, it is imposed that the overall European debit must be equal to the corresponding generated credit:

$$\sum_c debit_{j,c} = \sum_c credit_{j,c} \qquad \forall j \tag{6.7}$$

The significance of terms $debit_{j,c}$ and $credit_{j,c}$ is to be found in the choice of forcing countrywide total per capita cost $\widehat{TC}^{tot}_{j,c}$ [€/person] to fall within a predetermined range:

$$\widehat{TC}^{tot}_{j,c} = \frac{TC^{tot}_{j,c}}{P_c} \qquad \forall j, c \tag{6.8}$$

$$\widehat{TC}^{tot}_{j,min} \cdot \delta_c \leq \widehat{TC}^{tot}_{j,c} \leq \widehat{TC}^{tot}_{j,max} \cdot \delta_c \qquad \forall j, c \tag{6.9}$$

where P_c [people] represents the number of inhabitants of country c, while δ_c is the countrywide weighting factor. In this study, δ_c (Table 6.2) is implemented as a normalised parameter that represents the target levelling of per capita costs amongst countries c in cases of policies driven by: (i) countrywide CO_2 per capita emissions (i.e., δ^A_c); (ii) national CO_2 emissions· GDP (i.e.,δ^B_c); and (iii) a countrywide CO_2 emissions/GDP (i.e., δ^C_c). Accordingly, δ^A_c describes the reciprocal features of countries c in terms of CO_2 emissions from large stationary sources, whereas δ^B_c and δ^C_c combine differences in local emissions with the economic outcome described in terms of GDP. Overall, the so formulated δ_c parameter does not penalise countries with low CO_2 emissions, whereas it pushes towards an increase of the economic commitment for CCS for those countries whose per capita emissions are high (i.e., δ^A_c), or with both high per capita emissions and GDP (i.e., δ^B_c), or with low carbon efficiency at producing wealth (i.e., δ^C_c). δ_c is employed to shift the range of validity of $\widehat{TC}^{tot}_{j,c}$ according to the inner characteristics of countries c in terms of population, emissions and GDP. For instance, in the case of $\delta^c = \delta^A_c$, if a country c has lower per capita emissions with respect to another country c', the per capita contribution to cooperation of c must be lower than that of c' thus, $\delta_c < \delta_{c'}$ and consequently $\widehat{TC}^{tot}_{j,c}$ must be cheaper than $\widehat{TC}^{tot}_{j,c'}$. On the other hand, if c has higher per capita emissions than c' thus, $\delta_c > \delta_{c'}$ and $\widehat{TC}^{tot}_{j,c}$ must be more expensive than $\widehat{TC}^{tot}_{j,c'}$.
Both the lower bound $\widehat{TC}^{tot}_{j,min}$ [€/person] and the upper bound $\widehat{TC}^{tot}_{j,max}$ [€/person] are iteratively calculated according to the extreme target values of minimum (i.e., $\widehat{TC}^{network}_{min}$ [€/person]) and maximum (i.e., $\widehat{TC}^{network}_{max}$ [€/person]) infrastructural cost, chosen over all European countries from the best globally optimal CCS SC configuration (i.e., the optimal infrastructural network obtained by only minimising $TC^{network}_{j,c}$):

$$\widehat{TC}^{tot}_{j,min} = \widehat{TC}^{network}_{min} + \varepsilon_j \cdot (\widehat{TC}^{network}_{max} - \widehat{TC}^{network}_{min}) \qquad \forall j, loop \tag{6.10}$$

Tab. 6.2: Differential countrywide weighting factors δ_c^A, δ_c^B and δ_c^C for each country c (Eurostat, 2019a; 2019b).

	δ_c				δ_c		
c	δ_c^A	δ_c^B	δ_c^C	c	δ_c^A	δ_c^B	δ_c^C
fin	2.9723	4.7684	0.9294	mda	0.6702	0.0712	3.1630
dk	1.7997	3.5861	0.4531	pt	1.4427	1.0734	0.9727
uk	1.4864	2.0509	0.5404	esp	0.9294	0.9163	0.4728
ltu	0.7251	0.4225	0.6243	ba	1.6777	0.9733	4.5980
irl	1.7339	4.2133	0.3579	srb	1.9972	0.4074	4.9107
nl	0.1002	0.1690	0.0298	alb	0.6012	0.0952	1.9048
de	2.6800	4.2244	0.8529	mkd	1.5933	0.2947	4.3220
pl	2.3431	1.1205	2.4578	gr	1.7938	1.1811	1.3667
be	2.3077	3.5095	0.7612	tur	0.2880	0.1057	0.3936
ukr	0.2391	0.0245	1.1730	nor	0.0000	0.0000	0.0000
fr	0.3846	0.4981	0.1490	se	0.0000	0.0000	0.0000
cz	0.5226	0.3735	0.3668	ch	0.0000	0.0000	0.0000
svk	2.0148	1.2406	0.2931	aut	0.0000	0.0000	0.0000
ita	1.1570	1.2982	0.5173	est	0.0000	0.0000	0.0000
hrv	0.2679	0.1243	0.2897	lv	0.0000	0.0000	0.0000
hun	0.2126	0.1056	0.2148	si	0.0000	0.0000	0.0000
ro	0.2466	0.0926	0.3293	dz	1.8129	1.0596	1.5560

$$\widehat{TC}_{j,max}^{tot} = \widehat{TC}_{max}^{network} - \varepsilon_j \cdot (\widehat{TC}_{max}^{network} - \widehat{TC}_{min}^{network}) \qquad \forall j, loop \tag{6.11}$$

The j-iterative calculation of Eqs.(6.10,6.11) is set through ε_j, a parameter ranging from 0 to 0.5 that indicates the level of cooperation reached between countries at iteration j, and employed to force the convergence of $\widehat{TC}_{j,min}^{tot}$ and $\widehat{TC}_{j,max}^{tot}$ of Eq.(6.9) towards an average target value of total per capita cost. Accordingly, the combination of Eqs.(6.10,6.11) produces a shift of each countrywide total cost $\widehat{TC}_{j,c}^{tot}$ of Eq.(6.8), ultimately levelised around a satisfactory compromise with the resulting (and potentially more expensive) cooperative SC configuration. Countries whose expenditures are not within the bounds set through ε_j and δ_c by aim of Eqs.(6.9-6.11), are forced to compensate the differential investment for CCS through either $debit_{j,c}$ or $credit_{j,c}$ as defined by Eq.(6.2).

The final level of cooperation among countries is obtained as a result of the iterative formulation. In fact, the model optimises the level of cooperation along with other decision variables until the stop criterion is reached. This criterion is set through the definition of the threshold cooperation convergence rate ε_j^*, which sets the stop criterion for the j-iterative optimisation procedure. Considering two countries c and c', when $\varepsilon_j = \varepsilon_j^*$ the resulting SC will be characterised by a δ_c-based proportionality of per capita total costs:

$$\frac{\widehat{TC}_{j,c}^{tot}}{\delta_c} = \frac{\widehat{TC}_{j,c'}^{tot}}{\delta_{c'}} \qquad \forall j; c : \varepsilon_j = \varepsilon_j^* \tag{6.12}$$

On the other hand, when $\varepsilon_j > \varepsilon_j^*$ the resulting networks would entail a sudden and constant increase in both European total cost TC_j^{tot} and countrywide per capita costs $\widehat{TC}_{j,c}^{tot}$. Broadly speaking, the threshold ε_j^* corresponds to the first value of ε_j over iterations j, after which: (i) the derivatives of TC_j^{tot} become constant; and (ii) all per capita costs $\widehat{TC}_{j,c}^{tot}$ constantly increase. For each chosen δ_c, the threshold ε_j^* will define the first optimal cooperative SC, i.e. that configuration contemplating cooperation at the minimum possible total cost TC_j^{tot}, after which TC_j^{tot} will increase due to an additional and unwanted increase of the cooperation level in the solution.

6.5 Results and discussion

6.5.1 Scenarios

The model has been optimised through the GAMS modelling framework on an i7 core @2.60 GHz (32 GB RAM) computer by aim of CPLEX solver in less than 5 hours (each scenario comprised 26 iterations j). The European capture target was set equal to 50% of overall CO_2 emissions that is forecasted to generate over the next 20 years, in order to compare the results with those from previous Chapters. Four Scenarios have been here investigated (Table 6.3). The base-case Scenario 0 minimises the installation and operation costs of a European CCS SC, excluding any cooperation approach from the modelling framework. Its output will be briefly presented to be compared with the results from other scenarios. Oppositely, Scenario A, Scenario B and Scenario C employ the costs share-based methodology previously discussed in the mathematical formulation. In particular, in Scenario A the differential weighting factor δ_c is set equal to δ_c^A, imposing a per capita emission-driven costs share between countries c, whereas in Scenario B the factor δ_c is set equal to δ_c^B, imposing a CO_2 emissions·GDP-driven costs share between countries c. Scenario C assumes the differential weighting factor δ_c equal to δ_c^C, and thus imposes an emission/GDP-driven costs share between countries c. Then, a sensitivity analysis will be proposed to assess optimal cooperative configurations depending on the choice in the carbon reduction target α. Finally, an analysis on the European legal framework on onshore storage is proposed.

6.5.2 Policies and cooperation levels

The best CCS SC configuration (i.e., European global optimum) is obtained from the optimisation of Scenario 0, and entails an overall European investment of 448.8 B€, corresponding to 37.90 €/t of sequestered CO_2 of which capture costs are the main contributor with 35.59 €/t, against 2.29 €/t for transport and 0.02 €/t for sequestration costs. However, as previously mentioned, if each country had to pay for the SC installed within its borders, the resulting network would be characterised by a huge spread of costs among the different players (Figure 6.1). Moreover, if it

Tab. 6.3: Scenario 0-A-B-C, main computational data and results: European carbon reduction target α [%], countrywide differential weighting factor δ_c, resulting threshold cooperative convergence rate ε_j^* and corresponding European total cost TC^{tot} [B€ or €/t of sequestered CO_2], maximum optimality gap (Opt. gap [%]) and solution time (Sol. time [s]).

Scenario	α	δ_c	ε_j^*	TC^{tot}		Opt. gap	Sol. Time
				[B€]	[€/t]	[%]	[s]
0	0.50	-	-	448.8	37.90	2.0	46
A	0.50	δ_c^A	0.26	460.5	38.89	2.0	14000
B	0.50	δ_c^B	0.22	452.7	38.12	2.0	17196
C	0.50	δ_c^C	0.37	455.3	38.44	2.0	16788

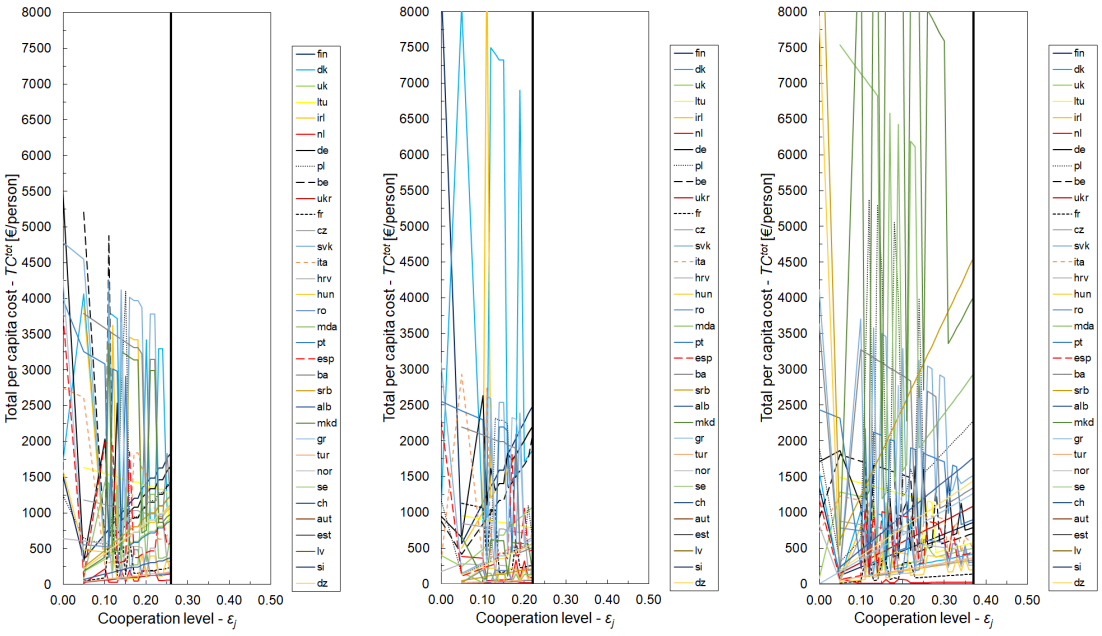

(a) *(b)* *(c)*

Fig. 6.3: Countrywide variation of total per capita cost $\widehat{TC}_c^{tot}$ [€/person] on cooperation level ε_j at iteration j (shown until the model reaches convergence for $\varepsilon_j = \varepsilon_j^*$), for Scenario A (a), Scenario B (b), and Scenario C (c). Black vertical bars represent the threshold cooperative configurations obtained for ε_j^*.

was chosen to equally divide these costs between all European inhabitants (independently from the local level of emissions and/or richness), this would likely cause the opposition of several countries judging the resulting costs to be highly unfair for their citizens. These issues make the SC resulting from Scenario 0 not likely to be implementable. Conversely, when it is chosen to employ a methodology based on costs cooperation ($j > 1$, $\varepsilon_j > 0$), both Scenario A (Figure 6.3a), Scenario B (Figure 6.3b) and Scenario C (Figure 6.3c) exhibit countrywide costs that start differentiating according to the policy imposed through δ_c and converge towards the optimal cooperative CCS SC for $\varepsilon_j = \varepsilon_j^*$ (Figure 6.3).

Differently from Scenario 0, Scenario A penalises countries with high per capita carbon intensity and therefore, balances the economic trade-offs between a SC designed on the basis of national per capita CO_2 emissions (from large stationary sources) and the overall European level of costs share. Under this assumption (Table 6.3), the resulting threshold configuration is obtained for $\varepsilon_j^* = 0.26$ and entails a total European expenditure TC^{tot} of 460.5 B€ (i.e., 38.89 €/t of sequestered CO_2), i.e. 2.6% more expensive with respect to Scenario 0. Accordingly, Scenario A exhibits a higher European cost for CCS than Scenario 0, and this increase is needed to obtain a configuration that accomplishes an emission-based policy for national investments. In particular (Figure 6.4), those countries characterised by high per capita CO_2 emissions (from large stationary sources) are forced to provide a larger per capita contribute to the installation and operation of the network (e.g., Finland with 1836 €/person, Germany with 1655 €/person, Poland with 1447 €/person and Belgium with 1425 €/person), whereas low emitters costs are either relatively low (e.g., Netherlands, Ukraine, Croatia, Hungary, Romania and Turkey pay less than 200 €/person, each), or almost null (e.g., Norway, Sweden, Switzerland, Austria, Estonia, Latvia, Slovenia). All the other countries with an intermediate level of per capita CO_2 emissions fill the gap of cost between 200 €/person and 1400 €/person.

Regarding Scenario B, it provides the optimal cooperation-based configuration according to the different countrywide products of per capita emissions·GDP thus, according to a compromise mechanism of cooperation that penalises, for instance, rich countries with high per capita CO_2 emissions. In this case, the threshold configuration is given by $\varepsilon_j^* = 0.22$ and entails again a higher total cost than Scenario 0 (+0.9%), with an overall expenditure TC^{tot} of 452.7 B€ (i.e., 38.12 €/t of sequestered CO_2). Scenario B exhibits (Figure 6.4) a spread of countrywide per capita total costs between about 2500 €/person (e.g., Finland with 2492 €/person, Germany with 2208 €/person, Ireland with 2202 €/person, Belgium with 2101 €/person and Denmark with 1874 €/person) and a minimum cost lower than 200 €/person. In fact, Netherlands, Czech Republic, Ukraine, Hungary, Romania, Moldavia, Albania, Macedonia and Turkey spend less than 200 €/person, each, while it is again almost null the contribution from Norway, Sweden, Switzerland, Austria, Estonia, Latvia and Slovenia. All other countries are ranked in intermediate costs share positions (e.g., Poland pays 586 €/person). As an interesting comparison with the

results from Scenario A, it should be observed the case of Germany and Poland, being these countries characterised by similar carbon intensities, but different values of GDP. Unlike Scenario A (i.e., an emission-driven policy entailing an almost identical per capita contribution from Germany and Poland), Scenario B penalises Germany, since it has higher GDP with respect to Poland. In this sense, Scenario B forces rich emitters to pay more for their generated CO_2. However, employing an emissions·GDP-based policy, could be penalising and not satisfactory for those countries characterised by relatively low per capita CO_2 emissions, together with a high value of GDP (e.g., Ireland). Broadly speaking, the richness of a country might not always constitute sufficient justification to invest in CCS, when the contribution of that country to overall emissions is already lower than that of many other players. An alternative is given by Scenario C, which aims at providing the best CCS SC configuration under a cooperation mechanism that combines nationwide CO_2 emissions and GDP, to penalise those countries whose richness is generated inefficiently in terms of environmental impact. The optimal cooperative network is obtained for $\varepsilon_j^* = 0.37$, corresponding to a total cost TC^{tot} of 455.3 B€ (i.e., 38.44 €/t of sequestered CO_2, +1.4% with respect to Scenario 0). Accordingly, the resulting SC entails almost the same total cost TC^{tot} of Scenario B, but with noteworthy differences when analysing results of each single country c. In fact, Scenario C suggests (Figure 6.4) very high per capita costs for Serbia (4557 €/person), Macedonia (4011 €/person) and Moldavia (2935 €/person), and significant contributions from Poland (2281 €/person), Albania (1768 €/person) and Slovakia (1523 €/person), whereas Netherlands and France pay less than 200 €/person, each. Analogously to Scenario A and Scenario B, also Scenario C suggests an almost null contribution on costs for Norway, Sweden, Switzerland, Austria, Estonia, Latvia and Slovenia. The optimal solution from Scenario C tends towards a high economic disadvantage for some of the Balkan countries, and particularly those characterised by high CO_2 emissions, low GDP and scarce population therefore, high per capita costs.
Overall, pushing towards the adoption of cooperative SCs determines an increase (+2.6% for Scenario A; +0.9% for Scenario B, +1.4% Scenario C) in the total European cost for CCS for all the investigated scenarios, having quantified the maximum economic penalty with respect to Scenario 0 for the case of Scenario A. Furthermore, from Scenario A, Scenario B, and Scenario C it emerges that the European design of an optimal cooperative CCS SC should possibly entail a significant economic per capita contribution from Finland, Germany, Poland and Belgium, whereas the choice of other major per capita contributors to costs (e.g., Ireland, Denmark, Serbia, Macedonia) is strictly related to the cooperation policy that is chosen to employ. None of the investigated scenarios suggests to expose Norway, Sweden, Switzerland, Austria, Estonia, Latvia and Slovenia to the costs for the optimal cooperative European CCS network, considering the negligible amount of per capita CO_2 emissions from large stationary sources generated by the aforementioned countries.

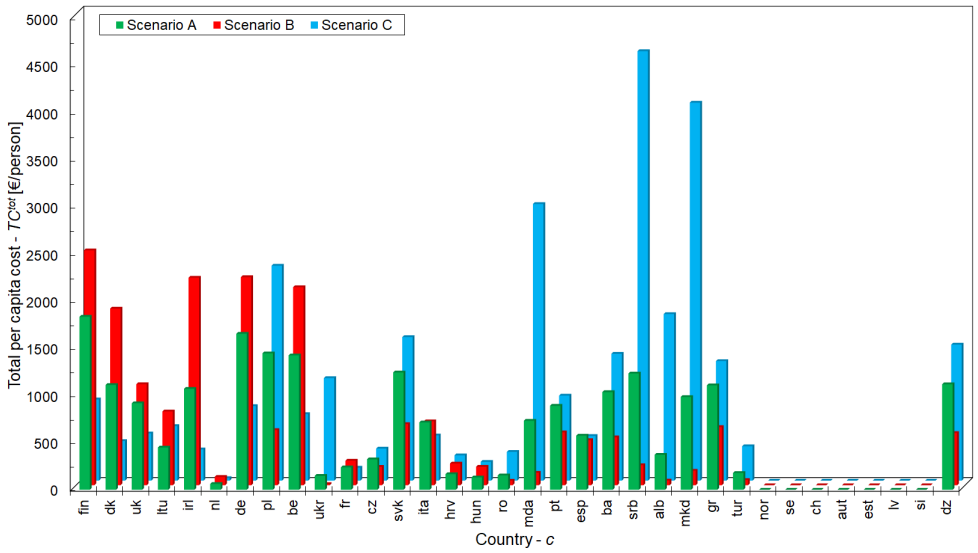

Fig. 6.4: Total per capita costs (TC_c^{tot} [€/person] for each country c, for Scenario A, Scenario B, and Scenario C.

6.5.3 Network configurations

This model provides the best CCS SC configurations according to the cooperation levels imposed through ε_j, and to the chosen policy determined through δ_c, which altogether define the different scenarios. The total contribution $\widehat{TC}_c^{tot}$ of each country c to the European total cost TC^{tot} is determined through either: (i) an active participation to the installation and deployment of the CCS infrastructures (i.e., $\widehat{TC}_c^{network}$); or (ii) a financial compensation (i.e., $debit_c$) towards those countries whose per capita expenditures are conversely high (i.e., $credit_c$). Therefore, it is of fundamental importance understanding the national exposure in terms of $\widehat{TC}_c^{network}$, $debit_c$ and $credit_c$ for each single country c, since these design variables provide clear indications on which countries might act as either active industrial partners or financial squaring entities, according to the optimised scenario (Figure 6.5).

Regarding Scenario A (Figure 6.5a), the debit/credit system acts as balancing force to obtain a final distribution of per capita costs that is proportional to countrywide per capita CO_2 intensity. The resulting optimal SC configuration (Figure 6.6a) entails large per capita infrastructural costs for the strategic CO_2 emitters, where the major capture nodes are consequently installed and operated (i.e., Denmark, Germany, Poland, Belgium, Slovakia, Bulgaria, Serbia and Macedonia), whereas minor per capita contributions to infrastructural costs are mainly spread between United Kingdom, Italy, Portugal and Spain. Regarding the remaining countries characterised by large per capita CO_2 emissions (i.e., Finland, Ireland and Greece), these pay an amount of per capita debit to balance the excess of investment (i.e., a corresponding per capita credit) mainly towards Denmark, Poland, Bulgaria, Serbia and Macedonia.

From the results of Scenario B, it can be noted that the per capita infrastructural

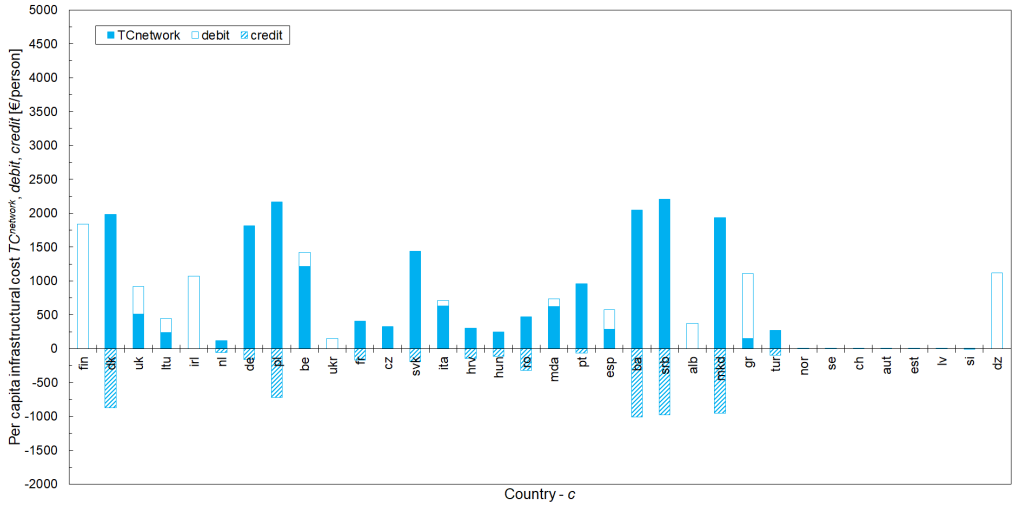

(a)

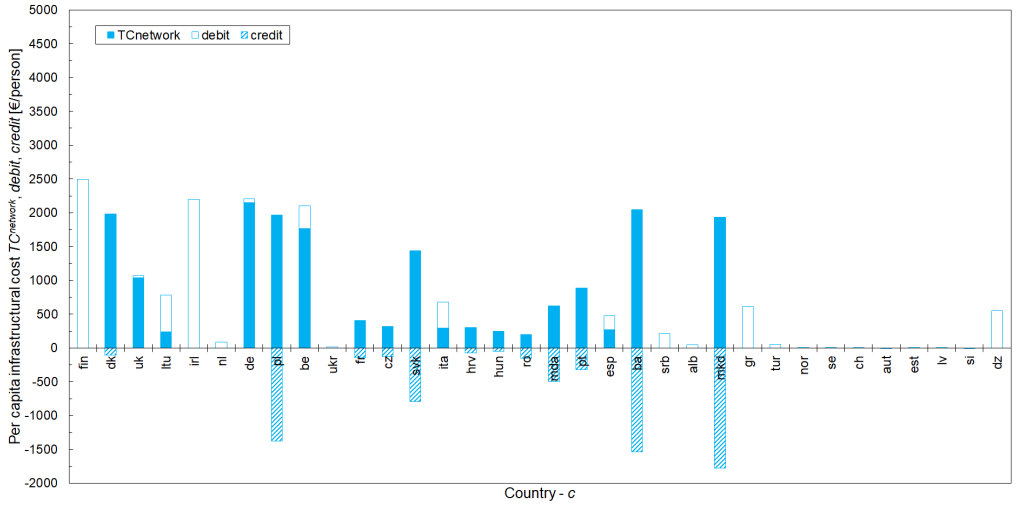

(b)

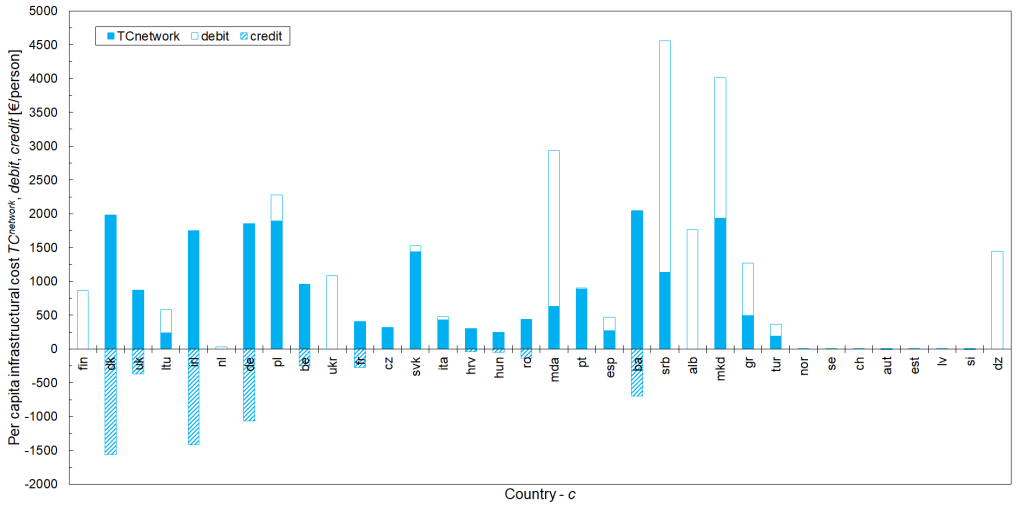

(c)

Fig. 6.5: Contribution each country c in terms of total network cost $\widehat{TC}_c^{network}$, debit ($debit_c$), and credit ($credit_c$), for Scenario (a), Scenario B (b), and Scenario C (c).

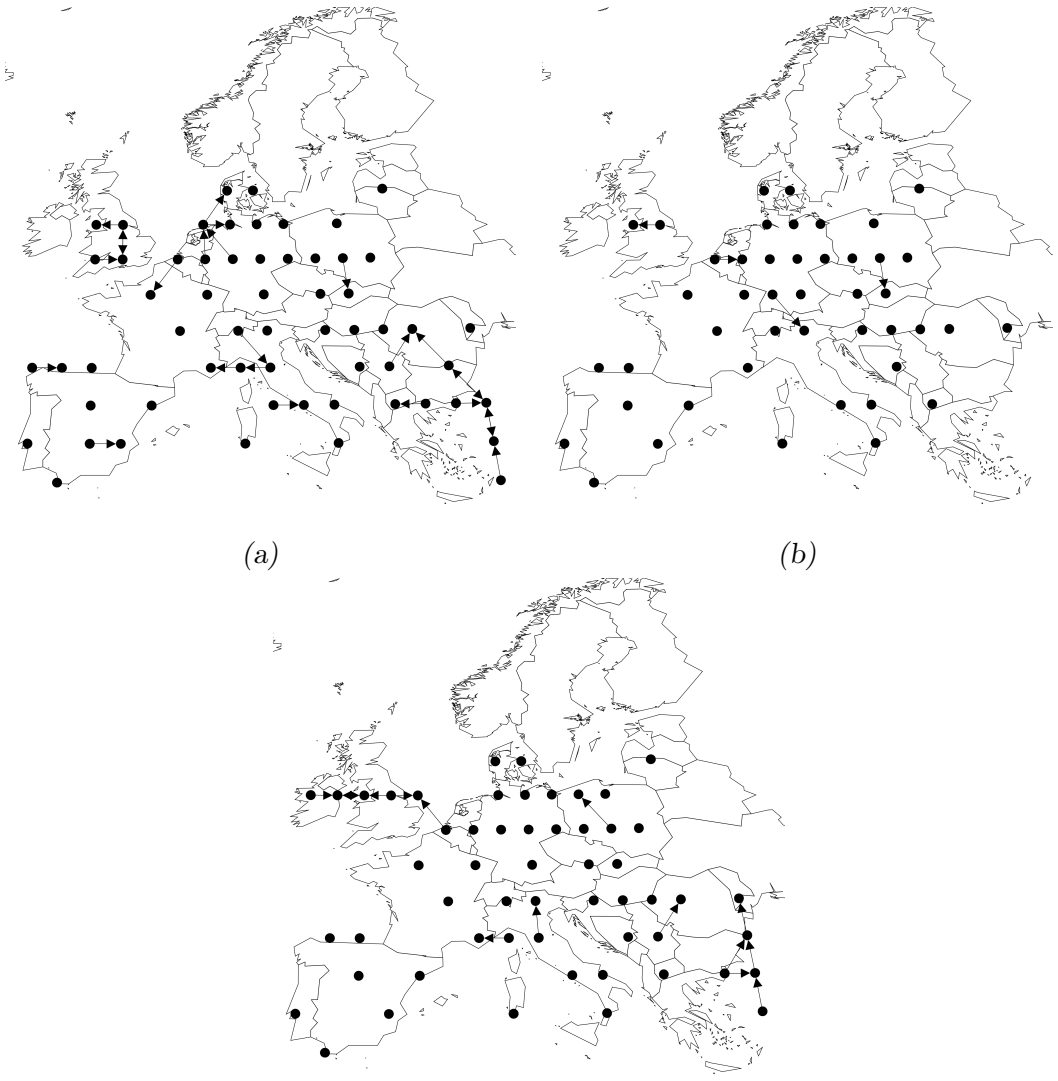

Fig. 6.6: Final SC configurations for Scenario A (a), Scenario B (b), and Scenario C (c). Dark dots represent capture and sequestration nodes.

commitment (Figure 6.5b) is slightly different compared to Scenario A. Indeed, Scenario B optimises the SC such that the countrywide per capita total cost is always proportional to both the contribution to emissions and the national GDP. Under this assumption, the critical capture nodes (Figure 6.6b), constituting the major cost item, are located in Denmark, Germany, Poland, Belgium, Slovakia, Bulgaria and Macedonia. Among these, Poland, Slovakia, Bulgaria and Macedonia, being characterised by lower values of GDP, receive from Finland, Ireland and others a large amount of credit to balance their excess of per capita investment. As a result, the optimal cooperative system under Scenario B exhibits a SC configuration (Figure 6.6b), which is mainly developed across central Europe, where the main capture and sequestration facilities are installed and operated.
Finally, from Scenario C (Figure 6.5c), which encourages the countrywide efficiency in producing high GDP while generating low CO_2 emissions, emerges that the main capture points (Figure 6.6c) are located (similarly to Scenario A) in Denmark, Ireland, Germany, Poland, Slovakia, Bulgaria and Macedonia, and constitute the main contribution to the per capita SC costs. On the one hand, the SC configuration resulting from Scenario C (Figure 6.6c) is particularly similar to that of Scenario B (Figure 6.6b) and almost identical to that of Scenario A (Figure 6.6a), in terms of overall infrastructural design. On the other hand, unlike Scenario A, Denmark, Ireland and Germany receive a squaring amount of per capita credit from those countries characterised by lower values of emissions/GDP ratio, i.e. Finland, Ukraine, Moldavia, Serbia, Albania, Macedonia, Greece, Tunisia and Algeria, these conversely characterised by a much larger per capita contribution in terms of debit rather than infrastructural investment.

6.5.4 Assessing the European carbon reduction target

Optimal cooperative CCS SCs (i.e., those resulting from the optimisation of Scenario A-B-C) are always slightly more expensive than those obtained from a globally-optimised European infrastructure (i.e., Scenario 0), independently from the level of carbon reduction target α that must be achieved. Indeed, when aiming at sequestering the 20% of overall emissions from large stationary sources ($\alpha = 20\%$) (Table 6.4), the most expensive SC is that resulting from the optimisation of Scenario C (+5.7% with respect to Scenario 0), whereas the total cost of both the emission-based Scenario A (+0.3%) and Scenario B (+0.0%) is unchanged with respect to Scenario 0. Also when it is chosen an $\alpha = 30\%$ (Table 6.4), all the cooperative scenarios entail just minor increases in total costs compared to the results from Scenario 0 (between +2.6% and 4.6%). In general, these increases in total costs are comparatively similar to those obtained from the optimisation of the base cases, which were characterised by a much larger carbon reduction target (i.e., $\alpha = 50\%$).

Tab. 6.4: Scenario 0-A-B-C, European carbon reduction target α [%], resulting threshold convergence rate ε_j^*, European total cost TC^{tot} [B€ or €/t of sequestered CO_2], and increase in European total cost ΔTC^{tot} [%] with respect to the α-corresponding economic result in Scenario 0.

Scenario	δ_c	α	ε_j^*	TC^{tot}		ΔTC^{tot}
				[B€]	[€/t]	[%]
0	-	0.20	-	164.7	34.92	0.0
0	-	0.30	-	258.5	36.45	0.0
0	-	0.50	-	448.8	37.90	0.0
A	δ_c^A	0.20	0.11	165.2	35.01	+0.3
A	δ_c^A	0.30	0.18	265.3	37.26	+2.6
A	δ_c^A	0.50	0.26	460.5	38.89	+2.6
B	δ_c^B	0.20	0.10	164.7	35.74	0.0
B	δ_c^B	0.30	0.16	270.3	37.51	+4.6
B	δ_c^B	0.50	0.22	452.7	38.12	+0.9
C	δ_c^C	0.20	0.17	174.1	36.57	+5.7
C	δ_c^C	0.30	0.26	268.0	37.60	+3.7
C	δ_c^C	0.50	0.37	455.3	38.44	+1.4

6.5.5 Assessing legal restrictions on onshore sequestration

During the last decade, national regulations on CO_2 onshore storage have generated a diversified legal framework among European countries (EC, 2017). On the one hand, Czech Republic, Germany, Poland, Sweden, the Netherlands and the United Kingdom decided to restrict the amount of CO_2 to sequester within their mainland. On the other land, Austria, Croatia, Estonia, Ireland, Latvia, Finland and Belgium are currently forbidding this practice, which would be vital for CCS considering its lower costs compared to offshore transport and storage. Besides, the United Kingdom, Poland and the Netherlands may authorise offshore CO_2 sequestration in the future. Anyway, the uncertain European policy on CO_2 geological storage might generate risk and increase the cost of CCS. Therefore, here we propose an analysis based on current policies on storage (Instance II), which prudently optimises the cooperative CCS SC while excluding all the aforementioned countries from those where CO_2 onshore sequestration is permitted.

Under the hypotheses of Instance II, all the investigated case studies entail an increase in specific total costs TC^{tot} (Figure 6.7), from a minimum growth of +1.48% (Scenario II.C) until a maximum growth of +6.98% (Scenario II.A). This additional expenditure is needed to install and operate a more complex CCS SC, to divert the CO_2 towards those countries that are still assumed to allow onshore sequestration. As a matter of facts, the share of injected CO_2 among European countries is strongly affected by the limitations introduced through Instance II (Figure 6.8). Germany

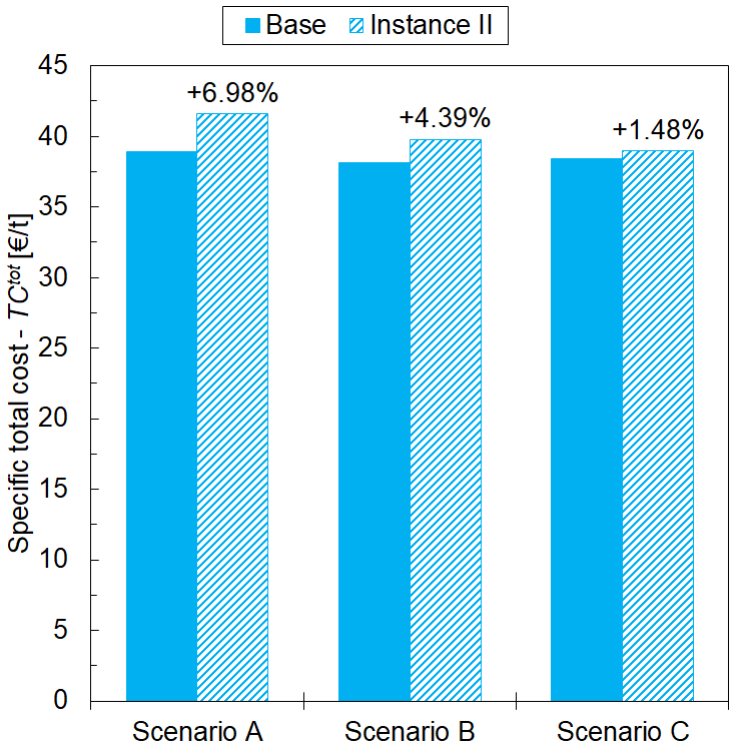

Fig. 6.7: Increase in specific total cost TC^{tot} [€/t] when limitations in onshore storage are taken into account (Instance II), with respect to base Scenarios A-B-C.

and Poland previously accounted for almost half of the basins to be exploited for storage (Figure 6.8a), whereas Instance II chooses to utilise the geological potential of other countries (Figure 6.8b).

6.6 Chapter conclusions

This Chapter 6 proposed a MILP model for the economic optimisation of cooperative European SCs for CCS. The modelling framework included different policies for costs share, based on countrywide characteristics in terms of population, CO_2 emissions, and GDP. The objective was to design optimal cooperative SCs, being characterised by a smaller spread of per capita costs among countries, whilst increasing the total cost of the network compared to the solution from a globally optimised European infrastructure.

The maximum European economic penalty was quantified in +2.6% (with respect to a globally optimised network) of total installation and operation costs, when an emission-driven differential policy was employed among countries. Regarding per capita infrastructural investment, it was shown that the optimal cooperative SC would entail significant contributions from Finland, Germany, Poland and Belgium, whereas the level of economic commitment of other countries depend on the chosen policy for costs share. Norway, Sweden, Switzerland, Austria, Estonia, Latvia and Slovenia were never exposed to costs, given their negligible contributions in terms

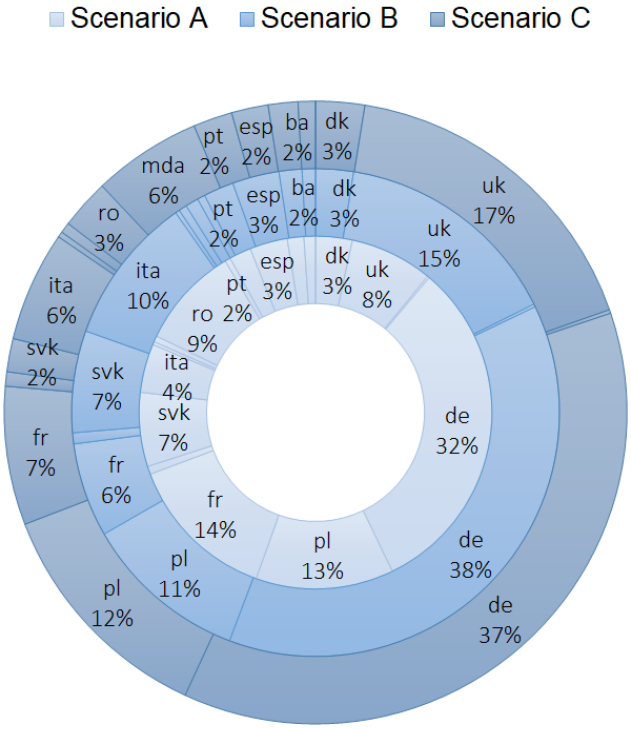

(a)

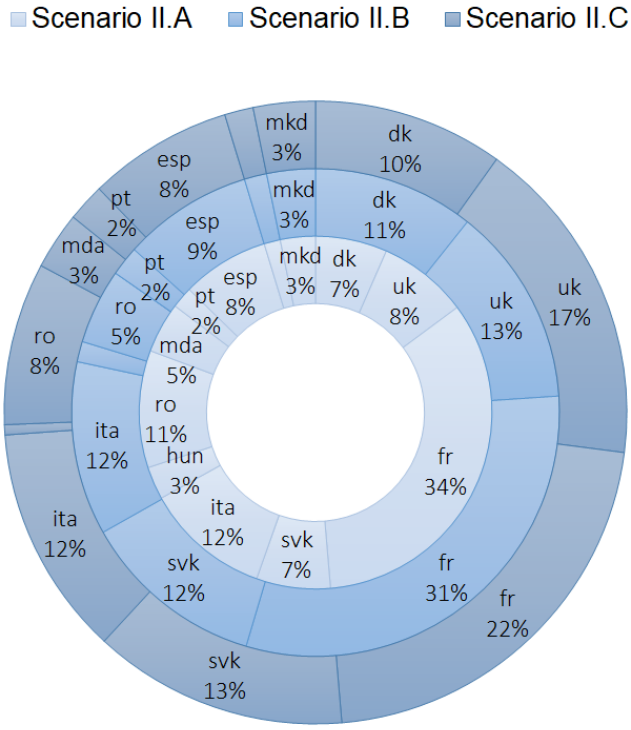

(b)

Fig. 6.8: Countrywide share of sequestered CO_2 for Scenario A-B-C in case of no constraints on storage (a) and for Instance II (b).

of per capita CO_2 emissions from large stationary sources. Independently from the chosen policy for cooperation, the optimal SC entailed almost the same design in all scenarios, meaning that the results are rather robust in terms of final infrastructure. On the other hand, it was demonstrated the possibility to decrease the spread of costs for CCS through a tailored debit and credit system, which might act as a balancing force depending on the considered policy. Overall, the model was shown capable of providing indications on possible cooperative networks in the large-scale and complex context of Europe, offering the opportunity to assess correctly the possible different policies for costs share and understand their implications in terms of both SC design and countrywide per capita commitment. In this work, three different cooperative policies were considered and analysed, but the modelling approach is quite general and makes it possible to assess the effect of alternative sharing criteria, too. At the same time, we do recognise that the actual definition and implementation of continent-wide strategies involving decision from diverse countries need take into account other complex political, social and economic factors. Furthermore, the region of interest was here represented as a closed system, whereas international trading and cooperation policies may have an impact, too. However, we believe that the proposed methodology may provide investors and policy-makes with a useful tool for assessing in a quantitative way how different strategies can facilitate or hinder cooperation, which players would mainly benefit or be disadvantaged, and how general costs would be affected.

Overall, Chapters 2-6 tackled the modelling of a European CCS frameworks in terms of both costs, risks, and policy. Chapter 7 will further expand on this by introducing CO_2 utilisation and proposing a comprehensive (although preliminary) CCUS optimisation.

7

A preliminary study to encompass CO_2 utilisation

7.1 Chapter summary

In the next few years, CCS will be strategic as a key technology for reducing anthropogenic emissions of greenhouse gases. Carbon utilisation (i.e., in the CCUS framework) has been often considered as a viable option to increase the environmental benefits, while decreasing costs of the mere CCS system. This Chapter proposes a preliminary study on a European CCUS SC. In particular, the model will neglet the possible utilisation pathways through mineral carbonation (e.g., to produce solid construction materials), or the biological conversion, and will only optimise the CCUS system considering chemicals and fuels as potential output candidates. Therefore, this preliminary study will investigate, through a MILP model, the strategic design of a European SC for CCUS, only considering chemical pathways as conversion and utilisation options. The goal is to reduce by 50% the European emissions from large stationary sources by 2030. Results highlight that, under our assumptions, the significance of carbon utilisation in terms of reduction of the environmental impact is likely to be a very minor one: considering the current state of technologies only about 0.6% of the overall CO_2 emitted from large stationary sources can be removed by chemical utilisation. Some benefits can be obtained in terms of overall cost reduction thanks to revenues deriving from the chemicals being produced. The model sets the basis for future work on a comprehensive (i.e., with more conversion options) CCUS SC.

7.2 Modelling framework

This Chapter proposes a static (to reduce the computational burden) MILP model for the economic optimisation of European CCUS SCs. In this preliminary study, that for simplicity considers only chemical conversion as possible utilisation pathway, the SC takes into account (Figure 7.1):

- location of European large stationary sources of CO_2, according to data provided by the EDGAR Database (JRC, 2016);
- technical and economic description of set k for carbon capture options, that includes post-combustion from coal-fired power plants, post-combustion from gas-fired power plants, pre-combustion from gas-fired power plants and oxy-fuel combustion;
- technical, economic and feasibility implementation of set l, that includes both pipelines (onshore and offshore) and ships as possible transport means;
- location of onshore basins that are able to efficiently trap the CO_2 for long term geological sequestration, according to data provided by the EU GeoCapacity Project (2009);
- technical and economic features of the CO_2 utilisation stage through a set ψ of chemical outputs.

Overall, this European CCUS model is capable of providing:

- the selection, location, scale and cost of capture nodes;
- the definition, scale and cost of the transport infrastructure between geographic nodes;
- the location, scale and cost of geological sequestration nodes;
- the selection, location, scale and profit of chemical conversion nodes;
- the final CCUS SC configuration according to chosen European carbon reduction target;
- the differences in SC behaviour according to rates of chemicals production;
- the differences in SC behaviour according to national regulations on onshore storage.

This study, given the high number of potential reaction mechanisms for CO_2 conversion (Aresta et al., 2013), proposes a screening of the processes according to the following principles:

- (*i*) *minimum production threshold*: a conversion path is taken into account only if the European demand for the chemical output is a relevant one; the reason for this relies on the large flowrates of CO_2 (i.e., ≥ 1 Mt/year) deriving from stationary sources and consequently on the necessity of exploiting these carbon streams at scale for producing chemicals. Therefore, this model assumes that at least 1 Mt/year of CO_2 should be converted in order to satisfy the market demand;

- (*ii*) *techno-economic data availability*: the maturity of the technology should be at least such that basic technical (productivity) and economic (production cost) information are available. This means that the current state of research and/or industrial application must be capable of providing complete techno-economic information on the specific conversion process;

- (*iii*) *environmentally promising*: the conversion process must produce in general less CO_2 than that employed to feed it thus, the process CO_2 net balance should be negative (i.e., CO_2 emissions are lower than CO_2 consumption); as regard energy intensive processes, it is here assumed to employ only renewable energy;

- (*iv*) *economically promising*: in order to be sustainable from an economic standpoint, the conversion process should be capable of providing a profit from the sale of the chemical output.

Furthermore, in order to avoid unrealistic results, here we assume that at maximum one conversion plant for producing chemical ψ can be installed in each region g. The plant scale ranges between the values found in the literature for existing commercial plants.
As a result, after excluding from the CCUS framework those products whose processes do not meet the requirements listed above according to information found in the scientific literature (Table 7.1), only two chemical products, i.e. polyether carbonate polyols (PPP) and methanol (MeOH), were selected and included as options for CO_2 utilisation in set $\psi = [PPP, MeOH]$. As regards the compliance with both the minimum production threshold and the availability of techno-economic data, PPP are bulk chemicals generally employed in the production of polyurethanes and are one of the most commonly produced polymers, with a yearly world production of 9.4 Mt, of which 2.4 Mt just in Europe (Covestro, 2017), whereas MeOH is one of the most versatile and produced chemicals, with a world plant capacity of 125 Mt/year and a European demand of 12 Mt/year (IHS, 2017). When studying the compliance with the environmental requirements, it is here assumed to exploit only low-carbon technologies to generate the energy required for the conversion processes (e.g., renewable or nuclear energy), in order to limit the generation of indirect CO_2 emissions due to utilisation. The chemical conversion of CO_2 into PPP (with 20% weight of CO_2) generates 2.65-2.86 kg CO_2-eq per kg of product, leading to a GHG

Tab. 7.1: List of chemicals that can be produced from CO_2 and their effective compliance with the design requirements: (*i*) *minimum production threshold*, (*ii*) *techno-economic data availability*, (*iii*) *environmentally promising* and (*iv*) *economically promising*. Only PPP and MeOH meet all the requirements.

		Compliances			
Chemical	Reference	(*i*)	(*ii*)	(*iii*)	(*iv*)
Urea	Heffer and Prud'Homme, 2016	V	V	X	V
Polyurethanes	Covestro, 2017	V	V	-	-
Mineral carbonates	Aresta et al., 2013	V	V	V	X
Syngas	Cairns, 2016	X	V	-	-
MeOH	IHS, 2017	V	V	V	V
Formaldehyde	MC group, 2014	V	X	-	-
Formic Acid	Aresta et al., 2013	X	V	V	X
Ethylene	Statista, 2013	X	X	-	-
Ethylene glycol	Aresta et al., 2013	X	X	-	-
Acetic acid	Aresta et al., 2013	X	V	-	-
Acrylic acid	Aresta et al., 2013	X	X	-	-
DMC	Aresta et al., 2013	X	V	V	V
Salicylic acid	Aresta et al., 2013	V	X	-	-
Polyoxymethylene	PIE, 2016	X	X	-	-
Polycarbonate	Covestro, 2017	X	X	-	-
Kerosene	CNN, 2014	X	V	V	X
Biodiesel	Lam et al., 2012	X	V	V	X
Dimethoxyethane	Methanol Institute, 2016	V	X	-	-
Methyl tert-butyl ether	Argus De Witt, 2015	V	X	-	-
PPP	Aresta et al., 2013	V	V	V	V

emission reduction of about 11% with respect to traditional production technologies (von der Assen and Bardow, 2014). Similarly, the conversion of CO_2 into MeOH allows saving about 1.2 kg of CO_2 per kg of MeOH with respect to its traditional production through steam reforming of natural gas (Roh et al., 2016). According to the literature, the two selected processes for CO_2 chemical conversion are also promising from an economic standpoint. As regards the conversion of CO_2 into PPP, this process can be specifically designed to generate profits (Fernandez-Dacosta et al., 2017), while concerning the production of MeOH, several options have been demonstrated to be economically feasible (Pérez-Fortes et al., 2016; Rivera-Tinoco et al., 2016; Mondal et al., 2016; Bellotti et al., 2017). It should be observed that the conversion into dimethylcarbonate (DMC), despite looking attractive from both an environmental and an economic point of view (Table 7.1), is not capable of guaranteeing a sufficient European production which complies with the minimum threshold requirement that is here imposed (Covestro, 2017). The following Sections will detail the characteristics and the implementation of the chosen conversion processes.

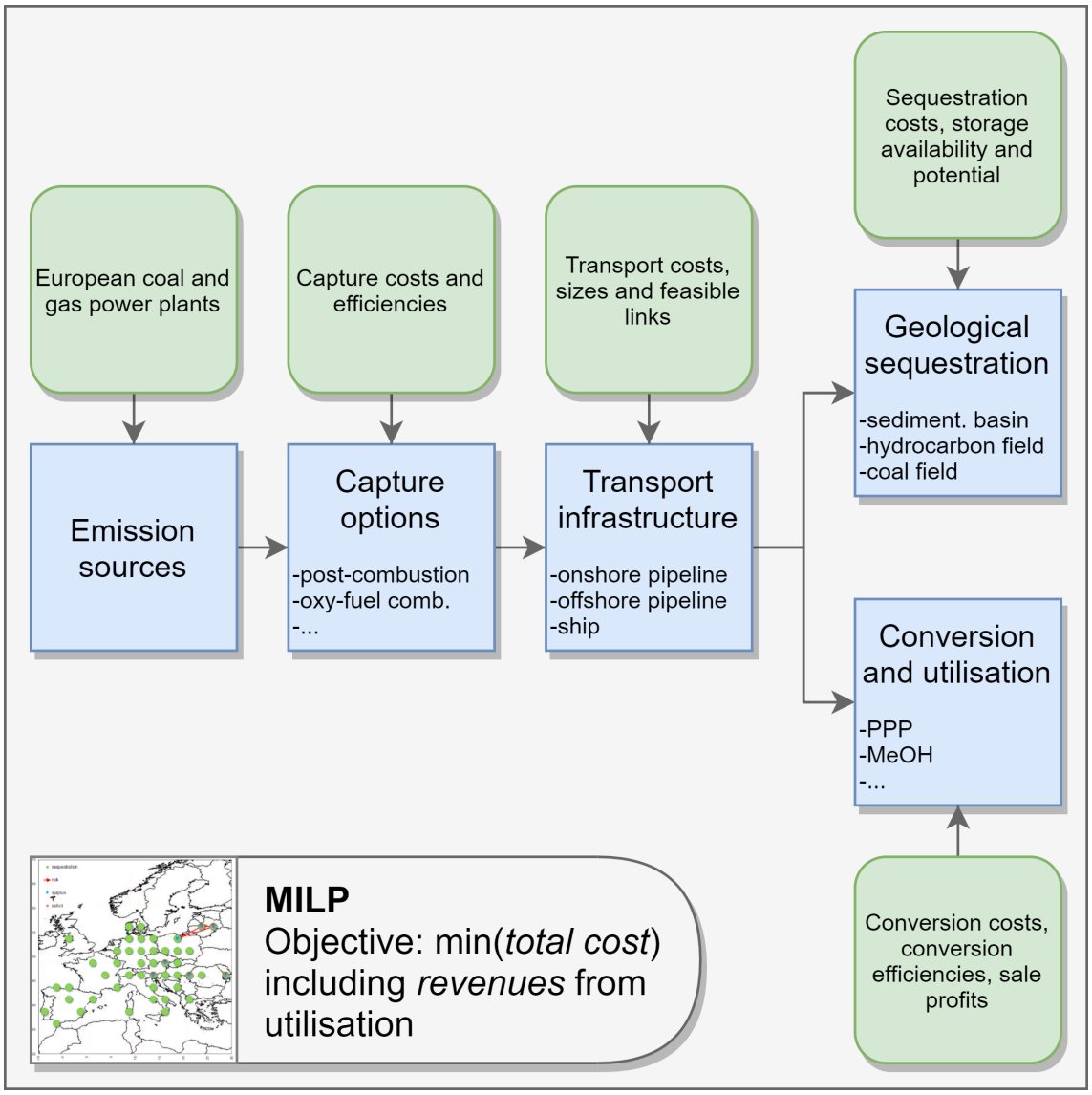

Fig. 7.1: Overview of the proposed framework for the CCUS SC optimisation.

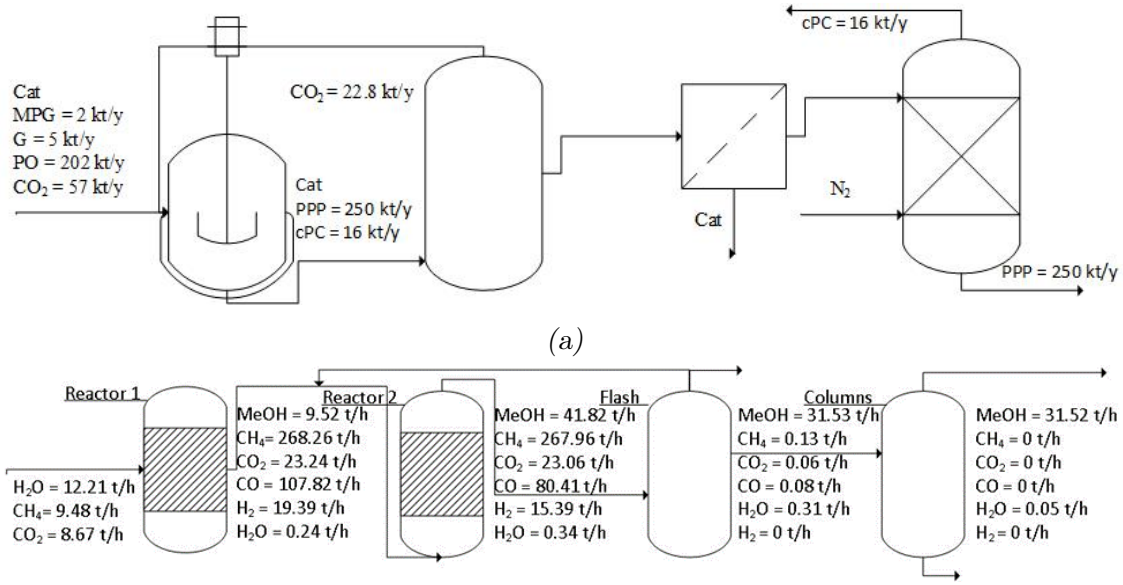

(a)

(b)

Fig. 7.2: Principal flowrates and conversion schemes for producing either (a) PPP (Fernández-Dacosta et al., 2017), or (b) MeOH (Wiesberg et al., 2016).

7.3 Mathematical formulation

The objective is to minimise the total cost TC [€] that occurs to install and operate the entire European CCUS network, which includes the total cost related to capture facilities TCC [€], the total cost of the transport infrastructure TTC [€], the total cost for geologically confining the CO_2 TSC [€], and the $profit$ [€] coming from the utilisation stage:

$$\begin{cases} objective = min(TC) \\ TC = TCC + TTC + TSC - profit \\ s.t. \\ capture\ problem\ model \\ transport\ problem\ model \\ sequestration\ problem\ model \\ utilisation\ problem\ model \end{cases} \tag{7.1}$$

In particular, the capture problem model, the transport problem model, and the sequestration problem model, have been already discussed in Chapter 2, thus, in order to avoid redundancy and to highlight the key challenge of this Chapter 7, just the utilisation problem model will be entirely described in the following, on the basis of the conversion processes that were modelled for producing either PPP (Figure 7.2a) or MeOH (Figure 7.2b). The total profit of Eq.(7.1) obtained from the conversion of CO_2 is calculated according to the cash flow $CF_{\psi,g}$ [€] that can be generated by the production and sale of chemical ψ in region g:

$$profit = \sum_{\psi,g} CF_{\psi,g} \tag{7.2}$$

In particular, $CF_{\psi,g}$ of Eq.(7.2) is defined as:

$$CF_{\psi,g} = (R_{\psi,g} + COM_{\psi,g}) \cdot (1 - tax_g) + d_{\psi,g} \qquad \forall \psi, g \tag{7.3}$$

The revenue $R_{\psi,g}$ [€] is calculated assuming to sell both the main product and all by-products the may derive from chemical ψ in region g, whereas $COM_{\psi,g}$ [€] represents the manufacturing cost of chemical ψ in region g. Furthermore, tax_g [%] (Table 7.2) is a country-based parameter that describes the amount of taxes in each region g, while $d_{\psi,g}$ [€] accounts for the depreciation of chemical ψ in region g.
As regards the revenue $R_{\psi,g}$ of Eq.(7.3) of chemical ψ in region g, it is given by:

$$R_{\psi,g} = \widehat{R}_{\psi,g} \cdot U^{chem}_{\psi,g} \qquad \forall \psi, g \tag{7.4}$$

where $U^{chem}_{\psi,g}$ [t] is the amount of chemical ψ that is produced in region g as a result of the model solution, whereas $\widehat{R}_{\psi,g}$ [€/t] is a parameter representing the unitary revenues that can be earned from chemical ψ in region g. In particular, $\widehat{R}_{\psi,g}$ of Eq.(7.4) is calculated according to the unitary price $P_{\zeta,g}$ [€/t] set on output products ζ in region g, and to the mass flowrates $\dot{m}_{\zeta,\psi}$ [t/year] of output commodities ζ that are that are generated along with chemical ψ:

$$\widehat{R}_{\psi,g} = \sum_{\zeta} \frac{P_{\zeta,g} \cdot \dot{m}_{\zeta,\psi}}{U^{ref}_{\psi}} \qquad \forall \psi, g \tag{7.5}$$

The parameter U^{ref}_{ψ} [set equal to 250 kt/year], representing the reference plant output capacity, the output flowrates $\dot{m}_{\zeta,\psi}$, and the unitary prices $P_{\zeta,\psi}$ set for the production, are retrieved from Fernández-Dacosta et al. (2017), Souza et al. (2014) and Wiesberg et al. (2016), and finally differentiated among the different European countries c according to the differential costs of natural price and electricity (Table 7.2), following the methodology proposed by Baldo (2018).
The manufacturing cost $COM_{\psi,g}$ of Eq.(7.3) is calculated according to the formulation proposed by Turton et al. (2015):

$$COM_{\psi,g} = U^{chem}_{\psi,g} \cdot [A^{\psi} \cdot (raw_{\psi,g} + util_{\psi,g})] + B^{\psi} \cdot FCI_{\psi,g} + C^{\psi} \cdot lab_{\psi,g} \cdot \delta^{chem}_{\psi,g} \tag{7.6}$$

Accordingly, the manufacturing cost depends on the amount of chemical $U^{chem}_{\psi,g}$ of Eq.(7.6), which is multiplied by a scalar $A^{\psi} = 1.23$, that conversely weights the sum of $raw_{\psi,g}$ [€/t] (Table 7.3) and $util_{\psi,g}$ [€/t] (Table 7.4), these representing the unitary costs of raw materials and utilities for chemical ψ in region g, respectively. These parameters have been evaluated following the procedure reported in Baldo (2018). Furthermore, $COM_{\psi,g}$ also depends on the fixed capital investment $FCI_{\psi,g}$ [€] for producing chemical ψ in region g (weighted by $B^{\psi} = 0.28$) and on the labour cost $lab_{\psi,g}$ [€/t] (the latter, reported for in Table 7.2, is weighted by $C^{\psi} = 2.73$ and assumed to scale linearly with the size of the plant). The binary variable $\delta^{chem}_{\psi,g}$ determines whether the productivity $U^{chem}_{\psi,g}$ of chemical ψ in region g falls to a null value, or not, and in that case also the contribution of labour costs is consequently

nullified. In fact, $\delta^{chem}_{\psi,g}$ represents if there is production of chemical ψ in region g, or not, according to the productivity upper bound $U^{max}_{\psi,g}$ [t of chemical] (retrieved from IHS, 2016 and Covestro, 2017) of chemical ψ in region g:

$$U^{chem}_{\psi,g} \leq \delta^{chem}_{\psi,g} \cdot U^{max}_{\psi,g} \qquad \forall \psi, g \tag{7.7}$$

As regards the term $FCI_{\psi,g}$ of Eq.(7.6), it has been evaluated following the non-linear formulation provided by Sinnot and Towler (2009). Then, given the MILP mathematical architecture of this optimisation problem, that formulation has been linearized and the following linear equation implemented to calculate $FCI_{\psi,g}$, given a non-null amount $U^{chem}_{\psi,g}$ of chemical ψ in region g, and according to the binary decision variable $\delta^{chem}_{\psi,g}$:

$$FCI_{\psi,g} = U^{chem}_{\psi,g} \cdot FCI^{slope}_{\psi} + \delta^{chem}_{\psi,g} \cdot FCI^{intercept}_{\psi} \qquad \forall \psi, g \tag{7.8}$$

where FCI^{slope}_{ψ} [€/t of chemical] and $FCI^{intercept}_{\psi}$ [€] (Table 7.5) are respectively the arrays of slope and the intercept coefficients of the linearized facility capital costs for producing each chemical ψ, and are calculated from the results provided by Aasberg-Petersen et al. (2008).

Having defined $FCI_{\psi,g}$ through Eq.(7.8), it is then possible to evaluate the depreciation $d_{\psi,g}$ of Eq.(7.3) of chemical ψ in region g as a fixed percentage (set equal to 10% according to d'Amore and Bezzo, 2016) over facility capital cost:

$$d_{\psi,g} = 0.1 \cdot FCI_{\psi,g} \qquad \forall \psi, g \tag{7.9}$$

As seen before in Eqs.(7.4,7.6), $U^{chem}_{\psi,g}$ represents the optimal amount of chemical ψ to be produced in region g according to the model solution. It is possible to link the chemical ouptut with the actual CO_2 exploited for utilisation, through the parameter U^{conv}_{ψ} [t of CO_2/t of chemical ψ] (Table 7.5):

$$U_g = \sum_{\psi} (U^{chem}_{\psi,g} \cdot U^{conv}_{\psi}) \qquad \forall g \tag{7.10}$$

Therefore, U^{conv}_{ψ} represents the amount of CO_2 that is needed to produce a unitary amount of chemical ψ (Langanke et al., 2014; Sakakura and Kohno, 2009; Roh et al., 2016), while U_g is the net amount of CO_2 that is exploited for utilisation purposes in region g.

Furthermore, when some CO_2 utilisation occurs in a specific region g, the totally emitted CO_2 P^{max}_g in that region must be decreased by that effectively saved because of its usage in a conversion process instead of a traditional input (i.e., $P^{saved}_{\psi,g}$):

$$P^{saved}_{\psi,g} = U^{chem}_{\psi,g} \cdot U^{saved}_{\psi} \qquad \forall \psi, g \tag{7.11}$$

$$P^{net}_g = P^{max}_g - \sum_{\psi} P^{saved}_{\psi,g} \qquad \forall g \tag{7.12}$$

In particular, U^{saved}_{ψ} [t of CO_2/t of chemical ψ] represents the quantity of CO_2 that is not emitted when substituting CO_2 as an input to the traditional process that typically would be employed to produce chemical ψ (von der Assen and Bardow, 2014; Roh et al., 2016) (Table 7.5).

Tab. 7.2: Prices of natural gas (gas p.) and electricity (el. p.), labour cost (lab_c [k€/y]) and corporate tax rate (tax_c, set then identical for each region g within country c) in the analysed countries c (Eurostat, 2017a; 2017b; 2017c).

c	gas p. [€/kWh]	el. p. [€/kWh]	lab_c [k€/y]	tax_c
Belgium	0.0244	0.113	55.691	0.340
Czech Republic	0.0238	0.069	17.480	0.190
Denmark	0.0327	0.082	62.756	0.220
Germany	0.0317	0.152	51.825	0.298
Ireland	0.0332	0.124	49.660	0.125
Greece	0.0283	0.107	28.179	0.290
Spain	0.0310	0.106	36.388	0.250
France	0.0326	0.099	53.384	0.333
Croatia	0.0246	0.087	16.659	0.200
Italy	0.0271	0.148	43.822	0.240
Lithuania	0.0246	0.084	10.263	0.150
Hungary	0.0261	0.074	13.136	0.090
Netherlands	0.0365	0.082	56.107	0.250
Poland	0.0273	0.086	13.227	0.190
Portugal	0.0279	0.114	22.321	0.210
Romania	0.0255	0.079	7.648	0.160
Slovakia	0.0282	0.112	15.205	0.210
Finland	0.0441	0.067	50.376	0.200
UK	0.0248	0.127	47.068	0.190
Macedonia	0.0300	0.056	6.626	0.100
Albania	0.0578	0.084	4.626	0.150
Serbia	0.0310	0.064	8.404	0.150
Turkey	0.0187	0.063	13.899	0.200
Bosnia	0.0343	0.059	9.702	0.100
Moldova	0.0263	0.083	3.600	0.120
Ukraine	0.0262	0.039	3.352	0.190

Tab. 7.3: Cost of raw materials $raw_{\psi,g}$ [€/t] for producing chemical ψ in region g (Eurostat, 2017a; 2017b; 2017c; Baldo, 2018), with null values for cells $g = [125-134]$.

	ψ			ψ			ψ	
g	PPP	MeOH	g	PPP	MeOH	g	PPP	MeOH
1	1386.6	326.9	43	1386.6	195.1	85	1386.6	210.1
2	1386.6	326.9	44	1386.6	195.1	86	1386.6	210.1
3	1386.6	326.9	45	1386.6	169.6	87	1386.6	210.1
4	1386.6	326.9	46	1386.6	169.6	88	1386.6	210.1
5	1386.6	326.9	47	1386.6	222.9	89	1386.6	210.1
6	1386.6	326.9	48	1386.6	222.9	90	1386.6	176
7	1386.6	326.9	49	1386.6	222.9	91	1386.6	176
8	1386.6	381.1	50	1386.6	219.4	92	1386.6	176
9	1386.6	326.9	51	1386.6	219.4	93	1386.6	176
10	1386.6	326.9	52	1386.6	166.7	94	1386.6	290.1
11	1386.6	326.9	53	1386.6	166.7	95	1386.6	198.6
12	1386.6	170.2	54	1386.6	170.2	96	1386.6	185.8
13	1386.6	170.2	55	1386.6	170.2	97	1386.6	185.8
14	1386.6	381.1	56	1386.6	169.6	98	1386.6	127.9
15	1386.6	381.1	57	1386.6	169.6	99	1386.6	199.1
16	1386.6	196.8	58	1386.6	169.6	100	1386.6	210.1
17	1386.6	196.8	59	1386.6	222.9	101	1386.6	210.1
18	1386.6	196.8	60	1386.6	222.9	102	1386.6	210.1
19	1386.6	213.1	61	1386.6	176	103	1386.6	210.1
20	1386.6	213.1	62	1386.6	176	104	1386.6	210.1
21	1386.6	170.2	63	1386.6	176	105	1386.6	176
22	1386.6	170.2	64	1386.6	178.3	106	1386.6	176
23	1386.6	256.5	65	1386.6	192.2	107	1386.6	176
24	1386.6	219.4	66	1386.6	184.1	108	1386.6	185.8
25	1386.6	219.4	67	1386.6	184.1	109	1386.6	185.8
26	1386.6	219.4	68	1386.6	184.1	110	1386.6	127.9
27	1386.6	219.4	69	1386.6	165	111	1386.6	127.9
28	1386.6	195.1	70	1386.6	199.1	112	1386.6	210.1
29	1386.6	195.1	71	1386.6	195.1	113	-	-
30	1386.6	195.1	72	1386.6	195.1	114	-	-
31	1386.6	195.1	73	1386.6	195.1	115	-	-
32	1386.6	195.1	74	1386.6	222.9	116	-	-
33	1386.6	170.2	75	1386.6	176	117	-	-
34	1386.6	170.2	76	1386.6	176	118	-	-
35	1386.6	170.2	77	1386.6	176	119	1386.6	176
36	1386.6	169.6	78	1386.6	233.3	120	1386.6	176
37	1386.6	219.4	79	1386.6	233.3	121	1386.6	185.8
38	1386.6	219.4	80	1386.6	197.4	122	1386.6	185.8
39	1386.6	219.4	81	1386.6	184.1	123	1386.6	185.8
40	1386.6	219.4	82	1386.6	184.1	124	1386.6	127.9
41	1386.6	195.1	83	1386.6	184.1			
42	1386.6	195.1	84	1386.6	199.1			

Tab. 7.4: Cost of utilities $util_{\psi,g}$ [€/t] for producing chemical ψ in region g (Eurostat, 2017a; 2017b; 2017c; Baldo, 2018), with null values for cells $g = [125 - 134]$.

	ψ			ψ			ψ	
g	PPP	MeOH	g	PPP	MeOH	g	PPP	MeOH
1	3.24	145.4	43	3.08	130.1	85	3.01	128.3
2	3.24	145.4	44	3.08	130.1	86	3.01	128.3
3	3.24	145.4	45	1.92	82.1	87	3.01	128.3
4	3.24	145.4	46	1.92	82.1	88	3.01	128.3
5	3.24	145.4	47	2.92	125.4	89	3.01	128.3
6	3.24	145.4	48	2.92	125.4	90	3.26	135.8
7	3.24	145.4	49	2.92	125.4	91	3.26	135.8
8	5.43	236.4	50	3.77	159.3	92	3.26	135.8
9	3.24	145.4	51	3.77	159.3	93	3.26	135.8
10	3.24	145.4	52	2.26	95.4	94	10.03	393.9
11	3.24	145.4	53	2.26	95.4	95	2.27	98.1
12	3.01	125.5	54	3.03	128.1	96	2.79	117.7
13	3.01	125.5	55	3.03	128.1	97	2.79	117.7
14	5.43	236.4	56	1.92	82.1	98	1.93	79.6
15	5.43	236.4	57	1.92	82.1	99	3.08	130.1
16	2.65	113.0	58	1.92	82.1	100	3.01	128.3
17	2.65	113.0	59	2.92	125.4	101	3.01	128.3
18	2.65	113.0	60	2.92	125.4	102	3.01	128.3
19	3.14	133.8	61	3.26	135.8	103	3.01	128.3
20	3.14	133.8	62	3.26	135.8	104	3.01	128.3
21	3.01	125.5	63	3.26	135.8	105	3.26	135.8
22	3.01	125.5	64	2.50	105.6	106	3.26	135.8
23	2.99	130.5	65	2.51	107.2	107	3.26	135.8
24	3.77	159.3	66	2.46	104.4	108	2.79	117.7
25	3.77	159.3	67	2.46	104.4	109	2.79	117.7
26	3.77	159.3	68	2.46	104.4	110	1.93	79.6
27	3.77	159.3	69	2.33	98.0	111	1.93	79.6
28	3.08	130.1	70	3.08	130.1	112	3.01	128.3
29	3.08	130.1	71	3.01	128.3	113	-	-
30	3.08	130.1	72	3.01	128.3	114	-	-
31	3.08	130.1	73	3.01	128.3	115	-	-
32	3.08	130.1	74	2.92	125.4	116	-	-
33	3.01	125.5	75	3.26	135.8	117	-	-
34	3.01	125.5	76	3.26	135.8	118	-	-
35	3.01	125.5	77	3.26	135.8	119	3.26	135.8
36	2.81	117.4	78	2.52	110.4	120	3.26	135.8
37	3.77	159.3	79	2.52	110.4	121	2.79	117.7
38	3.77	159.3	80	2.34	100.6	122	2.79	117.7
39	3.77	159.3	81	2.46	104.4	123	2.79	117.7
40	3.77	159.3	82	2.46	104.4	124	1.93	79.6
41	3.08	130.1	83	2.46	104.4			
42	3.08	130.1	84	2.58	107.9			

Tab. 7.5: Arrays of slopes FCI_{ψ}^{slope} [€/t of chemical] and intercepts $FCI_{\psi}^{intercept}$ [€] coefficients for the calculation of the facility capital costs for producing chemical ψ (Aasberg-Petersen et al., 2008). Carbon quantity U_{ψ}^{saved} [t of CO_2/t of chemical ψ] that is saved from the production of a unitary quantity of chemical ψ (von der Assen and Bardow, 2014; Roh et al., 2016), and carbon quantity U_{ψ}^{conv} [t of CO_2/t of chemical ψ] that is converted to produce a unitary quantity of chemical ψ (Langanke et al., 2014; Sakakura and Kohno, 2009; Roh et al., 2016).

	FCI_{ψ}			
	slope [€/t]	intercept [€]	U_{ψ}^{saved} [t/t]	U_{ψ}^{conv} [t/t]
PPP	33.96	20.97	0.15	0.23
MeOH	79.79	229.02	0.65	0.28

7.4 Results

The time-static CCUS model was optimised using the GAMS CPLEX solver for MILP problems on a 16 GB RAM laptop in about 27 hours (an optimality gap always lower than 1% was reached). Results from the optimal CCS network are reported as a matter of comparison (Scenario 0). The CCUS network is here optimised according to the selection of a minimum European reduction target of 50% of overall European CO_2 emissions from large stationary sources, therefore consistent with the recent directives (EC, 2017), and with the results from previous Chapters. Three scenarios have been here investigated (Table 7.6). In Scenario A it is assumed that the production of PPP and MeOH cannot be higher than the current European production. A subsequently described case-study takes into account the fact that some European countries do not allow onshore sequestration (Scenario B), while a conclusive case-study investigates the response of the model to hypotetical higher demands of the two chemicals (Scenario C).

Scenario A entails a total cost TC for installing and operating the CCUS network that is reduced by 5.5% with respect to Scenario 0. This is due to the fact that the introduction of chemical conversion brings in some revenues (the profit in Scenario A is equal to 1.57 €/t). Conversely, the possibility of chemical conversion of CO_2 allows just a slight reduction of 0.7% of total capture cost TCC, which decreases from 30.93 €/t (Scenario 0) down to 30.72 €/t (Scenario A). On the other hand, Scenario A entails a barely unchanged transport infrastructure with respect to Scenario 0, despite the necessity of transporting not only the CO_2 that is destined to sequestration, but also the CO_2 fed to the conversion plants (the latter quantity is so small that does not affect the overall structure of the transport network). This result is not surprising if we consider that the same total quantity of CO_2 is imposed to be captured from stationary sources in all scenarios, and therefore the same to-

Tab. 7.6: Scenarios 0-A-B-C, main assumptions and results. All scenarios aim at reaching a European carbon reduction target $\alpha = 50\%$ of emissions from large stationary sources. Results are summarised in terms of total cost TC total capture cost TCC, total transport cost TTC, total sequestration cost TSC, and $profit$. Intensive values (i.e., [€/t]) are referred to the overall captured quantity of CO_2. Results for Scenario C are those considering the triplication of the European production of chemicals with respect to the base case.

Scenario	Model	TC [€/t]	TCC [€/t]	TTC [€/t]	TSC [€/t]	$profit$ [€/t]
0	CCS	33.36	30.93	1.96	0.47	-
A	CCUS	31.52	30.72	1.90	0.46	1.57
B	CCUS	32.69	30.73	2.59	0.46	1.09
C	CCUS	29.34	30.28	1.79	0.45	3.18

tal flowrate must be shipped between the nodes (independently from the choice of either sequestration or utilisation). As a result, the total transport cost TTC just slightly varies from 1.96 €/t (Scenario 0) to 1.90 €/t (Scenario A). Conversely, the exploitation of geological storage slightly diminishes with respect to Scenario 0 (i.e., -1.44%). Total sequestration costs TSC are unchanged between Scenario 0 and Scenario A (0.47 €/t and 0.46 €/t, respectively). In terms of CO_2 emission reduction, the net impact of utilisation amounts to 0.58% of the overall captured amount (the result is comparable with the 1% upper bound for chemical conversion estimated by Mac Dowell et al., 2017).

The final SC configuration is reported in Figure 7.3 for both Scenario 0 (Figure 7.3a) and Scenario A (Figure 7.3b). It can be observed that the SC configuration is nearly identical. Capture points do not change and the main driver to establish the transport system is still the location of the sequestration sites. The three conversion facilities are situated in regions allowing for cost reduction, i.e. Hungary, Macedonia and Turkey, respectively. It was verified that the key parameters affecting the definition of the plant sites are corporate tax rate, cost of materials, and energy price. The country where the conversion plants are located allow for a good mix of the above parameters. Regarding the corporate tax rate, there is a large variability across Europe (Table 7.2), from a minimum of 9% (Hungary) up to a maximum of 34% (Belgium). The tax rate of Macedonia is just slightly higher than from that of Hungary, while the one of Turkey is close to the average (i.e. 20%). In fact, the construction of plants in Hungary and Macedonia is mainly justified by tax rate values. Turkey takes advantage of the low cost of raw materials (Table 7.3) and utilities (Table 7.4). In particular, the price of electricity is at its lowest in Turkey (0.0187 €/kWh) (Table 7.2). Therefore, the presence of a plant for producing energy-intensive MeOH in Turkey is quite justifiable. Summarising, the location of plants for CO_2 conversion into PPP is mainly chosen on the basis of low taxation,

since this process is less energy intensive. Conversely, as regards the production of MeOH, its location is mainly determined by the cost raw materials and utilities (and, in particular, of electricity). Labour costs (Table 7.6) do not seem to have a relevant impact for choosing the locations of conversion facilities.
Scenario B considers the fact that some countries restrict (Czech Republic, Germany, Poland, Sweden, the Netherlands, and UK) or forbid (Austria, Croatia, Estonia, Ireland, Latvia, Finland and Belgium) onshore sequestration (EC, 2017). Even though UK, Poland and the Netherlands are in the process of authorising it (EC, 2017), Scenario B prudently optimises the CCUS SC while excluding all the aforementioned states from those in which onshore storage is allowed. Results (Table 7.6) show that the total cost TC does not change significantly (about 2% more expensive with respect to Scenario A), whereas, analogously to what observed in Chapter 2 for CCS SCs, the optimal CCUS network entails a longer (+66%) and more expensive (+36.8%) transport infrastructure. Interestingly, the restrictive legal framework for onshore storage produces also a parallel decrease in the utilisation of CO_2 for chemical conversion (-29.8% with respect to Scenario A), since the design of the final SC configuration is mainly driven by capture and transport costs and utilisation would lead to an even more complex (and expensive) transport infrastructure, despite the beneficial effects of a positive profit.
Scenario C focuses on investigating how the cost of a CO_2 SC varies if the production of chemicals progressively increases with respect to the current European one (i.e., with respect to Scenario A) until three times the current production. Accordingly, tripling the production of both chemicals corresponds to an increase of the European production quota from $25.5\%^{PPP}$ and $9.6\%^{MeOH}$ (Scenario A) to $76.6\%^{PPP}$ and $28.8\%^{MeOH}$ (Scenario C) of actual world capacity. The results from the optimal CCUS configuration of Scenario C show that overproduction of the two chemicals mainly affects the total cost of the SC (Figure 7.4a), which could be reduced by about 6.92% in case productions of both chemicals are tripled with respect to current ones. On the other hand, the contribution of CO_2 utilisation over capture would go from 0.58% (Scenario A) to a maximum of about 1.75% (Scenario C) (Figure 7.4b). In order to completely avoid the necessity of CO_2 sequestration, an increase to over 70 times the current European production of PPP and MeOH would be required. In terms of GHG savings, Scenario C would allow a net CO_2 saving due to utilisation equal to 24.5 Mt (corresponding to 4.07% of the overall processed CO_2), against just 8.2 Mt for Scenario A.

7.5 Discussion and limitations

This preliminary analysis concluded that CCU in general can contribute very little to achieve the European climate target set for 2030, in terms of both emissions and CCS costs reduction. However, the authors recognise that the scope was limited by several simplifications, which are discussed in the following:

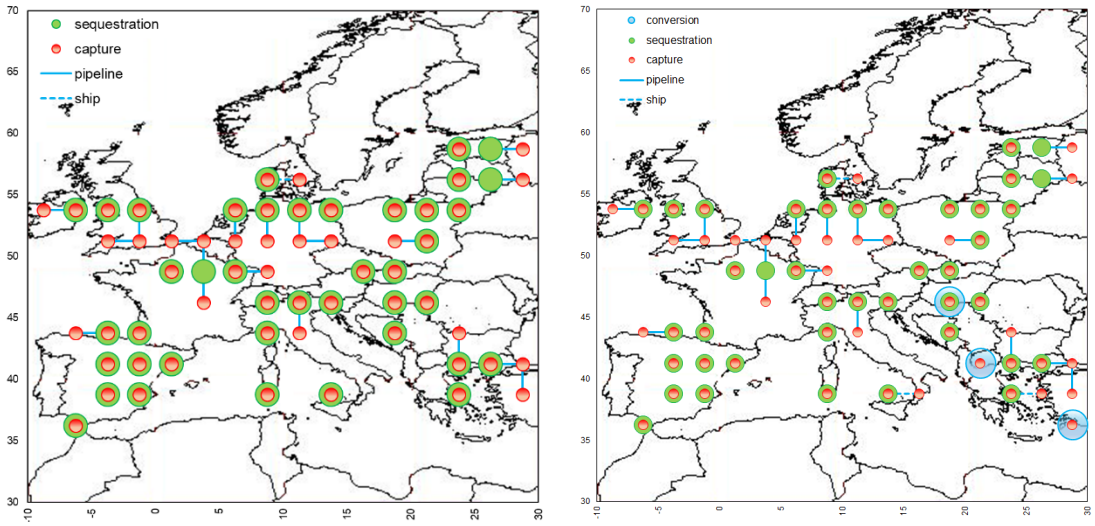

(a) (b)

Fig. 7.3: Final SC configurations for (a) Scenario 0 and (b) Scenario A.

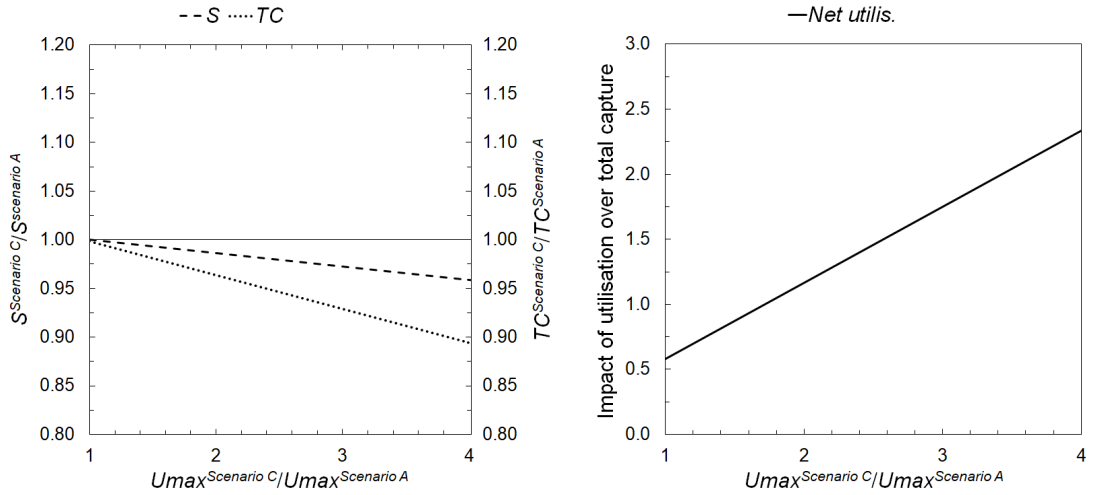

(a) (b)

Fig. 7.4: Comparison between Scenario C and Scenario A in terms of: (a) relative variations in total cost (TC) and exploitation of geological sequestration (S); and (b) effective net CO_2 utilisation ($Netutilis.$), with respect to the change in the productions of the chemical being considered (U^{max}).

- one major criticism about this work would rely on the fact that very few technologies and commodities were implemented for CO_2 conversion and that the demand for CO_2 to be utilised was forecasted for the mere production of chemicals. Therefore, alternative pathways were not taken into account (e.g., construction materials and fuels, as shown in Chapter 1). On the one hand, it should be recognised that this choice appears to be a sensible one, considering the current state of technologies. On the other hand, a comprehensive study to investigate other routes is needed. For instance, when focussing on the cement industry, an application of CCU technologies could foster the routing towards an 'ideally carbon-free' market in which construction materials are generated from the same CO_2 captured within the plant itself;

- regarding the demand of chemicals considered in this study, we recognise that new policies and technological changes may determine dramatic variations in the next few years. As a matter of facts, MeOH is currently envisioned for a wide range of applications beyond its current use, e.g. as fuel for transport and energy sectors and for synthesis of hydrocarbons, including several major large-volume chemicals (Olah et al., 2011; IEA, 2013). Hence, imposing the current production volumes as an upper limit for the utilisation potential may neglect a wide range of options;

- furthermore, this model assumed that traditional production technologies for PPP and MeOH would move to alternatives based on CO_2 conversion, so that all European production would rely on CO_2 as a feedstock. In the current situation, such scenario does not appear to be highly plausible unless some incentives are introduced or the whole world production follows a similar path;

- moreover, another limitation of this study entails the fact that the trasport stage is not modelled for final products, even though it should be recognised that a precise description of this aspect would require an accurate spatial definition of the market demand, which is currently beyond the scope of this work;

- finally, by having set the time-horizon to 2030, the temporal scale considered in this study represented a short-term perspective of the European situation. Although recognising that major changes in the techno-energetic mix might happen even in a medium term framework, this simplification was supported by the necessity of keeping this preliminary study computationally tractable and of reducing uncertainty in the foreseen scenarios.

7.6 Chapter conclusions

This Chapter assessed the potential impact of a European CCUS SC. Results showed that, as suggested by other studies, the environmental impact of CO_2 utilisation is

likely to be a minor one (about 0.6% reduction in GHG emissions for the chemicals considered in this study). The main benefit might be the reduction of the overall costs (decreasing by 5.5%), since conversion would provide for some revenues (differently from sequestration).
Furthermore, it was verified that even a huge increase in the production of the two commodities (up to three times the current European production) would not change the results dramatically. Although admittedly representing an approximated snapshot of a possible state of things, the presented results confirmed that CO_2 utilisation is not a viable option if the objective is to achieve a significant impact in terms of CO_2 emissions reduction. Nonetheless, it might be a sensible approach to slightly reduce the taxpayers' cost for establishing a CCS infrastructure as geological sequestration seems to be the only effective choice to take care of CO_2 emissions from stationary sources.

8

Conclusions and future work

The Thesis provided insights into the development of a mixed integer linear programming mathematical framework for the strategic optimisation of European carbon capture and storage and carbon capture utilisation and storage supply chains. Firstly, a deterministic carbon capture and storage supply chain economic optimisation was developed, in which the objective was to minimise the total cost to install and to operate the network over a chosen time framework. In that case, the investigated scenarios (capturing up to the 70% of 20 years' CO_2) demonstrated the good European potential for operating sequestration at scale and the good computational performance of the solution approach. Costs for capture emerged as the key economic challenge of the system, being transport- and sequestration-related costs a negligible part of the overall investment. Secondly, it was proposed a carbon capture and storage supply chain optimisation under uncertainty in geological sequestration capacities: here the objective was to quantify the financial risks arising from geological uncertainties in European supply chain networks, whilst also providing a tool for minimising storage risk exposure. It was shown that such risks can be minimised via careful design of the network, by distributing the investment for storage across Europe and by incorporating operational flexibility to improve network resiliency on uncertainty. Then, a subsequent pillar of this research analysed a societal risk-constrained supply chain optimisation: in this case, the economic optimisation was coupled with societal risk analysis and the optional installation of mitigation measures on the pipeline infrastructure. It turned out that mitigation actions never represent more than 10% of total cost for installing and operating the transport network, whereas no feasible solution could be found for a carbon reduction target higher than 50%, because of the unacceptable level of societal risk. Another model

dealt with a carbon capture and storage supply chain multi-objective optimisation with considerations on social acceptance-related issues through risk perception by the public. This analysis provided indications on the optimal trade-off configuration between the economic and socially acceptable networks. As a result, some offshore storage had to be exploited in order to limit the risk perception by the local communities. Then, in order to decrease the spread of costs for carbon capture and storage among European countries, a further study was presented here and dealt with the design of international networks under consideration of cooperation policies and compensation schemes among the European countries. Regardless of the chosen policy for cooperation (i.e., emission-driven policy, gross domestic product-driven policy, or a combination of both) the optimal supply chain entailed almost the same design in all scenarios, meaning that the results were rather robust in terms of final infrastructure. Finally, it was proposed a preliminary optimisation of a comprehensive carbon capture utilisation and storage system, considering the possible utilisation of CO_2 for the production of two chemicals (i.e., polyether carbonate polyols and methanol). The results showed that CO_2 conversion and utilisation mainly affects the total cost of the supply chain, which could be reduced with respect to a mere carbon capture and storage network. On the other hand, the contribution of CO_2 utilisation over capture was shown to be almost negligible.
Results from this Thesis provided preliminary insights into strategic policies for investment planning for carbon capture and storage at European scale, and may be improved by implementing further aspects such as:

- quantifying reliability issues such as component failures (e.g., injection well failure), in order to minimise operational risks in the inherent planning of the supply chain infrastructure, also in terms of a potential impact on the natural environment;

- considering the effects of varying the load factors of power plants on capture costs, as well as aspects related to ageing and potential decommissioning of those power plants not retrofitted with carbon capture technologies;

- evaluating the potential decrease in costs of carbon capture and storage technologies due to the effects of technology learning curves (e.g., Giarola et al., 2013); moreover, regarding capture cost, a deeper focus should be addressed on pre-combustion, to provide more reliable data and tackle uncertainty issues related to the early stage of development of such technology;

- assessing and optimising carbon capture, utilisation and storage networks through a proper environmental analysis, in order to consider the net global footprint of such systems in terms of CO_2-equivalent emissions and minimising risks towards natural ecosystems;

- further investigating CO_2 utilisation pathways as an alternative to geological storage. As a matter of fact, one aim for the future would be to evaluate the

effects of carbon capture and utilisation from an economic and environmental perspective and to further assess what contribution may derive from CO_2 utilisation for conversion into useful products through quantitative supply chain optimisation tools. In fact, the possibility to consider multiple conversion and utilisation options in the design of a large scale (i.e., European) network has thus far never been analysed;

- incorporating large industrial emissions clusters (particularly, cement industries) as possible sources of carbon to be captured. As a matter of facts, considering emission clusters rather than single point-source facilities, industry (and particularly, cement industry) could play an important role in the accounting of overall CO_2 generation in Europe. On the one hand, different (traditional) techniques have already been significantly employed and exploited to decrease these emissions, such as improving energy efficiency, using less carbon intensive fuels and alternative raw materials. On the other hand, carbon capture and storage was shown to be good at heavily decarbonising the cement industries, while in the meantime existing plants could be retrofitted with different options as capture technologies. In particular, cement plants constitute an ideal candidate for carbon capture and storage, considering their relatively high concentration of CO_2 in the flue gases, the small amount of (sufficiently) large emission points, the stable operational load of these facilities and, sometimes, the presence of waste heat for process integration.

Overall, the development of quantitative modelling techniques for supply chain optimisation problems (such those presented in this Thesis) may accomplish the determination of optimal network configurations and technological choices that would allow minimising the overall costs and risks for installing and operating a European carbon capture utilisation and storage infrastructure while pursuing a chosen carbon reduction target. In view of the above, this research represents a fundamental step forward in order to provide tools and methods for the strategic assessment of different policies, aiming at fostering an effective installation and operation of carbon capture, transport, utilisation and sequestration networks.

Bibliography

Aasberg-Petersen, K., Nielsen, C.S., Dybkjær, I., Perregaard, J., 2008. Large scale methanol production from natural gas. Haldor Topsoe 22.

Acar, C., Beskese, A., Temur, G.T., 2019. A novel multicriteria sustainability investigation of energy storage systems. *Int. J. Energy Res.* 43, 6419-6441.

Agnolucci, P., Akgul, O., McDowall, W., Papageorgiou, L.G., 2013. The importance of economies of scale, transport costs and demand patterns in optimising hydrogen fuelling infrastructure: An exploration with SHIPMod (Spatial hydrogen infrastructure planning model). *Int. J. Hydrogen Energy* 38, 11189-11201.

Ağralı, S., Üçtuğ, F.G., Türkmen, B.A., 2018. An optimization model for carbon capture and storage/utilization vs. carbon trading: A case study of fossil-fired power plants in Turkey. *J. Environ. Manage.* 215, 305-315.

AIChE, 2000. Chemical Process Quantitative Risk Analysis. Wiley-Interscience, New York, USA.

Akgul, O., Mac Dowell, N., Papageorgiou, L.G., Shah, N., 2014. A mixed integer nonlinear programming (MINLP) supply chain optimisation framework for carbon negative electricity generation using biomass to energy with CCS (BECCS) in the UK. *Int. J. Greenh. Gas Control* 28, 189-202.

Alcalde, J., Flude, S., Wilkinson, M., Johnson, G., Edlmann, K., Bond, C.E., Scott, V., Gilfillan, S.M.V., Ogaya, X., Stuart Haszeldine, R., 2018. Estimating geological CO_2 storage security to deliver on climate mitigation. *Nat. Commun.* 9, 1-13.

Alper, E., Yuksel Orhan, O., 2017. CO_2 utilization: Developments in conversion processes. *Petroleum* 3, 109-126.

Aminu, M.D., Nabavi, S.A., Rochelle, C.A., Manovic, V., 2017. A review of developments in carbon dioxide storage. *Appl. Energy* 208, 1389-1419.

An, J., Peng, S., 2016. Layout optimization of natural gas network planning: Synchronizing minimum risk loss with total cost. *J. Nat. Gas Sci. Eng.* 33, 255-263.

Anderson, S.T., 2017. Cost Implications of Uncertainty in CO_2 Storage Resource Estimates: A Review. *Nat. Resour. Res.* 26, 137-159.

Anthonsen, K.L., Hendriks, C., Wojcicki, A., van der Meer, B., Kirk, K., Le Nindre, Y.-M., Peter Christensen, N., Le Gallo, Y., Bossie-Codreanu, D., neele, F., Smith, N., Dalhoff, F., Vangkilde-Pedersen, T., 2009. Assessing European capacity for geological storage of carbon dioxide–the EU GeoCapacity project. *Energy Procedia* 1, 2663-2670.

Aresta, M., Dibenedetto, A., Angelini, A., 2013. The changing paradigm in CO_2 utilization. *J. CO_2 Util.* 3-4, 65-73.

Argus De Witt, 2015. Argus DeWitt 2015 Fuels and Oxygenates Annual [WWW Document]. `https://www.argusmedia.com/~/media/files/pdfs/petchems/mtbe-2015-annual-flyer.pdf?la=en`

Arnette, A.N., 2016. Renewable energy and carbon capture and sequestration for a reduced carbon energy plan: An optimization model. *Renew. Sustain. Energy Rev.* 70, 254-265.

Arning, K., Offermann-van Heek, J., Linzenich, A., Kaetelhoen, A., Sternberg, A., Bardow, A., Ziefle, M., 2019. Same or different? Insights on public perception and acceptance of carbon capture and storage or utilization in Germany. *Energy Policy* 125, 235-249.

Ashworth, P., Bradbury, J., Wade, S., Ynke Feenstra, C.F.J., Greenberg, S., Hund, G., Mikunda, T., 2012. What's in store: Lessons from implementing CCS. *Int. J. Greenh. Gas Control* 9, 402-409.

Ashworth, P., Wade, S., Reiner, D., Liang, X., 2015. Developments in public communications on CCS. *Int. J. Greenh. Gas Control* 40, 449-458.

Bachu, S., 2003. Screening and ranking of sedimentary basins for sequestration of CO_2 in geological media in response to climate change. *Environ. Geol.* 44, 277-289.

Bahn, O., Haurie, A., Kypreos, S., Vial, J.-P., 1998. Advanced mathematical programming modeling to assess the benefits from international CO_2 abatement co-

operation. *Environ. Model. Assess.* 3, 107-115.

Bakken, B.H., von Streng Velken, I., 2008. Linear models for optimization of infrastructure for CO_2 capture and storage. *IEEE Trans. Energy Convers.* 23, 824-833.

Baldo V, 2018. Economic optimisation of a European supply chain for CO_2 utilisation and sequestration. http://tesi.cab.unipd.it/59680/

Barker, R., Hua, Y., Neville, A., 2016. Internal corrosion of carbon steel pipelines for dense-phase CO 2 transport in carbon capture and storage (CCS) – a review. *Int. Mater. Rev.* 6608, 1-31.

Bassani, A., van Dijk, H.A.J., Cobden, P.D., Spigno, G., Manzolini, G., Manenti, F., 2019. Sorption Enhanced Water Gas Shift for H 2 production using sour gases as feedstock. *Int. J. Hydrogen Energy* 31, 16132-16143.

Beamon, B., 1998. Supply chain design and analysis: models and methods. *Int. J. Prod. Econ.* 3, 281-294.

Bellotti, D., Rivarolo, M., Magistri, L., Massardo, A.F., 2017. Feasibility study of methanol production plant from hydrogen and captured carbon dioxide. *J. CO_2 Util.* 21, 132-138.

BP, 2017. BP Statistical Review of World Energy 2017 [WWW Document]. http://www.bp.com/content/dam/bp/en/corporate/pdf/energy-economics/statistical-review-2017/bp-statistical-review-of-world-energy-2017-full-report.pdf

Braun, C., 2017. Not in My Backyard: CCS Sites and Public Perception of CCS. *Risk Anal.* 37, 2264-2275.

Bui, M., Adjiman, C.S., Bardow, A., Anthony, E.J., Boston, A., Brown, S., Fennell, P.S., Fuss, S., Galindo, A., Hackett, L.A., Hallett, J.P., Herzog, H.J., Jackson, G., Kemper, J., Krevor, S., Maitland, G.C., Matuszewski, M., Metcalfe, I.S., Petit, C., Puxty, G., Reimer, J., Reiner, D.M., Rubin, E.S., Scott, S.A., Shah, N., Smit, B., Trusler, J.P.M., Webley, P., Wilcox, J., Mac Dowell, N., 2018. Carbon capture and storage (CCS): The way forward. *Energy Environ. Sci.* 11, 1062-1176.

Cairns, H., 2016. Global trends in Syngas, technical report, Stratas Advisors [WWW Document]. https://stratasadvisors.com/Insights/072216-Global-Sybgas-Trends

Calderón, A.J., Papageorgiou, L.G., 2018. Key aspects in the strategic development of synthetic natural gas (BioSNG) supply chains. *Biomass and Bioenergy* 110, 80-97.

CCSNetwork, 2015. 2015 Situation Report on the European Large Scale Demonstration Projects Network: Public Summary [WWW Document]. https://hub.globalccsinstitute.com/sites/default/files/publications/199478/2015-situation-report-european-large-scale-demonstration-projects-network.pdf

CDIAC, 2017. Fossil-Fuel CO_2 Emissions [WWW Document]. https://cdiac.ess-dive.lbl.gov/trends/emis/meth_reg.html

Chen, W., Le Nindre, Y.M., Xu, R., Allier, D., Teng, F., Domptail, K., Xiang, X., Guillon, L., Chen, J., Huang, L., Zeng, R., 2010. CCS scenarios optimization by spatial multi-criteria analysis: Application to multiple source sink matching in Hebei province. *Int. J. Greenh. Gas Control* 4, 341-350.

Chen, Z.A., Li, Q., Liu, L.C., Zhang, X., Kuang, L., Jia, L., Liu, G., 2015. A large national survey of public perceptions of CCS technology in China. *Appl. Energy* 158, 366-377.

CIESIN, 2017. Gridded Population of the World, Version 4 (GPWv4): Population Count, Revision 10 [WWW Document]. https://doi.org/10.7927/H4PG1PPM

CNN, 2014. Desert plants and green diesel: Meet the jet fuels of the future [WWW Document]. http://edition.cnn.com/travel/article/boeing-biofuel/index.html

Covestro, 2017. Investor Presentation technical report [WWW Document]. http://investor.covestro.com/en/presentations/presentations/

Cuéllar-Franca, R.M., Azapagic, A., 2015. Carbon capture, storage and utilisation technologies: A critical analysis and comparison of their life cycle environmental impacts. *J. CO_2 Util.* 9, 82-102.

Czernichowski-Lauriol, I., Berenblyum, R., Bigi, S., Car, M., Gastine, M., Persoglia, S., Poulsen, N., Schmidt-Hattenberger, C., Stead, R., Vincent, C.J., Wildenborg, T., 2018. CO_2 GeoNet actions in Europe for advancing CCUS through global cooperation. *Energy Procedia* 154, 73-79.

d'Amore, F., Bezzo, F., 2016. Strategic Optimisation of Biomass-Based Energy Supply Chains for Sustainable Mobility. *Comput. Chem. Eng.* 87, 68-81.

d'Amore, F., Bezzo, F., 2017. Economic optimisation of European supply chains for CO_2 capture, transport and sequestration. *Int. J. Greenh. Gas Control* 65, 99-116.

d'Amore, F., Mocellin, P., Vianello, C., Maschio, G., Bezzo, F., 2018a. Economic optimisation of European supply chains for CO_2 capture, transport and sequestration, including societal risk analysis and risk mitigation measures. *Appl. Energy* 223, 401-415.

d'Amore, F., Mocellin, P., Vianello, C., Maschio, G., Bezzo, F., 2018b. Towards the economic optimisation of European supply chains for CO_2 capture, transport and sequestration, including societal risk analysis. *Comput. Aided Chem. Eng.* 44, 2305-2310.

d'Amore, F., Sunny, N., Iruretagoyena, D., Bezzo, F., Shah, N., 2019a. European supply chains for carbon capture, transport and sequestration, with uncertainties in geological storage capacity: insights from economic optimisation. *Comp. Chem. Eng.*, 129, 106521.

d'Amore, F., Sunny, N., Iruretagoyena, D., Bezzo, F., Shah, N., 2019b. Optimising European supply chains for carbon capture, transport and sequestration, including uncertainty on geological storage availability. *Comput. Aided Chem. Eng.* 46, 199-204.

d'Amore, F., Lovisotto, L., Bezzo, F., 2019c. Introducing social acceptance into the design of CCS supply chains: a case study at a European level. *J. Clean. Prod.*, Accepted. `https://doi.org/10.1016/j.jclepro.2019.119337`

d'Amore, F., Bezzo, F., 2019d. Optimal design of European cooperative supply chains for carbon capture, transport and sequestration with costs share policies. *AIChE J.*, Accepted. `https://doi.org/10.1002/AIC.16872`.

Davis, S.J., Cao, L., Caldeira, K., Hoffert, M.I., 2013. Rethinking wedges. *Environ. Res. Lett.* 8.

DNV, 2011. Report for Australian Maritime Safety Authority: Ship Oil Spill Risk Models. Det Norske Veritas, Project PP002916, Appendix IV.

Dütschke, E., 2011. What drives local public acceptance - Comparing two

cases from Germany. *Energy Procedia* 4, 6234-6240.

EC, 2017. Report from the commission to the European Parliament and the Council on Implementation of Directive 2009/31/EC on the Geological Storage of Carbon Dioxide [WWW Document]. https://ec.europa.eu/commission/sites/beta-political/files/report-carbon-capture-storage_en.pdf

EC, 2018. 2030 climate and energy framework, greenhouse emissions [WWW Document]. https://ec.europa.eu/clima/policies/strategies/2030_en

EC, 2019. The European CCS Demonstration Project Network [WWW Document]. https://ccsnetwork.eu/

EIA, 2007. About U.S. Natural Gas Pipelines - Transporting Natural Gas [WWW Document]. https://www.eia.gov/pub/oil_gas/\%0Anatural_gas/analysis_publications/ngpipeline/develop.html

Elahi, N., Shah, N., Korre, A., Durucan, S., 2014. Multi-period least cost optimisation model of an integrated carbon dioxide capture transportation and storage infrastructure in the UK. *Energy Procedia* 63, 2655-2662.

Ervural, B.C., Evren, R., Delen, D., 2018. A multi-objective decision-making approach for sustainable energy investment planning. *Renew. Energy* 126, 387-402.

Eurobarometer, 2011. Public awareness and acceptance of CO_2 capture and storage. Bruxelles, Belgium.

Eurostat, 2016. Energy Balances [WWW Document]. http://ec.europa.eu/eurostat/web/\%0Aenergy/data/energy-balances

Eurostat, 2017a. Labour costs database [WWW Document]. http://ec.europa.eu/eurostat/web/labour-market/labour-costs/database

Eurostat, 2017b. Energy price statistics [WWW Document]. http://ec.europa.eu/eurostat/statistics-explained/index.php/Energy_price_statistics

Eurostat, 2017c. Natural gas price statistics [WWW Document]. http://ec.europa.eu/eurostat/statistics-explained/index.php/Natural_gas_price_statistics

Eurostat, 2019a. Demography and migration, population [WWW Document].

https://ec.europa.eu/eurostat/web/population-demography-migration-projections/data/main-tables?p_p_id=NavTreeportletprod_WAR_NavTreeportletprod_INSTANCE_YsjeL9sUx9xO\&p_p_lifecycle=0\&p_p_state=normal\&p_p_mode=view\&p_p_col_id=column-2\&p_p_col_count=2

Eurostat, 2019b. Annual national accounts, GDP and main components [WWW Document]. https://ec.europa.eu/eurostat/web/national-accounts/data/database?p_p_id=NavTreeportletprod_WAR_NavTreeportletprod_INSTANCE_HxOU2oGtTuFV\&p_p_lifecycle=0\&p_p_state=normal\&p_p_mode=view\&p_p_col_id=column-2\&p_p_col_count=3

Farquharson, D.V., Jaramillo, P., Schivley, G., Klima, K., Carlson, D., Samaras, C., 2017. Beyond Global Warming Potential: A Comparative Application of Climate Impact Metrics for the Life Cycle Assessment of Coal and Natural Gas Based Electricity. *J. Ind. Ecol.* 21, 857-873.

Fernández-Dacosta, C., Van Der Spek, M., Hung, C.R., Oregionni, G.D., Skagestad, R., Parihar, P., Gokak, D.T., Strømman, A.H., Ramirez, A., 2017. Prospective techno-economic and environmental assessment of carbon capture at a refinery and CO_2 utilisation in polyol synthesis. *J. CO_2 Util.* 21, 405-422.

Feron, P.H.M., 1994. Membranes for Carbon Dioxide Recovery from Power Plants, in: Paul, J., Pradier, C.-M. (Eds.), Carbon Dioxide Chemistry. Woodhead Publishing, pp. 236-249.

Galán-Martín, A., Pozo, C., Azapagic, A., Grossmann, I.E., Mac Dowell, N., Guillén-Gosálbez, G., 2018. Time for global action: An optimised cooperative approach towards effective climate change mitigation. *Energy Environ. Sci.* 11, 572-581.

García, J.H., Torvanger, A., 2019. Carbon leakage from geological storage sites: Implications for carbon trading. *Energy Policy* 127, 320-329.

Gastine, M., Berenblyum, R., Czernichowski-Lauriol, I., De Dios, J.C., Audigane, P., Hladik, V., Poulsen, N., Vercelli, S., Vincent, C., Wildenborg, T., 2017. Enabling Onshore CO_2 Storage in Europe: Fostering International Cooperation Around Pilot and Test Sites. *Energy Procedia* 114, 5905-5915.

Geske, J., Berghout, N., van den Broek, M., 2015. Cost-effective balance between CO_2 vessel and pipeline transport: Part II - Design of multimodal CO_2 transport: The case of the West Mediterranean region. *Int. J. Greenh. Gas Control* 33, 122-134.

Giarola, S., Bezzo, F., Shah, N., 2013. A risk management approach to the economic and environmental strategic design of ethanol supply chains. *Biomass and Bioenergy* 58, 31-51.

Gibon, T., Arvesen, A., Hertwich, E.G., 2017. Life cycle assessment demonstrates environmental co-benefits and trade-offs of low-carbon electricity supply options. *Renew. Sustain. Energy Rev.* 76, 1283-1290.

Global CCS Institute, 2017. Database of Current CCS Projects [WWW Document]. `https://www.globalccsinstitute.com/status`

Goel, V., Grossmann, I.E., 2004. A stochastic programming approach to planning of offshore gas field developments under uncertainty in reserves. *Comput. Chem. Eng.* 28, 1409-1429.

Götz, M., Lefebvre, J., Mörs, F., McDaniel Koch, A., Graf, F., Bajohr, S., Reimert, R., Kolb, T., 2016. Renewable Power-to-Gas: A technological and economic review. *Renew. Energy* 85, 1371-1390.

Gough, C., O'Keefe, L., Mander, S., 2014. Public perceptions of CO_2 transportation in pipelines. *Energy Policy* 70, 106-114.

Groothuis, P.A., Groothuis, J.D., Whitehead, J.C., 2008. Green vs. green: Measuring the compensation required to site electrical generation windmills in a viewshed. *Energy Policy* 36, 1545-1550.

Grossmann, I.E., Apap, R.M., Calfa, B. a., Garcia-Herreros, P., Zhang, Q., García-Herreros, P., Zhang, Q., 2016. Recent advances in mathematical programming techniques for the optimization of process systems under uncertainty. *Comput. Chem. Eng.* 91, 3-14.

Han, J.H., Lee, I.B., 2012. Multiperiod Stochastic Optimization Model for Carbon Capture and Storage Infrastructure under Uncertainty in CO_2 Emissions, Product Prices, and Operating Costs. *Ind. Eng. Chem. Res.* 51, 11445-11457.

Han, J.H., Lee, I.B., 2013. A comprehensive infrastructure assessment model for carbon capture and storage responding to climate change under uncertainty. *Ind. Eng. Chem. Res.* 52, 3805-3815.

Hasan, M.M.F., First, E.L., Boukouvala, F., Floudas, C.A., 2015. A multi-scale framework for CO_2 capture, utilization, and sequestration: CCUS and CCU.

Comput. Chem. Eng. 81, 2-21.

Havens, J.A., Spicer, T.O., 1985. Development of an atmospheric dispersion model for heavier-than-air gas mixtures.

Hedlund, F.H., 2012. The extreme carbon dioxide outburst at the Menzengraben potash mine 7 July 1953. *Saf. Sci.* 50, 537-553.

Heffer, P., Prud'homme, M., 2016. 84th IFA Annual Conference, Moscow, 30 May-1 June 2016, in: Fertilizer Outlook 2016-2020. International Fertilizer Industry Association (IFA), Moscow.

Herzog, H., Golomb, D., Zemba, S., 1991. Feasibility, modeling and economics of sequestering power plant CO_2 emissions in the deep ocean. *Environ. Prog.* 10, 64-74.

Heuberger, C.F., Staffell, I., Shah, N., Mac Dowell, N., 2018. Impact of myopic decision-making and disruptive events in power systems planning. *Nat. Energy* 3, 1-7.

Hillebrand, M., Pflugmacher, S., Hahn, A., 2013. Toxicological risk assessment in carbon capture and storage technology. *Toxicol. Lett.* 221, 118-143.

HO, J., 2017. Juyuan starts up polyether polyol plant.

Hofstede, G., Hofstede, G.J., Minkov, M., 2010. Cultures and Organizations, Software of the Mind, Intercultural Cooperation and Its Importance for Survival, 3rd Ed. ed. MacGraw-Hill, New York, USA

Huijts, N.M.A., Midden, C.J.H., Meijnders, A.L., 2007. Social acceptance of carbon dioxide storage. *Energy Policy* 35, 2780-2789.

IEA, 2013. Technology Roadmap: Energy and GHG Reductions in the Chemical Industry via Catalytic Processes [WWW Document]. `https://www.iea.org/publications/freepublications/publication/TechnologyRoadmapEnergyandGHGReductionsintheChemicalIndustryviaCatalyticProcesses.pdf`.

IEA, 2015. Key World Energy Statistics 2015.

IEA, 2018. World Energy Outlook 2018 [WWW Document]. `https://www.iea.org/weo2018/`.

IEAGHG, 2002. Transmission of CO_2 and Energy [WWW Document]. http://www.ieaghg.org/publications/technical-reports/17-publications/technical-evaluations/82-recently-published-technical-papers

IHS, 2003. Ethylene Carbonate From Ethylene Oxide.

IHS, 2017. Global Methanol Demand Growth Driven by Methanol to Olefins as Chinese Thirst for Chemical Supply Grows, IHS Markit Says [WWW Document]. http://news.ihsmarkit.com/press-release/country-industry-forecasting-media/global-methanol-demand-growth-driven-methanol-olefi

IPCC, 2005. IPCC Special Report on Carbon Dioxide Capture and Storage. Prepared by Working Group III of the Intergovernmental Panel on Climate Change [WWW Document]. Cambridge Univ. Press. https://www.ipcc.ch/pdf/special-reports/srccs/srccs_wholereport.pdf

IPCC, 2018. Global warming of 1.5 °C. An IPCC special report on the impacts of global warming of 1.5 °C above pre-industrial levels and related global greenhouse gas emission pathways, in the context of strengthening the global response to the threat of climate chang [WWW Document]. http://report.ipcc.ch/sr15/pdf/sr15_spm_final.pdf

Jarvis, S.M., Samsatli, S., 2018. Technologies and infrastructures underpinning future CO_2 value chains: A comprehensive review and comparative analysis. *Renew. Sustain. Energy Rev.* 85, 46-68.

Jensen, M.D., Pei, P., Snyder, A.C., Heebink, L. V., Botnen, L.S., Gorecki, C.D., Steadman, E.N., Harju, J.A., 2013. Methodology for phased development of a hypothetical pipeline network for CO_2 transport during carbon capture, utilization, and storage. *Energy and Fuels* 27, 4175-4182.

Jeong, H., Sun, A.Y., Zhang, X., 2018. Cost-optimal design of pressure-based monitoring networks for carbon sequestration projects, with consideration of geological uncertainty. *Int. J. Greenh. Gas Control* 71, 278-292.

Jin, S.W., Li, Y.P., Nie, S., Sun, J., 2017. The potential role of carbon capture and storage technology in sustainable electric-power systems under multiple uncertainties. *Renew. Sustain. Energy Rev.* 80, 467-480.

Joshi, P., Bikkina, P., Wang, Q., 2016. Consequence analysis of accidental release of supercritical carbon dioxide from high pressure pipelines. *Int. J. Greenh. Gas Control* 55, 166-176.

JRC, 2016. Emission Database for Global Atmospheric Research (EDGAR) [WWW Document]. edgar.jrc.ec.europa.eu/index.php

Kallrath, J., 2000. Mixed integer optimisation in the chemical process industry: experience, potential and future perspectives. *Chem. Eng. Res. Des.* 78, 809-822.

Kalyanarengan Ravi, N., Van Sint Annaland, M., Fransoo, J.C., Grievink, J., Zondervan, E., 2016. Development and implementation of supply chain optimization framework for CO_2 capture and storage in the Netherlands. *Comput. Chem. Eng.* 102, 40-51

Karimi, F., Khalilpour, R., 2015. Evolution of carbon capture and storage research: Trends of international collaborations and knowledge maps. *Int. J. Greenh. Gas Control* 37, 362-376.

Karimi, F., Toikka, A., 2018. General public reactions to carbon capture and storage: Does culture matter? *Int. J. Greenh. Gas Control* 70, 193-201.

Karimi, F., Toikka, A., Hukkinen, J.I., 2016. Comparative socio-cultural analysis of risk perception of Carbon Capture and Storage in the European Union. *Energy Res. Soc. Sci.* 21, 114-122.

Khan, L.R., Tee, K.F., 2016. Risk-cost optimization of buried pipelines using subset simulation. *J. Infrastruct. Syst.* 22, 1-9.

Kim, M., Kim, K., Kim, T. hyun, Kim, J., 2019. Economic and environmental benefit analysis of a renewable energy supply system integrated with carbon capture and utilization framework. *Chem. Eng. Res. Des.* 147, 200-213.

Klokk, Schreiner, P.F., Pagès-Bernaus, A., Tomasgard, A., 2010. Optimizing a CO_2 value chain for the Norwegian Continental Shelf. *Energy Policy* 38, 6604-6614.

Knoope, M.M.J., Raben, I.M.E., Ramírez, A., Spruijt, M.P.N., Faaij, A.P.C., 2014. The influence of risk mitigation measures on the risks, costs and routing of CO_2 pipelines. *Int. J. Greenh. Gas Control* 29, 104-124.

Koornneef, J., van Keulen, T., Faaij, A., Turkenburg, W., 2008. Life cycle assessment of a pulverized coal power plant with post-combustion capture, transport and storage of CO_2. *Int. J. Greenh. Gas Control* 2, 448-467.

Kwak, D.H., Kim, J.-K., 2017. Techno-economic evaluation of CO_2 enhanced oil recovery (EOR) with the optimization of CO_2 supply. *Int. J. Greenh. Gas Control* 58, 169-184.

L'Orange Seigo, S., Dohle, S., Siegrist, M., 2014. Public perception of carbon capture and storage (CCS): A review. *Renew. Sustain. Energy Rev.* 38, 848-863.

Lam, M.K., Lee, K.T., Mohamed, A.R., 2012. Current status and challenges on microalgae-based carbon capture. *Int. J. Greenh. Gas Control* 10, 456-469.

Langanke, J., Wolf, A., Hofmann, J., Böhm, K., Subhani, M.A., Müller, T.E., Leitner, W., Gürtler, C., 2014. Carbon dioxide (CO_2) as sustainable feedstock for polyurethane production. *Green Chem.* 16, 1865-1870.

Lee, S.Y., Lee, I.B., Han, J., 2019. Design under uncertainty of carbon capture, utilization and storage infrastructure considering profit, environmental impact, and risk preference. *Appl. Energy* 238, 34-44.

Lees, F., 2004. Loss prevention in the process industries, 3rd ed. Butterworth-Heinemann, London, United Kingdom.

Leonzio, G., Foscolo, P.U., Zondervan, E., 2019. An outlook towards 2030: Optimization and design of a CCUS supply chain in Germany. *Comput. Chem. Eng.* 125, 499-513.

Leung, D.Y.C., Caramanna, G., Maroto-Valer, M.M., 2014. An overview of current status of carbon dioxide capture and storage technologies. *Renew. Sustain. Energy Rev.* 39, 426-443.

Li, H., Jiang, H.D., Yang, B., Liao, H., 2019a. An analysis of research hotspots and modeling techniques on carbon capture and storage. *Sci. Total Environ.* 687, 687-701.

Li, C., Negnevitsky, M., Wang, X., Yue, W.L., Zou, X., 2019b. Multi-criteria analysis of policies for implementing clean energy vehicles in China. *Energy Policy* 129, 826-840.

Liang, X., Reiner, D., Li, J., 2011. Perceptions of opinion leaders towards CCS demonstration projects in China. *Appl. Energy* 88, 1873-1885.

Lisbona, D., McGillivray, A., Saw, J.L., Gant, S., Bilio, M., Wardman, M., 2014. Risk assessment methodology for high-pressure CO_2 pipelines incorporating

topography. *Process Saf. Environ. Prot.* 92, 27-35.

Mac Dowell, N., Fennell, P.S., Shah, N., Maitland, G.C., 2017. The role of CO_2 capture and utilization in mitigating climate change. *Nat. Clim. Chang.* 7, 243-249.

MC Group, 2017. World Formaldehyde Production to Exceed 52 Mln Tonnes in 2017 [WWW Document]. `https://mcgroup.co.uk/news/20140627/formaldehyde-production-exceed-52-mln-tonnes.html`

Medina, H., Arnaldos, J., Casal, J., Bonvicini, S., Cozzani, V., 2012. Risk-based optimization of the design of on-shore pipeline shutdown systems. *J. Loss Prev. Process Ind.* 25, 489-493.

Methanol Institute, 2016. DME: an emerging global fuel, technical report [WWW Document]. `http://www.methanol.org/wp-content/uploads/2016/06/DME-An-Emerging-Global-Guel-FS.pdf`

Middleton, R.S., Keating, G.N., Viswanathan, H.S., Stauffer, P.H., Pawar, R.J., 2012a. Effects of geologic reservoir uncertainty on CO_2 transport and storage infrastructure. *Int. J. Greenh. Gas Control* 8, 132-142.

Middleton, R.S., Kuby, M.J., Wei, R., Keating, G.N., Pawar, R.J., 2012b. A dynamic model for optimally phasing in CO_2 capture and storage infrastructure. *Environ. Model. Softw.* 37, 193-205.

Middleton, R.S., Yaw, S., 2018. The cost of getting CCS wrong: Uncertainty, infrastructure design, and stranded CO_2. *Int. J. Greenh. Gas Control* 70, 1-11.

Molag, M., Raben, I.M.E., 2006. Externe veiligheid onderzoek CO_2 buisleiding bij Zoetermeer.

Mondal, K., Sasmal, S., Badgandi, S., Chowdhury, D.R., Nair, V., 2016. Dry reforming of methane to syngas: a potential alternative process for value added chemicals-a techno-economic perspective. *Environ. Sci. Pollut. Res.* 23, 22267-22273.

Morbee, J., Serpa, J., Tzimas, E., 2012. Optimised deployment of a European CO_2 transport network. *Int. J. Greenh. Gas Control* 7, 48-61.

Moreno-Benito, M., Agnolucci, P., Papageorgiou, L.G., 2017. Towards a sustainable hydrogen economy: Optimisation-based framework for hydrogen infrastructure development. *Comput. Chem. Eng.* 102, 110-127.

Mukherjee, A., Okolie, J.A., Abdelrasoul, A., Niu, C., Dalai, A.K., 2019. Review of post-combustion carbon dioxide capture technologies using activated carbon. *J. Environ. Sci.* 83, 46-63.

Mula, J., Peidro, D., Díaz-Madroñero, M., Vicens, E., 2010. Mathematical programming models for supply chain production and transport planning. *Eur. J. Oper. Res.* 204, 377-390.

National Accademies of Sciences, 2019. Gaseous Carbon Waste Streams Utilization: Status and Research Needs. The National Accademies Press, Washington, DC.

Nie, Z., Korre, A., Elahi, N., Durucan, S., 2017. Real Options Analysis of CO_2 Transport and Storage in the UK Continental Shelf under Geological and Market Uncertainties and the Viability of Subsidies for Market Development. *Energy Procedia* 114, 6612-6622.

Noureldin, M., Allinson, W.G., Cinar, Y., Baz, H., 2017. Coupling risk of storage and economic metrics for CCS projects. *Int. J. Greenh. Gas Control* 60, 59-73.

Odenberger, M., Johnsson, F., 2010. Pathways for the European electricity supply system to 2050-The role of CCS to meet stringent CO_2 reduction targets. *Int. J. Greenh. Gas Control* 4, 327-340.

Odenberger, M., Kjärstad, J., Johnsson, F., 2008. Ramp-up of CO_2 capture and storage within Europe. *Int. J. Greenh. Gas Control* 2, 417-438.

Ogden, J.M., 2003. Modeling Infrastructure for a Fossil Hydrogen Energy System with CO_2 Sequestration, in: Gale, J., Kaya, Y. (Eds.), Greenhouse Gas Control Technologies - 6th International Conference. Pergamon, Oxford, pp. 1069–1074.

Ogden, J.M., 2004. Conceptual Design of Optimized Fossil Energy Systems with Capture and Sequestration of Carbon Dioxide [WWW Document]. `https://www.osti.gov/scitech/\%0Abiblio/829538`

Olah, G.A., Goeppert, A. Prakash, G.K.S., 2011. Beyond Oil and Gas: The Methanol Economy, 2nd ed. Wiley-VCH, Weinheim.

Oltra, C., Upham, P., Riesch, H., Boso, À., Brunsting, S., Dütschke, E., Lis, A., 2012. Public Responses to CO_2 Storage Sites: Lessons from Five European

Cases. *Energy Environ.* 23, 227-248.

Onyebuchi, V.E., Kolios, A., Hanak, D.P., Biliyok, C., Manovic, V., 2017. A systematic review of key challenges of CO_2 transport via pipelines. Renew. Sustain. *Energy Rev.* 81, 1-21.

Pacala, S., Socolow, R., 2004. Stabilization wedges: Solving the climate problem for the next 50 years with current technologies. *Science* 305, 968-972.

Perdan, S., Jones, C.R., Azapagic, A., 2017. Public awareness and acceptance of carbon capture and utilisation in the UK. Sustain. *Prod. Consum.* 10, 74-84.

Pérez-Fortes, M., Schöneberger, J.C., Boulamanti, A., Tzimas, E., 2016. Methanol synthesis using captured CO_2 as raw material: Techno-economic and environmental assessment. *Appl. Energy* 161, 718-732.

Petrosjan, L., Zaccour, G., 2003. Time-consistent Shapley value allocation of pollution cost reduction. *J. Econ. Dyn. Control* 27, 381-398.

Petvipusit, K.R., Elsheikh, A.H., Laforce, T.C., King, P.R., Blunt, M.J., 2014. Robust optimisation of CO_2 sequestration strategies under geological uncertainty using adaptive sparse grid surrogates. *Comput. Geosci.* 18, 763-778.

PIE, 2016. POM technical report [WWW Document]. `https://pieweb.plasteurope.com/Default.aspx?pageid=302\&node=100212`

Pietzner, K., Schumann, D., Tvedt, S.D., Torvatn, H.Y., Næss, R., Reiner, D.M., Anghel, S., Cismaru, D., Constantin, C., Daamen, D.D.L., Dudu, A., Esken, A., Gemeni, V., Ivan, L., Koukouzas, N., Kristiansen, G., Markos, A., Ter Mors, E., Nihfidov, O.C., Papadimitriou, J., Samoila, I.R., Sava, C.S., Stephenson, M.H., Terwel, B.W., Tomescu, C.E., Ziogou, F., 2011. Public awareness and perceptions of carbon dioxide capture and storage (CCS): Insights from surveys administered to representative samples in six European countries. *Energy Procedia* 4, 6300-6306.

Poulsen, N., Holloway, S., Neele, F., Smith, N.A., Kirk, K., 2014. CO_2StoP Final Report Assessment of CO_2 storage potential in Europe European Commission Contract No ENER/C1/154-2011-SI2.611598.

QGIS, 2017. QGIS Geographic Information System. Open Source Geospatial Foundation Project. [WWW Document]. `http://qgis.osgeo.org`

Rasmussen, N., 1975. Reactor safety study. An assessment of accident risks in U.S. commercial nuclear power plants. Executive Summary. WASH-1400 (NUREG-75/014). Rockville, MD, USA.

Reiner, D.M., 2015. Where can I go to see one? Risk communications for an 'imaginary technology. *J. Risk Res.* 18, 710-713.

Reiner, D.M., 2016. Learning through a portfolio of carbon capture and storage demonstration projects. *Nat. Energy* 1, 1-7.

Ridgway, P., 2007. Summary derivation of provisional SLOT and SLOD DTLs for CO_2.

Rivera-Tinoco, R., Farran, M., Bouallou, C., Auprêtre, F., Valentin, S., Millet, P., Ngameni, J.R., 2016. Investigation of power-to-methanol processes coupling electrolytic hydrogen production and catalytic CO_2 reduction. *Int. J. Hydrogen Energy* 41, 4546-4559.

Roddis, P., Carver, S., Dallimer, M., Norman, P., Ziv, G., 2018. The role of community acceptance in planning outcomes for onshore wind and solar farms: An energy justice analysis. *Appl. Energy* 226, 353-364.

Roffel, B., Rijnsdorp, J.E., 1982. Process dynamics, control and protection. Ann Arbor, MI.

Roh, K., Frauzem, R., Nguyen, T.B.H., Gani, R., Lee, J.H., 2016. A methodology for the sustainable design and implementation strategy of CO_2 utilization processes. *Comput. Chem. Eng.* 91, 407-421.

Rubin, E.S., Davison, J.E., Herzog, H.J., 2015. The cost of CO_2 capture and storage. *Int. J. Greenh. Gas Control* 40, 378-400.

Rubinstein, R.Y., Kroese, D.P., 2017. Simulation and the Monte Carlo Method, Wiley, Hoboken, New Jersey.

Rusin, A., Stolecka, K., 2015. Reducing the risk level for pipelines transporting carbon dioxide and hydrogen by means of optimal safety valves spacing. *J. Loss Prev. Process Ind.* 33, 77-87.

Sabio, N., Gadalla, M., Guillén-Gosálbez, G., Jiménez, L., 2010. Strategic planning with risk control of hydrogen supply chains for vehicle use under uncertainty in operating costs: A case study of Spain. *Int. J. Hydrogen Energy* 35,

6836-6852.

Sakakura, T., Kohno, K., 2009. The synthesis of organic carbonates from carbon dioxide. *Chem. Commun.* 11, 1312-1330.

Schumann, D., 2017. Public Perception of CO_2 Pipelines. *Energy Procedia* 114, 7356-7366.

Selosse, S., Ricci, O., 2017. Carbon capture and storage: Lessons from a storage potential and localization analysis. *Appl. Energy* 188, 32-44.

Sinnot, R., Towler, G., 2009. Chemical Engineering Design, 5th ed.

Small, M.J., Wong-Parodi, G., Kefford, B.M., Stringer, M., Schmeda-Lopez, D.R., Greig, C., Ballinger, B., Wilson, S., Smart, S., 2019. Generating linked technology-socioeconomic scenarios for emerging energy transitions. *Appl. Energy* 239, 1402-1423.

Smit, B., Reimer, J.A., Oldenburg, C.M., Bourg, I.C., 2014. Introduction to Carbon Capture and Sequestration. Imperial College Press, London, United Kingdom.

Statista, 2013. Ethylene production capacity worldwide in 2013 by region [WWW Document]. `https://www.statista.com/statistics/270007/capacity-of-ethylene-by-region/`

Stephanopoulos, G., Reklaitis, G. V., 2011. Process systems engineering: From Solvay to modern bio- and nanotechnology. A history of development, successes and prospects for the future. *Chem. Eng. Sci.* 66, 4272-4306.

Sternberg, A., Jens, C.M., Bardow, A., 2017. Life cycle assessment of CO_2-based C1-chemicals. *Green Chem.* 19, 2244-2259.

Strachan, N., Hoefnagels, R., Ramírez, A., van den Broek, M., Fidje, A., Espegren, K., Seljom, P., Blesl, M., Kober, T., Grohnheit, P.E., 2011. CCS in the North Sea region: A comparison on the cost-effectiveness of storing CO_2 in the Utsira formation at regional and national scales. *Int. J. Greenh. Gas Control* 5, 1517-1532.

Sustainable Gas Institute, 2016. White Paper 2: Can technology unlock unburnable carbon? [WWW Document]. `https://www.sustainablegasinstitute.org/technology-unlock-unburnable-carbon/`

Szulczewski, M.L., MacMinn, C.W., Herzog, H.J., Juanes, R., 2012. Lifetime of carbon capture and storage as a climate-change mitigation technology. *Proc. Natl. Acad. Sci.* 109, 5185-5189.

Tapia, J.F.D., Lee, J.Y., Ooi, R.E.H., Foo, D.C.Y., Tan, R.R., 2018. A review of optimization and decision-making models for the planning of CO_2 capture, utilization and storage (CCUS) systems. *Sustain. Prod. Consum.* 13, 1-15.

ter Mors, E., Terwel, B.W., Daamen, D.D.L., 2012. The potential of host community compensation in facility siting. *Int. J. Greenh. Gas Control* 11, 130-138.

ter Mors, E., Terwel, B.W., Daamen, D.D.L., Reiner, D.M., Schumann, D., Anghel, S., Boulouta, I., Cismaru, D.M., Constantin, C., de Jager, C.C.H., Dudu, A., Esken, A., Falup, O.C., Firth, R.M., Gemeni, V., Hendriks, C., Ivan, L., Koukouzas, N., Markos, A., Næss, R., Pietzner, K., Samoila, I.R., Sava, C.S., Stephenson, M.H., Tomescu, C.E., Torvatn, H.Y., Tvedt, S.D., Vallentin, D., West, J.M., Ziogou, F., 2013. A comparison of techniques used to collect informed public opinions about CCS: Opinion quality after focus group discussions versus information-choice questionnaires. *Int. J. Greenh. Gas Control* 18, 256-263.

Terwel, B.W., Harinck, F., Ellemers, N., Daamen, D.D.L., Best-Waldhober, M.D., 2009. Trust as predictor of public acceptance of CCS. *Energy Procedia* 1, 4613-4616.

Terwel, B.W., ter Mors, E., 2015. Host community compensation in a carbon dioxide capture and storage (CCS) context: Comparing the preferences of Dutch citizens and local government authorities. *Environ. Sci. Policy* 50, 15-23.

Thomas, G., Edgar, G.H., Anders, A., Bhawna, S., Francesca, V., 2017. Health benefits, ecological threats of low-carbon electricity. *Environ. Res. Lett.* 12, 34023.

Treut, L., Somerville, R., Cubasch, U., Ding, Y., Mauritzen, C., Mokssit, A., Peterson, T., Prather, M., Qin, D., Manning, M., Chen, Z., Marquis, M., Averyt, K.B., Tignor, M., Kingdom, U., 2007. Historical Overview of Climate Change Science [WWW Document]. `https://www.ipcc.ch/site/assets/uploads/2018/03/ar4-wg1-chapter1.pdf`

Turk, G.A., Cobb, T.B., Jankowski, D.J., Wolsky, A.M., Sparrow, F.T., 1987. CO_2 Transport: A new application of the assignment problem. *Energy* 12, 123-130.

Turton, R., Baile, R.C., Whiting, W.B., Shaeiwitz, J.A., Bhattacharyya, D.,

2015. Analysis, synthesis, and design of chemical processes, Fourth Edi. ed. Pearson Education, Inc.

Unger, T., Ekvall, T., 2003. Benefits from increased cooperation and energy trade under CO_2 commitments—the nordic case. *Clim. Policy* 3, 279-294.

Upham, P., Oltra, C., Boso, À., 2015. Towards a cross-paradigmatic framework of the social acceptance of energy systems. *Energy Res. Soc. Sci.* 8, 100-112.

USDOE, 2014. FE/NETL CO_2 Transport Cost Model: Description and User's Manual, Report No. DOE/NETL2014/1660. Pittsburg, PA.

van den Broek, M., Ramirez, A., Groenenberg, H., Neele, F., Viebahn, P., Turkenburg, W., Faaij, A., 2010. Feasibility of storing CO_2 in the Utsira formation as part of a long term Dutch CCS strategy. An evaluation based on a GIS/MARKAL toolbox. *Int. J. Greenh. Gas Control* 4, 351-366.

van der Horst, D., Toke, D., 2010. Exploring the landscape of wind farm developments; local area characteristics and planning process outcomes in rural England. *Land use policy* 27, 214-221.

van Egmond, S., Hekkert, M.P., 2012. Argument map for carbon capture and storage. *Int. J. Greenh. Gas Control* 11, 148-159.

Vianello, C., Mocellin, P., Macchietto, S., Maschio, G., 2016. Risk assessment in a hypothetical network pipeline in UK transporting carbon dioxide. *J. Loss Prev. Process Ind.* 44, 515-527.

Vögele, S., Rübbelke, D., Mayer, P., Kuckshinrichs, W., 2018. Germany's "No" to carbon capture and storage: Just a question of lacking acceptance? *Appl. Energy* 214, 205-218.

von der Assen, N., Bardow, A., 2014. Life cycle assessment of polyols for polyurethane production using CO 2as feedstock: insights from an industrial case study. *Green Chem.* 16, 3272-3280.

Wallquist, L., Seigo, S.L.O., Visschers, V.H.M., Siegrist, M., 2012. Public acceptance of CCS system elements: A conjoint measurement. *Int. J. Greenh. Gas Control* 6, 77-83.

Wang, X., Qie, S., 2018. Study on the investment timing of carbon capture and storage under different business modes. *Greenh. Gases Sci. Technol.* 8,

639-649.

WBGU, 2011. World in Transition: A Social Contract for Sustainability [WWW Document]. https://www.wbgu.de/fileadmin/user_upload/wbgu/publikationen/hauptgutachten/hg2011/pdf/wbgu_jg2011_kurz_en.pdf

Wiesberg, I.L., de Medeiros, J.L., Alves, R.M.B., Coutinho, P.L.A., Araújo, O.Q.F., 2016. Carbon dioxide management by chemical conversion to methanol: HYDROGENATION and BI-REFORMING. *Energy Convers. Manag.* 125, 320-335.

Witkowski, A., Rusin, A., Majkut, M., Rulik, S., Stolecka, K., 2015. Advances in Carbon Dioxide Compression and Pipeline Transportation Processes.

Wolsink, M., 2018. Social acceptance revisited: gaps, questionable trends, and an auspicious perspective. *Energy Res. Soc. Sci.* 46, 287-295.

Wu, Q., Lin, Q.G., Wang, X.Z., Zhai, M.Y., 2015. An inexact optimization model for planning regional carbon capture, transportation and storage systems under uncertainty. *Int. J. Greenh. Gas Control* 42, 615-628.

Yang, L., Zhang, X., McAlinden, K.J., 2016. The effect of trust on people's acceptance of CCS (carbon capture and storage) technologies: Evidence from a survey in the People's Republic of China. *Energy* 96, 69-79.

Yue, D., You, F., 2016. Optimal Supply Chain Design and Operations Under Multi-Scale Uncertainties: Nested Stochastic Robust Optimization Modeling Framework and Solution Algorithm. *AIChE J.* 62, 3041-3055.

ZEP, 2011. The cost of CO_2 transport: post-demonstration CCS in the EU, European Technology Platform for Zero Emission Fossil Fuel Power Plants.

Zhang, Z., Huisingh, D., 2017. Carbon dioxide storage schemes: Technology, assessment and deployment. *J. Clean. Prod.* 142, 1055-1064.

Zhang, S., Liu, L., Zhang, L., Meng, Q., Du, J., 2018a. Optimal Planning for Regional Carbon Capture and Storage Systems under Uncertainty. *Chem. Eng. Trans.* 70, 1207-1212.

Zhang, S., Liu, L., Zhang, L., Zhuang, Y., Du, J., 2018b. An optimization model for carbon capture utilization and storage supply chain: A case study in Northeastern China. *Appl. Energy* 231, 194-206.

Zheng, Z., Larson, E.D., Li, Z., Liu, G.J., Williams, R.H., 2010. Near-term mega-scale CO_2 capture and storage demonstration opportunities in China. *Energy Environ. Sci.* 3, 1153-1169.